Biofortification of potato (*Solanum tuberosum*) using metal oxide nanoparticles

Karen Elizabeth Davies

A thesis submitted in partial fulfilment of the
requirements of Nottingham Trent University
for the degree of Doctor of Philosophy

This research programme was carried out in collaboration with AHDB Potatoes and BBSRC

2018

Abstract

The project aimed to increase the phytoavaiablilty of calcium (Ca), iron (Fe) and zinc (Zn) in order to fortify tubers for human consumption to aid the reduced global micronutrient malnutrition (MNM). Simultaneously improve quality of tubers (dry mass), reduction of disease occurrence (soft rot), and uniformity of tuber size.

There are three strategies commonly adopted to improve plant fortification: enhanced fertilisers, breeding and nutritional genetic modification. While genetic modification has produced some interesting results, the commercialisation is hindered by public perception and legislation, therefore selective breeding programmes are now being developed to circumvent these issues and help address the global issue of micronutrient malnutrition. This programme of work adopts a more holistic approach, whereby a plant food additive has been developed that can be fed to all varieties of crop without the need to develop new strains through breeding or genetic modification.

The work here in produced a number of key findings:

- Increase in mineral content of tubers from skin to pith in all applications
- Increased foliar growth rate and tubers >30mmm
- Iron increased the consistency of tuber size
- Retention on minerals in growth media, decreasing leaching and increasing phytoavailability. Also beneficial to decreasing the minerals realised in the environment.

Using patented technology, the reactor allows accurate and consistent size production of nanoparticles metal oxide nanoparticles with a production rate of 1 kg per hour whereas previous this rate was approximately 5 grams a day. The bulk production allows nanoparticles to be applied in numerous ways that were previously unfeasible.

Sustainable application of iron fortification that retains in the soil strata for a longer period of time than conventional applications Coating of amino acid to the nanoparticle increases the efficiency of nitrogen assimilation, in turn increasing the metabolism of the plant and accumulation of other minerals present in the soil or fertiliser. Costing less than current Fe-chelated with less requirement for application.

Significant increases in the mineral content of the tubers means a more nutritional food for human consumption. Increases in weight, yield and faster maturity can mean a solution to sustaining agriculture for a fast growing population.

The fortification method can be added to current fertiliser applications, requiring no drastic changes to current methods**.**

The implications of the project are summarised in the below figure.

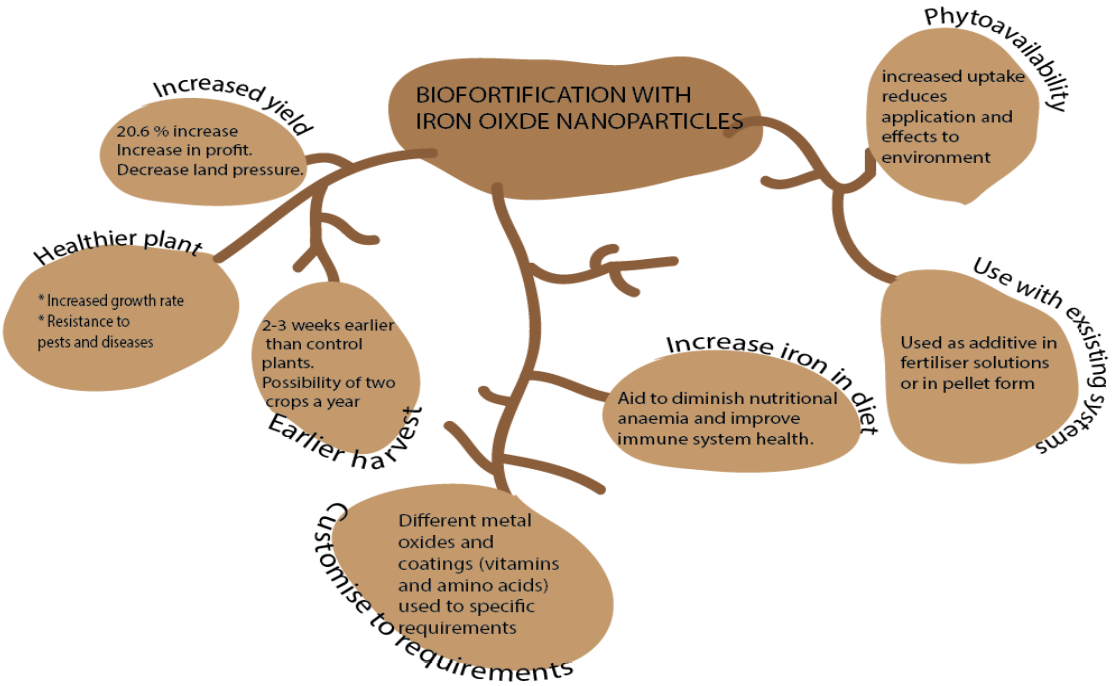

Contents

Tables and figures

Abbreviations

AHDB	Agriculture and Horticulture Development Board
CaFeNP	Calcium ferrite nanoparticle ($CaFe_2O_4$)
CaFeNP+His	Calcium ferrite nanoparticle ($CaFe_2O_4$) coated with histidine 1:1, w/w
CaNP	Calcium oxide nanoparticle (CaO)
CaNP+His	Calcium oxide nanoparticle (CaO) coated with histidine 1:1, w/w
CFU	Colony forming unit
CSRC	Crop Storage Research Centre. AHDB Potatoes, Sutton Bridge, Lincolnshire
d.a.p	days after planting
DM%	Dry mass percentage
FeNP	Iron oxide nanoparticle (Fe_3O_4)
FeNP+His	Iron oxide nanoparticle (Fe_3O_4) coated with histidine 1:1, w/w
FTIR	Fourier-transform infrared spectroscopy
H_1	Alternative hypothesis
His	Histidine
HNS	Hydroponic nutrient solution
H_o	Null hypothesis
ICP-OES	inductively coupled plasma optical emission spectrometry
MONP	Metal oxide nanoparticle
MONP+His.	Metal oxide nanoparticle coated with histidine 1:1, w/w
NP	Nanoparticle
SDR	Spinning disc reactor
SEM	Scanning electron microscope
W.a.p.	Weeks after planting
XRD	X-ray powder diffraction
ZnNP	Zinc oxide nanoparticle (ZnO)
ZnNP+His	Zinc oxide nanoparticle (ZnO) coated with histidine 1:1, w/w

1 Introduction

1.1 Nanoparticle synthesis

Research into the use of nanoscale science and technology, enables the characterisation and manipulation of synthesised structures (Schmid, 2010), has intensified in the last years due to increase in realisation of potential or improved chemical novel applications and productivity (Parak *et al*., 2008; Schmid, 2010; Khot *et al*., 2012; Sirvastava *et al*., 2013). Particles measuring less than 100 nm, in one dimension are classified as nanoparticles, NP, see figure 1.1. (Mamalis, 2007; Nair *et al*., 2010; Hasany *et al*., 2012; Sirvastava *et al*., 2013). Nanoparticles are found in the natural environment in forms of dust particulates, volcanic ash, some pollens and antibodies (Parak *et al*., 2008). Due to the nano size, particles properties have been investigated for the unique ability to improve function, performance and increase cost-effectiveness in engineered materials resulting in an extremely diverse research field.

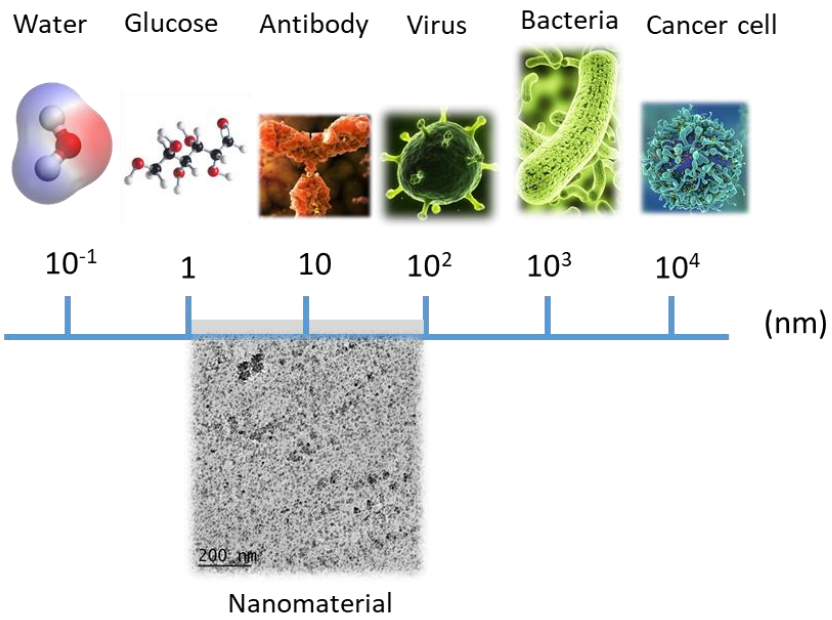

Figure 1.1: Schematic comparing the nm range. Adapted from Amin et al. (2014)

Previously nanotechnology has evolved from the scientific fields of physics, chemistry and molecular biology, material science and micro electrons (Malalis, 2007; Parka *et al*. 2008) in order to manipulate structures to nano size, to enhance and improve functionality. Primarily nanotechnology developments have focused on applications in electronics (microchip technology), medicines and life

sciences (drug delivery) and energy (Parak *et al*., 2008; Mamalis, 2007; Niar *et al*., 2010). The synthesis and isolation of monodispersed NP, with an emphasis on the control over size, shape and composition are of increased importance when synthesising nanoparticles especially when scaling up for commercial production (Parak *et al*. 2008; Schmid, 2010 Khot *et al*., 2012).

There are two approaches to nanomaterial formulation (Parak *et al*., 2008) as represented in figure 1.2. Top down production uses physical mechanical methods such as bore mills to reduce the size of the particles, i.e. in the production of corn flour, pharmaceuticals and utilised in the micro electrical industry (Parak *et al.*, 2008). The second approach is known as 'bottom up', involving the synthesis of precursor solutions, resulting in a precipitation reaction. Many synthesis techniques involve solutions of metal salt or salts with a controlled addition to a base in excess.

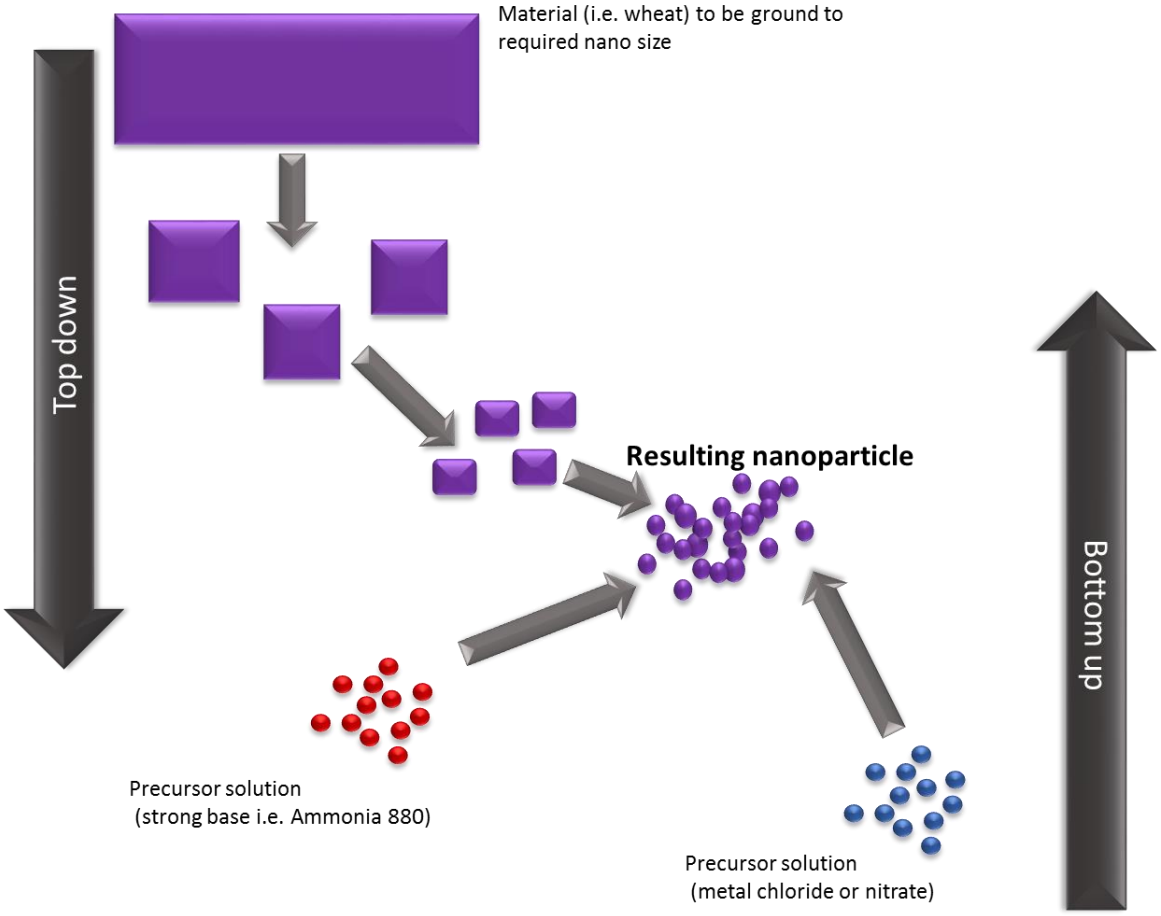

Figure 1.2: Bottom up and top down approaches to the formation of nanoparticles

A number of synthesis techniques have been developed to satisfy the growing demand for nanomaterial, such as iron (III) oxide nanoparticles, FeNP (Roth *et al*., 2015), with size controlling techniques such as sol-gel synthesis (Albornoz and Jacobo, 2006), hydrothermal reactions (Wan *et al*., 2005), sonochemcial procedures (Kim *et al*., 2005), hydrolysis and thermolysis of precursors (Limata *et al*., 2003), electrospray synthesis (Baska *et al*., 2007), and synthesis forming microelmulsions (Chin and Yaacob, 2007). Nanoparticles are generally synthesised in a controlled environment where oxygen concentration (and other gases i.e. nitrogen in excess) and pressure are regulated along with precursor solutions used in precipitation techniques of monodisperse NP, were the following factors are varied to produce the required nanoparticles (Laurent *et al*., 2008):

- pH
- Temperature
- Concentration of precursor solutions
- Rates and ratio of precursor solutions
- Degree of suspension

Variation in the synthesis conditions are critical to obtain the desired nanoparticle characteristics, however, the ripening process in which larger particles grow known as Ostwald ripening (figure 1.3) and uncontrolled growth through nucleation, are problematic as this can increase the particles size beyond the nano range. This is an implication to metal oxide nanoparticle (MONP) synthesis as they are formed as a dispersant in a medium, which renders them unstable with respect to agglomeration to a more stable bulk form.

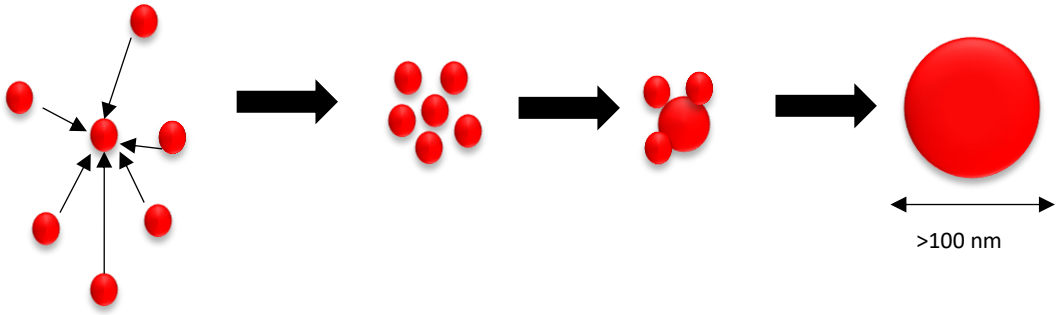

Figure 1.3: Ostwald ripening of NP.

The top down approach is commonly used in large-scale production as it can economically mass produce NP in contrast to bottom up approaches that are still laboratory based, low yielding and not cost efficient as the mechanical top down approaches. However, with developments focused on the

bottom up approach as these techniques yield narrow range of particulate sizes and increase the formation control resulting in increased control over the final product. Formation of MONP's in this project used bottom up approach, where two precursor solutions formulate a coprecipitation reaction.

A widespread method in the absence of a stabilising surfactant agent, is the co-precipitation of metal salts within an alkali environment (Roth *et al*., 2015), known as the Massart process (Morrison *et al*., 2004; Sun *et al*., 2004). The reduction of transition metal salts with in an aqueous solution is a widely practiced form of MONP synthesis (Schmid. 2010). Iron NP and ZnNP (Srivastava *et al*., 2013) are commonly formed this way, with stoichiometric mixture of ferrous and ferric salts forming the metal salt precursor for the co-precipitation synthesis of FeNP (Laurent *et al*., 2008).

There are sixteen phases of pure iron oxide (Laurent *et al*., 2008; Carvalho *et al*., 2013; Ramimoghadam *et al*., 2014), the most synthesised is the cubic ferromagnetic magnetite (Fe_3O_4) which contains oxidation states of Fe^{2+} and Fe^{3+}. The superparamagnetic properties of Fe_3O_4 are utilised due to ease of particle size manipulation for that applications of magnetic resonance imaging (MRI) contrast reagents, drug delivery, magnetic data storage and magnetic ink jet printing (Laurent *et al*., 2008; Carvalho *et al*., 2013; Ramimoghadam *et al*., 2014).

A second bulk synthesis of NP that requires a longer retention time uses a sol-gel / polymeric precursor method involves the development of networks through an arrangement of colloidal suspension (sol) and gelation to form a system in continuous liquid phase (gel) (Srivastava *et al*., 2013; Ramimoghadam *et al*., 2014). A sol gel is a dispersion of polymetrix precursors developed by Pechnini (Pechnini, 1967; Candeia *et al*., 2004) consisting of the formation of a metallic citrate polymerization using ethyl glycol as the basis of sol-gel reactions (Morrison *et al*., 2004; Candeia *et al*, 2004; Khanna and Verma, 2013). Depending on the nature of the precursors, may be divided into two classes namely inorganic precursors (chlorides, nitrates, sulfides, etc.) and alkoxide precursors. The sol gel procedure has been developed to produce NP on a bulk scale that require a greater precursor retention time without the requirement for heat or alternations to atmospheric pressure. In the formation of calcium oxide nanoparticles (CaNP) (Safaei-Ghomi *et al*., 2013) and calcium ferrite (CaFeNP) calcium nitrate was used and iron nitrate when synthesising CaFeNP (Candia *et al*., 2004; Khanna and Verma, 2013). Citric acid was added to provide fuel for the combustion (Khanna and Verma, 2013), especially for CaFeNP synthesis, which in turn served as a chelating agent to form complexes with metal ion (Khanna and Verma, 2013) preventing the precipitation of hydroxylated compounds (Thant *et al*., 2010), with metallic cations homogeneously distributed throughout the matrix (Candeia *et al*., 2004).

To exploit novel applications of NP requires the preparation and isolation of monodispersed, stable metal nanoparticles with a great degree of control over size, shape and composition (Schmid, 2010) in significant quantities (Parak *et al*., 2008; De Caprariis *et al*., 2012; Khot *et al*., 2012) that is replicable. The Spinning disc reactor, SDR (figure 1.4) developed and patented by Dr G.W.V. Cave, WO 2017033005A1, (Cave, 2017) is based upon a continuous flow system allowing large quantities of MONP to be synthesised at any one time thus allowing the application of MONP as a fertiliser via adaptation of co-precipitation and sol-gel synthesis. The rotation of the disc, seen in figure 5, creates a high centrifugal force that promotes film flow (De Caprariis *et al*., 2012). The stepped surface on the disc and the bowl shape; wall height, diameter of disc, bowl shape, gives rise to mixing and control over NP size synthesised. The precursor solutions are fed into the reactor (figure 1.4) and dispersed onto the disc via peristaltic pumps on the top of the rotating disc (figure 1.5). The feed rates and ration of the disc are controlled via a control panel, therefore altered to a specific MONP requirements and size formation.

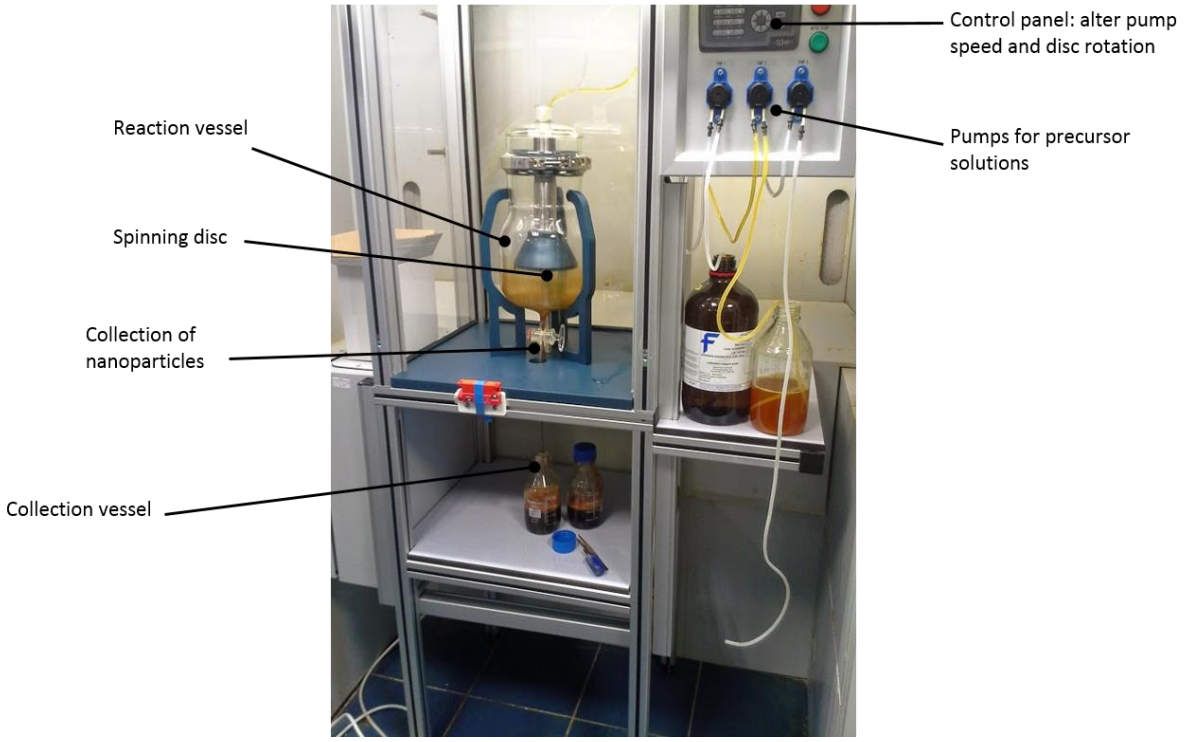

Figure 1.4: SDR allows bulk production of uniform sized nanoparticles

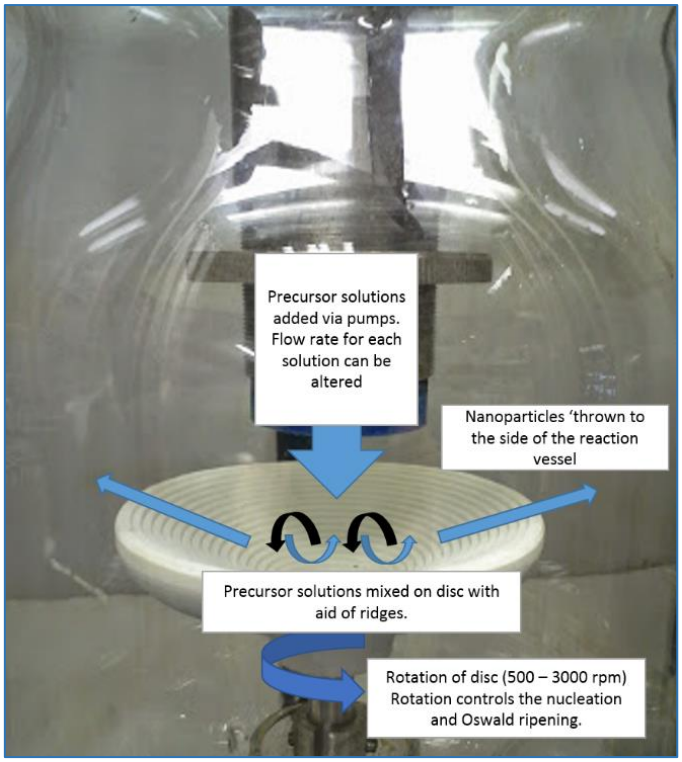

Figure 1.5: SDR disc, demonstrating the morphology of the disc effecting the mixing of the precursor solutions

Control over mixing intensification to precipitation formation is to reduce mixing time, leading to a decrease reaction time and nucleation resulting maximised monodispersed MONP synthesis.

When NP precipitation takes place (figure 1.6), the size distribution of the NP formed are mainly determined by a two-step process, nucleation and aggregation (De Caprariis *et al*., 2012). Complete macromixing between the two precursor solutions, almost all of the supersaturation is consumed during aggregation, therefore producing uniformed sized particles (De Caprariis *et al*., 2012) figure 1.6, to avoid further aggregation and the occurrence of Ostwald ripening (figure 1.3).

When formed, the centrifugal force disperses the NP onto the side of the reaction vessel, figure 1.6. A short interparticle distance allows the interaction of two particles via van der Waals forces. In the absence of repulsive forces to counteract the attraction Ostwald ripening occurs (Schmid, 2010) once the MONP are suspended. With the aid of washing and gravitational force, the NP moves towards the collection tap and into the collection vessel where the NP solution is quickly filtered and dried accordingly to avoid Ostwald ripening.

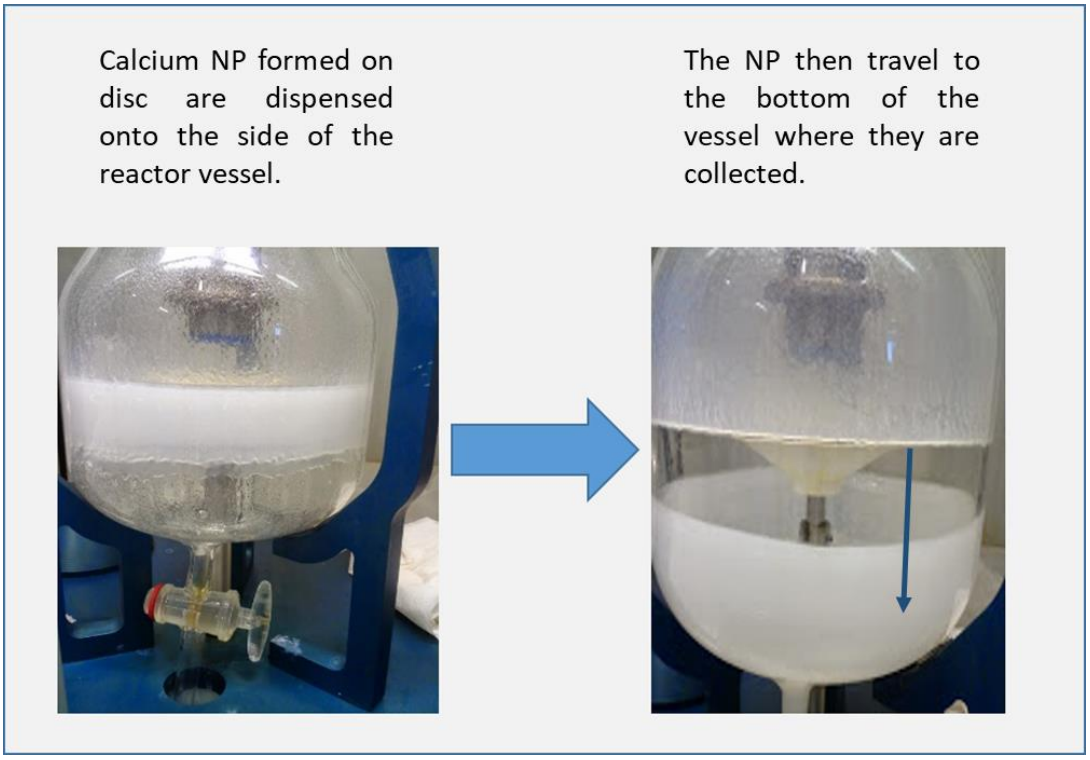

Figure 1.6: Synthesis of CaNP on the SDR

To counteract the particle attraction and aid MONP suspension, two methods are used 1) electrostatic stabilization 2) steric stabilization (De Caprariis *et al.*, 2012). In this instance the electrostatic coating of the amino acid histidine patented by Cave and Mundell (2014), WO 2013136082 A3, prevents agglomeration of particles into larger particles (> 100 nm) and the suspension of MONP in an aqueous solvent.

In summary, the SDR enables the increased production of narrow ranged NP that can be tailor synthesised to specific requirements using coprecipitation and sol gel methods. This enables new materials to be developed which require mass produced nanomaterial applying nanotechnologies ethos of improved material efficiency into areas such as agriculture. The use of silver NP has been successfully transferred from medical applications as an antifungal and anti-bacterial agent (Singh *et al.*, 2008; Panacek *et al.*, 2009), to a pathogen control in the prevention of fungal diseases (Jo and Kim, 2009) like powdery mildew (Park *et al.*, 2006).

1.2 Minerals: Fortification of food

The work herein focused on the biofortification of plants using Ca, Fe and Zn minerals although other minerals are required in addition to oxygen, carbon dioxide and water. Generally, plants require at

least fourteen mineral elements to maintain growth and production of crops (Marschner, 1995; Mengel *et al*., 2001). A depletion in phytoavailable elements results in deficiency, consequently reducing plant growth, yields and increases the plants susceptibility for disease. If the crop is deficient in a mineral, this will pass onto the consumer (Kelling and Schilte, 2008; Gupta and Gupta, 2014), causing micronutrient malnutrition, MNM (Hirschi, 2004) also known as 'Hidden hunger'. MNM is a globe issue (FAO, 1996; Hirschi, 2004; Kelling and Schilte, 2008) with in ever-increasing population placing greater pressure on land to provide food as well as housing and amenities, therefore emphasis is placed on food security (Kalpana *et al*., 2011).

Food security is achieved when food systems operate such that; *'all people, at all times, have physical and economic access to sufficient, safe and nutritious food to meet their dietary needs and food preferences for an active and healthy life'* (FAO, 1996; Kalpana *et al*., 2011). There are three components to food system to achieve security: (i) food availability (production, distribution and exchange) (ii) food access (affordability, allocation and preference) and (iii) food utilization; nutritional value, social value and food safety, (Gregory *et al*., 2005). Food security status is diminished, or a state of food insecurity occurs, when any one of the three components of the food system deteriorates (Kalpana *et al*., 2011).

The human body requires 22 minerals to maintain health which can be obtained from a varied diet (table 1.1) (Welch and Graham, 2002; Welch and Graham, 2005; White and Broadley, 2005[a]; White and Broadley, 2009; Saltzman *et al*., 2013). The mineral elements most commonly lacking in human diets are Fe, Zn, I, Se, Ca, Mg and Cu (White and Broadley, 2009; Stein, 2010). Mineral nutrition in humans is defined as the process by which substances in foods are transformed into body tissues and provide energy for the full range of physical and mental activities that make up human life (Bouis *et al*., 2011; Saltzman *et al*., 2013). The most abundant global plant-based foods (rice, wheat cassava and maize) are nutritionally inadequate to sustain human health (Hirschi, 2004). Cereal grains have inherently low concentrations of micronutrients such as Zn and Fe. Translocation of Fe from senescing leaves to the grain, particularly when cultivated in nutrient deficient soils, is particularly poor (Grusak and Dellapenna, 1999). A majority of population cannot obtain such a varied diet and as a consequence 60% of the world population are Fe deficient, over 30 % deficient in Zn and majority of the developing world deficient in Ca (Fossard *et al*., 2000; Welch and Graham, 2002; Welch and Graham, 2005; Grusak and Cakmak, 2005; Rude and Gruber, 2005; Thacher *et al*., 2006). Everything fluctuates in content and concentration of minerals; however, the crop can only provide minerals that are derived from the soil unless a fertiliser is applied (Hirschi, 2009). It is also recognised that the

growing reliance upon cereals as a stable food inhibits absorption of Fe, Zn and Ca due the presence of phytic acids that are prolific in the composition of cereal based food, contributing to MNM (Frossard *et al*., 2000).

	Sources	*Functions*	*RDA*
Calcium	Milk, cheese, yogurt, sardines, canned fish with bones	Structural in bones and teeth, signal transduction	1500 – 2000 mg
Iron	Meat, fish, poultry, firm tofu, dried beans, peas, like soybeans, chickpeas, split pea, lentils, nuts and seeds, organ meats such as liver and heart; blackstrap molasses	Oxygen transport, signal transduction, energy production and immune defence.	18 - 30 mg
Zinc	Yogurt, milk, cheese; dried beans like kidney, navy, pinto and soybeans, lentils, pumpkin seeds and sunflower seeds, liver, meat, poultry, fish and seafood	Cofactor for enzymes, growth and development; immune function	30 - 50 mg

Table 1.1 Ca, Fe and Zn sources from food. Adapted from Cole and Kramer (2016). RDA data source Bach and Bach (2000).

Iron deficiency leading to iron deficient anaemia is the most common dietary deficiency globally (Akhter *et al*., 2005; Paesano *et al*., 2010). Low iron reduces the production of haemoglobin (blood oxygen carrier). Low concentrations of hemoglobin, adversely affect cognitive and motor development and cause fatigue and low productivity (Balarajan *et al*., 2011). Due to the recent decline in the consumption of red meat, the UK gains 5% of Fe intake from potatoes reasoning that agrimony biofortification is an attractive strategy to increase Fe in the diet (White, 2017). Calcium like iron, is an abundant mineral and therefore should be easily available to dietary intake. However, 75 million people worldwide suffer from osteoporosis, a disease in which bones of the skeleton become fragile and more likely to fracture due to low bone density caused by loss of calcium minerals (Vavrusova and Skinsted, 2014). It is estimated that only 50–60% of post-menopausal women consume the adequate intake of dietary calcium per day (Breitman *et al*., 2003). This deficiency can be controlled by maintaining the daily calcium intake to the adequate level (Soto *et al*., 2014). Improved calcium absorption would probably have a major role on the reduction of bone fractures and osteoporosis in the body.

In 2012, the 65th World Health Assembly approved an action plan and global targets for maternal, infant, and child nutrition, with a commitment to halve anemia prevalence in women of reproductive age by 2025, from 2011 levels. As such, attention to nutritional interventions, such as the 'Scaling Up Nutrition' initiative, has increased with global projects by the World Health Organization (WHO) (WHO, 2002) with HarvestPlus initiative. Founded in 2003, HarvestPlus is part of the CGIAR Research Program on Agriculture for Nutrition and Health (formally Consultative Group for International Agricultural Research), coordinated by the International Centre for Tropical Agriculture (CIAT) and the International Food Policy Research Institute (IFPRI) (Chugh and Dhaliwal, 2013). The program uses biofortification to breed higher amounts of vitamins and minerals in staple foods, including bean, cassava, orange sweet potato, rice, maize, pearl millet, and wheat (WHO, 2002; White and Broadley, 2009; Chugh and Dhaliwal, 2013). Biofortification, the process of breeding and / or supplying nutrients into food crops (White and Broadley, 2009; Bouis *et al*., 2011; Saltzman *et al*., 2013), aims to provide an economically viable and sustainable method of delivering micronutrients. Over the past forty years, agricultural development has focused on the increase in yield, particularity on staple crops such as cereals (Bouis *et al*., 2011; Saltzman *et al*., 2013), to meet the demand to feed a growing global population. Genetic engineering approaches have been also deemed successful for biofortification of a few traits in cereals (Naqvi *et al*., 2009; Wirth *et al*., 2009; Masuda *et al*., 2012). Introduction of genes that code micronutrient-binding proteins, overexpression of storage proteins (i.e. ferritin) (Chugh and Dhaliwal, 2013) and / or increased expression of proteins that are responsible for micronutrient uptake into plants (Lonnerdal, 2003). Exhale of a successful program of biofortification through GM is the Golden Rice Project, which has been genetically engineered to produce β-carotene, to control vitamin A deficiency (Ye *et al*., 2000; Stein *et al*., 2008).

Introduction of crops genetically modified or bred to increase mineral uptake may be deemed success full, however, research has demonstrated that cultivation of genotypes of high yielding grains, coincided with the mineral content decline (Jarrell and Benerly, 1981; Loladze, 2002; Thomas, 2003; White and Broadley, 2005[b]; Fan *et al*., 2008). The long running Broadbalk Wheat Experiment at the Rothamsted Research Facility, published data on the mineral content of the semi-dwarf high yielding wheat, (*Triticum aestivum L.*) (Fan *et al*., 2008). Observation on yield has been taken since 1843, with the introduction of the modern variety, *T. aestivum L.*, in 1968 with mineral content analysis of harvested dried grain (Fan *et al*., 2008). Decline in the Fe, Zn and Cu minerals in the grain were observed since the experiment commenced to present day suggesting the exhaustion of phytoavailable minerals (Thomas, 2003; White and Broadley, 2005[b]). These results reflect what other studies have found using other high yield crops, *Sorghum bicolor* (Reddy *et al*., 2005), leading to the

conclusion that new agronomic strategies are required to increase mineral concentration in edible tissues rather than focusing on yield (White and Broadley, 2005[a]; White and Broadley, 2005[b]; Reddy *et al*., 2005; White and Broadley, 2009). In 2002 the World Health Organisation highlighted the inadequacies of crops in mineral content, leading to malnutrition, health implications and detrimental economic impacts (Welch and Graham, 2005; Bouis *et al*., 2011).

1.3 Plant mineral uptake

The uptake of mineral elements by plant roots/tubers and their subsequent distribution within the plant have been the subject of studies for many decades (Marshner, 1995; Mengal *et al*., 2001; Karley and White, 2009; Miller *et al*., 2009; Miwa *et al*., 2009; Puig and Peñarrubia, 2009; White and Broadley, 2009).

There are several barriers that impede mineral uptake and not just the phytoavailability of minerals at the root to soil, or tuber to soil interface (i.e. rhizosphere) (Welch and Grahmam, 2005). Free metal ions that are released via weathering of parent material, decomposition of organic matter or added via fertiliser (Evans, 1989; White, 2001; Kelling and Schilte, 2008), the ions interact with the charged particulates that may form weak complexes through cation exchange or strong bond through ligand exchange. Elements may precipitate immediately or remain in a solution depending on the ionic potential (Salisbury and Ross, 1991). The associations these ions form largely depends on the nature of the ion and absorbing surface (Evans, 1989). Metal ions of calcium, iron and zinc (Ca^{2+}, Fe^{3+}, Fe^{2+}, Zn^{2+}) are taken up by the root system in a solution form (Mousavi, 2011), are unavailable as they form strong bonds with clay and organic matter in the form of oxides and hydroxides binding the metals into the soil / compost matrix (Mousavi, 2011). Insoluble complexes are unable to move through the matrix to the rhizosphere where reduction in the pH enables chelation and uptake, see figure 1.7. The mobility of metals within the soil are conditions are influenced by a number of factors; irrigation (via precipitation or application), pH (varying from 4.0-9.0, exerting a strong influence over free ion concentration) (Marschner, 1993; D'Imperio *et al*., 2016), CO_2, temperature, organic matter content, microorganism activity, metal species present and aeration (Oviedo and Rodríguez, 2003; Welch and Graham, 2005). Species and variety of crop also determines mineral acquisition as the complex nature of the highly regulated homeostasis governing metal absorption, translocation within the plant, regulating transportation and redistribution (thus control over the prevention of toxic accumulation) may impede accumulation (Welch and Graham, 2005). Interactions between the mineral cations and

anions are rare but there is influence indirectly through membrane potential, protein electrical gradient or via feedback regulation through the rate of plant growth or metabolism (Marschner, 1993).

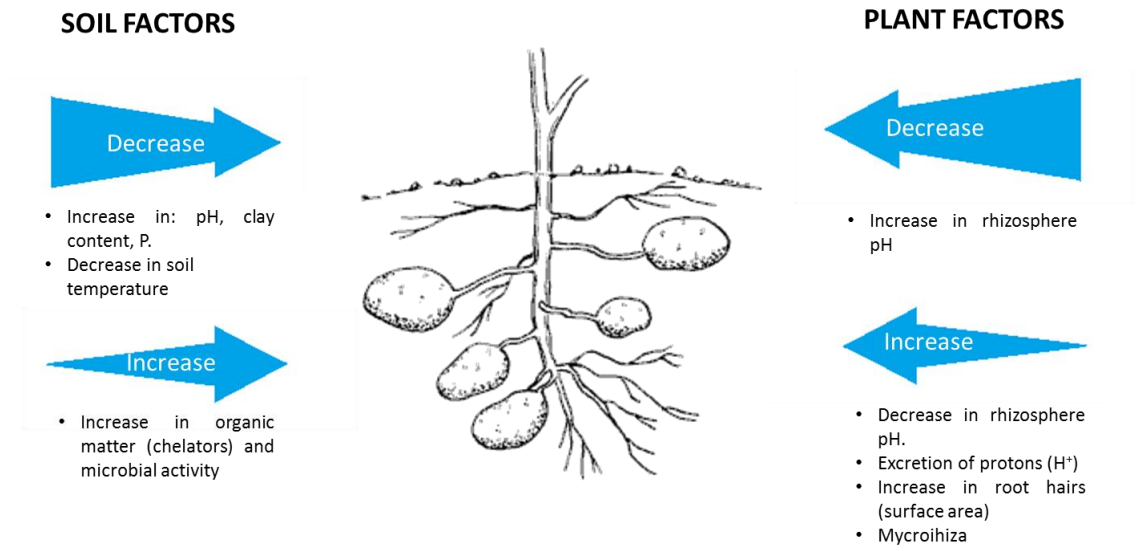

Figure 1.7: Summery of factors effecting uptake of minerals (Marschner, 1993; Hirischi, 2004; Welch and Graham, 2005).

Ca, as with many elements is abundant in the parent rocks of the soil, however a majority of Ca compounds are insoluble, reducing mobility in the soil and consequently to the root system of the plant (Fossard *et al*., 2000). Calcium ion, Ca^{2+} is a large divalent cation in contrast to Fe and Zn ions (Hirischi, 2004) and moves in conjunction with water when free, however, this a rare occurrence as it forms a tight bond with particulates so much that Ca leaching through the soils strata does not normally occur (White, 2001; Hirschi, 2004). Unlike other minerals such as Fe and Zn, Ca^{2+} passively diffuses into the root / tuber via a gradient caused by transpiration in the leaves (Hirischi, 2004; Kelling and Schilte, 2008; Palta, 2010). Calcium is less mobile in the plant and is retained in the root or tuber upon acquisition (Marschner, 1995; Kelling and Schilte, 2008). The xylem delivers Ca^{2+} to transpiring leaf tissues, where it is taken up from the apoplast by specific cell types (Hirschi, 2004). Translocation of Ca^{2+} to non-transpiring or xylem-deficient tissues, occurs via the phloem (Palta, 2010).

Iron is essential nutrient to photosynthetic organisms as it has numerous metabolic functions and functions as a co-factor in photosynthetic and electron transport chains (Carmel *et al*., 2014). There are two strategies for Fe uptake known as strategy I and strategy II. Both employ an up-regulation under Fe deficiency to increase Fe availability. Strategy I, used by dicotyledons and non-grass monocotyledons, yeast and most algae (Kelling and Schilte, 2008; Raven, 2013; Carmel *et al*., 2014), thus including the potato, tomatoes and chillies. The acidification by the release of organic acids and

phenolic compounds, increase the concentration of Fe^{3+} in the soil solution, further chelated to Fe^{2+} by ferric reductase, which is taken up by an iron transporter as seen in figure 1.8 (La Fontaine *et al*., 2002; Kim and Guerinot, 2007).

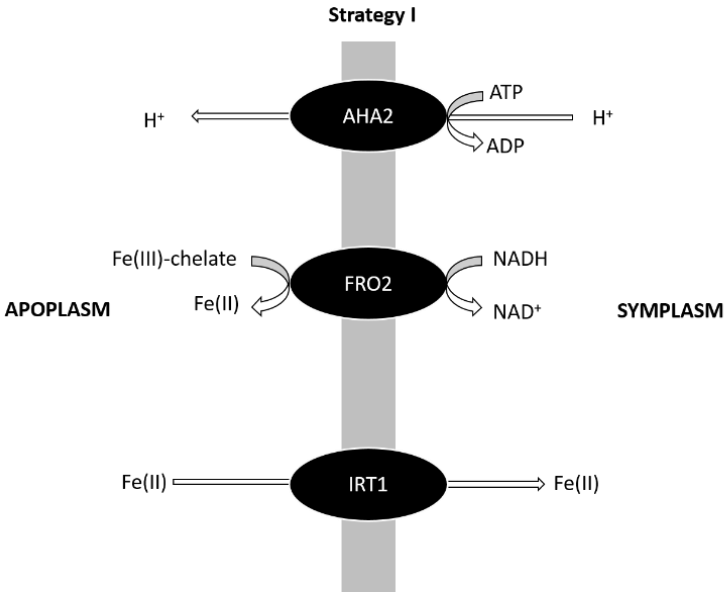

Figure 1.8: Strategy I uptake of iron as used by potato plants. Adapted from La Fontaine et al. (2002).

Strategy II including grasses, microalgae and cyanobacteria. Muginieic acid family of phytosiderophores bind Fe^{3+} in the rhizosphere which is recognised by the plant and thus taken up as well as Fe^{2+} (La Fontaine *et al*., 2002). Strategy II increases the efficiency of Fe uptake compared to strategy I, allowing grass species to grow in areas of Fe-deficiency (Hirschi, 2004).

Free Zn ions are bound in the soils matrix similarly to Fe (Salisbury and Ross, 1991) and thus highly dependent in the pH of the growth media. Normality the Zn content of non-polluted soils is approximately $3 \times 10^{-8} – 5 \times 10^{-7}$ M (Tegeder, 2012) with 15 – 30 % as free ions. Zinc acts similarly to Fe ions with release in the rhizosphere due to decrease of pH are a result of proton pump (Ghasemi *et al*., 2012), figure 1.9.

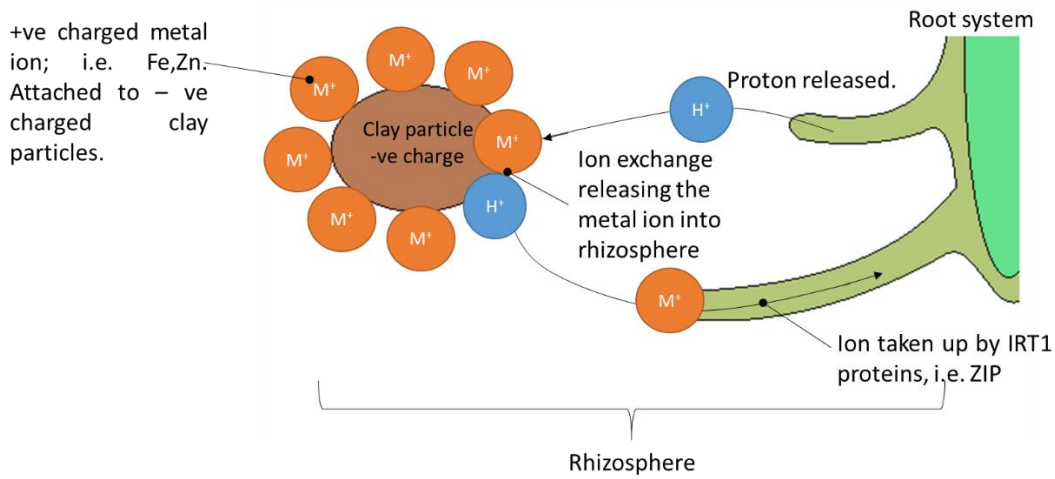

Figure 1.9: Simplified proton pump mechanism.

Zinc is taken up as Zn^{2+} or Zn-phytosidphore complexes across the plasma membranes of the root membranes from the rhizosphere (Grotz and Guerinot, 2006). It is commonly assumed to be transported across the root to the xylem (Colangelo and Guerinot, 2006; Broadley *et al*., 2007). As with Fe uptake, ZIP family of IRT1 (Iron-regulated transporter) (Guerinot, 2000).

1.4 Forms of fortification for propagation

The three main constituents in fertilisers are nitrogen, phosphorous and potassium (N, P and K). N promotes leaf growth, formation of proteins and chlorophyll. P promotes flower, fruit development and root growth. K is involved in the synthesis of proteins and contributes to health of the stem and root too (Corradini *et al*., 2010). Modern agricultural methods have been successful in meeting needs of the population with the focus on cereals as they are the primary consumed and produced globally (Bouis, 2000; Welch and Graham, 2002; Bouis, 2003; Hirschi, 2004; Welch and Graham, 2005). However, in recent year's fortification of micro and macro nutrients in order to improve human health has been brought to the forefront of research in the content of micronutrient malnutrition (MNM) (Mayer *et al*., 2008), also termed hidden hunger.

There are three main methods of fortification; enhanced fertilisers, conventional breeding and nutritional genetic modification (GM). Conventional breeding for desirable characteristics takes a number of seasons / years to produce a crop for commercial, along with expert knowledge and cost this method is not usually a feasible option but is used in developing countries. Genetic modification

has focused on genes to accelerate Fe acquisition. Initiatives such as HarvestPlus, (Hirschi, 2009; Bouis *et al*., 2011; DellaValle *et al*., 2013) and the Golden Rice Project (Ye *et al*., 2000; Painem *et al*. 2005) has seen success, however the negative image of GM in the developed world has prevented widespread use of GM crops in the developing world where such crops are needed (Ye *et al*., 2000; Painem *et al*. 2005; Hirschi, 2009; Bouis *et al*.,2011; DellaValle *et al*., 2013). Biofortification relies on the plant's capacity to produce or accumulate biosynthetic (vitamins) or physiological (minerals) nutrients (Mayer *et al*., 2008).

Manipulation to diversify the genetic spectrum enables the plant to increase Ca, Fe or Zn uptake, however if the deficient mineral is unavailable in the soil, no accelerated increase will occur (Bouis *et al*., 2011).

Fertilising arable land has taken place for thousands of years and it is the widest spread technique in fortification. Costs, reapplication and transportation have negative impacts on fertiliser use globally. Unfortunately, 40 – 70% of N, 80 – 90 % of P and 50- 70% of K content are lost to the environment therefore unavailable to the plant to utilise (Trenkel, 1997; Saigusa, 2000). Therefore, application of mineral fertilisers must ensure stability and retention in the soil for long term availability to maintain a sustainable supply of nutrients without the requirement for frequent application.

Calcium is the third-most important nutrient element available in soil and is an essential element for the plants (D'Imperio *et al*., 2016). From weathering of the soil parent material Ca is available in various sources including feldspar, apatite, limestone and gypsum (Frossard *et al*., 2000; D'Imperio *et al*., 2016). The concentration of Ca^{2+} in neutral and calcareous soils solution (between 0.1 and 20 x 10^{-3} M) deemed adequate for cultivation (Frossard *et al*., 2000), however these condition impede the uptake of Fe and Zn. It is well documented that high content of Ca in calcareous soil limits the reduction of Fe^{3+} and uptake of Fe^{2+} coursing the deficiency chlorosis (Kelling and Schilte, 2008). The high pH of calcareous soils reduces the solubility of iron oxides by reducing H^{+}. This also effects uptake of other minerals including Zn, K and Mg (Bouis *et al*., 2011).

Most Ca compounds are generally insoluble and thus making the Ca unavailable to plant therefore application of Ca compounds such as Ca carbonate, Ca phosphate, Ca sulfate, Ca gluconate, Ca chloride and others to increase phytoavailability (Pilbeam and Marley, 2006). Due to implications associated with the transport of this element to phloem-fed tissue, Ca fertiliser has limited success, (Karley and White, 2009; D'Imperio *et al*., 2016). Foliar Ca application in the form of lime (CaO, $CaCO_3$), gypsum ($CaSO_4$) calcium nitrate calcium phosphate is commonly applied in horticulture to fortify seeds and fruits (White, 2005; Bouis *et al*., 2011).

Iron is Fe is one of the most abundant elements in soil only small amounts are phytoavailable as Fe shows a low mobility in soil as $Fe^{2+}$is rapidly bound to soil particles and converted into Fe^{3+} becoming unavailable to the plant (Carvalho and Vasconcelos; 2013), resulting in a global nutritional disorder (Grusak and Dellapenna, 1999; Hirschi, 2004; Chatterjee *et al*., 2006; Kim and Guerinot, 2007; White and Broadley, 2009; Winkler, 2011). Iron uptake is in accordance to the plants requirements, maintaining a Fe concentration of 10^{-9} – 10^{-4} M to achieve optimal growth (Abadía *et al*., 2011).

Iron fertilisers can be grouped into three classes; inorganic Fe compounds (sulphates, oxides and hydroxides), synthetic Fe-chelates (ethylenediamine tetraacetic acid (EDTA), and natural form of Fe complexes (humate and amino acids) (Abadía *et al*., 2011). Commercial fertilisers utilise Fe in the forms of $FeSO_4.7H_2O$ and synthetic Fe-chelate such as Fe-EDTA (ethylenediamineteraacetic acid) HEDTA, 2-hydroxyethylenediaminetriacetic acid; DTPA, diethylenetriaminepentacctic acid; EDDSA, ethylenediaminediscuccinic acid and IDSA, iminodisuccinic acid (Schaider *et al*., 2006; Wagner and Baran, 2010; López-Rayo *et al*., 2015) that are applied either as a foliar or root solution to increase Fe availability. Salts are extremely soluble and easily leached through the soil (Lucena, 2006), therefore only used as a sort-term delivery. Chelates are also highly soluble, but are more retentive in the soil than Fe-salts, however, prove costly and unobtainable for farmers where Fe fortification is in demand (White and Broadley, 2009; Ghasemi *et al*., 2012).

Plants display Zn deficiencies in calcareous or alkaline soils, particularly in sandy soils, i.e. Turkey, China, Western Australia and in Central and Western Africa (Marschner, 1993; Alloway, 2004; White and Broadley, 2009; Abadía *et al*., 2011; Mousavi, 2011; Winkler, 2011). Concentration of Zn ranges from 10^{-8} to 10^{-6} M in non-polluted soils (Stein *et al*., 2005; White and Broadley, 2009). The concentration of Zn in the soil solution decreases from 10^{-4} to 10^{-10} M with an increase from pH 5 to pH 8 (Kiekens, 1995). Zn is applied as inorganic sources , ZnO, $ZnC0_3$, $ZnS0_4$, $Zn(N0_3)_2$ and $ZnCl_2$, with $ZnSO_4$ as the most commonly used (Alloway, 2004). Chelated forms of Zn are also applied, majority as ZnEDTA, Na_2Zn-ethylenediamine tetra-acetate, however, as reflected by Fe-chelates, cost implication favour the Zn salts (Hotz and Brown, 2004).

1.5 Use of metal oxide nanoparticles as a mineral supply

*Current agronomic strategies rely on mineral fertiliser application to increase the mineral content in edible tissues of the crop with increasing focus on the stabilisation and phytoavailability of the mineral (*White and Broadley, 2005[a]; White and Broadley 2005[b]; White and Broadley, 2009). The novel application of MONP+His as a form of fortification, hypothesises that the size of the NP can penetrate

through the cell wall pores (5 to 20 nm) (Fleischer *et al*., 1999; Navarro *et al*., 2008; Nair *et al*., 2010) allowing nanoparticles and nanoaggregates less than the pore size to pass passively into the plant without chelation (Navarro *et al*., 2008). The histidine coating of the nanoparticles, increases mobility through the strata due to the ability to suspend the nanoparticle and move with water. This allows passive diffusion into the tuber/root membrane through a concentration gradient. The amino acid coating provides a barrier, reducing the MONP to complexing with ligands in the compost that would otherwise decrease phytoavailability. The MONP+His. is a sustainable application of mineral fortification, due to the increase in retention capabilities in the soil strata over conventional metal salts and chelates, consequently decreasing the requirement for repeated applications and having a positive economic impact. The application of FeNP+His. allows the delivery of both Fe^{3+} and Fe^{2+} as a stoichiometric ratio of 2:1 (Fe^{3+}/Fe^{2+}) (Laurent *et al*., 2008) allowing a duel delivery of Fe that is phytoavailable immediately (Fe^{2+}) and a more stable Fe supply (Fe^{3+}) (White and Broadley, 2009) that will not be as readily complexed as Fe^{2+} but available to the plant when Fe^{3+} is reduced in the rhizosphere via a proton pump mechanism (Sánchez *et al*., 2005; White and Broadley, 2009).

An additional benefit of MONP+His application is the coating of amino acid, histidine. Sánchez, *et al.*, (2005) reported that the use of amino acids in nutrient solutions improves Fe uptake by crops. The presence of the amino acid increases the efficiency of nitrogen assimilation (Ghasemi *et al*., 2012), in turn increasing the metabolism of the plant and accumulation of other minerals present in the soil or fertiliser (Tegeder, 2012). Amino acids have highly diverse and essential roles in plants, by being the building blocks for enzymes and proteins, they provide important components for plant metabolism and structure (Fischer *et al*., 1998; Gupta and Gupta, 2004), therefore providing an additional benefit to the application of MONP+His.

1.6 Potato history and consumption

Since the introduction of the potato (*Solanum tuberosum*) to Europe in the mid-16th century (Lisinska and Leszczynsk, 1989), the vegetable has become a staple in the global diet, becoming the fourth largest crop cultivated with 318 million tonnes produced in 2014 (CIP, 2017). China produces 2.50 % of the global total (9.5 million tonnes in 2014) and is the long-standing highest producer. United Kingdom contributes 0.15% in 2014 with 591,100 tonnes over 1.9 million ha involved in production in 2014 (FAO, 2016), figure 1.10, with a global production exceeding 300 million metric tonnes produced from 155 countries, considered a staple food for more than a billion people (CIP, 2017).

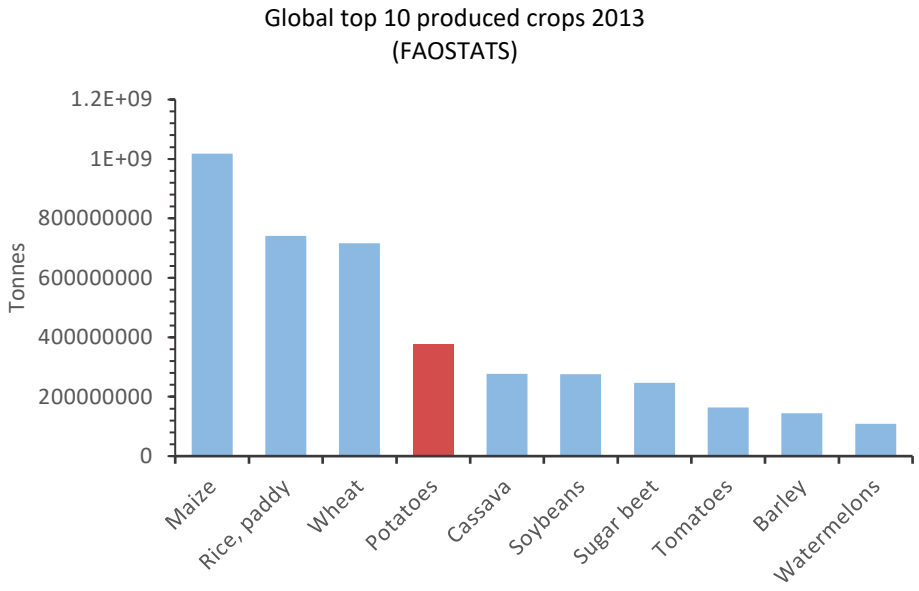

Figure 1.10: Highest produced global crops, data obtained from FAO-stat (FAO, 2016).

In the early 1990's Europe and Northern America were the primary growers and consumers. In recent times the increased global trend in potato production (figure 1.11) has seen a substantial increase from Asia, Africa and Latin America. In the 1960's Asia, Africa and Latin America produced 30 million tonnes, increasing to 165 million tonnes by 2014 (FAO, 2016).

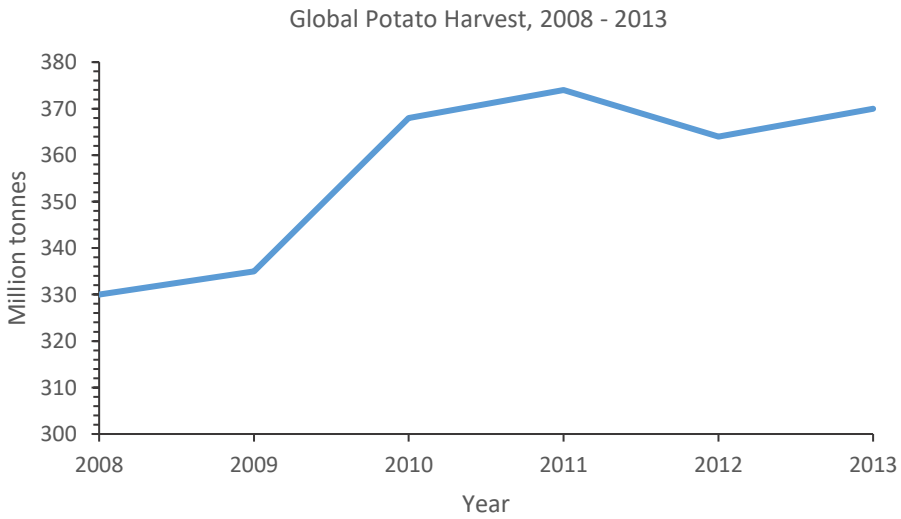

Figure 1.11: Taken from Potato Council 2015 Yearbook and Buyers Guide (FAO, 2016).

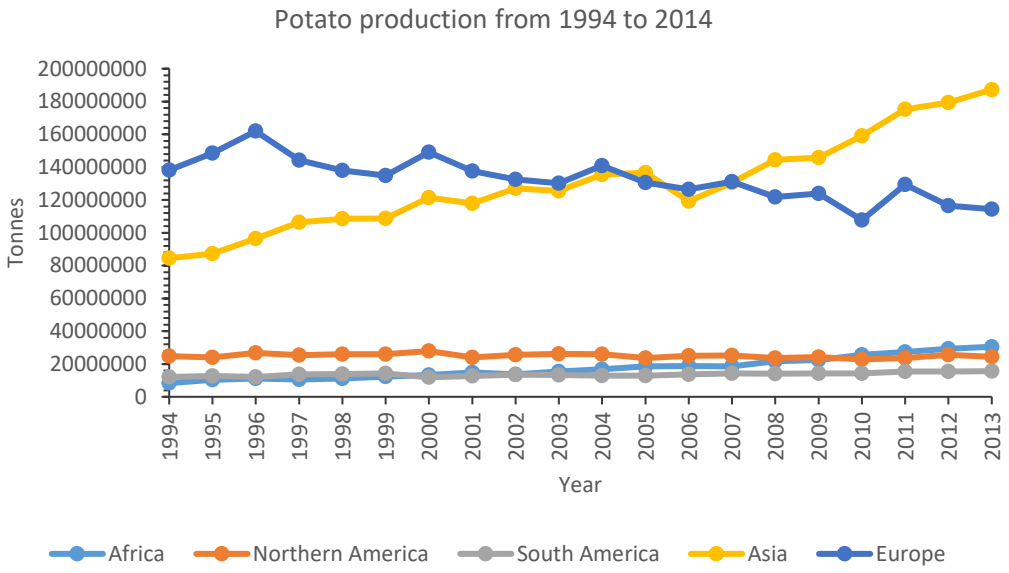

Figure 1.12:Data from FAO displaying the global potato production over a 14-year period (CIP, 2017).

In 2005, a landmark event in global potato production occurred as developing countries out produced the developed world (figure 1.12). In 2013, China produced the most potatoes with 89 million tonnes, equivalent to 24 % of the global production and twice as many as the next highest producer (Kolbe and Stephan-Beckmann, 1997; Potato council, 2015). The UK market yields 5.58 million tonnes of potato a year (table 1.2), with an increasing import into fresh potatoes, table 1.3 (Potato Council, 2015; FAO, 2016) showing a local and global importance of the potato.

Crop	Produced in United Kingdom 2013 (Tonnes)
Wheat	11921000
Sugar beet	8000000
Barley	7092000
Potatoes	5580000
Rapeseed	2128000
Oats	964000
Carrots and turnips	696200
Cabbages and other brassicas	271800
Cauliflowers and broccoli	155700
Peas, green	152570
Tomatoes	93600
Leeks, other alliaceous vegetables	35220
Rye	33000
Chillies and peppers, green	23500

Table 1.2 UK crop yield, 2013 (FAO, 2016).

	United Kingdom potato export and imports (Tonnes)			
	2009	2010	2011	2012
Fresh				
Import	281839	248841	267081	465206
Export	256180	336699	384622	287623
Frozen				
Import	501942	501022	524712	524222
Export	37084	26812	32290	39967

Table 1.3: UK import and export of fresh and frozen potatoes (FAO, 2016).

1.7 Propagation and mineral composition of potato.

The potato plant has a short life span ranging from 80 to 150 days from planting to maturity, with variation between varieties (Lisinska and Leszczynski, 1989; Kolbe and Stephan-Beckmann; 1997). Its developmental stages are often described in terms of tubulisation and tuber development (Gray and Hughes, 1978; Lisinska and Leszczynski, 1989), with life cycle of a potato tuber is characterised by initiation and growth followed by a period of dormancy and finally sprouting resulting in the next (vegetative) generation (Gray and Hughes, 1978; Kolbe and Stephan-Beckmann; 1997), figure 1.13.

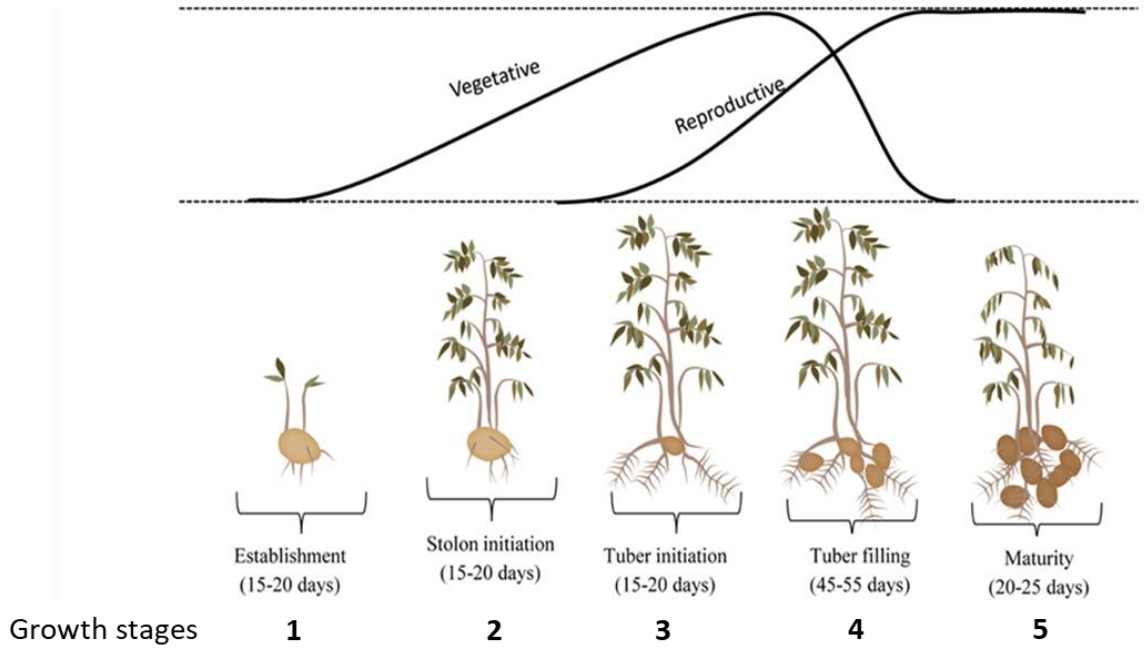

Figure 1.13: Generic growth cycle of potato. Adapted from Obidiegwu et al. (2015).

Stages 1 and 2 last from 30 to 70 days depending on planting date, soil temperature and other environmental f actors, the physiological age of the tubers (Lisinska and Leszczynski, 1989; Johnson, 2008), and the characteristics of particular cultivars.

Sprouting tuber Growth stage 1; the onset of sprout appearance at break of dormancy, also known as 'chitting' (Lisinska and Leszczynski, 1989). Possible application of MONP as a spray coating to promote sprouting. Also a 'drench' application can be applied at planting, whereby a highly concentrated solution of MONP is applied in the soil surrounding the seed potato. Vegetative Growth stage 2; The plant is established, seeing the formation of leaves, branches, roots and solons. Tuber initiation

Growth stage 3; approximately 30-60 days after the seed tuber is planted, tuber formation begins. Tubers are derived from lateral underground buds developing at the base of the main stem that when kept underground develop into stolon due to diagravitropical growth (Gray and Hughes, 1978; Lisinska and Leszczynski, 1989). When the conditions are favourable for tuber initiation, the elongation of the stolon stops, and cells located in the pith and the cortex of the apical region of the stolon first enlarge and then later divide longitudinally (Gray and Hughes, 1978; Lisinska and Leszczynski, 1989; Johnson, 2008). At this stage, fertiliser with increased N is applied. The FeNP+His. application at this stage would benefit chlorophyll production and growth with addition Fe and the assimilation of N from the presence of His. developing tuber Growth stage 4; during enlargement tubers become the largest sink of the potato plant storing massive amounts of carbohydrates (mainly starch) and also significant amounts of protein (Gray and Hughes, 1978; Johnson, 2008). Furthermore, tubers decrease their general metabolic activity and as such behave as typical storage sinks. MONP+His. would benefit the loading of potatoes and assist in the fortification of the tubers for human consumption and plant / crop development.

Mature tuber Growth stage 5; potato tubers are harvested from 90 to 160 days after planting and this may vary with cultivars, production area, and marketing conditions. Starch the typically represents 20% of the fresh weight of mature tuber. After potato vines die back the skin of tuber thickens and hardens, which provides greater protection to tubers during harvest and blocks entry of pathogens to the tuber (Gray and Hughes, 1978; Lisinska and Leszczynski, 1989). MONP+His application has the potential to regulate starch content, therefore produce a consistent starch content, an attribute that is of interest to the potato processing industry (Lulai and Orr, 1979). At dormancy, defined as 'absence of visual growth' (Lisinska and Leszczynski, 1989), cellular rates are supressed (Kolbe and Stephan-Beckmann; 1997), with tuber meristems are arrested (Obidiegwu *et al*., 2015).

Initially consumed for medicinal proposes by the aristocracy (Lisinska and Leszczynski, 1989), and recently implicated in contributing towards diabetes and obesity due to high glycaemic index, it seems to be forgotten the potatoes provision as a staple crop preventing malnutrition over the centuries in many countries (Camire *et al*., 2009). The tuber provides the consumer with highly digestible carbohydrate, nutritionally complete protein and excellent source of essential nutrients with the exception of Fe, Cr, and Cu, although specific cultivars may provide significant contributions to the intake of several elements (Lisinska and Leszczynski, 1989; White and Broadley, 2005[a], Suttle, 2008). In areas of the world the vitamin C content is an important constitute of the diet together with several B vitamins (folic acid, niacin, pyridoxine, riboflavin, and thiamine) plus pyridoxine (vitamin B6) (Camire *et al*., 2009). With all crops, the mineral content, yield, dry matter %, storage feasibility and disease

resistance are somewhat dependant on the genic features which can fluctuate within the same variety (Lisinska and Leszczynski, 1989). Mineral content can further depend on age of tuber at time of consumption, storage technique, environmental conditions, disease and soil composition without the influence of chemical's. It has been long associated the mineral content of crops are influenced by the soils mineral content, particularly those with close proximity such as the potato. Due to the potato's stability as a staple food, an increase in uptake of essential trace elements may be a desired when considering that half of the world's population is estimated to affected by microelement deficiencies (Zhoa and M^{C}Garth, 2009). Trace elements occur in low quantities in the environment, typically below 1 g/kg (Kabata-Pendias, 2010).

Initiatives calls have been made to promote the nutritional value and cooking methods of potatoes in order to increase in the fresh market sector. The year 2014 marked the tenth anniversary of the 'Grow Your Own' which has reached 2.1 million British school children (71 % primary schools). In 2015 the Potato Council lunched 'More than a bit on the side' campaign to highlight the diversity of the potato in the diet (Potato Council, 2015).

1.8 Other crops in the *Solanaceae* family

Other members of the deadly nightshade family *Solanum lysopersicum*, which potatoes are a member, includes chilli pepper and tomatoes. Tomato is popular worldwide fruit and the second most produced and consumed in the western countries (Willcox *et al*., 2003). The tomato fruit is a sink organ and provides an excellent source of many nutrients and antioxidants including vitamin C, lycopene and phenolic acids (Bressy *et al*., 2013; Verma *et al*., 2015). Chilli peppers are fruits of plants from the genus *Capsicum* of which are several domesticated species of chili peppers, among them *Capsicum annuum*, C. *frutescens* and *C. chinense*, which include many common varieties. These various peppers are widely used in many parts of the world and are particularly noted for their pungency, due to the unique presence of chemicals from the antioxidant capsaicinoid family of fatty acids (Arora *et al*., 2011, González-Zamora *et al*., 2013).

It was of interest in the application of MONP to observe the translocation and storage of minerals applied as MONP to fruit as well the effect to other constituents (i.e. capsacinoids). This would substantiate the MONP as a non-phytotoxic source that is potentially utilised by other varieties of crop such as brassicas and cereals as a method of sustainable fortification.

2 Nanoparticle synthesis and functionalisation

To allow nanoparticles to be utilised in a commercial application such as a fertiliser, the synthesis must be formulated to large-scale production, allowing control over the particle size.

The aims of the following synthesis:

- Bench top reactions converted to SDR.
- Consistent synthesis of narrow range nanoparticles.
- Synthesis to take place at ambient temperature under normal atmosphere
- Efficient precursor chemicals.
- Maximise yield by increasing the efficiency of the reaction.

To allow the suspension and uptake of the MONP by the plant, coating and compatibility tests carried out to improve availability and coating efficiency. Seed germination rate and percentage allowed to

2.1 Materials and methods

The following co-precipitation and sol gel synthesise were adapted for the SDR, patent WO 0013136082 A1 unless stated (Cave, 2017).

All chemicals supplied by Sigma-Aldrich unless stated otherwise. Ammonia, acids and solvents used in the following synthesis obtained from Fisher Scientific (laboratory, analytical or HPLC grade) without prior purification. Characterisation carried out by XRD (powder X-ray diffraction microscopy) and FT-IR with average particle size analysed via TEM. Metal content of coated MONP suspensions analysed via inductively coupled plasma optical emission spectrometry (ICP-OES), Perkin Elma ICP-OES Optima 2100 DV.

2.1.1 Calcium oxide nanoparticle synthesis via a sol gel method.

The following bench top synthesis was adapted from Safaei-Ghomi, (2013) for the SDR. A solution of calcium nitrate tetrahyrate, $Ca(NO_3)_2.4H_2O$ (1 M dm^{-1}, 118.07 g,) in ethylene glycol (500 mL) was consistently used in each reaction. A separate base solution of sodium hydroxide (3 M dm^{-1}, 60 g) in distilled water (500 mL) added to the SDR. These concentrations found to form a white precipitate instantaneously when tried on a 100 mL scale on the bench therefore ideal to transfer into the SDR.

The two precursor solutions fed into the SDR as a 1:1 ratio, 60 ml/s, via peristaltic pumps at room temperature. The disc rotational speed was a) 2000 rpm then b) 3000 rpm. The CaNP instantaneously formed for the both rotational speeds, however the 2000 rpm prevented free flow of the CaNP, coursing blockages and potential interference of particulate size through the prolong exposure to surplus precursor materials. The 3000 rpm disc speed allowed free flow of the CaNP through the reactor later collected and filtered using a grade 2 sintered glass funnel by vacuum filtration, washed with distilled water (3 x 200 mL) then with ethanol (2 x 200 mL) while the CaNP collected *in situ* in the funnel. The nanoparticles collected from the funnel, dried in a vacuum oven at 60^{o}C for 12 hours, followed by calcination of the NP at 500^{o}C for 5 hours.

It was found necessary to use ethylene glycol as the viscosity (1.113 g/mL at 25 °C) increased retention time between the two precursor solutions necessary for instant particle formation. The method using water-based precursor solutions, the particles failed to form even at low disc speeds (500 rpm) and increased solution concentrations.

The process of heating to a constant temperature for a period of 2 hours, calcination, removed remaining ethylene glycol remaining from washing. The formation of the CaNP as formulated in equation 1.

Equation 1: formation of CaO

$$Ca(NO_3)_2.4H_2O + 2NaOH \rightarrow Ca(OH)_2 + 2NaNO_3 + 4H_2O \quad \text{(Step1)}$$

$$\text{Heating at } 500^0C \rightarrow \ CaO + H_2O \quad \text{(Step 2)}$$

2.1.2 Synthesis of iron oxide nanoparticles (Fe_3O_4)

A precursor solution of Fe^{2+} and Fe^{3-} was prepared using $FeCl_2.4H_20_9$ (0.05 mol^{-1}, 9.94 g) dissolved in distilled water (1000 mL) with $FeCl_3.6H_2O$ (0.10 mol^{-1}, 27.03 g). Ammonia 8’80 (1000 mL) was used as the base precursor in the synthesis as adapted from previous reported reactions (Chatterjee *et al*., 2003; Laurent *et al*., 2008; Khalil, 2015). The two precursor solutions (at room temperature) added at equal volume via separate peristaltic pumps at a flow rate of 60 ml / s, combining at the surface of the spinning disc (rotating at 2000 rpm). The co-precipitation reaction formed a black precipitate upon the disc. The rotation and ridges on the disc allow the two precursor solutions to mix, with centrifugal force of the rotation dispels the crude FeNP onto the sides of the reactor where crude FeNP flows into a Duran bottle, 2.5L. The crude FeNP was formulated as in equation 2.

Equation 2: Formation of Fe_3O_4

$$Fe^{2+} + 2Fe^{3+} + 8OH^- \rightarrow Fe_3O_4 + 4H_2O \quad \text{(step 1)}$$

$$Fe_3O_4 + 2H + \rightarrow \gamma Fe_2O_3 + Fe^{2+} + H_2O \quad \text{(step 2; in the presence of oxygen forming } \gamma Fe_2O_3\text{)}$$

Once the precursor solutions have been processed through the SDR, the reactor was washed (2 x 250 mL) with distilled water to collect any residual crude FeNP, as it was found to accumulate around the reactors surface. The crude FeNP was initially decentred with the use of magnets (2 x 25mm dia x 20 mm thick, N52 neodymium with 24 kg pull) purchased from first4magnets.com, positioned at the base of the collection vessel. Using magnets exploits he superparamagnetic nature of FeNP (Laurent *et al*., 2008). The magnets pull the crude FeNP towards the base of the Durnan bottle, 2 L, enabling solution to be decanted. Some nanomaterials maybe lost due to mishandling, or lack of magnetic field, so caution must be taken to prevent loss of yield. Removal of the magnets from the base of the Duran enabled the resuspension of the nanomaterial. To remove excess precursor material, a further wash (3 x 500 mL) with distilled water, using the magnets to separate the nanomaterial from the washing each time. The FeNP was filtered using a 1 Litre sintered glass funnel, (grade 3), and finally washed with ethyl acetate (1 x 200 mL). The FeNP was dried for 6 hours under vacuum to air (at room temperature) before being transferred to an oven at 60^{o}C for 24 hours.

To suspend the FeNP in a solution for application, the FeNP were coated using amino acid histidine hydrochloride, 1:1, w/w (patent 20150027050) ground together to form an electrostatic bond with a pestle and mortar.

2.1.3 Synthesis of zinc oxide nanoparticles, water based: ZnNP method 1

Incorporating synthesis methods from Srivastava, *et al*., (2013), and Akbar and Anal (2014), a synthesis technique was optimised to incorporate the SDR.

Using an aqueous solution of zinc chloride ($ZnCl_2$) and base solutions (ammonia hydroxide, and sodium hydroxide), a number of variations in molarity of both precursor solutions, feed ratio and rpm of the disc were made to maximise instantaneous formation of zinc oxide nanoparticle output from the SDR (table 2.1).

	Zinc chloride molarity (mol^{-1})	*Base*	*Base molarity (mol^{-1})*	*Feed ratio Zn: base (mLs / s))*	*SDR speed (rpm)*	*Percentage yield (%)*
1	0.2	NaOH	0.5	60:30	500	No instant formation
2	0.2	NH_4	Conc	60:30	500	No instant formation
3	0.5	NaOH	0.5	60:30	500	No instant formation
4	1	NaOH	0.5	60:60	500	77.6
5	1	NaOH	0.5	60:60	1000	No instant formation

Table 2.4: Variation in synthesis conditions, using water as the solvent in the translation of ZnO synthesis to SDR.

After a number of alterations, a solution of sodium hydroxide (0.5 M, 40 g) in deionised water (2000 mL) added to a solution of zinc chloride (1 M, 272.63 g) in deionised water (2000 mL). The two colourless precursor solutions fed onto the spinning disc at a feed rate of 1:1, on the SDR at a 1:1 feed rate of 60 mL/s with a disc rotation of 1000 rpm, resulting in the formation of a white precipitate.

The nanoparticles were filtered under vacuum using 15 cm dia. grade 2 sintered glass funnel and washed with distilled water (4 x 250 mL) once with ethanol (200 mL), drying for 24 hours in a vacuum oven at 40°C. The nanoparticles were calcined at 200°C for 12 hours (Akbar and Anal (2014), to remove excess water to obtain ZnO as in equation 3.

Equation 3: Formation of ZnO

$$ZnCl_2 + NH_4OH \rightarrow Zn(OH)_2 + NH_4Cl \quad \text{(step 1)}$$

$$Zn(OH)_2 \rightarrow ZnO + H_2O \quad \text{(step 2)}$$

2.1.4 Synthesis of zinc oxide nanoparticles using methanol and acetone: ZnNP method 2

The ZnNP synthesis adapted further to remove the requirement for calcination and presence of NaCl. Removal of water as the precursor solvent to be replaced by methanol and acetone (technical grade) was adopted from Zak, *et al.* (2011), using $ZnCl_2$ (0.4 M, 27.26 g) dissolved in methanol (500 mL) as the metal precursor solution. In a separate solution, NaOH (0.8 M, 48 g) dissolved in acetone (1500 mL) as the base precursor solution. The two precursor solutions were fed into reactor 1:3 ratio ($ZnCl_2$: NaOH). A white precipitated was instantly formed when mixed on the spinning disc. The ZnO was filtered using vacuum filtration with a 15 cm dia. sintered glass funnel (grade 3) and washed acetone (3 x 200 mL). Dried in oven at 50^{o}C for 4 hours.

2.1.5 Synthesis of calcium ferrite nanoparticles

The synthesis of calcium ferrite ($CaFe_2O_4$) was carried out using a conventional Sol-gel method employing a polymetirc precursor solution as in the Pechini method (Pechini, 1967; Candeia *et al*., 2004). The process is based on metallic citrate polymerization using ethylene glycol (Livage *et al*., 1989; Khanna and Verma, 2013). Citric acid or another hydrocarboxylic acid, is used in an aqueous solution to act as a chelating agent to form complexes with the metal ions, in this instance iron and calcium, preventing a hydroxilated compound from being hydrolysed. Secondarily citric acid provides fuel for combustion in the Sol-gel auto-combustion process (Pechini, 1967; Livage *et al*., 1989; Candeia *et al*., 2004; Wu *et al*., 2006; Wu and Wang, 2011; Khanna and Verma, 2013) initiating oxidation-reduction which in turn provides energy to form the ferrite nanocrystallites (Wu and Wang, 2011; Khanna and Verma, 2013). The oxidising nature of the nitrate salts of calcium and iron contribute to the oxidation of the metals as well as providing cation sources (Hwang *et al*., 2004). The addition of a polyalcohol, such as ethylene glycol, leads to the formation of an organic ester. Heating promotes polymerisation and results in a homogeneous resin in which metal ions are uniformly distributed (Candeia *et al*., 2004). Residual citric acid that had not been used in the combustion stage can be removed by thermal treatment without effecting the properties of calcium ferrite. The process results in the formation of a spinel structure RO.R2O3, by association of a trivalent oxide (acid character) with a bivalent oxide (alkaline character) which usually leads to a high thermal stability Candeia *et al*., 2004). A conventional sol-gel method was used for the synthesis, using ethylene glycol as the basis of this process as used by Khanna and Verma, (2013) with modifications. Initially a 10 mL solution of calcium

nitrate (1 M, 23.62 g) was mixed with 10 mL solution of ferric nitrate (2 M, 80.80 g) in a 250 mL pyrex beaker. Citric acid (2 M, 38.42 g) 10 mL, was added to the solution along with 7 ml ethylene glycol. The solution with consciously stirred with a magnetic stirrer and heated between 90-100 ^{o}C to evaporate water and to form a gel. After ca. 30 mins heating, the gel becomes very viscous and increases in viscosity as the combustion continues. The auto-combustion stage is signified by the liberation of a brown gas (CO_2, H_2O, N_2) and the appearance of crystals of $CaFe_2O_4$, equation 4. At this stage, the temperature increased to 200^{o}C to compete the combustion. Once the gel has completely converted to a brown powder signalling the completion of the auto-ignition process. The brown powder was washed with ethanol (2 x 100 mL) via a glass-sintered funnel (grade 1) via vacuum. The powder was then dried overnight in an oven at 60^{o}C.

Equation 3: Formation of $CaFe_2O_4$

$$CaO + Fe_2O_3 \rightarrow CaFe_2O_4$$

2.2 Nanoparticle coating

Metal oxide nanoparticles do not suspend or dissolve in an aqueous solution. To enable MONP suspension a coating is required that is soluble in water but also creates an electrostatic attachment to the MONP in question, figure 2.1 (Cave and Mundell, 2014).

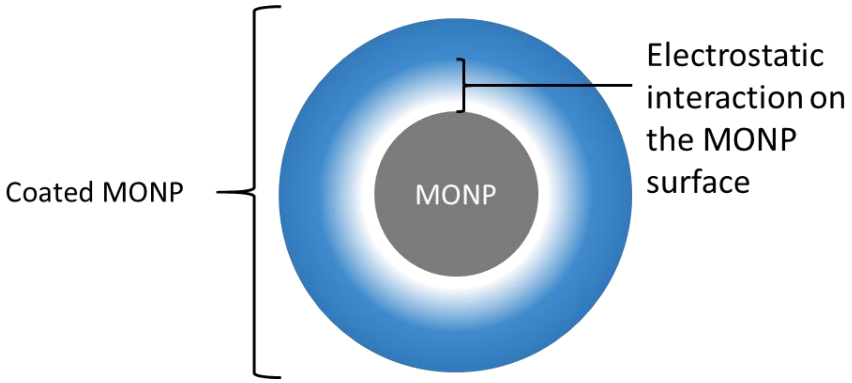

Figure 2.1: Coating of a MONP: Electrostatic charge is aided H^+ bond via the addition of HCl and the patented coating technique ensures the MONP is stable.

2.2.1 Hydrolysing amino acid

To ensure an electrostatic attraction between the amino acid and the MONP, the H^+ bond was increased by hydrolysation. Amino acid, 50g, was dissolved into 100 mL of hydrochloric acid, 4 M. The water was evaporated using a rota evaporator until a slurry was obtain, then using the continuous mode an off-white crystalline solid was obtained (42 g, 84% yield).

Starting weight = 50.00 g

End weight = 42.05g

Percentage Yield = (42.05/50)100 = 84.1 %

2.2.2 Coating MONP

The amino acid and MONP was ground using a pestle and mortar with a w/w ratio of 1:1, and ground for 10 minutes. For larger scale trials (CB2015, PFT2015 and PFT2016), the amino acid and MONP was ground using a KitchenAid KCG0702ER Burr Coffee Grinder, purchased from Amazon.co.uk (Cave and Mundell, 2014).

To ensure coating method was successful, MONP+His (0.001g) was suspended in to distilled water (10 mL). The suspension was filtered through a 20 µL syringe to remove excess MONP+His. Using a round bottom flask (50 mL) the suspension was evaporated (Buchi R-210 rotary evaporator) till the dry thus retrieving coated MONP+His. The powder was then analysed on the FT-IR to show the presence of the MONP and His.

To establish an effective coating, coatings applied to FeNP 1:1, w/w as described above. The following coating were tested: ascorbic acid, citric acid, ethylenediaminetetraacetic acid (EDTA), folic acid and hydrolysed amino acids histidine, leucine, lysine, threonine, phenylalanine and valine. The amount of FeNP suspended by the coating was determined by suspending 100 mg in to 10 mL of distilled water and sonicated at 40^{o}C for 15 mins. The solutions were then filtered with a 20 µl syringe filter then analysed via the ICP-OES.

2.2.3 Determining amino acid for FeNP application, AAFeNP

Using tomato seed, variety Gardeners Delight (purchase from Simply Seeds, Nottingham), a trail was conducted to establish an effective amino acid to allow suspension but one that would not affect the physiosology of the plant to allow the observation of the effect of the application the MONP.

The seeds were sown directly in Jiffy compost plugs in propagators, 400 x 250 x 180 mm (purchased from LBS Horticulture, Lancashire) and germinated at ambient temperature under greenhouse conditions (average 26 °C) with no additional heat or light. Eighteen seeds were sown per cohort; one seed per plug. The Jiffy plugs were hydrated in an amino acid (100 mg / L), solution (100 mL) and watered (10 mL of 100 mg / L) with the designated solution every two days. A record of shoot emergence (appearance of plumlar hook / hypocotyl above the surface) and height (soil and stem intercept to shoot tip, figure 2.2) taken once a week for a period of 14 days.

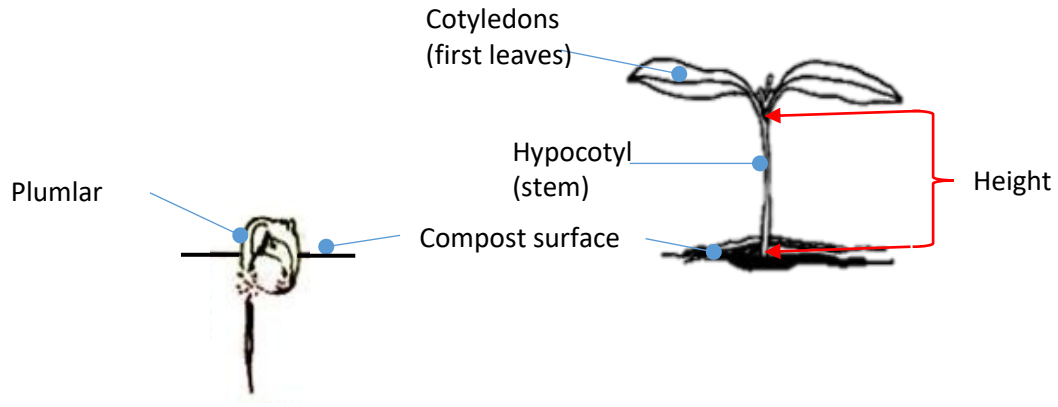

Figure 2.2. Measuring emergence and shoot height to ascertain amino acid suitable for the observation of the effect of MONP application.

2.3 Results of nanoparticle synthesis and functionalisation

2.3.1 Synthesis of calcium oxide nanoparticles

Calcium oxide (CaNP) nanoparticles average size was 3.62 – 20.18 nm with an average of 16.6 nm (n=20) (figure 2.3), showing some NP synthesised below the reported size of 30-40 nm by Safaei-Ghomi, *et al*., (2013) and the size Tang, (2008) reported, between 14 and 18 nm. Both methods used precursor solutions with similar concentrations and drip feed rates to that used when translating the synthesis to the SDR. The large size distribution considered the result of using ethylene glycol in the SDR system. The Ethylene glycol enables to extend the retention between the base and calcium nitrate solution that is beyond the remit of the SDR allowing CaO nanoparticle formation. However, this synthesis technique allows some uncontrolled Ostwald ripening to occur in the reaction vessel, resulting in the wide range of particle size. Further adaptation of the synthesis method to reduce the retention will enable a narrow nanoparticle range to be obtained.

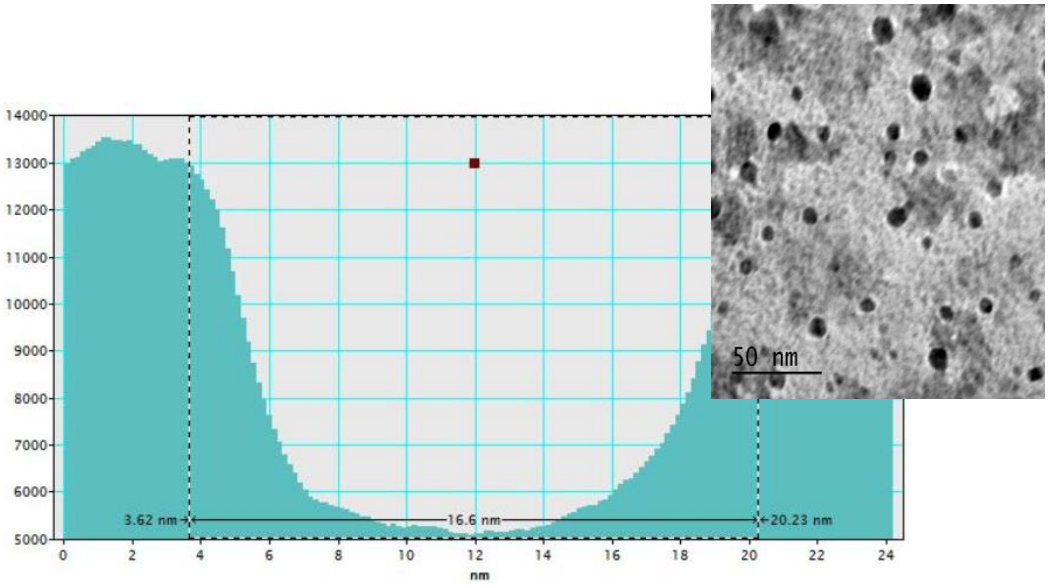

Figure 2.16 Average dimensions of CaO nanoparticles (n=25). Inserted is the TEM of CaO, depicting the nanoparticles spherical shape.

Theoretical yield at step 1 = 37.046g per 500 mL, giving 0.5 mol^{-1}

Percentage yield at step 1 (none calcined): a = 81.01 %*, b = 91.43 %

Theoretical yield after Step 2 (calcinated) = 28.085g

Percentage yield at step 2: a = 78.89 %**, b = 81.97 % **

** loss of product due to smaller particles lost during washing and retention in sintered filter and retention of CaNP in reactor due to viscosity of product.*

*** Some yield loss due to fine particulates in the atmosphere*

FT-IR of step 1 confirmed $Ca(OH)_2$ peaks: 871.737 cm^{-1}, 1037.749 cm^{-1}, 1082.617 cm^{-1}, 1209.383 cm^{-1}, 1341.588 cm^{-1}, 1407.702 cm^{-1}, 1595.917 cm^{-1}, 2123.767 cm^{-1}, 2217.617 cm^{-1}, 2711.311 cm^{-1}, 2874.943 cm^{-1}, 3307.073 cm^{-1}, 3340.2 cm^{-1}, 3642.648 cm^{-1}.

FT-IR of step 1. CaO (calcinated CaNP) peaks; 703.532 cm^{-1}, 873.779 cm^{-1}, 950.673 cm^{-1}, 1407.206 cm^{-1}, 1776.076 cm^{-1}, 2180.493 cm^{-1}, 2511.294 cm^{-1}.

From the FT-IR obtained (figure 2.4a), the uncalcined CaNP are characteristic of calcium hydroxide nanoparticles (Lui *et al*., 2010; Mirghiasi *et al*., 2014) with a sharp peak at 3642 cm^{-1} of O-H stretching in the $Ca(OH)_2$ crystals (Liu *et al*., 2010). The board peak around 3340-3307 cm^{-1} indicates the presence of physisorbed (Darroudi *et al*., 2016) OH which is reduced when calcined (figure 2.5). The absorption peaks in figure 2.4 a 1407.702 and 871.737 cm^{-1} indicates the C–O bond related to carbonation of CaO published by Darroudi *et al*., (2016) (1421 – 1433 and 877 cm-1, figure 2.4 b) and Lui *et al.*, (2010),1460 and 874 cm−1.

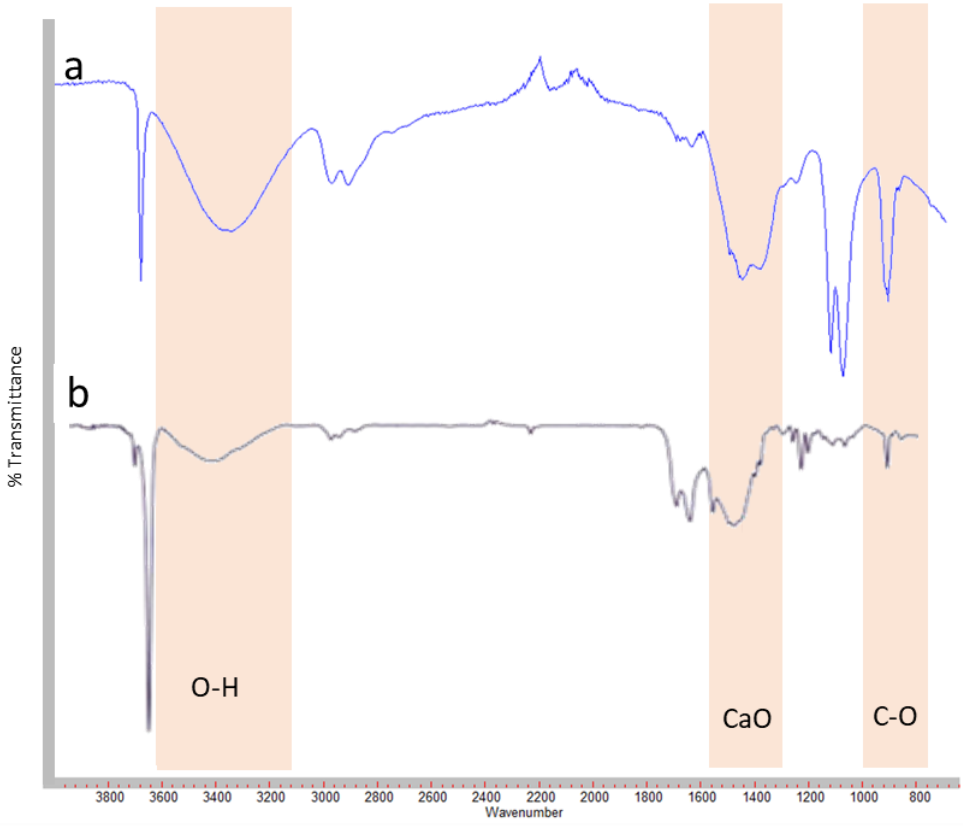

Figure 2.4 Comparison of FT-IR *of none calcined calcium oxide nanoparticles; a) CaNP synthesised from SDR, b) published by Darroudi et al., 2016.*

When calcined, the presence of H_2O in the form of OH bond decreases (peak 3340 cm^{-1} figures 2.5a and 2.5b, to form CaO as in the following equation:

$$Ca(OH)_2 \xrightarrow{\text{CALCINATION}} CaO + H_2O$$

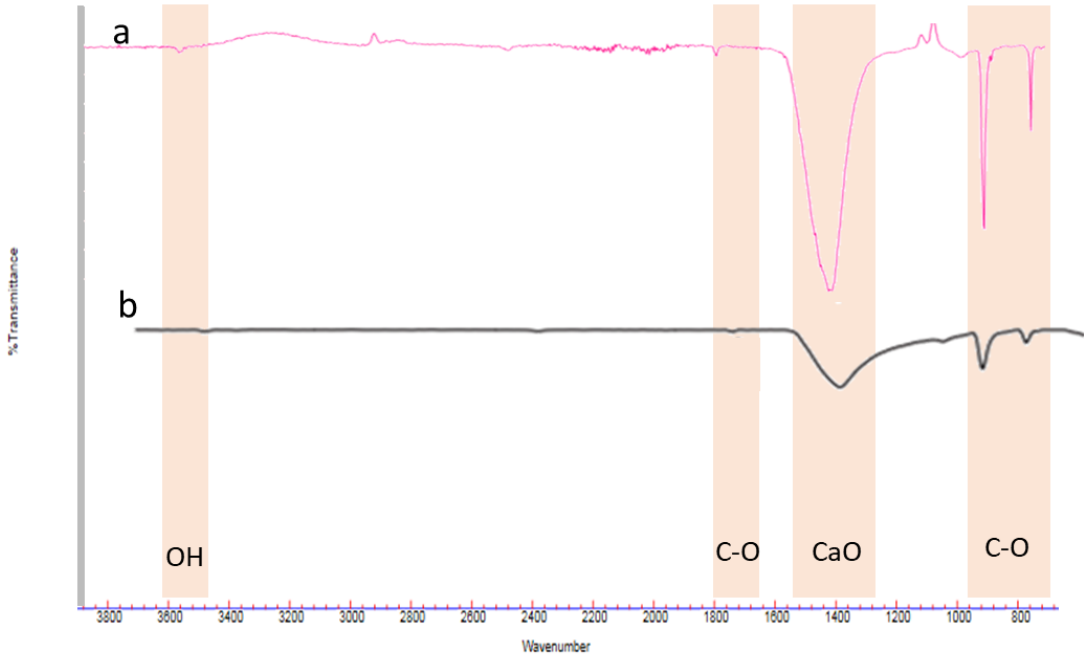

Figure 2.5 Comparison of calcined CaO NP; a) CaO synthesised via SDR and calcined at 500°C; b) reproduced from FT-IR published by Patel et al, 2009. C-O = bonds of calcite highlighted matching those published with OH bond showing a depreciation of water when heated, figure 2.4.

The transformation of uncalcined CaO ($Ca(OH)_2$) to CaO, was supported by XRD data. XRD of $Ca(OH)_2$, 2theta potential lines (figure 2.6); 18.1 °2Θ, 28.9 °2Θ, 34.0 °2Θ, 47.2 °2Θ, 50.8 °2Θ, 62.6 °2Θ, 64.3 °2Θ, 84.7 °2Θ. Upon calcination XRD of CaO, 2theta potential lines (figure 2.7a and 2.7b); 23.0 °2Θ, 29.5 °2Θ, 32.1 °2Θ, 37.3 °2Θ, 39. °2Θ 5, 43.2 °2Θ, 47.5, °2Θ 48.5 °2Θ 53.9 °2Θ, 57.5 °2Θ, 61, 63.3 °2Θ, 64.6 °2Θ, 67.4 °2Θ, 70.3 °2Θ, 74 °2Θ, 77.2 °2Θ, 79.6 °2Θ, 81.5 °2Θ.

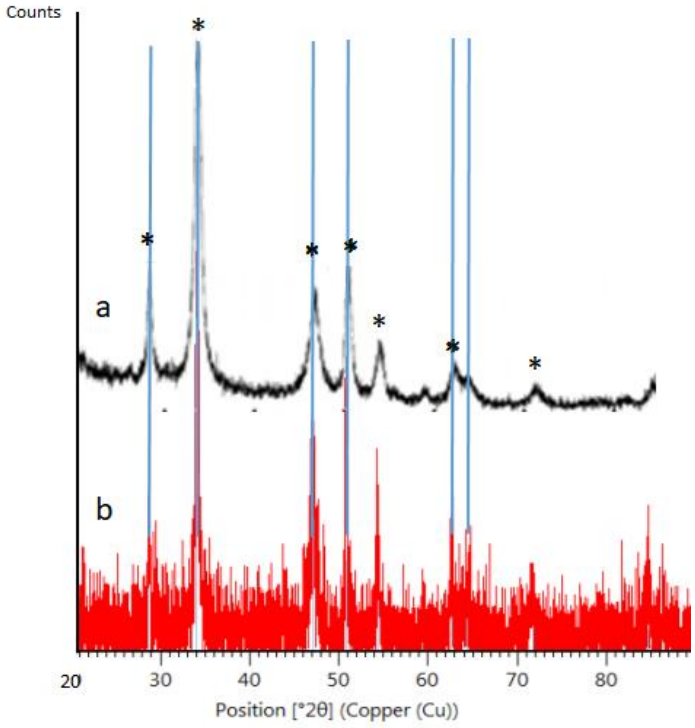

*Figure 2.6: XRD of none calcined CaO (Ca(OH)2). Published XRD of Ca(OH)2, a) (Mirghiasi et al., 2014) overlaid with particles synthesised from SDR, b). * represents the corresponding peaks between the two spectra, confirming Ca(OH)2.. Blue lines indicate Ca(OH)2 peaks obtained via High Score software (Malvern Panalytical) data library.*

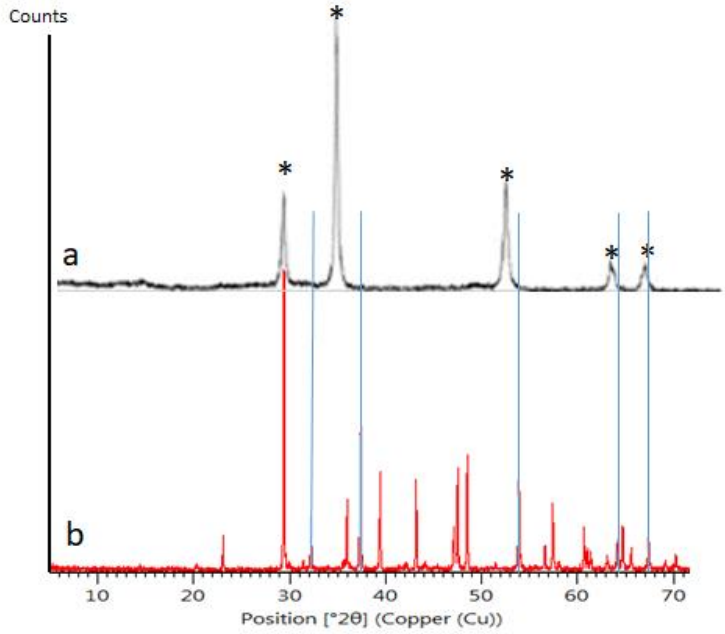

*Figure 2.7 XRD of calcined CaNP. XRD of calcium oxide nanoparticles publish by Ramos et al., 2015, a); overlaying calcined CaNP synthesised by SDR, b). * represents corresponding peaks between the two spectra. Blue lines indicate CaO peaks obtained via High Score software (Malvern Panalytical) data library.*

Figure 2.6 shows the reference peaks $Ca(OH)_2$ (High Score Plus ref: 01-084-1263), with a 66% certainty respectively. After calcination the CaO nanoparticles XRD, there is an absence of peak 18.190°, identified in the standard $Ca(OH)_2$ as a 59% certainty of CaO present in the calcined CaNP, with no matches of that peak in $CaCO_3$ and $Ca(OH)_2$ (figure 2.7a and 2.7b). Published XRD of $Ca(OH)_2$ and CaO nanoparticles are shown in figure 4.5 and 4.7. The published XRD of $Ca(OH)_2$ by Mirghiasi *et al*., (2014) confirms the uncalcined CaO is more likely to be $Ca(OH)_2$ as the presence of the peaks at 18.190° and 50°. Figure 2.7b presents cubic CaO XRD as published by Ramo *et al*., (2015) were as the calcined CaO nanoparticles synthesised by the SDR, figure 2.7a, are spherical as determined by the SEM (figure 2.3). The absence of strong peaks above 70° are noted in the SDR CaNP and the published CaO (Tang *et al*., 2008; Safaei-Ghomi *et al*., 2013; Ramos *et al*., 2015).

2.3.2 Synthesis of iron oxide nanoparticles (Fe3O4)

Adapted co-precipitation synthesis of iron oxide nanoparticles (Chatterjee *et al*., 2003; Laurent *et al*., 2008; Khalil, 2015) via the SDR, produced a NP ranging from 3 to 7.6 nm with an average of 4.732 nm (n- 20) (figure 2.8) as confirmed by TEM.

Theoretical yield = 11.58 g

Percentage yield =86%

In comparison to the commercially available Fe_3O_4, figure 2.9 (Chatterjee *et al*., 2003), the range is decreased and smaller when synthesised on the SDR.

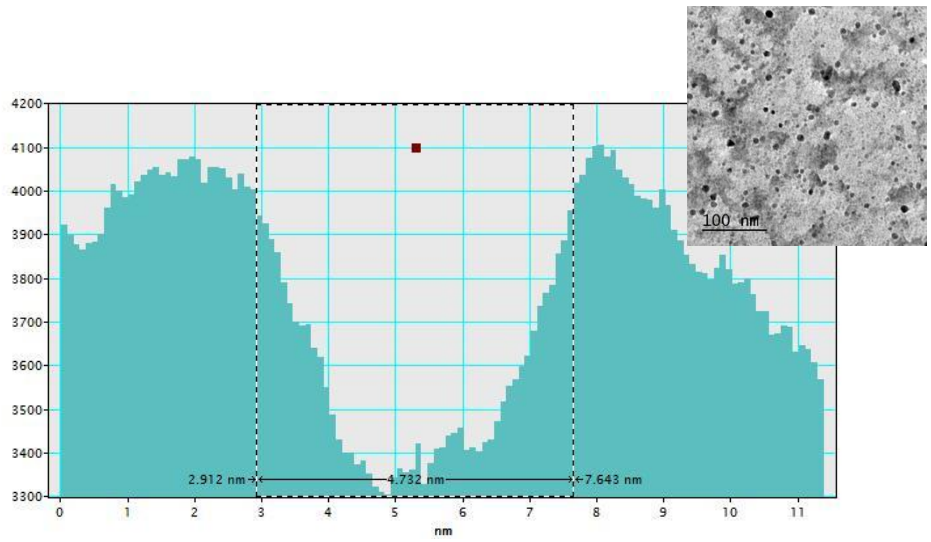

Figure 2.8 FeNP synthesised via SDR (left) and size range (right) produced by SDR (TEM).

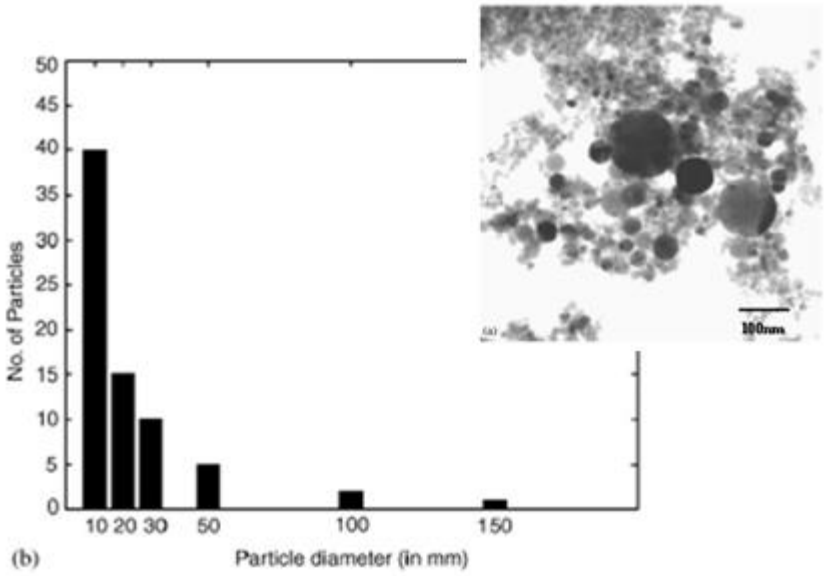

Figure 2.9 Reproduced from Chatterjee, J. et al., 2003; the TEM and size distribution of commercial (supplier undisclosed) Fe_3O_4.

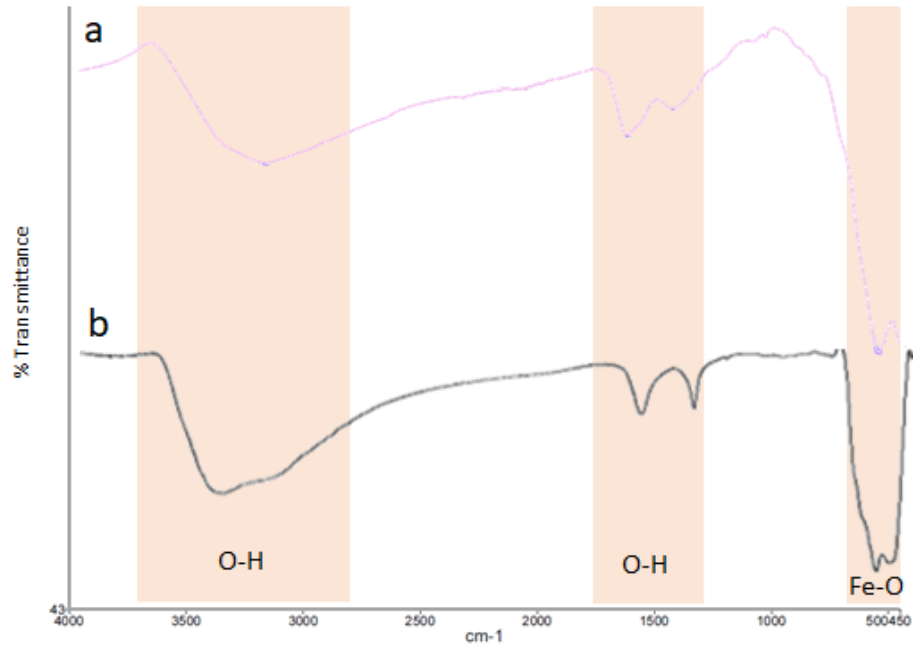

*Figure 2.*10 FT-IR spectra of FeNP synthesised *via SDR, a. Published* FT-IR *of Fe_3O_4 from Khalil,2015*

The FT-IR spectrum for uncoated $Fe_3O_{4,\ FT}$-IR peaks of FeNP: 531.94 cm^{-1},1419.92 cm^{-1}, 1618.31 cm^{-1}, 3180.06 cm^{-1}, coordinates with that of published FTRI as seen figure 2.10 (Khalil, 2015) displaying a stretching vibration at 3180 and cm^{-1}, which incorporates the contributions from both symmetrical and asymmetrical modes of the O–H bonds, which are attached to the surface iron atoms (Luo *et al.*,

2007). The bands at low wave numbers (≤ 700 cm^{-1}) come from vibrations of Fe–O bonds of iron oxide, in which for the bulk Fe_3O_4 samples appear at 570 and 375 cm^{-1} (Kassaee *et al*., 2011). The presence of an adsorbed water layer is confirmed by a stretch for the vibrational mode of water found at 1620 cm^{-1}.

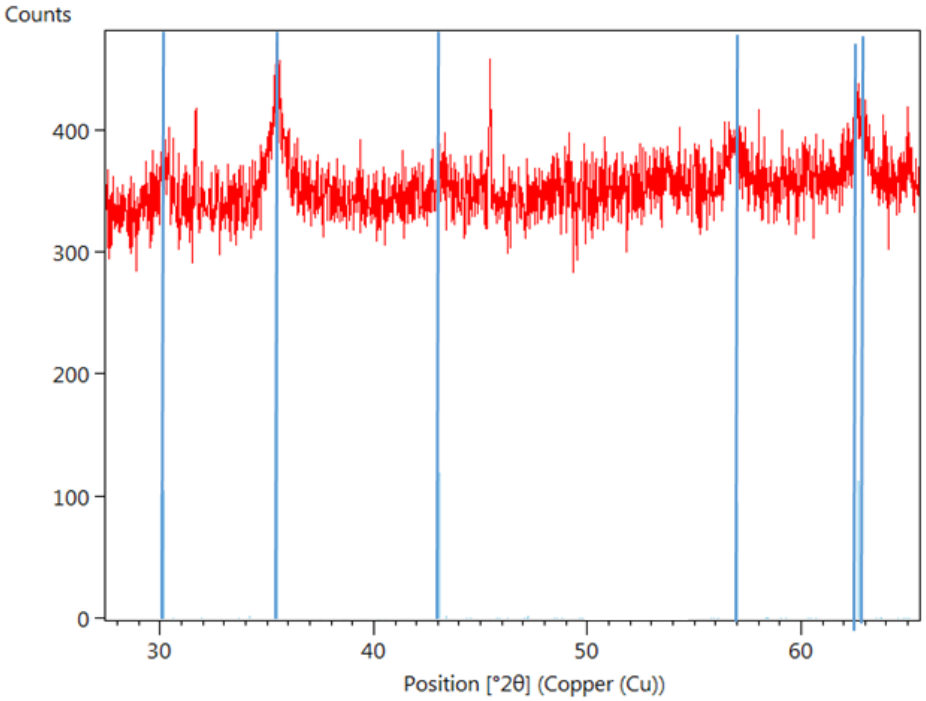

Figure 2.11 XRD of FeNP. Blue lines indicate peaks of Fe_3O_4 obtained by software, High Score, library data.

The FeNP synthesised by the SDR was further confirmed to be Fe_3O_4 via the XRD, figure 2.11, as prominent peaks are in conjunction with library data obtained from the High Score software.

2.3.3 Synthesis of zinc oxide nanoparticles

The zinc oxide nanoparticles synthesised using water as a solvent for the precursor solutions as described in section 2.1.3, (Srivastave *et al*., 2013; Akbar and Anal, 2014) produced particle averaging 8.39 nm with a range of 7.03 to 15.41 nm displaying a hexagonal wurtzite structure (figure 2.12) further confirmed by XRD in figure 4.15

Theoretical yield of $Zn(OH)_2$ = 99.423 g

Percentage yield = 78.050 %

Theoretical yield of ZnO = 82.4117g

Percentage yield of ZnO = 78.51 %

FT-IR peaks ZnO: 717.855 cm^{-1}, 902.892 cm^{-1}, 1041.579 cm^{-1}, 1141.810 cm^{-1}, 1246.666 cm^{-1}, 1342.355 cm^{-1}, 1412.040 cm^{-1}, 1448.817 cm^{-1}, 1586.035 cm^{-1}, 1627.660 cm^{-1}, 3484.952 cm^{-1}

ZnO nanoparticles synthesised with solvents methanol and acetone (Zak *et al*., 2011) achieved a narrower range of 2.277 to 6.376 n with an average of 4.099nm (n = 20) which also displayed a hexagonal wurtzite structure (figure 2.13).

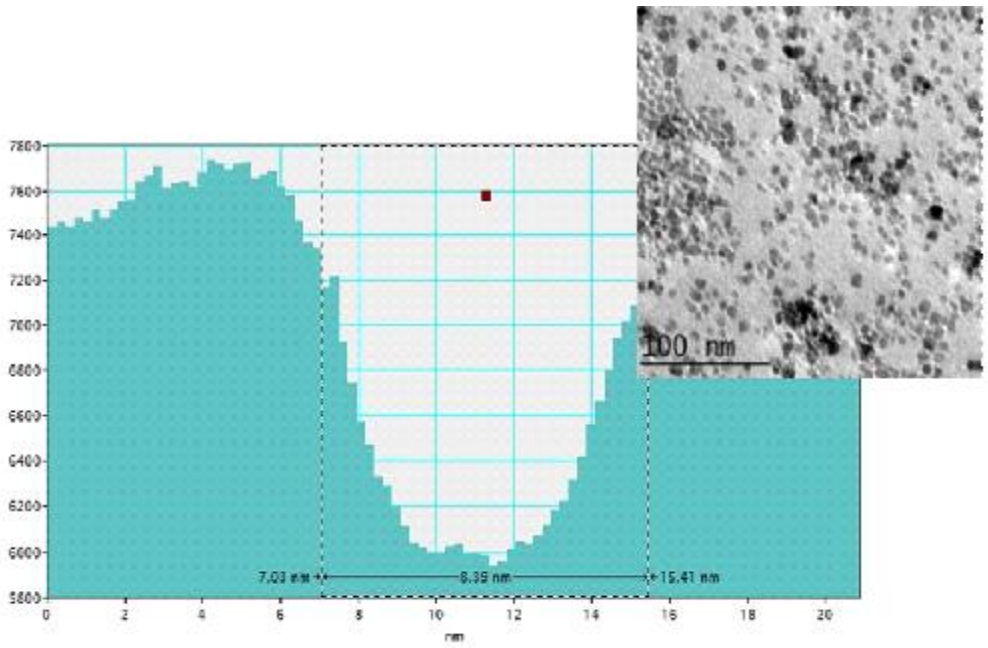

Figure 2.12 Nanoparticle size range and TEM (insert) of zinc nanoparticles synthesised via SDR with techniques adapted from Srivastava et al., (2013) and Akbar and Anal (2014).

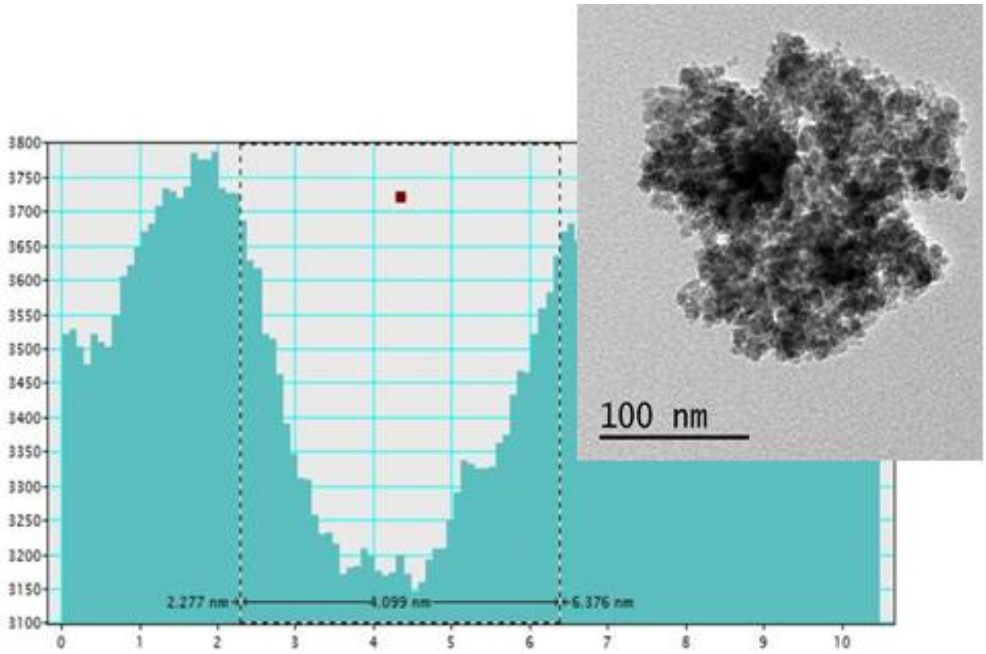

Figure 2.13 Size range of ZnO nanoparticles synthesised from method adapted from Zak, et al. (2011) [15] with insert of TEM.

The FT-IR spectra of the samples measured in the range of 4000–400 cm−1 are presented in figure 2.14. The as-prepared ZnO shows IR peaks at 457 cm−1, 1063 cm−1, 1390 cm−1, 1602 cm−1 and 3423 cm−1. The sharp peak positioned at 457 cm−1 is attributed to the Zn–O stretching bonds. The IR bands shown are in the region of 1700–600 cm−1 and correspond to C=O, C–O and C–H vibrations respectively (Vazquez-Arenas *et al*., 2012). Remaining peaks are due to the O–H stretching vibrations and bending modes of the adsorbed water. With the increase of temperature, the intensity of peaks centred at 1063 cm−1, 1390 cm−1 and 1602 cm−1 are deteriorated and at 500 ℃ these peaks are almost disappeared. It indicates that organic species are completely removed at 500 ℃ (Long *et al*., 2009; Babu *et al*., 2013).

.

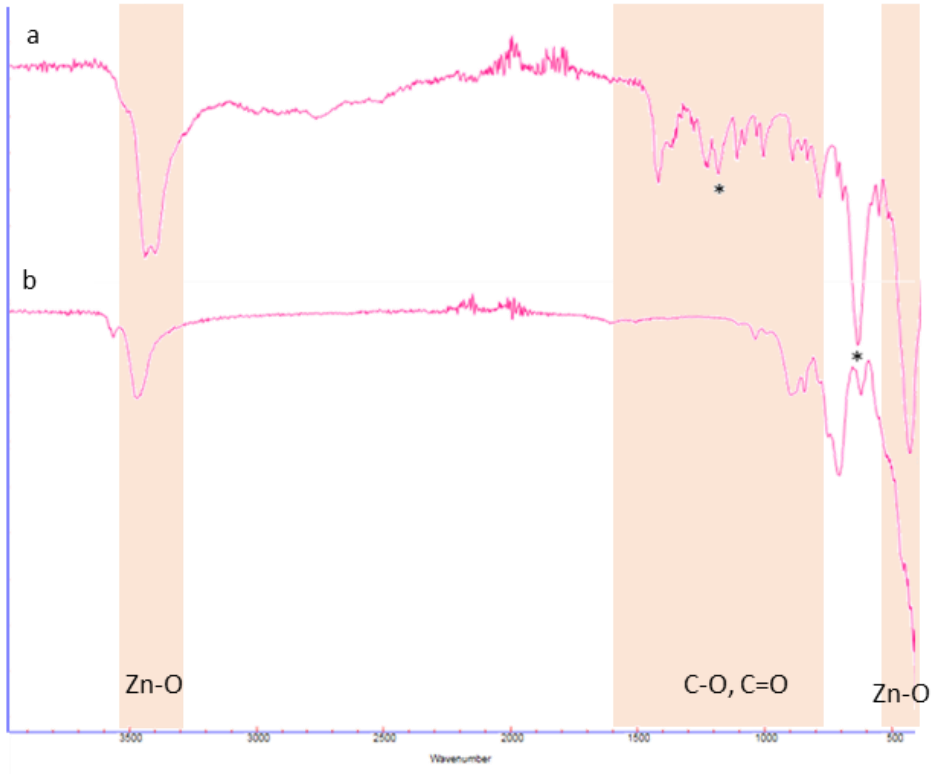

Figure 2.14 FT-IR *of a) ZnO nanoparticles synthesised with water as the precursor solvent, b) ZnO nanoparticles synthesised with methanol and acetone as the precursor solvent. * indicates peaks matching zinc hydroxychloride (Rao and Roa, 2015)*

The FT-IR also confirm the removal of the hydroxychloride and the completion of the reaction when using the modified method of ZnO synthesis using methanol and acetone as the solvent for NaOH and $ZNCl_2$ precursor solution.

The XRD of ZnO nanoparticles synthesised in H_2O display a number of peaks below 20° which were initially through to be NaCl. Comparing the XRD with reference XRD provided by High Score Plus software, the XRD of NaCl, ref: 01-071-3741 (figure) does not match the peaks below 20° XRD. In an attempt to remove the material, the number of washes were increase two fold together with calcination at 160°C for 4 hours (figure 2.15). The modification failed to move the peaks. Upon investigation, the synthesis using H_2O as precursor solvent did not complete the reaction with the $ZnCl_2$ due too insufficient NaOH, thus forming zinc hydroxychloride in the presence of excess H_2O formed as follows:

$4ZnO + ZnCl_2 + 5H_2O \longrightarrow Zn_5(OH)_8Cl_2.H_2O$

The solvent the precursor materials modified to acetone and methanol (Zak *et al*., 2011) with a 1:2 molecular ratio of $ZnCl_2$ to NaOH as in the previous method.

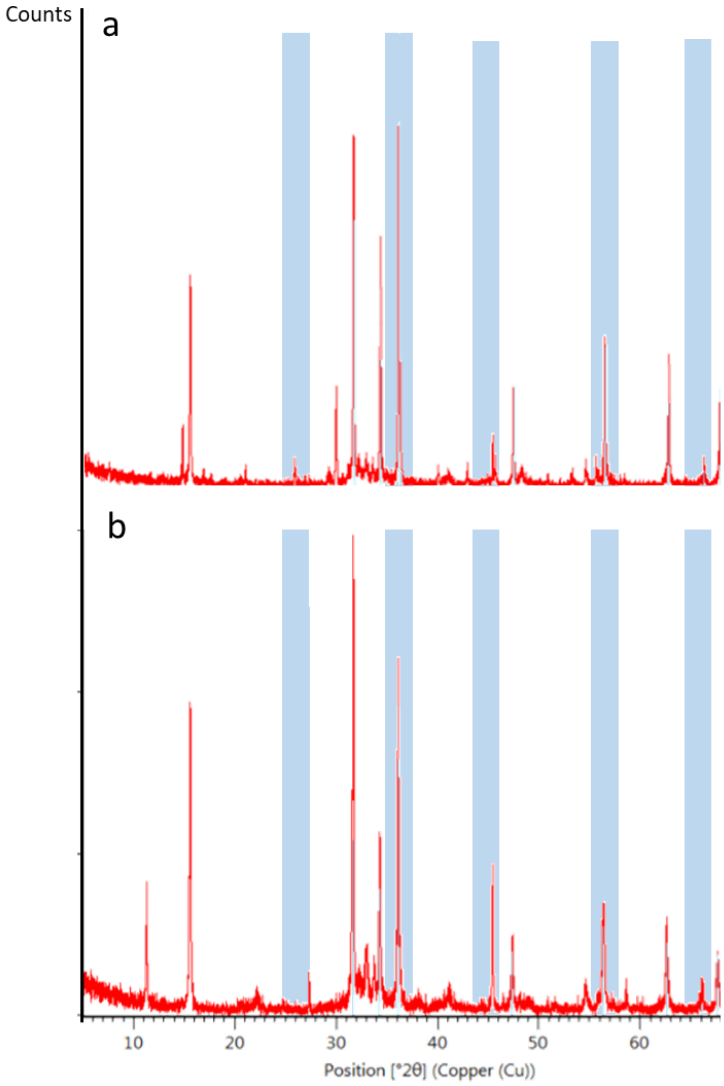

Figure 2.15 Two XRDs of ZnO synthesised from method adapted from Srivastava et al. (2013) and Akbar and Anal (2013); a) with four distilled water washes, and b) with eight distilled water washes and heated to 160°C for 4 hours in an unsuccessful attempt remove NaCl. Blue lines high light reference XRD of NaCl obtained from High Score software showing no peaks below 20°.

As observed in the XRD of the ZnO nanoparticles synthesised by the modified method, (figure 2.16) the peaks below 20° are removed and gave a comparable XRD to those published by Vazquez-Arenas *et al.* (2012), Rao and Rao (2015), Vanaja *et al.* (2016) and, displaying the distinctive ZnO peaks at 31.51, 34.658, 36.453, 47.74, 56.78, 62.99, 66.38, 68.06, 69.16 and 79.96. The XRD's suggest a completion of the co-precipitation reaction to form purer ZnO nanoparticle that will not require a calcination when the presence of water is kept to a minimum.

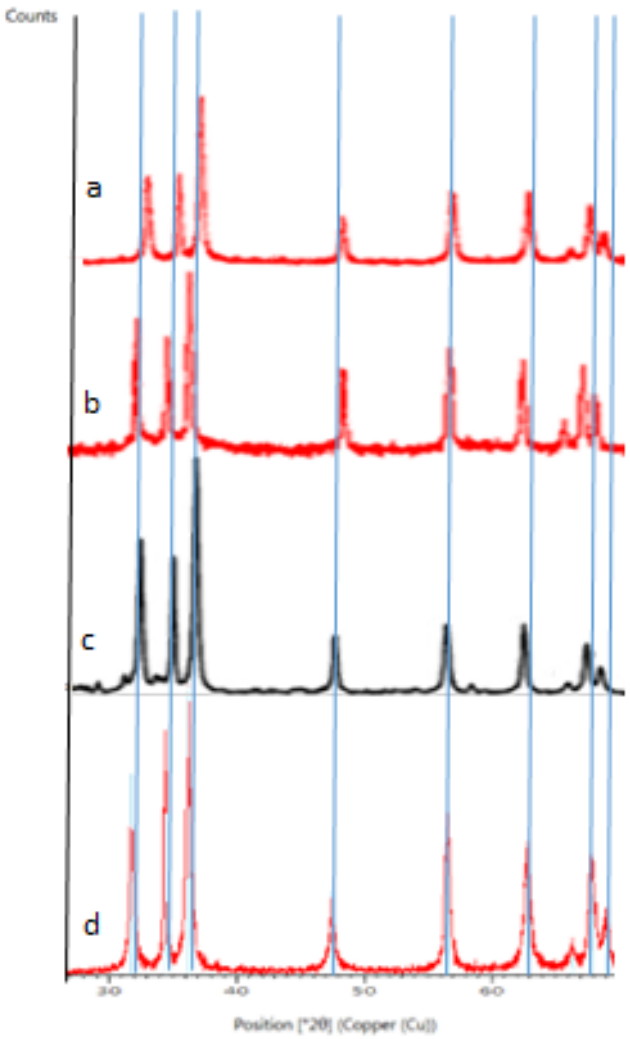

Figure 2.16 Published XRD of ZnO confirming the modified SDR synthesis produced ZnO a) Vanaja et al. (2016), b) Vazquez-Arenas et al. (2012), c) Rao and Rao (2015), d) Modification of the ZnO synthesis. The crude nanoparticles, washed three times in acetone with no calcination. Blue lines high light reference XRD of ZnO obtained from High Score software.

2.3.4 Synthesis of calcium ferrite nanoparticles

Calcium ferrite nanoparticles synthesised as reported by Khanna and Verma (2013). The results from TEM, figure 2.17, show a large range of nanoparticles (11.83 – 25.3 nm, average 13.47 nm, n = 20). Co-precipitation methods that do not use the SDR, result in a broad range of nanoparticle produced. Results from the ICP showed a ratio of 1:2, Fe to Ca respectively. An EDX of the CaFeNP only recorded the Fe content (figure 2.18), concluding the Ca is encapsulated by Fe (Pirouz *et al.*, 2015). Cu, Co and B are part of the instrument's element.

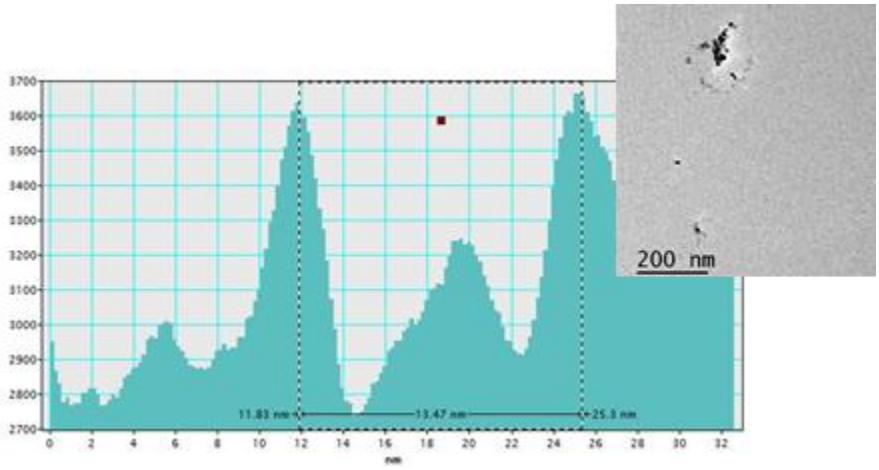

Figure 2.17 Calcium ferrite nanoparticles (TEM) produced by sol-gel and thermal decomposition method.

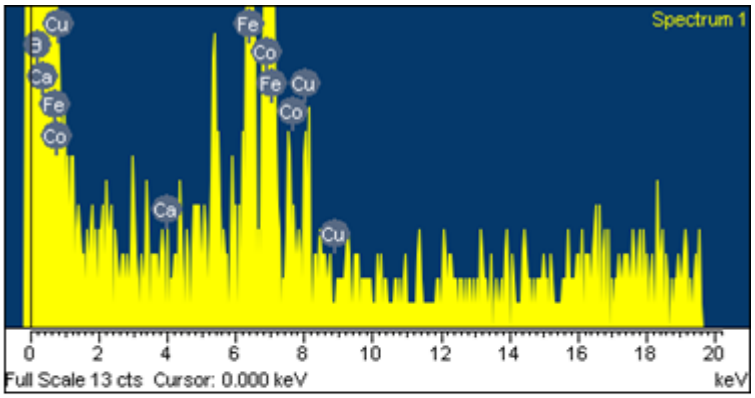

Element	Weight%	Atomic%
B K	96.33	99.29
Ca K	-0.03	-0.01
Fe K	1.93	0.39
Co K	1.47	0.28
Cu K	0.29	0.05
Totals	100.00	

Figure 2.18 EDX of calcium ferrite, synthesised via sol-gel method (Khanna and Verma, 2013).

Due to the presence of Fe, a clear XRD was not obtained, regardless of alterations to configuration, therefore unable to compare with published XRD, figure 2.19.

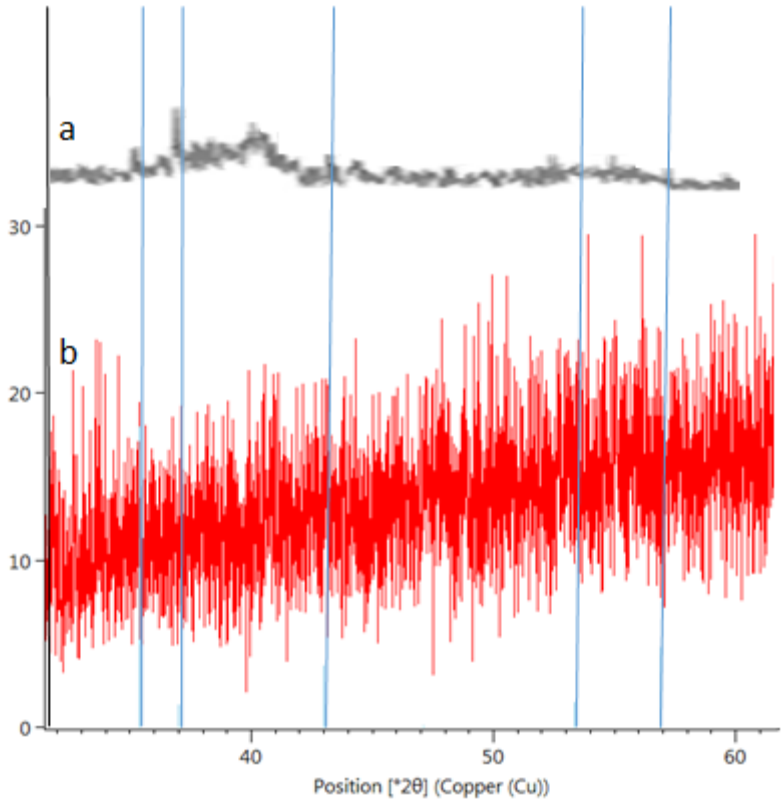

Figure 2.19 a) published XRD (Khanna and Verma, 2013), b) XRD from calcium ferrite synthesised using adapted sol-gel method. Blue lines high light reference XRD of ZnO obtained from High Score.

To identify the different bond formations in the sample of CaFeNP an FT-IR was performed. The synthesised and published FT-IR spectra contain bands at 3400 -3000 cm^{1} bands that correspond to O–H stretching vibration, that diminish with heating, figure 2.20. Absorption due to stretching in nitro compounds (containing NO_2 group) results in a strong band in the region 1661–1410 cm-1 as observed in figure 2.20, the conjugation further lowers the frequency of bands resulting in absorption E1550 cm^{-1} (Khanna and Verma, 2013; Khanna and Verma, 2013b; Pirouz *et al*., 2015). The stretching vibrations of C–O were detected at bands 1295 and 1289 cm-1 but were only present in the not calcined calcium ferrite figure 2.20a (Khanna and Verma, 2013). The bands at 560 and below are in correspondence to correspond to the stretching vibrations of the metal oxygen bonds i.e., Ca–O and Fe–O bonds (Rana and Philip, 2010; Khanna and Verma, 2013b; Pirouz *et al*., 2015). The spectra obtained for the adapted synthesis, displayed a band at 870 and 874 cm-1, possibly indicating the presence of starting material (i.e. citric acid or ethylene glycol) that remained after calcination at 300°C, further investigation into the removal and transfer onto the SRD is required to increase productivity and to decrease particle range.

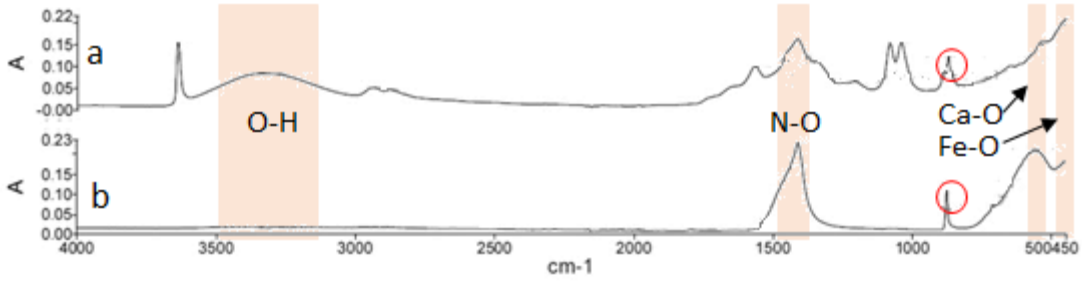

Figure 2.20 FT-IR *of calcium ferrite not calcined (a) and calcinated at 300°C (b) shows the removal of O-H bonds after calcination. The presence of bonds C-Cl at 872 – 875 cm-1 (circled in red) are residue from starting material.*

2.3.5 Coating technique

Hydrolysed histidine with a 1:1, w/w ratio was found to be adequate to coat MONP of Ca and Fe. With trial and error, ZnNP required an increase in coating to 2:1 (His.: ZnNP) for successful and maintained suspension. Uncalinated CaFeNP was found to suspend without requirement for coating, however when calcined, the residual starting material and O-H removed, coating was required as a 1:1 to be in accordance with Ca and Fe. The initial use of a pestle and mortar was very subject to the user and impropriate for large quantities required, therefore the use of a KitchenAid KCG0702ER Burr Coffee Grinder removed human error and provided an increased output of coated material with an increase in coating uniformity.

As initial trials focused upon FeNP, the coating suitability was primary established for this MONP with subsequent trails using the same coating for continuity. From the ICP results, table 2; ascorbic acid, citric acid, EDTA proved most efficient at suspending the FeNP. The use of EDTA, is cost effective but locks the FeNP / MONP in to a complex, figure 2.21, limiting availability for plant uptake.

Ascorbic and citric acid also bind tighly to FeNP, with increased H^+. This decreases the pH of the solution from pH 6.8 to 4.8, potentially coursing harm / inference to the uptake mechanisms of the plant.

Coatings of FeNP	***Fe mg / L***
Ascorbic acid	25.98
Citric acid	41.2
EDTA	21.87
Folic acid	0.489
Histidine	1.589
Leucine	1.871
Lysine	0.359
Threonine	0.384
Phenylalaine	0.379
Valine	0.394

Table 2.5 ICP-OES results of coating materials for FeNP.

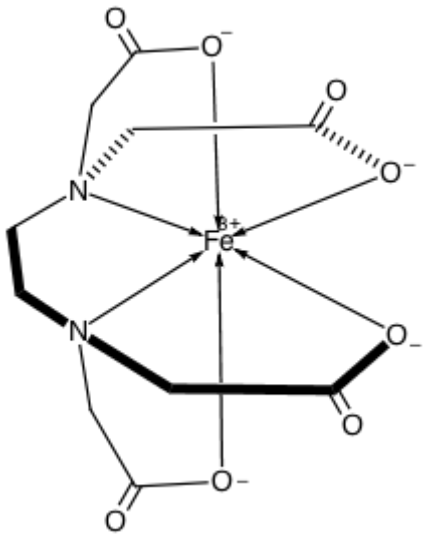

Figure 2.21 Fe-EDTA complex. The metal ion, Fe forms 6-valent coordination complexes with the EDTA, 4 bonds negatively charged oxygen and 2 bonds to a lone pair of nitrogen atoms.

Trials into the effect of suspension in an aqueous solution required further investigation into the agglomeration and longevity of NP suspension, particularly on a range of potential coating materials, (e.g. lysine, ascorbic acid and sugars) and a range of pH that the solution may be added to in potential commercial applications (hydroponic proration or as an antibacterial agent).

2.3 The effect of MONP on seed emergence

The ideal coating for MONP will not significantly increase or decrease the germination or growth rate of the seedlings to permit the observation of the effect of the MONP. Using the statistical analysis ANOVA and t-test unequal variances, a significant difference (sig. dif.) between the control and tested amino acid seedling heights was observed as seen in figure 2.22. Amino acids with the mean steam heights similar to that of the control seedlings, 23.63 mm were identified as; histidine (23.44 mm), valine (23.00 mm), cysteine (22.14 mm) and phenylalanine (22.67 mm), with histidine the closest to control measurement. These amino acid treatments did not significant effect the growth rate of the seedlings.

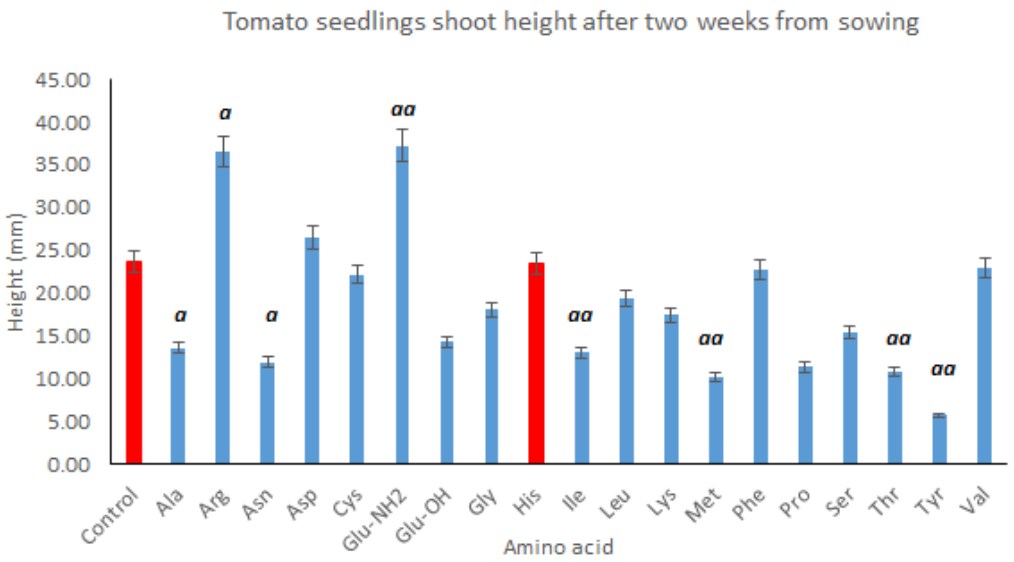

Figure 2.22 Results from tomato trial with essential amino acids. Using Excel, statistical analysis using ANOVA single factor (a) and t-test (*) was performed. The significant difference was ranked according to Duncan multi comparison (Duncan, 1955). <p=0.05, a; <p=0.01, aa and <p=0.005, aaa. Highlighted in red is the control and His. No significant difference in growth was found therefore highlighting His. as a good coating as it would have no significant influence in the tomato plant growth.

The influence of the amino acid on the emergence rate of the seedlings was taken into consideration. As for the growth rate, the percentage emerged would ideally be approximately that of the control seeds, 33.33%, table 2.3. Collaborating the results, it was concluded to use histidine (His) as the MONP coating.

Test solution	Percentage emergence (%)
Control	33.33
Alanine (Ala)	77.78
Arginine (Arg)	50.00
Asparagine (Asn)	55.56
Aspartic acid (Asp)	27.78
Cysteine (Cys)	77.78
Glutamic acid (Glu-NH2)	44.44
Glutamic acid (Glu-OH)	16.67
Glycine (Gly)	33.33
Histidine (His)	50.00
Isoleucine (Ile)	44.44
Leucine (Leu)	66.67
Lysine (Lys)	44.44
Methionine (Met)	33.33
Phenylalanine (Phe)	27.78
Proline (Pro)	16.67
Serine (Ser)	27.78
Threonine (Thr)	27.78
Tyrosine (Tyr)	16.67
Valine (Val)	11.11

Table 2.6 Results from tomato trial with essential amino acids, percentage of tomato seeds emerged. The amino acids are highlighted in red as those identified as to having the closest growth rates as the control seedlings.

3 Potato trials

As a key compliant in the global diet, the potato also provides an ideal candidate to for fortification via a soil or foliar applied MONP. The tubers proximately to the soil allowed the analysis of MONP behaviour in the growing media, uptake and utilisation of the metals provided by the MONP.

A number of growing conditions used to substantiate the use of MONP as fortification method. Using a hydroponic propagation system to initially eliminate environmental efforts such as light fluctuations, extremes of temperature and influence of growing media that would affect the physiology of the plants the nutrient requirement, plus the availability of the MONP. When establishing the optimal concentration of MONP with hydroponic system, the propagation was then moved to greenhouse / poly tunnel with the introduction of multi-purpose compost as a growing media, without addition lighting and some protection against temperature extremes. The data collated from these trials enabled experimental propagation to move to a field environment, where the uptake of the FeNP was observed in conditions of commercial application and propagation.

To substantiate the claims found from the previous trials of increased availability and plant utilisation plus an increase in the sustainability in the compost, a head to head trail was conducted using the radioactive isotope ^{59}Fe against the principle commercial source of Fe, Fe-EDTA.

3.1 Materials and methods

3.1.1 Growth pattern of stem; potato trials

The growth pattern of the potatoes grown in Clifton and Brackenhurst were recorded. Measurement of the height of a stem was taken from the based at the substrate level to the upper shoot apex. The height of three allocated stems per plant was recorded from two weeks from planting (when the MONP was introduced), to week 5. In the growth cycle of the potato plant, this period of time is focused on the development of the plants foliage, hence essential in monitoring effects the MONP's may have on the development.

3.1.2 Yield and harvested weight: Potato crop

At the point of harvest the fresh weights (2 d.p.) and numbers for trials conducted in Clifton and Brackenhurst were obtained and divided into two categories, >30mm and <30 mm.

Branston Ltd provided the number and average harvested weights for Field2015, divided into sizes <20, 20-40, 41-65 and <65mm. Field2016, physical data was not deemed essential to the trial.

3.1.3 Dry mass percentage (DM%); potato tubers

Previously, dry matter obtained by specific gravity, first developed in mid-19th century (Lisinska and Leszczynski, 1989). This determination of matter produced large discrepancies; therefore, a slow drying method to remove water without determination of the material was developed and adopted as the standard method, (Lisinska and Leszczynski, 1989).

For trials Sax2015, Sax2016, Feload2016 and Fieldrep2016, the DM% of Dry mass of a similar sized tubers (100 mm length, 30 g) were selected (n >10 per application). Using this regulatory system enabled tubers of similar age / growth stage to be analysed. Branston supplied the tubers from Field2015 (n=8 per treatment) and Field2016 (n=10 per treatment).

Each tuber was washed with distilled water twice, patted dry and left to dry at room temperature for 30 mins. A central core of a potato taken (diameter 15mm) using a cork border from the bud end to the stem end (figure 3.1) and immediately weighed. The sample was then place in dehydrator at 65^{o}C, and reweighed until a consistent dry weight was obtained (10-15 hours).

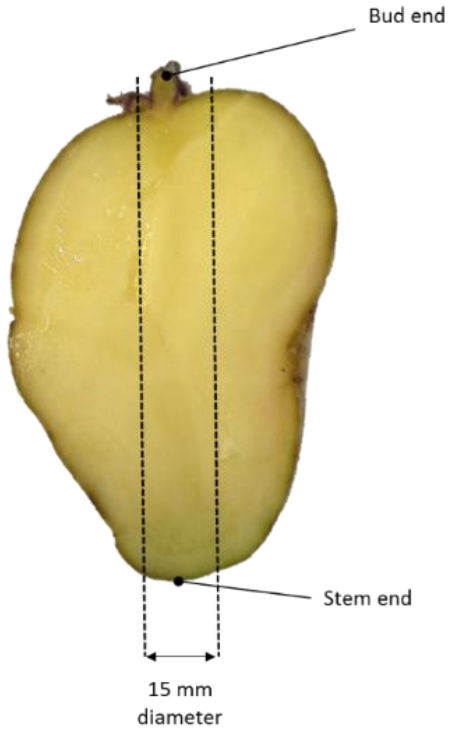

Figure 3.23 Sampling a potato tuber for DM%.

3.1.4 Determination of mineral content of potato tubers

Soil particles could interfere with mineral content analysis therefore contamination was avoided by toughly washing the tubers in deionised water twice, patted dry and left to dry at room temperature for 30 mins. Using a cork border (diameter 15mm), a core sample taken from the bud end to the stem end (figure 3.1) used in DM% was use to give an over view of the mineral content of the whole tuber. The autotomy of the potato as identified in figure 3.2. Two horizontal core samples were taken and divided into three parts central core of a potato was taken (figure 3.3). Each sample was dried as previously described for DM%. All samples where ground to a fine powder using a Tefal GT203840 Coffee Grinder.

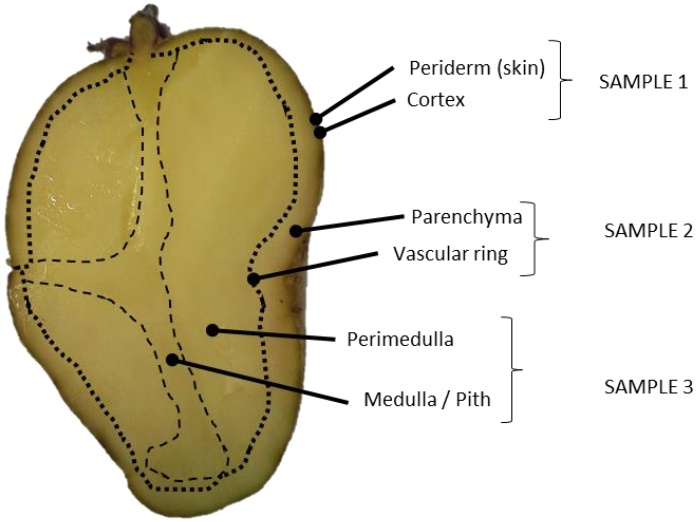

Figure 3.37 Constituent parts of potato (Lisinska and Leszczynski, 1989).

Digestion of dried potato tubers was carried out using ETHOS UP High Performance Microwave Digester System using the pre-set methodology '*Dried plant material*', figure 3.4.

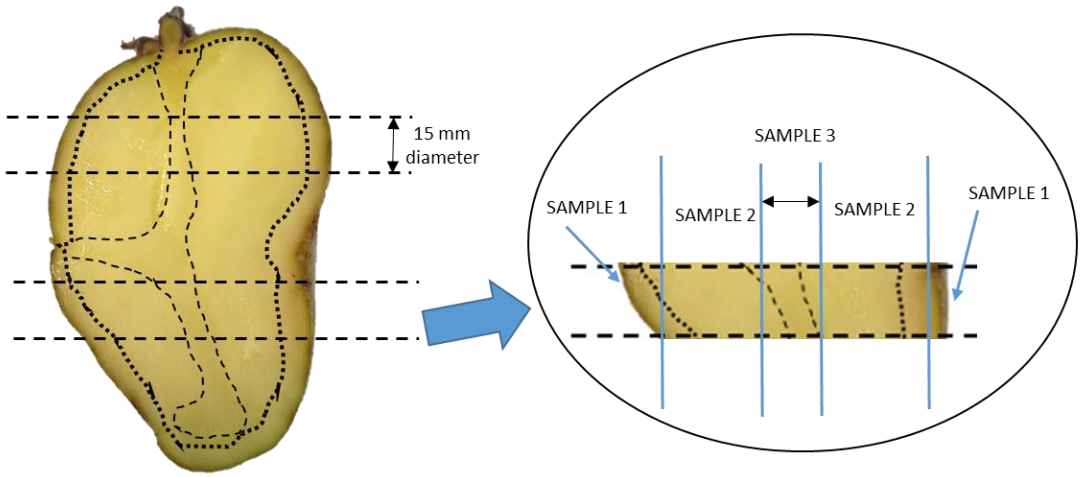

Figure 3.25 Samples taken to for ICP analysis for constituent parts of the tuber to observe the distribution of Fe, Ca and Zn through the tuber.

Sample weight and reagents

Sample weight	Up to 500 mg
Reagents	8 mL HNO3 2 mL H2O2

Microwave program

Step	Time	T1	Power
1	00:15:00	200°C	1800 W*
2	00:15:00	200°C	1800 W*

Figure 3.26 ETHOS UP program for digestion of dried plant material', left using the EHTOS UP high performance digester, right. www.milestonesrl.com

Chemicals used for the digestions purchased from Sigma-Aldrich (hydrogen peroxide) and Thermo Fisher (Nitric acid, 36 %, analytical grade). The mineral content of the samples was obtained by Perkin Elma ICP-OES Opmtima 2100 DV, using calibrated using serially diluted standards purchased from

Fluker by a factor of ten. The fully digested material solution diluted to 20% for ICP analysis, to avoid nitric acid corroding the feed lines.

The mineral content was then calculation to 1g of dried sample. The data was statically analysed using ANOVA single factor, SD <p=0.05.

3.1.5 Hydroponic: Trials H2014 and H2015

Nutrients	M_r	*mol* L^{-1}	*g* L^{-1}
KNO_3	101.1032	0.0025	0.252758
$Ca(NO_3)_2$	164.088	0.00	0.41022
KH_2PO_4	136.086	0.0005	0.068043
H_3BO_3	61.83	9.50E-06	0.000587385
$MnCl_2.4H_20$	197.9052	7.40E-06	0.001464498
$ZnSO_4.7H_2O$	287.5799	9.60E-07	0.000276077
$CuSO_4.5H_2O$	249.6861	5.20E-07	0.000129837
$(NH_4)_6Mo_7O_{24}$	1235.873	1.00E-08	1.23587E-05

Table 3.7 Nutrient soluation formulation adapted from Wheeler, 2003. Used in trials Hydro2014 and Hydro2015.

An Atami Wilma 8 pot hydroponic drip feed system (purchased from NPK Technology, Liverpool) consisting of eight 11 L pots was used with a clay particle substrate (Dutch Pro) in pots, supplied by a 70 litre nutrient feed tank (120 x 60 cm), where the nutrient solution was recirculated and replaced every 2 weeks. The nutrient solution used was adapted from Wheeler, (2006) with an N:P:K, 7.5:0.5:3 mol L^{-1}, with removal of Ca, Fe and Zn constituents when equivalent MONP where tested. (table 3.1).

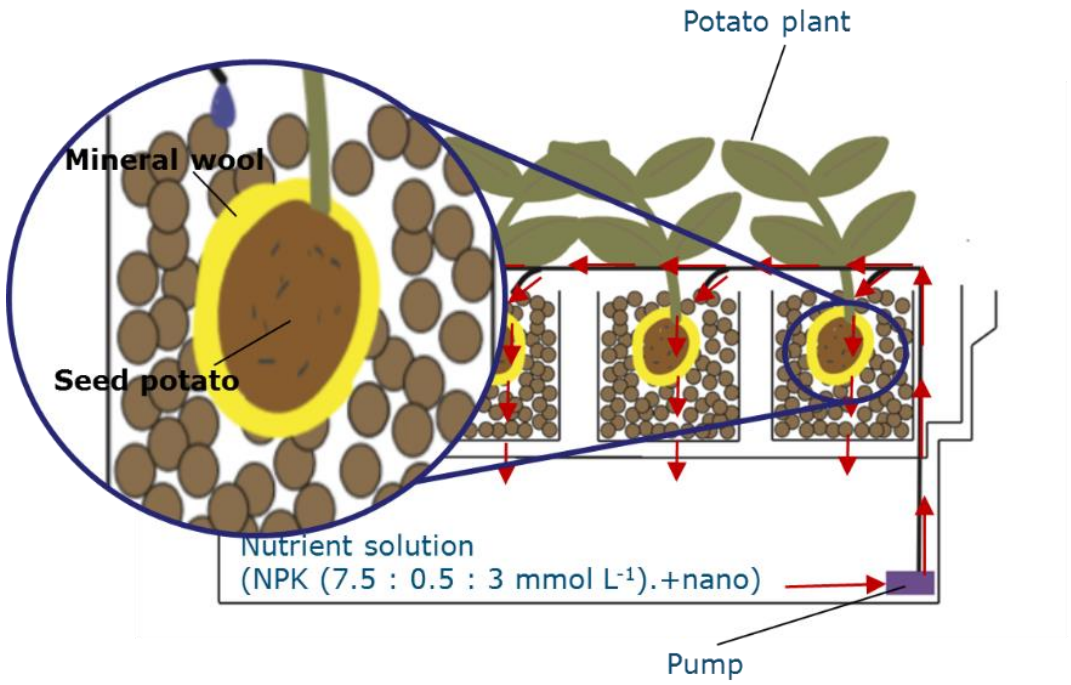

Figure 3.40 Schematic of the Wilma drip feed hydroponic system used in hydro2014 and hydro2015 trials.

One chitted tuber per pot was planted a third down of the way down the pot, and wrapped in mineral wool to maintain moisture immediately around the tuber (figure 3.5). Natural light and temperature fluctuations were limited by insulation of 0.5 mm polystyrene (radiator reflector foil), purchased from Screwfix, UK. Diurnal length was twelve hours (6.00 am to 18.00 light and 18.00 to 6.00 darkness) with two periods of feeding comprising of two, six-hour periods (6.00 till 13.00 and 18.00 till 1.00). Lighting provided by Philips 600W HPS Grow Master Son-T PIA Green Power lights at a 1.5 M distance from the top on the pots. The lights provided a full spectrum, illuminating 1.5 M^2 and providing 86500 lumens (www.lighting.philips.co.uk). Test solutions added to individual tanks with maintenance of the EC, pH and additional MONP levels.

Trials conducted under hydroponic conditions, tested FeNP, CaNP and ZnNP, as seen in table 3.2. All MONP's used in the following trials were coated with hydrolysed histidine. Each trial lasted 12 weeks or until the plants showed signs of senescence. The Saxon cultivar was used as the plant grew to a shorter height and tuber size is small to accommodate for height restrictions of the room and small dimensions of the hydroponic pots. The potatoes where provided from AHDB Potato, Sutton Bridge Crop Storage Research Centre, to ensure all were grown and stored in the same conditions at the same

time. The seed potatoes where allowed to chit until a shoot height of 2-3cm was produced. The seed potatoes planted into the clay particulate with a mineral wool jacket, with one shoot per potato.

Trial	Application	Concentration of MONP (mg/L)	Number of tubers
H2014	Control	0	8
	Fe-EDTA	8	8
	His.	8	8
	His.	20	8
H2015	Control	0	8
	CaNP+His	12	8
	CaNP+His	32	8
	FeNP+His	8	8
	FeNP+His	12	8
	FeNP+His	26	8
	ZnNP+His	8	8
	ZnNP+His	16	8

Table 3.8 Applications and concentrations used in H2014 and H2015 trials.

Growth rates noted on a weekly basis during propagation. Due to the restriction on tuber formation in the pots, only the Fe, Ca and Zn content of the tubers harvested were analysed via ICP-OES.

3.3.2 Saxon trials: Sax2015 and Sax2016

Greenhouse trials conducted at Clifton campus and poly-tunnel trials conducted at Brackenhurst campus, followed the same strategy: three chitted seed tubers, planted in an equal lateral triangle 20 cm apart. The plants were cultivated in 40 L sacks (purchased for LBS Horticulture), planting a third of the way down.

The growth medium was a peat based Erin Multipurpose compost. The growing sacks were laid out 50 cm, Sax2016 and 15 cm apart, Sax2015 (accordance to field propagation) so the foliage did not impinge on the adjacent sack (figure 3.6). Test solutions were applied once a week after two weeks from planting, unless stated otherwise. Dosage per plant of allocation treatment (500 mL) was applied directly at the base of the plant avoiding foliar contact. All plants were watered at the same time at twice a week between applications', although this increased in June and July to four times a week

watering. For all greenhouse / poly-tunnel, trials the planning took place in April and lasted 14 weeks for Saxon and 10 weeks for Swift, this was in accordance to the varieties growth pattern.

Where fertiliser was used, the organic granular slow release Chempak Potato fertiliser (N:P:K, 4-6-12+4MgO) was applied as directed by the manufacture. Table 3.3 summarises the applications of MONP in the trials.

Trial	*Application*	*Concentration of MONP (mg/L)*	*Chempak applied*	*Number of tubers*
Sax2015	Control	0	Y	21
	CaNP+His	12	Y	9
	CaNP+His	36	Y	9
	CaFeNP+His	Fe:12 Ca:24	Y	9
	FeNP+His	8	Y	21
	FeNP+His	12	Y	21
	FeNP+His	16	Y	21
	ZnNP+His	8	Y	9
	ZnNP+His	16	Y	9
Sax2016	Control (water only)	0	N	18
	Control with Chempak	0	Y	18
	CaNP+His	32	Y	18
	CaNP+His	64	Y	18
	FeNP+His	16	Y	18
	FeNP+His	32	Y	18
	His.	16	Y	18
	His.	32	Y	18
	His.	64	Y	18

Table 3.9 MONP solutions tested in trials using the potato cultivar 'Saxon' for trials Sax2015 (conducted under unheated greenhouse conditions at Clifton Campus) and Sax2016 (conducted in poly-tunnel, Brackenhurst Campus). All applications, including control, had an application of Chempak, apart from control (water only) Sax2016 where no additional feritlers were applied.

Observation of stem growth, harvest number and weights, were taken along with Dry mass (DM%) of similar sized tubers (100 mm length, 30 g) were selected. The Ca, Fe and Zn content of the tubers, and soil obtained via ICP-OES and statistically analysed. The Saxon cultivar as used previously in the hydroponic trials and transferred to the larger greenhouse / poly-tunnel investigations for continuity. The tubers were supplied by AHDB Potatoes, Sutton Bridge Research Facility, Lincolnshire. Planting for both trials took place in the second week in April and lasted 14 weeks, figure 3.6

Figure 3.28 Right Sax2015 trial under greenhouse conditions at Clifton Campus. Left, Sax2016 under poly-tunnel conditions at Brackenhurst campus, allowing more space and increase in sample number.

3.3.3 Optimising Fe application using 'Swift' (FeLoad2016)

Seed potatoes, 'Swift' obtained from Hollybeck Nursery, Southwell. The potatoes were cultivated as described in section 3.3.2, in the absence of Chempak, in the poly-tunnel at the Brackenhurst Campus.

Application with FeNP+His, 32 mg / L				
	Control	*L1*	*L2*	*L3*
Week 1				
Week 2				
Week 3				
Week 4				
Week 5				
Week 6				
Week 7				
Week 8				
Week 9				
Week 10				
Week 11				
Week 12				
Week 13	Harvested			

Table 3.10 Timetable of loading trial. Loading 1 (L1) commenced from week 2, with weekly applications thereafter to coincide with foliar growth. Loading 2 (L2), commenced from week 5 with weekly applications thereafter to coincide with tuber development. Loading 3 (L3), application commenced from week 8, with weekly applications thereafter to coincide with nutrient loading of the tubers.

The Fe application timetable is summarised in table 3.4, consisting of 15 plants per trial. Weekly applications of FeNP+His 32 mg / L were administrated from when indicated, with an application of 500 mL per plant, and irrigated as for Sax2015 and Sax2016 trials. Height was recorded for 3 weeks, harvest data obtained as in previous Sax2015 and Sax2016 trial DM % and mineral content.

3.3.4 Field trials in collaboration with Branston Limited (Field2015, Field2016)

Field trials carried out in collaboration with Branston Limited. Growth period Field2015 was conducted on a singular site near Branston, Lincolnshire 53°09'30.9"N+0°26'32.4"W using the red variety 'Mozart'. The second trial, Field2016, conducted on number of sites around Lincolnshire, propagating 'Inca Bella' and the commercially leading 'Maris Piper'. All sites are regarded as iron enriched and have not been treated for iron deficiency in the past. The FeNP+His was supplied to Branston as a solution for Field2015 and as a solid for Field2016 with application instructions for the desired concentration of Fe.

Field2015 FeNP+His application methods used are summarised in table 3.6 and segregated into a grid system of nine plants per replicate, table 3.5. T2 applied a solution of FeNP+His at a concentration of 30 mg / L directly around the seed potato tubers at the time of planting. T3 and T4 applied Fe+HisNP solution as a foliar application at a concentration of 30 mg / L. For both of the foliar applications the initial spray carried at 7 weeks after planting when the potato plants foliage has achieved 50 % growth. T4 treatment was applied twice, same time as T3 and 4 weeks thereafter at week 11, the areas for both field trials in to a grid system as seen in figure 3.7.

	Application	*Weeks since planting (planting = week 0)*
T1	Control - no iron	N/A
T2	Drench	0
T3	Drench + 1 foilar	0 + 7
T4	Drench + 2 foliar	0 + 7 + 11

Table 3.11 Details of Fe+HisNP application for Field2015 trial, using Mozart cultivar. T1 donates the first foliar application at 50% foliar growth. For Mozart cultivar this was 7 weeks after planting.

In field2016 trial, only the drench application method used with FeNP+His. 50 mg / L. Both field trials were harvested at week 21.

At harvest, the mean height of the steams collected from potatoes grown Field2015, along with tuber number and weights. A selection of potatoes was received from the trials for Fe content analysis

(Field2015 and Field2016). Soil samples were also analysed for Fe content. All Fe analysis was obtained using ICP-OES.

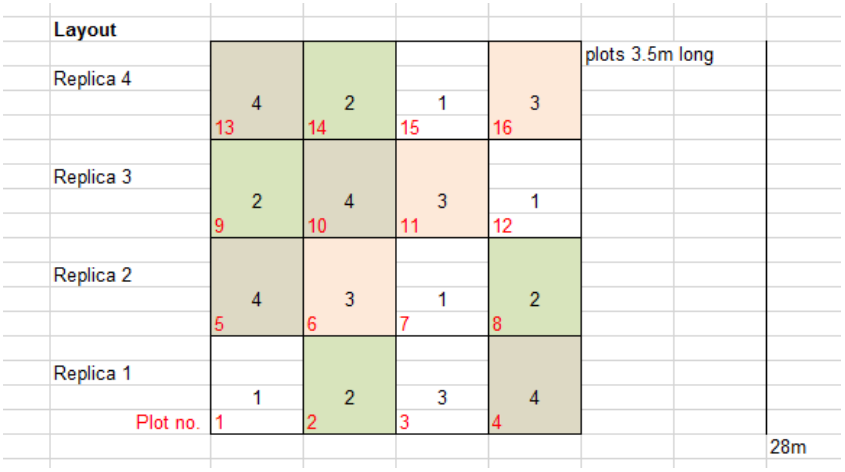

Figure 3.42 Grid layout of both field trials conducted in collaboration with Branston Ltd.

3.3.5 Replication of field trials (FieldRep2016)

The cultivar 'Swift' used to replicate the field trial conducted in collaboration with Branston Limited, section 3.3.4. All applications commenced with a drench application at planting, FeNP+His., 50 mg/L, (coinciding with Field2016, section 3.3.3) with foliar application at week 5, FeNP+His., 50 mg/L (Field2015). In order to protect the surrounding plants from contamination the plants where protected by two layers (1 mm thick) of plastic sheeting screen. A Hozelock 4122 Spraymist 1.25L, purchased from B&Q, was used to apply 1L FeNP+His., 50 mg/L, to each bag consisting of three potato plants. The chitted tubers were cultivated as in previous trials, at the Brackenhurst Campus, consisting of 15 tubers per treatment. At week 13, the tubers were harvested. This trial was used to observe the growth rate response to the Fe applications.

3.3.5: Observation of Fe uptake using radioactive isotope 59Fe. (59Fe trial)

To directly compare the uptake of Fe from FeNP+His. and commonly used iron delivery method of Fe-EDTA, both iron compounds were synthesised using the radioisotope ^{59}Fe, 1 mCi, purchased from Perkin Emler. The isotope allows tracking of the iron through the plant as well as quantity of iron utilised through the plant. Thirdly, the retention of iron in the soil can be observed. Chemicals for Fe-EDTA synthesis were purchases from Sigma Aldrich and the precursor chemicals for the FeNP+His synthesis was purchased as for pervious method.

The synthesis of this trial was adapted from Lauret *et al*. (2008) ^{59}Fe solution (10 mL) was added to a solution of iron (III) chloride (0.1 mol^{-1}, 30 mL) and iron (II) chloride (0.05 mol^{-1}, 30 mL), a 2:1 ration by molarity. This mix was added by continuous drip via a pressure equalising funnel, into sodium hydroxide (3 mol^{-3}, 60 mL). The sodium hydroxide was heated to 60^{o}C with continuous stirring at 500 rpm in a 250 mL a round bottom flask for 1 hour. The black nanoparticles were filtered through a grade 2 glass sintered funnel via vacuum filtration and washed with deionised water (3 x 50 mL) then ethanol (20 mL) and left to dry over night before in fume hood being ground for further use. Equal weight of histidine monochloride to iron oxide nanoparticle was ground using a pestle and mortar. The ^{59}FeNP+His., (3.30 g) was suspended into distilled water (1000 mL) making a stock solution. The stock solution (66.6 mL) was diluted to into distilled water (433.4 mL) before application to the plants.

The synthesis of Fe-EDTA (Stiener and Van Winde, 1970) involved the preparation of two precursor solutions; Solution A: Disodium EDTA (1.9g) into a solution of sodium hydroxide (1 mol^{-1}, 5 mL); Solution B: Iron (III) chloride hexahydrate (1.25 g) into distilled water (2.5 mL). Solution A was added to solution B with continual stirring and heated to 60 ^{O}C until a yellow precipitate formed. The precipitated was obtained by filtration and washed with ice cold water (2 x 50 mL) and once with ethanol (20 mL). No coating method was required as Fe-EDTA is soluble. Fe-EDTA (4.64 g) into distilled water (1000 mL). The stock solution (66.6 mL) was diluted with distilled water (433.4 mL) before application to plants.

The treatment (500 mL) was added once a week to the potato plants (planted in multipurpose compost as in previous trials) and watered every other day with tap water for six weeks. Three replicates of each application were cultivated. Samples of the compost, tuber and stem (lower, mid and upper) were taken and analysed for gamma radiation activity using a Hidex AMG Gamma Counter.

3.2 Results and discussion

3.2.1 H2014 and H2015 growth rate

From the data collected in trial H2014, figure 3.8 and table 3.6, it is observed the 8 ppm FeNP+His 8 mg / L and His. 8 mg / L has the optimal growth. Overall, the Zn+HisNP treated potatoes significantly suppressed by the presence of ZnNP with increases of 13.73 mm and 13.18 mm, ZnNP+His 8 and 16 mg / L respectively.

	p-Value
Control against ZnNP+His 8 mg / L	1.81×10^{-9}
Control against ZnNP+His 16 mg / L	1.4×10^{-9}

Table 3.12 p-value of stem heights (trial H2015) at week 5 of cultivation showing significant (<p=0.05) decrease in heights using ANOVA single factor analysis.

Ca+HisNP 12 mg / L did not grow as rapidly as expected with a height increase of 31.43 mm when compared to the increase of 216.63 mm obtained by Ca+HisNP 32 mg /L (figure 3.9a).

The tubers treated with His 8 mg / L significantly increase in height ($p = 1.09 \times 10^{-4}$) compared to the increase in height gained by control plants, figure 3.8. The height increase gained by His. 20 mg / L. although an increase over control was not significant.

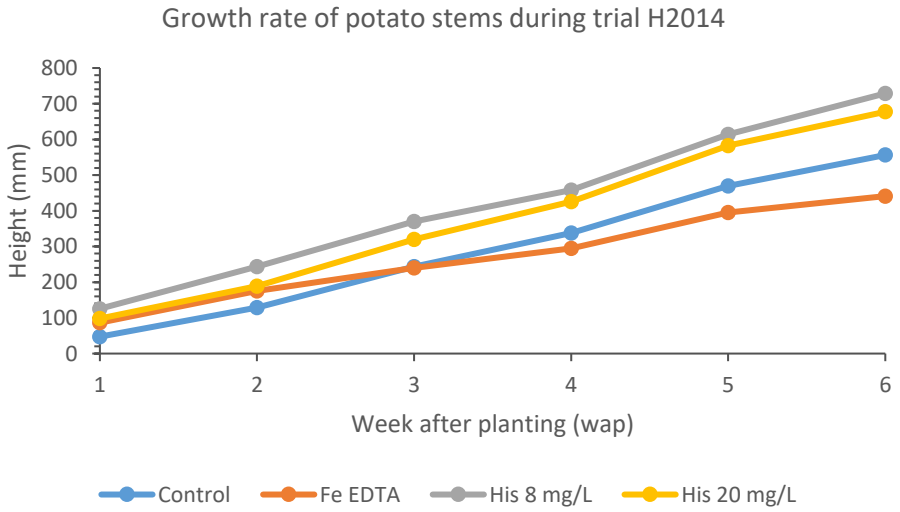

Figure 3.30 Growth rate of potatoes in trial H2015. Control plants increased by av. 304.22 mm, Fe-EDTA by 237. 22, His. 8 mg /L by 368.94 and His. 20 mg / L by 340.17 mm.

a) CaNP+His:Average growth rate of potato , H2015

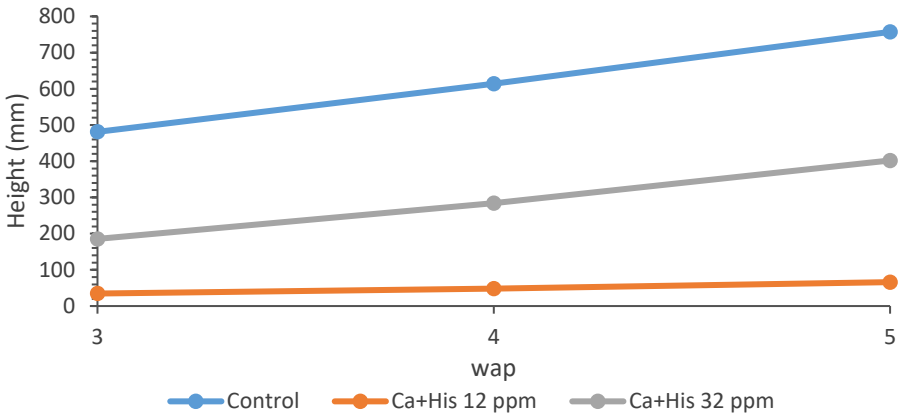

b) FeNP+His:Average growth rate of potato , H2015

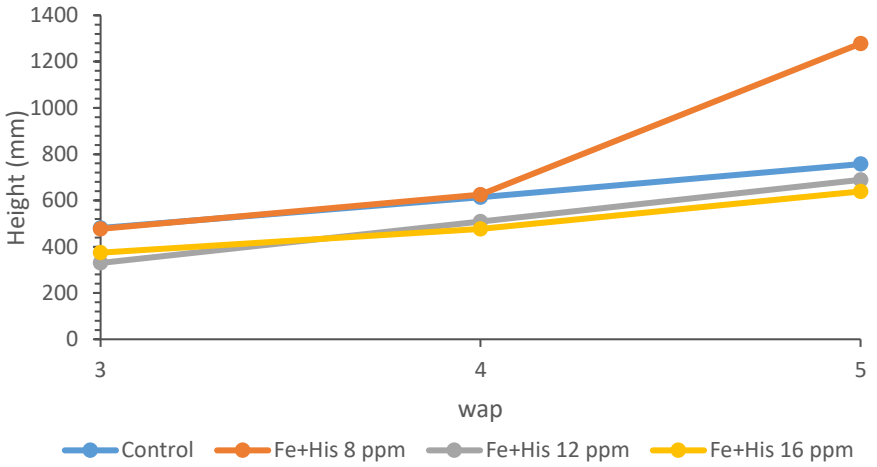

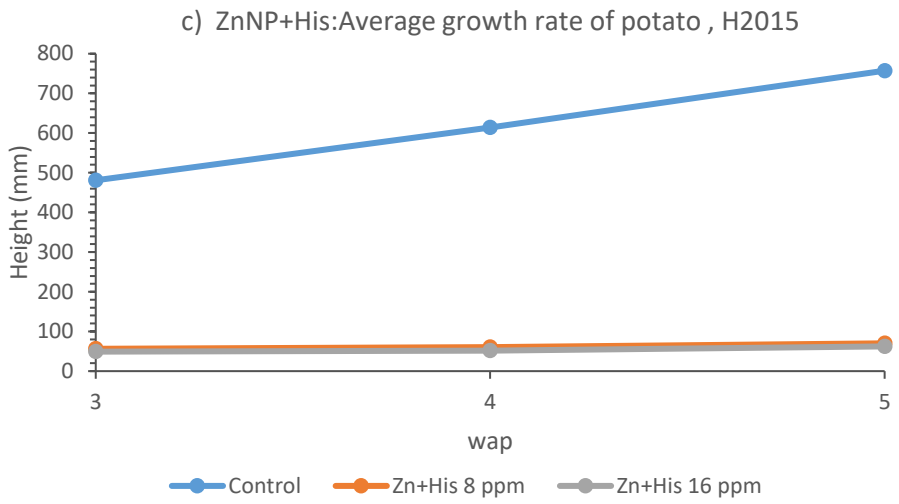

Figure 3.31 The growth rates of plants treated with CaNP+His (a) and ZnNP+His (c), have suppressed growth when compared to control. FeNP+His 8 mg / L (b) is the only treatment in the trial that demonstrated an increase in growth rate over control plants.

3.2.2 Saxon trials: Sax2015 and Sax2016

There was no sig. dif. when comparing the increase in height between weeks 3 and 5 (in conjunction with H2015) in Sax2015, figure 3.10 A percentage increase in height over control plants can be observed for treatments FeNP+His 16 mg / L, 9.90 %, CaFeNP+His., 5.40 % and ZnNP+His. 16 mg / L.

Potato stem heights after six weeks from planting, a 2.98 % increase over control gained by plants treated with FeNP+His. 12 mg / L and 0.26%, with plants treated with FeNP+His. 16mg / L, these increases were not found to be of significance, table 5.3. Plants fed with CaNP+His. 12 mg/ L gained 7.03 % increase over control height but was not found to be significant. However, CaFeNP+His and ZnNP+His 8 mg / L gained significant difference over control height stems, table 3.74. It was observed that between week 5 and 6 (figure 3.11) the control plants growth rate reduces as the plant commences the tuber filling stage (40 + days after planting). Plants treated with CaNP, FeNP and CaFeNP sustained growth rates during this period.

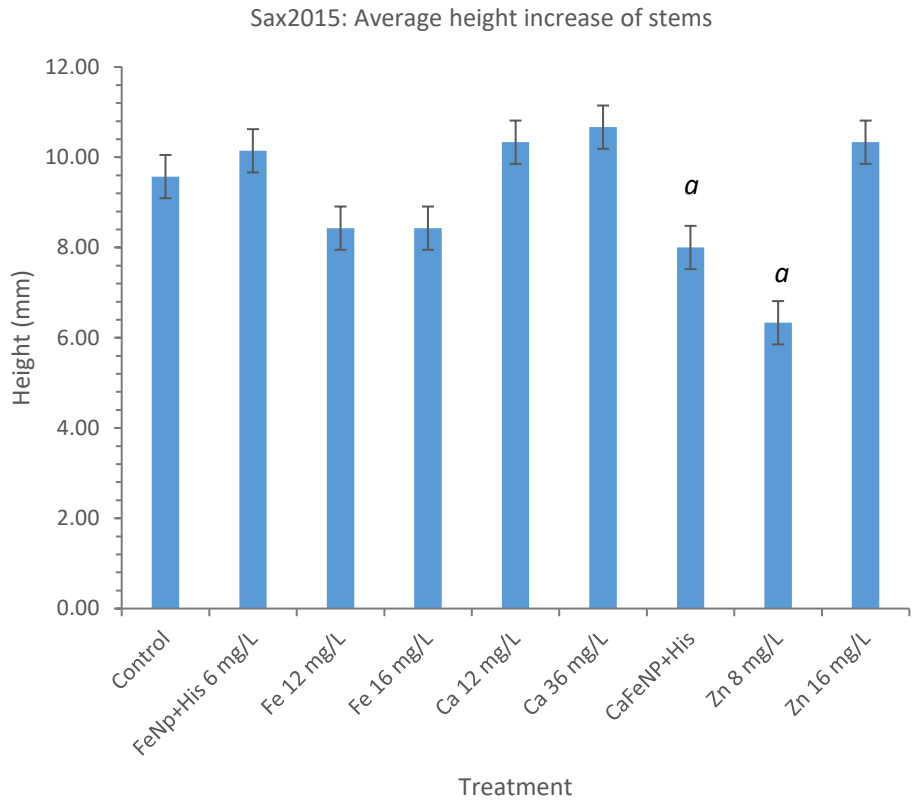

Figure 3.32 Average height increase of potato stems between weeks 3 to 5 after planting. p-values attained from ANOVA single factor comparing control heights and treated plant stem heights at six weeks of growth. A p value < 0.05 was deemed significantly different against control 'a'.

	Mean height (mm) at 6 weeks	*Percentage + or - in height against control*	*p value using ANOVA single factor*
Control	1198.73	N/A	N/A
FeNP+His 8 mg / L	1140.47	-4.86	0.2023
FeNP+His 12 mg / L	1234.40	2.98	0.2023
FeN+His 16 mg / L	1201.87	0.26	0.9246
CaNP+His 12 mg / L	1283.00	7.03	0.0501
CaNP+His 36 mg / L	1164.70	-2.84	0.2982
Ca.FeNP+His	1318.00	9.95	0.0210
ZnNP+His 8 mg / L	1300.80	8.51	0.0201
ZnNP+His 16 mg / L	1169.50	-2.44	0.7160

Table 3.13 Height (mm) of potato stems, percentage of height increase or decrease when compared to control six weeks after planting.

a) Sax2015: Stem growth rate of Ca treated plants

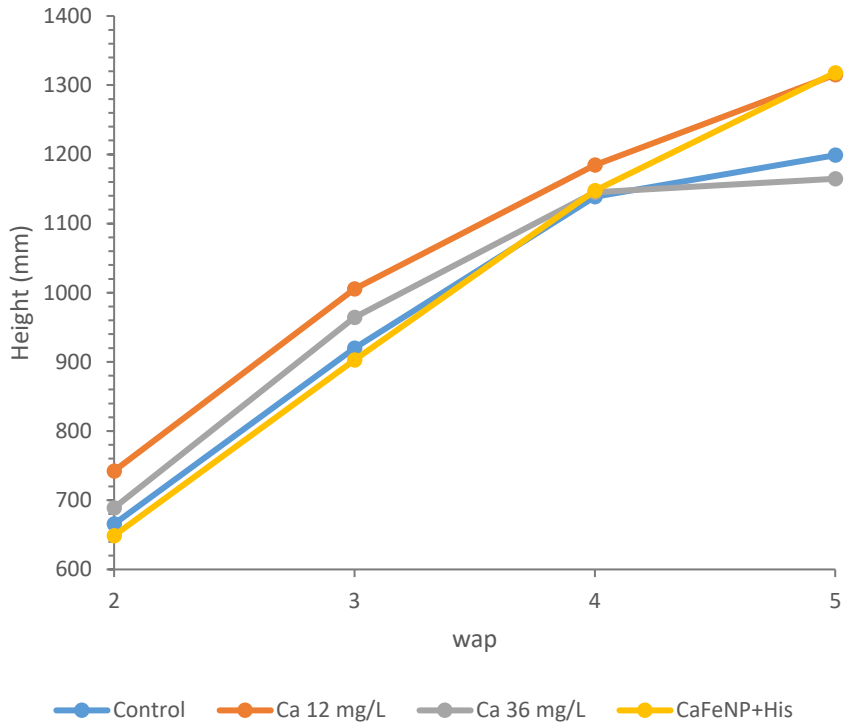

b) Sax2015: Stem growth rate of Fe treated plants

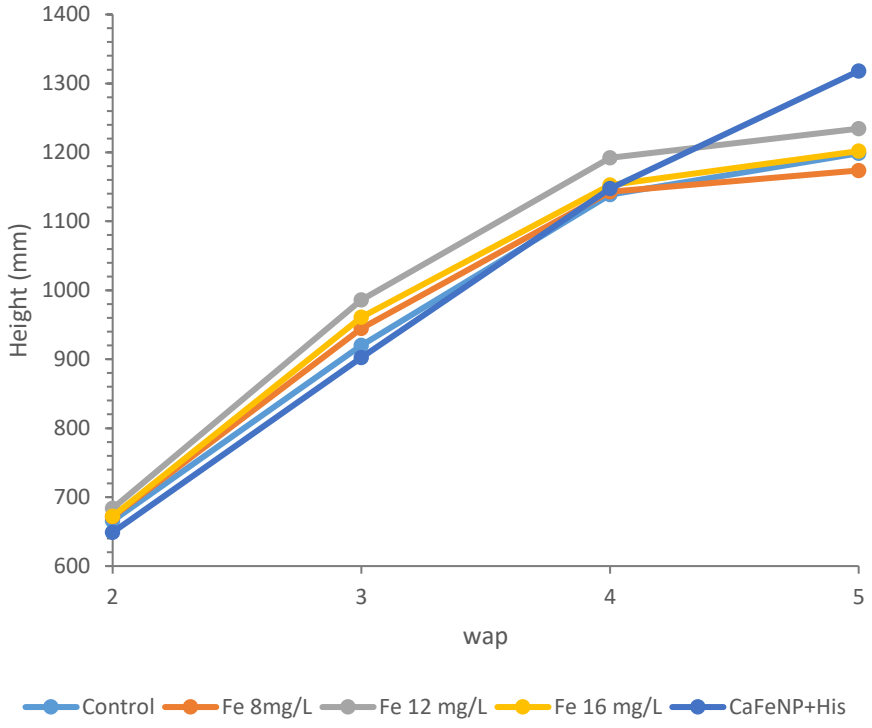

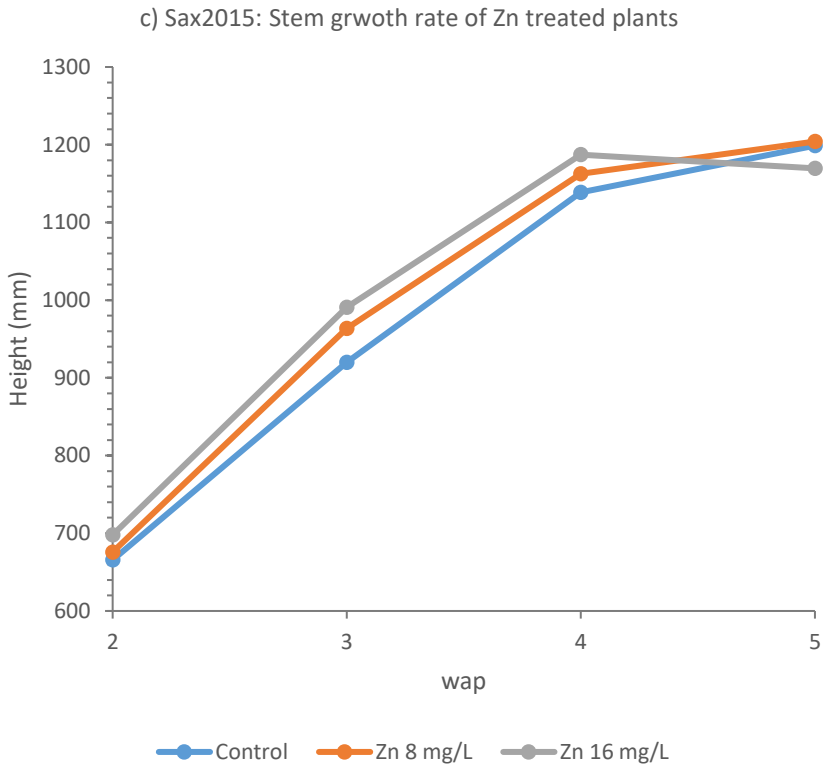

Figure 3.33 Average growth of potato stems during trial Sax2015. Observation suggests the presence of ZnNP (c) does not supress the growth of the potato stems as seen in the previous trial H2015

Growth rate data collected from trial Sax2016 showed sig. dif. of stem heights gained between week 3 to 5, figure 3.12, CaNP+His 32 and 64 mg / L has a significant increase in height over control, Chempak and the His. equivalent suggesting an influence in the presence of CaNP. This is supported by figure 5.7a where there in an increase in growth rate in stems treated with CaNP+His 32 mg /L.

His. only applications increase the growth rate of the stems as observed in figure 3.13, with a greater significance at lower concentrations.

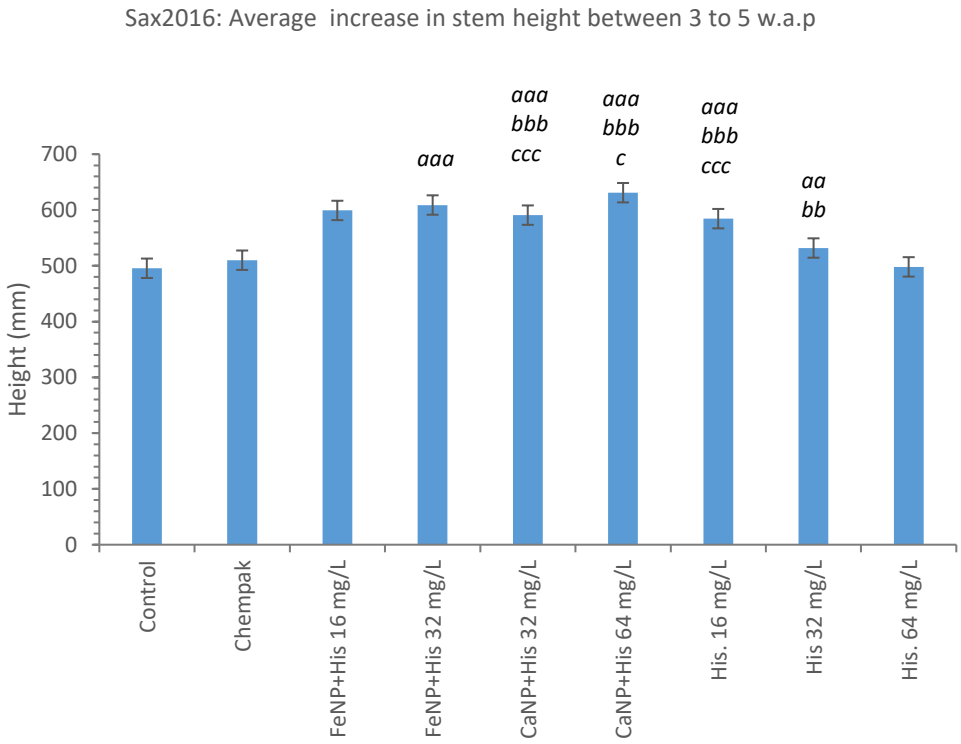

*Figure 3.47 Average increase in height of potato stems between weeks 3 and 5 after planting to be in conjunction with previous trials. Using ANOVA single factor statistical analysis, p-values were ranked; * p=0.05>, ** p=0.01, *** p=0.005. Letters a, against Control*

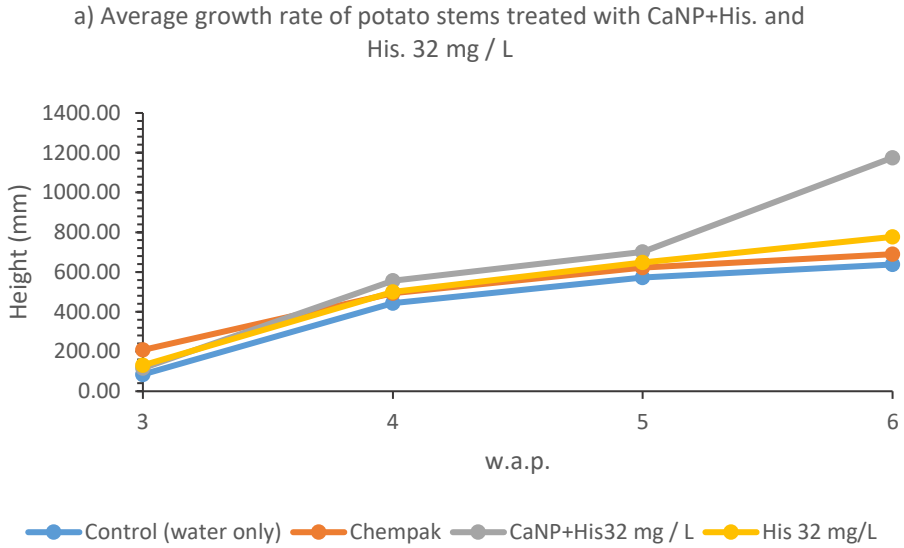

b) Average growth rate of potato stems treated with CaNP+His. and His. 64 mg / L

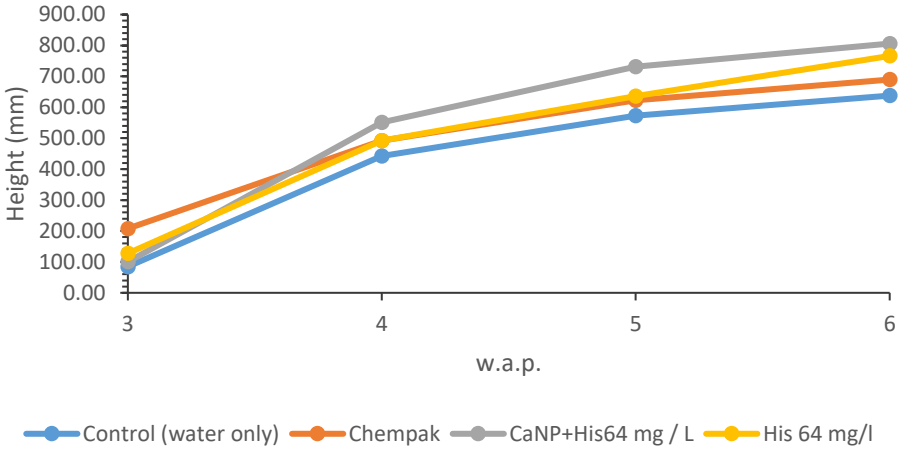

c) Average growth rate of potato stems treated with FeNP+His. and His. 16 mg / L

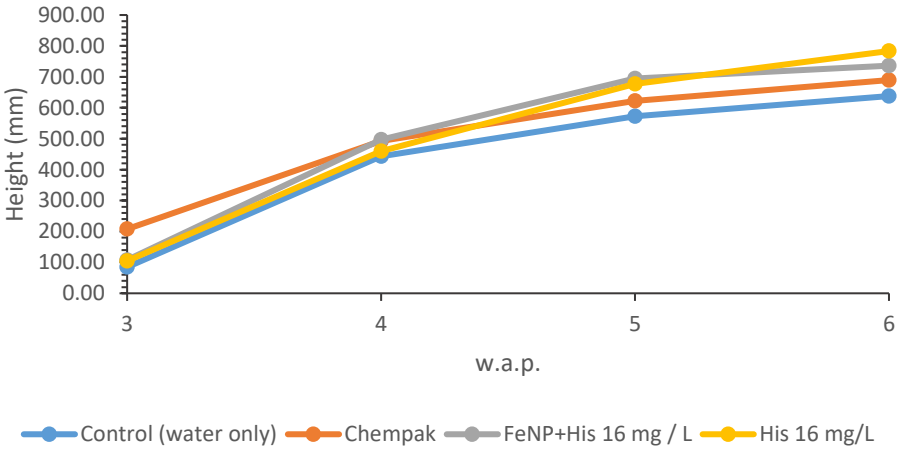

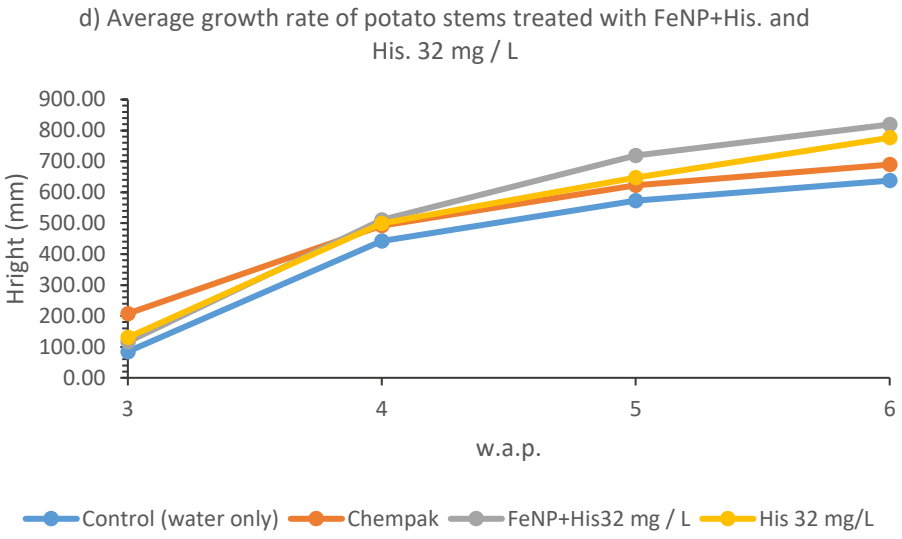

Figure 3.35 Average growth rates of potato stems in trial Sax2016. Control and those treated with commercial fertiliser, Chempak has a reduced height in stems than those treated with amino acid histidine or MONP's.

3.2.3 FeLoad2016

There was a significant difference between stem heights between control and L1 (p=0.006566) although the height increased between 4 to 6 weeks after planting (w.a.p) in the same applications were similar, control increase by 204.67 mm and L1, 202.44 mm, figure 3.14. No significant difference in time period was found between control and L2 growth, p=0.54231 and control against L3 growth, p=0.54231 but this was to be expected.

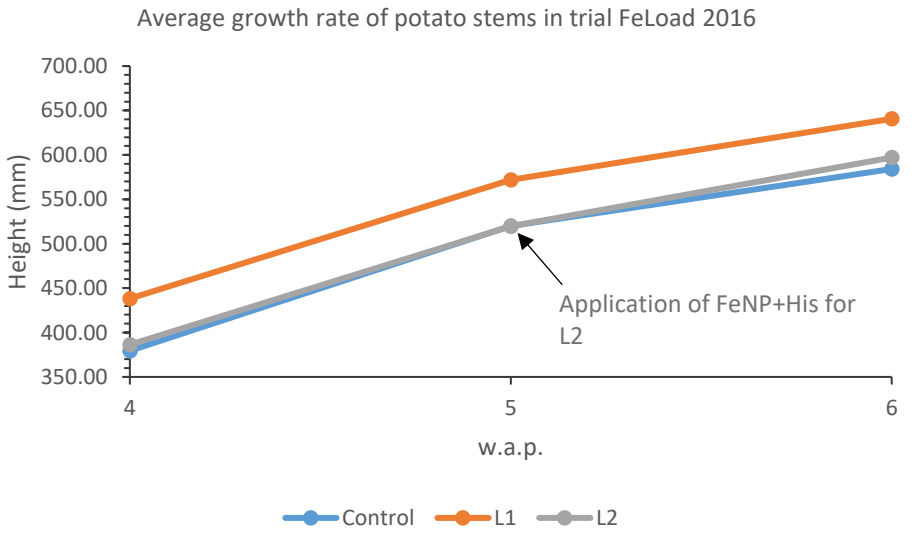

Figure 3.49 Average growth rate of potato stems during weeks 4 to 6 after planting. L3 was not represented in the graph as no application had been applied at this time.

3.2.4 FieldRep 2016

From the average stem growth rates (figure 3.15) the growth rate of the stem is sustained into the tuber loading phase of the potato plants growth cycle. Using ANOVA single factor there is a sig. dif., p=0.000109, between 'control' and 'Drench + 5-week app.'

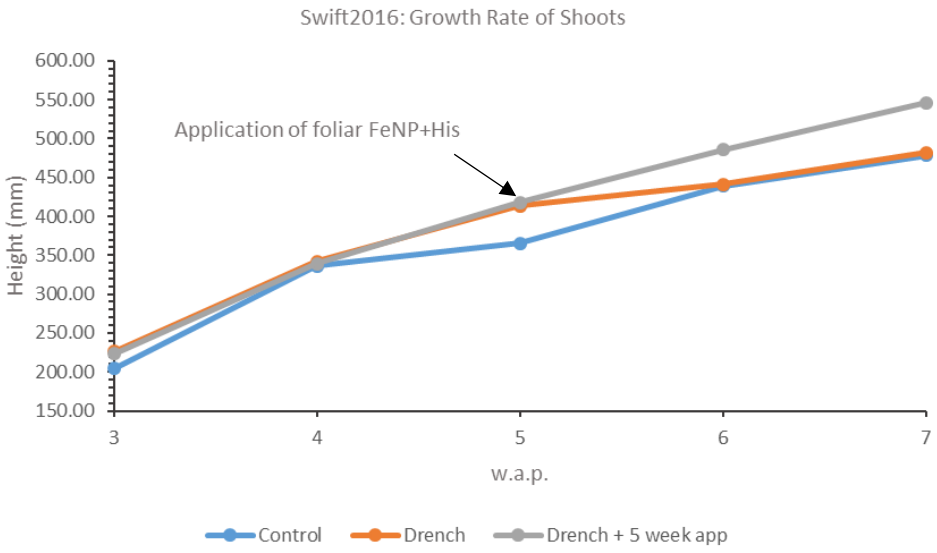

Figure 3.37 Average growth rates of potato stems in FieldRep2016 trial

3.3 The effect of MONP on yield

3.3.1 Saxon trials: Sax2015 and Sax2016

When comparing percentages variations, a 10 % increase or decrease was taken to be of significance with a H_0; "*applications of MONP do not influence the number of tubers harvested or the physiological maturation of the tubers*". This H_o was used when performing a Chi Squared statistical analysis, X^2.

The average number of tubers harvested per plant in Sax2015 were observed to increase over control when treated with FeNP+His 8 mg / L (10.31 %), CaNP+His 32 mg / L (25.83 %) which can be deemed as significant. FeNP+His 12 mg / L yield was not significantly less than control, however, FeNP+His 16 mg / L produced a significantly lower yield (-17.05 %) compared to control. The higher CaNP+His application had the opposite effect the 32 mg / L had on yield, with a significant loss of 33.59 %.

Although other FeNP and CaNP treatments obtained a lower number of tubers, when comparing growth data (FeNP+His 16 mg / L gained increased stem height, surmising there is no overall negative effect of Fe or CaNP application.

It was observed in figure 3.16 a, the application of ZnNP+His and CaFe+His had a significant negative effect on the number of tubers, producing a 15.14% and 13.74 % reduction in tuber tubers from ZnNP+His 8 and 16 mg / L respectively. The application of CaFeNP+His obtained the least number of tubers with a reduction of 33.59 %.

Sax2016 trial control (no champak or MONP) gained a higher yield than those treated with Chempak by 2.95 concluding that the Chempak did not significant impact on yield. Those treatments that gained a higher yield than Chempak where FeNP+His 16 mg / L (3.49 %) and His. 64 mg / L (12.44 %). Yield loss compared against control ranged from 22.19 to 6.36 % ad loss of 17.91 to 3.49 % against champak. Sax2015 losses had a more significant and wider range of percentage loss of 33.59 to 4.33 %.

In figure 3.16 b, it was observed a lower variance of ± 3.39 (n) was achieved in Sax2016, compared to Sax2015 ± 4.64 (n). Comparing FeNP+His. 16 mg / L application yields between Sax2015 and Sax2016 are inconsistent leading to question the influence of viability of seed potato and environmental conditions. Variations of this kind are due to environmental and genetic variation within the cultivar (Lisinska and Leszczynski, 1989; Genet, 1992) as the strata, time of year and treatment application was identical in both trials. Sax2015 were subjected to higher temperatures, due to the nature of the greenhouse conditions were as the Sax2016 plants were in a well ventilated poly-tunnel Increasing the sample number, repetitions and a focus on temperature and light fluctuations would establish the impact on such influences.

An observation of any correlation between the number of tubers harvested (figure 3.16) and the proportion of tubers that are above 30 mm and below the 30 mm commercial grade. Taking control (Sax2015) and Chempak (Sax2016) data as a reference point, a relationship was found to the total number of tubers and the percentage of >30 mm. Sax2015, those treatments obtaining a yield below control (n = 7.86) all acquired a larger percentage of >30 mm, whereas Sax2016 treatments all obtained higher percentages of > 30 mm tubers than Chempak.

The H_o for the percentages of > 30 and < 30 mm of harvested tubers were tested using X^2 with < p = 0.05. A sig. dif. between control and His. applications in trial Sax2015. Further sig. dif. was found in Sax2015, figure 5.20A, between FeNP+His 12 mg /L and CaFeNP+His; FeNP+His. and ZnNP+His 16 mg / L; CaNP+His 12 mg / L and CaFeNP+His. thus rejecting the H_o and recognising the treatments have an impact on the size of tubers harvested. The analysis was also carried out for data collated from the

harvest of Sax2016, were sig. dif. against champak was found between, control and all other treatments apart from FeNP+His 16 mg / L as observed in figure 5.20A. His. 16 mg / L significantly

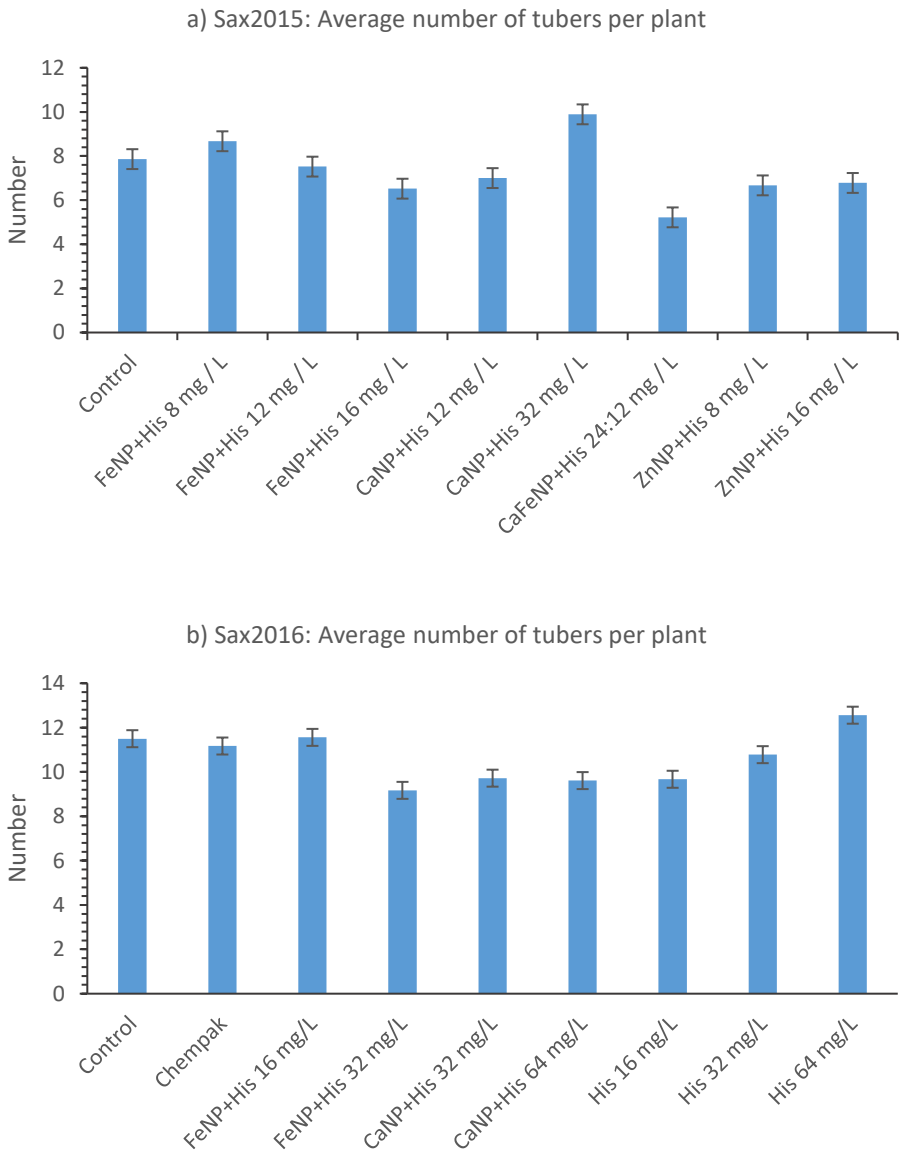

Figure 3.38 Average number of tubers harvested per plant. Comparing Sax2015 (A) and Sax16 (B) trials using Saxon cultivar.

increased the proportion of > 30 mm tubers when compared to the MONP equivalent application of FeNP+His. 16 mg/ L.

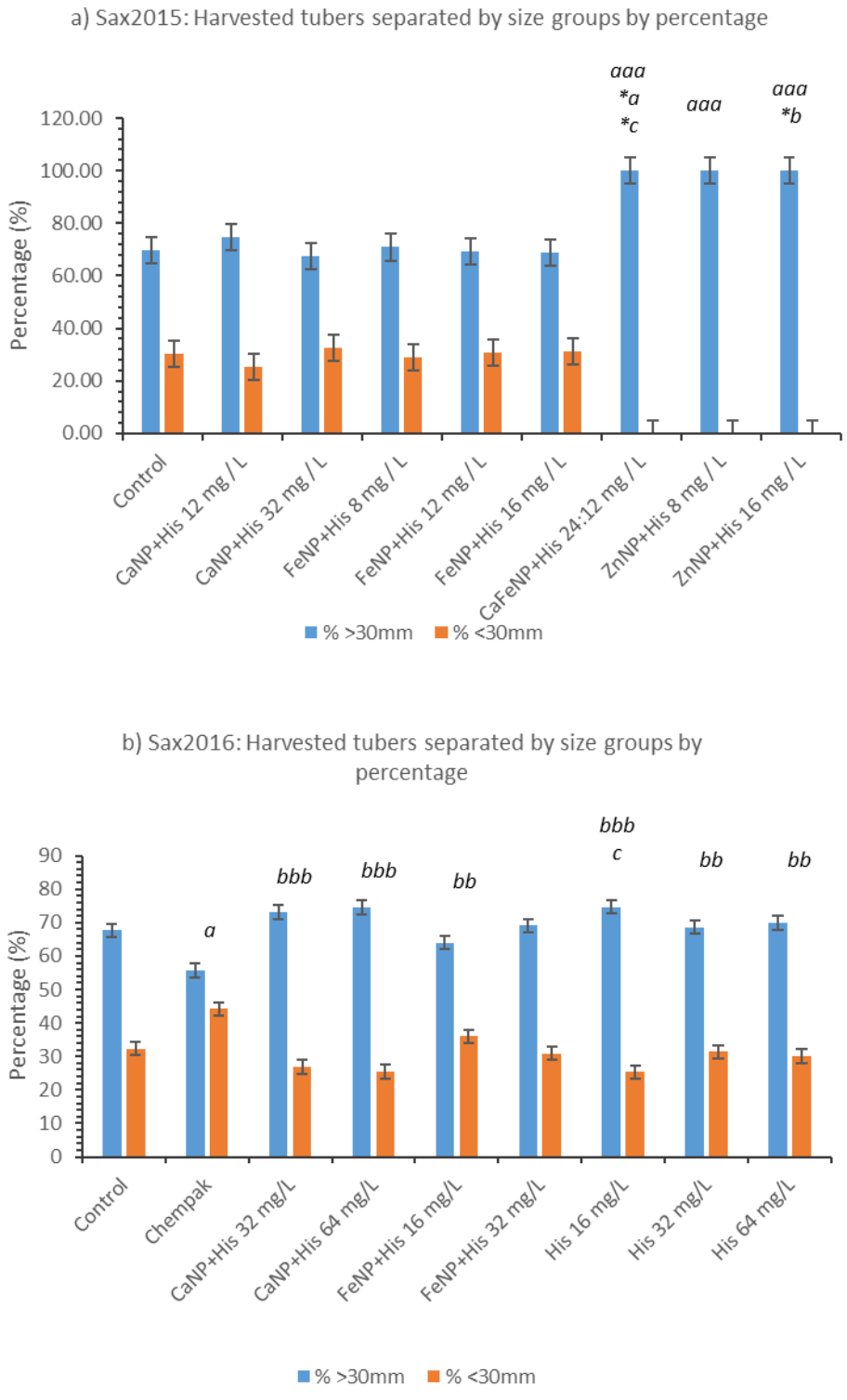

*Figure 3.39 Segregation of tubers into commercial acceptable size (> 30 mm) and < 30 mm. Sax2015 (a) indicates sig.dif. analysed via Chi Squared and ranked * p=0.05>, ** p=0.01, *** p=0.005. 'a' indicates a sig. dif. Between control and treatment; '*a', FeNP+His 12 against CaFeNP+His; '*b', FeNP+His 16 mg / L against ZnNP+His 16 mg / L and '*c' CaNP+His 12 mg / L against CaFeNP+His. Saxon2016 (B) using the ranking system as in A, 'a' indicated sif. dif against control, 'b' against Chempak and 'c' against MONP equivalent.*

Comparing harvested data statistically via ANOVA single factor analysis, from trial Sax2015, a significant increase between control plants overall average weight (OAW) in grams, and treatments, CaNP+His 12 mg / L ($p = 0.01$), CaFeNP+His ($p = 1.43 \times 10^{-4}$), ZnNP+His. 8 mg / L ($p = 3.21 \times 10^{-5}$) was found.

No sig. dif. was found in the data collected at the time of harvest between control harvested weights of > 30 mm. It was observed that CaNP+His. 32 mg / L and FeNP+His 8 mg / L produced 25.86 and 10.30 % more tubers per control plant respectively.

The tubers harvested measuring under the commercial acceptable level of 30 mm, had a significant difference in weight against control were FeNP+His 8, 12 and 16 mg /L. Treatments CaFeNP+His and both ZnNP+His did not produce any sub 30 mm tubers. Due to the harvest occurring at 14 weeks, approximately 20 days short of commercial harvest, the occurrence of <30 mm tubers would be expected as these tubers would go onto to produce 'salad' crop. The absence of these bud tubers (sub 30 mm) indicated the plant has halted tuber initiation early into the growth cycle. The presence of ZnNP or CaFeNP did not supress the vegetable development of the treated plants, nor did individual application of FeNP and CaNP supress development as previous discussed. This anomaly required further investigation in the form of repetition of the trial on a larger scale and investigation in to possible suppression of signalling pathways involved in tuber formation.

Data collated form the trial Sax2016 display a repletion of no sig. dif. ($< p = 0.05$) found between control / Chempak treatments and MONP's repeated in Sax2016, for OAW of the tubers. Treatment CaNP+His 32 mg / L displayed a 15.68 % weight increase when compared to champak, and a 15.60% increase against control; which is contradictory to Sax2015 results of control against CaNP+ His 32 mg / L of a 10.78 % loss.

As in Sax2015, there was a sig. dif. comparing < 30 mm between control (Sax2015) and Chempak (Sax2016) against FeNP+His 16 mg / L: $p = 0.0239$ in Sax2015 and a higher significance of $p = 3.38 \times 10^{-6}$ in trial Sax2016. In the Sax2015, control treated with Champak, as was the MONP treatments in both trials; subsequently the 'Chempak' treatment in Sax2016 is the equivalent to Sax2015 'control'.

3.3.2 FeLoad2016

The data collected from Feload2016 enabled the observation of the effects the application of FeNP+His. 32 mg / L had on the tubers physiological and chorological maturation (Lisinska and

Leszczynski, 1989; Lemaga and Caesar, 1990). Using control potatoes, cultivated with no additional N:P:K other than that provided by the compost, aimed to demonstrate correlation to the application of FeNP+His. to yield and tuber size distribution.

With a H_o, "*The application of FeNP+His. 32 mg / L has no effect on yield number or weight*" would have to be accepted as no significant difference was found when applying X^2 statistical analysis. Taking ≥10 % as a significant percentage increase / decrease, it can be stated the application of FeNP+His. 32 mg / L significantly decreased the average number of tubers per plant for Loading 2 (5 w.a.p), - 18.76 % and Loading 3 (8 w.a.p), - 15.11 % (figure 3.18 a). Loading 1 (2 w.a.p) significantly increased > 30 mm tubers (22.53 %), as did application Loading 2, 15.94 %). As seen in figure 3.18 b, Loading 3 application produced tubers of a similar size distribution as control, although producing a lower yield. Application of FeNP+His. 32 mg / L at Loading 1 and 2 produced lower yield but higher number of commercially viable tubers.

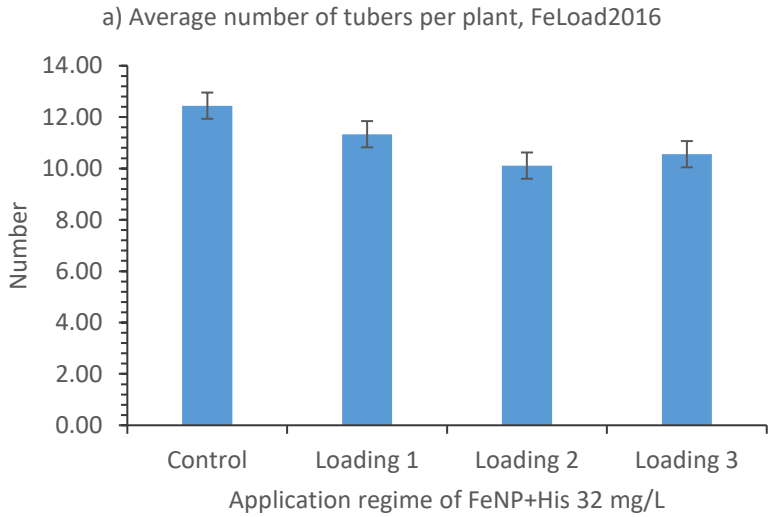

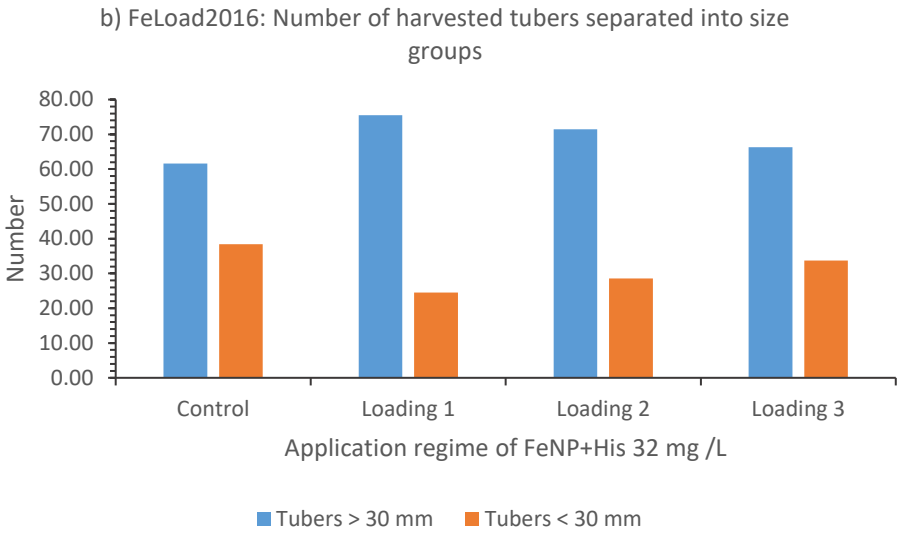

Figure 3.40 Average number of tubers harvested, (a) and the tuber size distribution (b) from trial Feload2016.

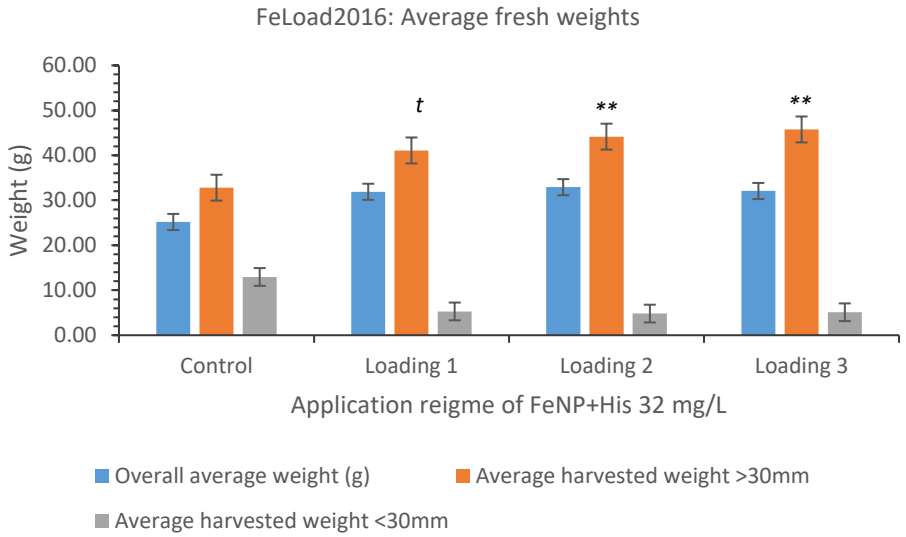

Figure 3.54 Comparison of fresh weights obtained from FeLoading2016 trial. Significant differences found using ANOVA analysis ''. Significant difference found with t-Test 't'. Difference ranked as previously described.*

Using ANOVA single factor statistical analysis, no sif. dif was found when overall all average weights, however, significant increases in percentage fresh weight (> 10%) were found; loading 1 = 26.85 %, Loading 2 = 30.74 and Loading 3 = 27.36 %. From figure 3.19 loading 2 and 3 produced significantly higher number of > 30 mm tubers than control using ANOVA analysis, p = 0.0068 and p = 0.0038 respectively. Loading 2 obtained a p = 0.057, therefore a t-Test one tail was performed and found a sif. dif. of p = 0.0283 against control.

3.3.3 Field2015

Using a H_o *"The application of FeNP+His. 30 mg / L would not influence the yield; number of tubers, size distribution and weight."* This was tested using AVOVA, X^2 and percentage increase/ decrease using levels of significance previously used.

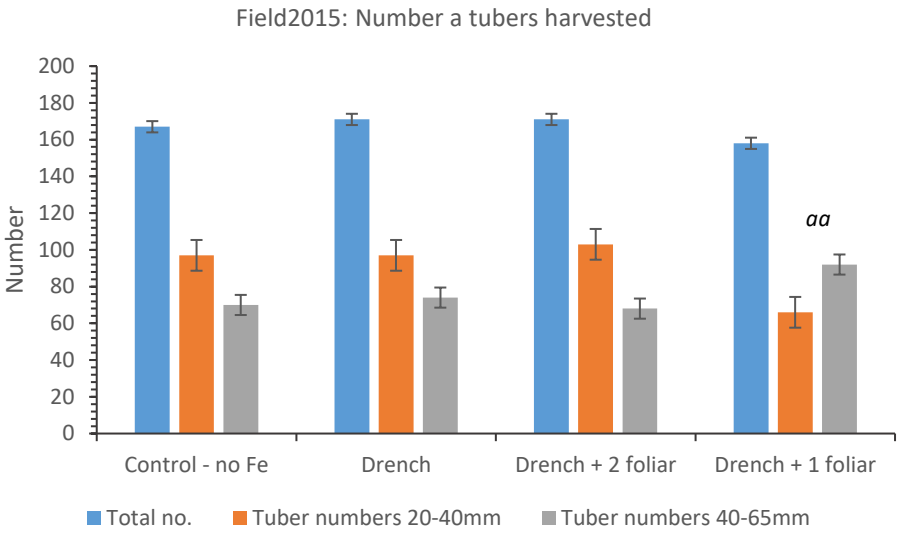

Figure 3.55 Number of tubers harvested from trial Field2016 in collaboration with Branston Ltd, cultivated in Lincolnshire. The "aa" indicates the level of sig.dif. obtained via X2 statistical analysis between 'Control' and 'Drench + 2 foliar" application of FeNP+His 30 mg/L.

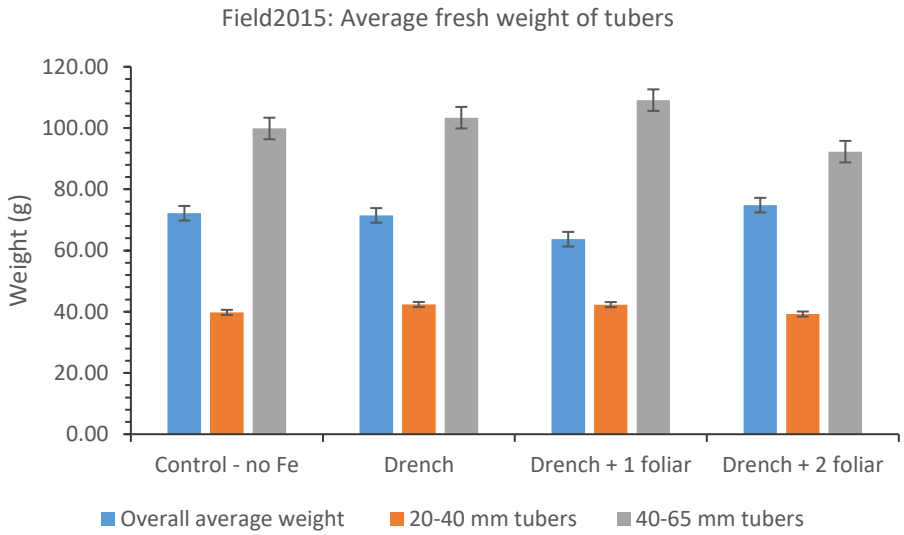

Figure 3.43 Harvested weights of tubers cultivated in trial Field2015 and segregated in to sizes.

Comparing the total number of tubers harvested per application, no significant difference was found using ANOVA single factor or percentage increase / decrease. Using X^2 to distinguish changes to tuber size distribution instigated by application of FeNP+His. 30 mg / L, a significant change was found between 'Control' and application 'Drench + 2 foliar', figure 3.20. This was supported with significant decrease in the number of tubers 20-40mm (-31.96%) and number of tubers 40-65mm (-31.43%) concluding a second application of FeNP had a detrimental effect on yield but not on the weight of the tubers, figure 3.20.

3.3.4 Field rep 2016

To replicate the loading of the FeNP+His. used in the Field2015 trial, a concentration of 50 mg / L was applied at planting as a 'drench' for both 'L1' and 'L2'. A second foliar application was applied at 8 w.a.p for 'L2' application, sooner than in the field trials as a rapid cultivar Swift was used for trial 'Field rep 2016', therefore shortening the growth period and bringing forward the midway foliar application as seen in Field2015. No addition fertiliser was used for control. Due to unforeseen circumstances the trial was harvested five weeks earlier than planned, therefore an increased number of bud tubers (< 30 mm) than usual were harvested. For this reason, figure 5.27 presents the average number of tubers per plant without size segregation.

Using the H_0^1; The application of FeNP+His. 50 mg / L had no effect on the number of tubers harvested" and a second null hypothesis H_o^2; "*the application of FeNP+His. 50 mg / L had no effect on the tuber size distribution*". Figure 3.22 represents the average number of tubers prematurely harvested at 10 w.a.p. L1, drench at planting only, produced 70.18 % more tubers than the control plants with L2, drench and a second foliar application at 8 w.a.p, producing 30.83 %. It can be said the application of FeNP+His. 50 mg / L increased the number of tubers produced thus H_o^1 can be rejected as both 'L1' and 'L2' > 10%.

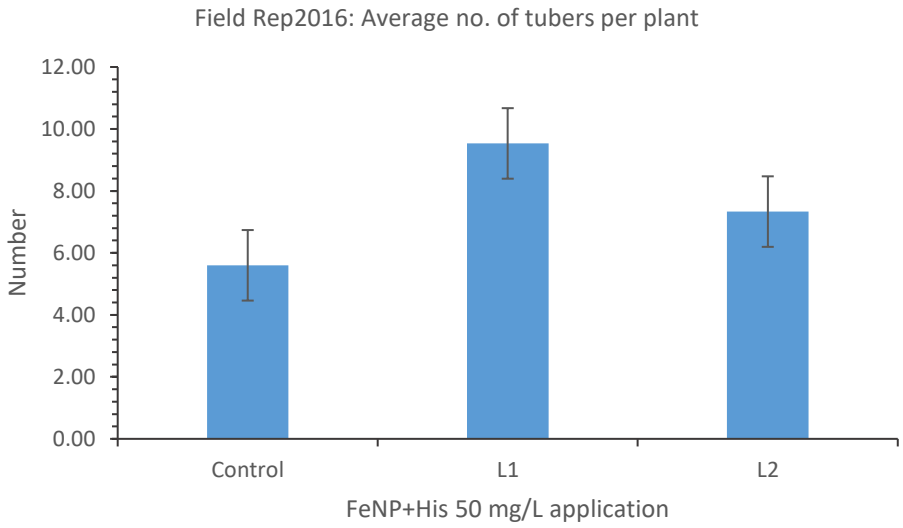

Figure 3.44 Average number of tubers harvested, Field rep 2016.

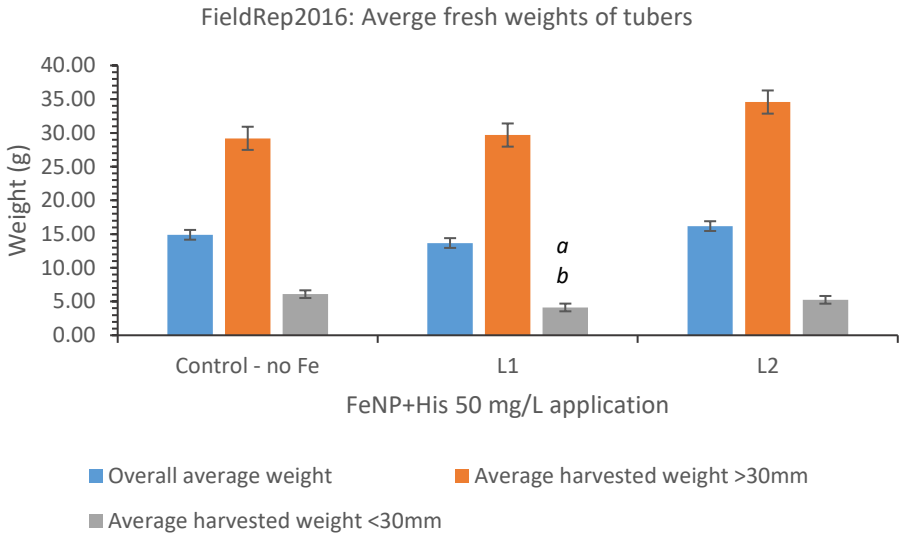

Figure 3.45 Harvested weights of tubers from 'Field rep 2016. 'a' represents sig. dif. between control and L1; 'b' sif dif between L1 and L2.

No sig.dif was found between overall weights, however a significant decrease in tubers < 30 mm can be observed in figure 3.23, between 'Control' and 'L1' (p = 0.0250, *t*-Test one way), 'L1' and 'L2' (p=0.0282, ANOVA single factor). A pattern of increased Fe concentration producing less < 30mm can also in observed in trials Sax2015 and Sax2016, figures 5.20, 5.21 and 5.23 (Feload2016) where the increased exposure of Fe (loading 1) decrease the <30mm tubers. The < 30mm harvested in 'L2' are not credible in the accounting for effect of the second foliar application, as only 2 weeks had preceded since application, not allowing time for the tubulisation / loading response to be observed.

3.4 The effect of MONP on Dry matter (%)

3.4.1 Saxon trials: Sax2015 and Sax2016

The DM % results from Sax2015 trial, presented a sig.dif. decrease when compared to control against treatments FeNP+His. 12 mg / L ($p = 1.5 \times 10^{-3}$), CaFeNP+His. ($p = 1.26 \times 10^{-2}$) and both ZnNP+His applications (8 mg / L, $p = 1.28 \times 10^{-2}$; 16 mg / L, $p = 0.05$) when using ANOVA single factor analysis. It was also noted that the standard deviations for DM% was higher than control in treatments FeNP+His. 8 and 12 mg / L and CaNP+His. 32 mg / L, table 3.8. Treatments that have similar DM % to control (36.67% ± 3.33) are FeNP+His. 16 mg / L (33.03 % ± 2.32) and CaNP+His. 32 mg / L (36.29 % ± 3.60). FeNP+His. 16 mg / L treatment gain a similar yield to control 6.52 tubers per plant to 7.86, whereas the CaNP+His. 32 mg / L gained a significant 25.83 %, concluding that this treatment would be preferable for fry processing and long term storage.

Treatments Sax2015	*Average % DM (± SD)*
Control (with Chempak)	36.67 ± 3.33
FeNP+His 8 mg / L	35.69 ± 3.35
FeNP+His 12 mg / L	32.67 ± 4.24 ^{aa}
FeNP+His 16 mg / L	35.03 ± 2.32
CaNP+His 12 mg / L	35.24 ± 2.45
CaNP+His 32 mg / L	36.29 ± 3.60
CaFeNP+His (24:12)	33.44 ± 2.14 ^{a}
ZnNP+His 8 mg / L	33.39 ± 2.85 ^{a}
ZnNP+His 16 mg / L	34.17 ± 2.01 ^{a}

Table 3.14 Dry mass of tubers (n = 10) harvested from Sax2015, ± SD. Significant difference found using single factor ANOVA are indicated and ranked by 'a' against control.

The industry requires a reliable high DM % ,20-25% (Lulai and Orr, 1979) in order for an optimise production and continuity of product quality. Tubers below DM = 20 % increase in bruising during harvest, disintegrate during cooking and take more time and energy to process resulting in darker product which is less desirable by the consumer. Those with a good DM absorb less oil when frying with a higher chip yield (Pritchard and Scanlon, 1997), desirable texture and flavour. Both trials are

produced tubers above 25 % as the tubers did into undergo prolonged storage, thus retaining matter that would normally degrade.

Treatments Sax2016	*Average % DM (± SD)*
Control	39.59 ± 3.87
Chempak	38.08 ± 3.19
FeNP+His 16 mg/L	38.95 ± 2.53
FeNP+His 32 mg/L	37.87 ± 2.79
CaNP+His 32 mg/L	35.61 ± 3.08 *aaa b*
CaNP+His 64 mg/L	39.67 ± 2.64
His 16 mg/L	36.69 ± 4.04 *a*
His 32 mg/L	37.72 ± 2.71 *aaa*
His 64 mg/L	49.92 ± 5.45 *b*

Table 3.15 Dry mass of tubers (n = 10) harvested from Sax2016, ± SD. Significant diffrences using ANOVA are indicated by 'a' against control and 'b' against Chempak. Differences are ranked as previously described.

The DM % data collected form Sax2015 ranged from 32.67 % (FeNP+His. 12 mg / L) to 36.67% (Control), 4% difference; where as Sax2016 ranges from 35.61 % (CaNP+His. 32 mg / L) to 49.92 % (His. 64 mg / L), a 14.31 % difference, table 3.9.

Significant differences were found, but as significant decreases in all treatments apart from His. 64 mg / L. Chempak obtained a slightly lower DM than control but this could be due to a number of factors. DM % can vary between tubers from the same plant, between cultivar, storage conditions, location, mineral composition of strata and tuber (Lulai and Orr, 1979; Lisiniska and Leszczynski. 1989). Locational changes affect DM, yield and growth rates are concerned with soil, large altitude range, weather influenced i.e. temperature and rainfall, strata composition and mineral availability. To eliminate these influences, the same cultivar was used from the same seed potato producer, brand of compost, time of year, as well as containers with the application and watering regime. The DM samples were taken from tubers of similar size, to ensure similar chronological age and taken within 72 hours of harvest thus reducing storage influence. Location changes between trials were minimal as Clifton greenhouse coordinate are; 52.90594N, 1.19332W, altitude 53 m; Brackenhurst poly-tunnel 53.06321N. 0.96585W, altitude 72 m.

3.4.1 FeLoad2016, DM %

No sig.dif was found using ANOVA or t-test. Percentage increase and decreases were also found to be insignificant. It can be concluded that with a H_o "*The application as no effect on the dry mass percentage of tubers*" is to be accepted, table 3.10.

FeNP+His 32 mg / L application	*Average % DM (± SD)*	*Percentage difference against 'control' (%)*
Control	38.56 ± 3.22	
Loading 1	37.01 ± 3.95	- 4.02
Loading 2	37.93 ± 2.81	- 1.63
Loading 3	39.44 ± 3.68	2.28

Table 3.16 DM % obtained from tubers harvested from trial Feload2016.

5.4.3 Field2015 and Field2016

The DM % of tubers exponentially increase after tuber initiation occurring 30 – 40 days after planting at a liner increase until a foliage senescence at approximately 90-120 days (Lisinska and Leszcaynski, 1989; Kolbe and Stephan-Beckmann, 1997). This rate is influenced by genetic and environmental variations. Comparing data with that published by Kolbe and Stephan-Beckmann, 1997, the DM % loss at harvest was comparable, figure 3.24. When comparing the two data sets, Kolbe and Stephan-Beckmann (1997) use d.a.e (days after emergence) which commences on the day the seed tubers are taken out of storage and allowed to chit. A period of 14 days is allocated until the seed tuber is planted, therefore in order to compare two data sets, 2 weeks is added to the data collected from trial Field2015 where the period of time is measured in weeks after planting (w.a.p.).

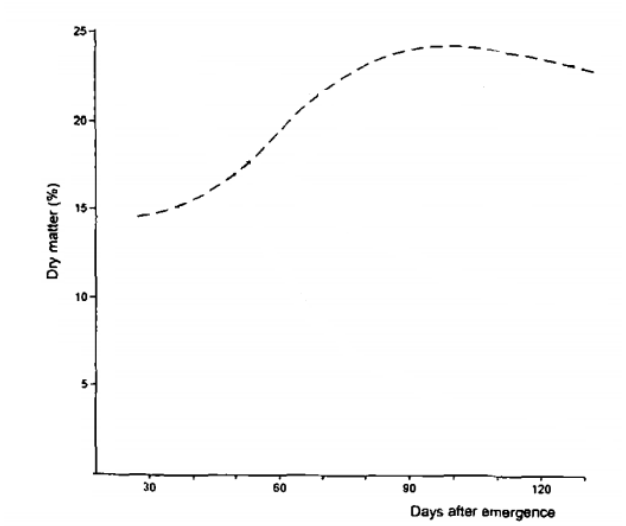

Figure 3.46 Development of dry matter percentage in potato tuber over time. Adapted from Kolbe and Stephan-Beckmann, 1997.

Using the following null hypothesis H_o^1 *"The application of FeNP+His. 30 mg / L does not affect the DM % of the tuber at harvest"*; and an alternative hypothesis H_1 *"The application of FeNP+His. affect the DM % loss."* which will be signified by the lack of sig.dif. DM % decrease.

Published data collated over two seasons (Kolbe and Stephan-Beckmann, 1997) demonstrating the DM % variations throughout the tubers growth stage (figure 3.24) with a decreased of 6.25 % from optimal dry weight (378 g, 24 %) at 105 days after emergence (17 w.a.p.) until harvest at 135 days after emergence (21 w.a.p), 356 g (22.5 % DM).

A number of tubers were collected at 12 w.a.p, n = 20, during trial Field2015. Using ANOVA single factor statistical analysis, there was a very high sig. dif. (<p=0.001) of DM % loss between DM % 12 and 22 w.a.p for 'Control', 'Drench' and 'Drench + 2 foliar' (figure 3.25). The application 'Drench + 1 foliar' attained a lower DM% loss of 3.45 %. All applications of FeNP+His. reduced the DM % loss compared to 'Control'. Therefore, H_1 is accepted for the application 'Drench + 1 foliar' due to the lack of significant decrease in DM %.

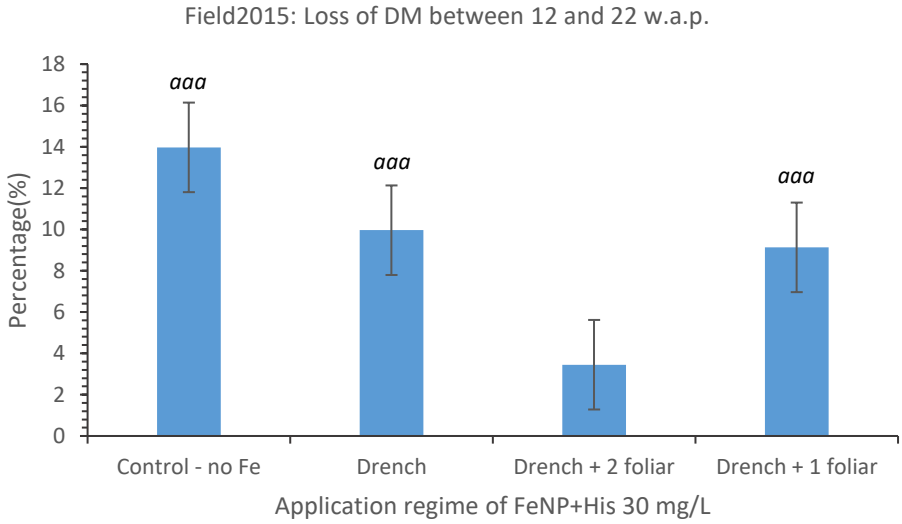

Figure 3.60 Percentage loss of DM % between 12 and 22 w.a.p. Sig.dif. ranked and noted by 'a' between DM% 12 and 24 w.a.p.

From table 3.10, no sig.dif. between 'Control' and other applications of FeNP+His. 30 mg / L at 12 w.a.p in Field2015. There was a significant increase in DM %. between 'Drench' application and 'Drench + 1 foliar' and Drench + 2 foliar' indicating an increase in tuber growth rate when FeNP+His. 30 mg / L was applied at planting thus rejecting H_o^1. At harvest, 22 w.a.p, all applications were found to have a sig. dif. higher DM % than that achieved by 'Control' plants, therefore rejecting H_o^1, table 3.11. It was noted that SD was constantly lower for 'Control' plants and greatest for 'Drench + 1 foliar' which attained the lowest DM % and percentage loss.

Treatment	*Average DM % ± SD at 12 weeks*	*Average DM % ± SD At harvest*
Control - no Fe	39.94 ± 2.69	34.36 ± 2.97
Drench	41.06 ± 3.52	36.97 ± 3.41 ^{aa}
Drench + 1 foliar	38.82 ± 3.05 ^{bb}	37.48 ± 4.73 ^{a}
Drench + 2 foliar	40.76 ± 3.45 ^{bb}	37.04 ± 3.99 ^{aa}

Table 3.17 DM % obtained from trial Field2015. Sif. dif is depicted against 'control' by 'a' and between application 'Drench + 1 foliar' and other applications as 'b'.

Dry mass percentage from Field2016 obtained insignificant different data, apart from Maris piper from the second site, table 3.12 (p=0.0160, ANOVA single factor). It was observed the Fe applications from

all Fe treatments across the two sites produced tubers with a slight increase in DM % than the commercial controls.

Variety and treatment	*Site 1*	*Site 2*
Maris piper - Control	39.49 ± 3.62	36.86 ± 3.50
Maris piper - Treated	39.91 ± 3.31	38.87 ± 3.79 [a]
Inca bella - Control	38.38 ± 2.19	39.13 ± 1.94
Inca bella Treated	39.06 ± 2.01	39.71 ± 2.18

Table 3.18 DM % from Field2016. Control tubers were cultivated with commercial fertilisers, with 'treated' applied with an additional drench application of FeNP+His at planting, replicating Field2015 application 'Drench'.

Comparing 'drench' application from Field2015 and Field2016 trials, an increase in DM% of 7.59 and 5.45 % were consistently found with a fluctuation of 0.38 SD.

3.4.4 Field rep 2016

From table 3.13 below, applications 'L1' and 'L2' produce tubers higher in DM than those from control. Only 'L1' application of FeNP+His. 50 mg / L produced tubers with a sig. dif. increase in DM% ($p=0.0438$, ANOVA single factor). Using H_0; "*application of FeNP+His. does not affect the DM% of tubers*" can be rejected for 'L1'.

Application of FeNP+His. 50 mg / L	*Average DM %*
Control	28.61 ± 2.91
L1	32.56 ± 4.97 [a]
L2	31.35 ± 4.84

Table 3.19 DM % data from trial replicating applications from Field2015 under poly-tunnel conditions.

Unlike data collected from Field2015, the second application using application via foliar spray, there was no influence of FeNP+His. 50 mg / L. As discussed in section 5.3.4, the time between foliar

application and harvest was not sufficient for a response to be determined, however, both L1 and L2 saw a 66.32 to 70.79 % increase.

3.5 The effect of MONP on mineral content of crop

3.5.1 Ca fortification in potato tubers hydroponic and compost propagation: H2015, Sax2015, and Sax2016.

Under hydroponic conditions, CaNP+His. 12 mg / L obtained a sig. dif. increase in Ca content compared to control and the higher Ca application of 32 mg / L, which tubers contained similar amounts of Ca to the control tubers. This pattern was repeated in Sax2015 trial, with significant decrease obtained using ANOVA single factor analysis. Using a null hypothesis, H_o; "*application of CaNP does not influence the content of Ca in potato tubers",* is rejected for applications of CaNP+His. 32 mg / L in H2015 and Sax2015. The H_o is again rejected for the application if CaFeNP, as the Ca content of the tuber is significantly higher than other CaNP applications and control. Comparing Ca fortification of concentrations 12 and 32 mg / L, the average concentration of 221.45 mg / L from the tubers fortified with calcium ferrite suggested the presence of Fe, increases Ca uptake resulting in fortification of the whole tuber. It has been published that the uptake of Ca^{2+} is not only regulated by the available Ca^{2+} in the rhizosphere but also by the presence of other ions, including Fe (Lisinska and Leszcaynski, 1989; Mäder *et al*., 2002).

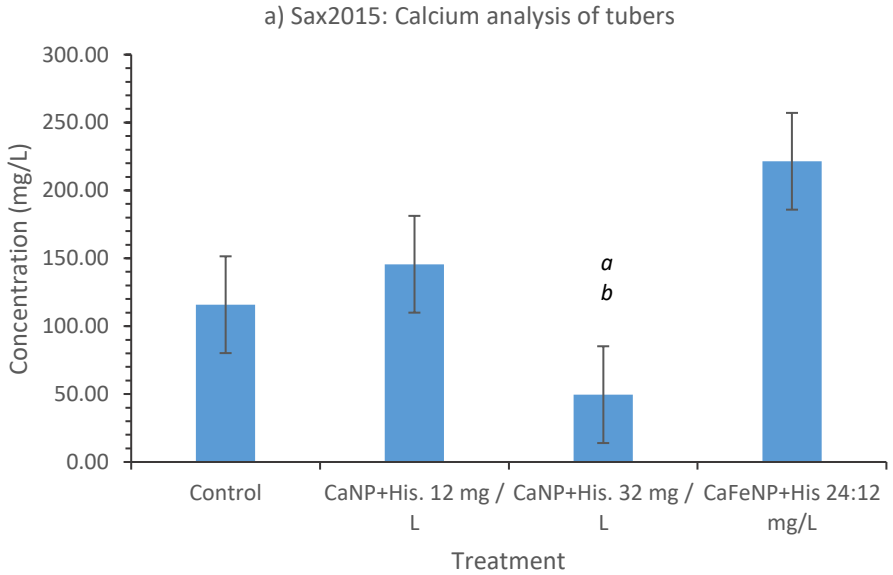

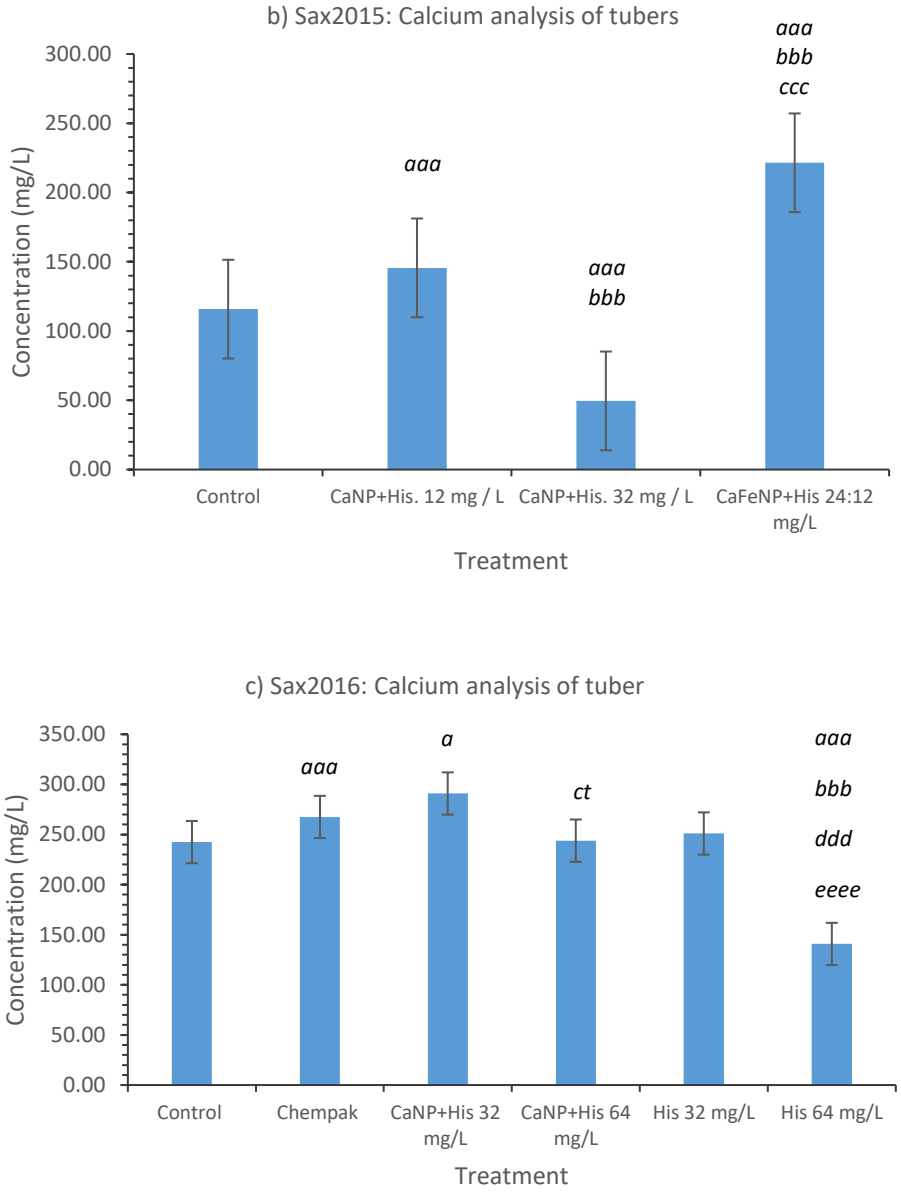

Figure 3.48 Ca content of whole tuber a) H2015; influence of MONP in a hydroponic system on the mineral content of tubers. Sig.dif. found between Ca applications 'a' against control, 'b' bwteen Ca applicationsa. b) Sax2015; calcium content of tubers propagated in greenhouse conditions in multipurpose compost. Sig. dif. indicated by the following: a = against control, b = against 12 mg / L, c = against 32 mg / L. c) Sax2016; Ca of tubers cultivated under poly-tunnel conditions in multipurpose compost. Sig. dif. indicted by: a = against control, b = against Chempak, ct = CaNP+His. 32 mg / L, d = CaNP+His. 64 mg / L, e = His. 32 mg / L. Sig. dif. obtained via ANOVA, where indicated by 't' the sig. dif. obtained via t-Test two sample.

Sax2015 and H2015 results (figures 3.26a and 3.26b) suggested the optimal Ca fortification feed would be 12 mg / L in the absence of Fe. This was not repeated in Sax2016 (figure 3.26c) as the results display a significant increase between control and 'CaNP+His. 32 mg / L', p = 0.0202, and a significant decrease in Ca content between Ca concentrations 12 and 32 mg / L when analysed using t-Test, p = 0.0374. There was no significant increase or decrease in the Ca content when compared to 'control' or

'Chempak', therefore accepting H_o for this application. The influence of histidine was investigated and found to achieve Ca concentrations that are of no significance (His. 32 mg/ L) or a significant loss, indicating the presence of calcium oxide nanoparticles have successfully increased the content of the potato tubers.

Fluctuations in uptake (i.e. preference in Ca concentration) are possibly due too climatic (extremes of heat) and genetic conditions (Lisinska and Leszcaynski, 1989; Tekalign and Hammes, 2005; White and Bradshaw *et al*., 2009) that are beyond the remit of these trials and present the possibility of further investigation.

To observe Ca uptake, the samples were segregated as previous described in section 3.1.4. A high concentration of Ca is retained in the skin than in the flesh of the tuber, figure 5.40. It is expected that the skin of the tuber will contain a higher proportion of Ca compared to the rest of the tuber as this is the interactive surface to the rhizosphere. The second highest area would be the pith as this area of the tuber contains the xylem, where the Ca^{2+} is exclusive transported with transpiration as the main driving force for transportation (Kirby and Pilbeam, 1984; Busse and Palta, 2006). It has been published that the main uptake of calcium occurs via the stolon root system and tuber rather than the main root system due to a more established xylem system (Kirby and Pilbeam, 1984), however Ca retention in the tuber is relatively low due to low transpiration rates as tubers are surrounded by moist soil, therefore low transpiration rate occurs in the tuber (Busse and Palta, 2006).

Figure 3.27a and 3.27b, show the concentration of Ca through the tuber with table 3.14, representing the percentage of Ca distributed through the tuber. Displaying percentage of mineral distribution allows observation of the transfer factor (TF) of the MONP (Bradfield *et al*., 2017). The TF allows to establish the ability of the CaNP to fortify the tuber (Ebbs *et al*., 2016; Bradfield *et al*., 2017).

Significant increase in Ca concentration in the skin was found in tubers fed with calcium ferrite. These tubers also gained significant amount of Ca in the flesh of the tuber and other Ca applications. As previously observed in figure 3.27b, the amount of Ca is significantly lower than other applications, leading to the suggestion that the Ca concentration is at a phytotoxic level and retained in the skin to avoid cellular damage. Sax2016 trial contradicts this, as the Ca concentration in the flesh areas of the tuber obtain significant increases in Ca over 'control' and 'Chempak' treatments, especially in the perimedulla / medulla region where transportation to the rest of the plant occurs (Lisinska and Leszcaynski, 1989).

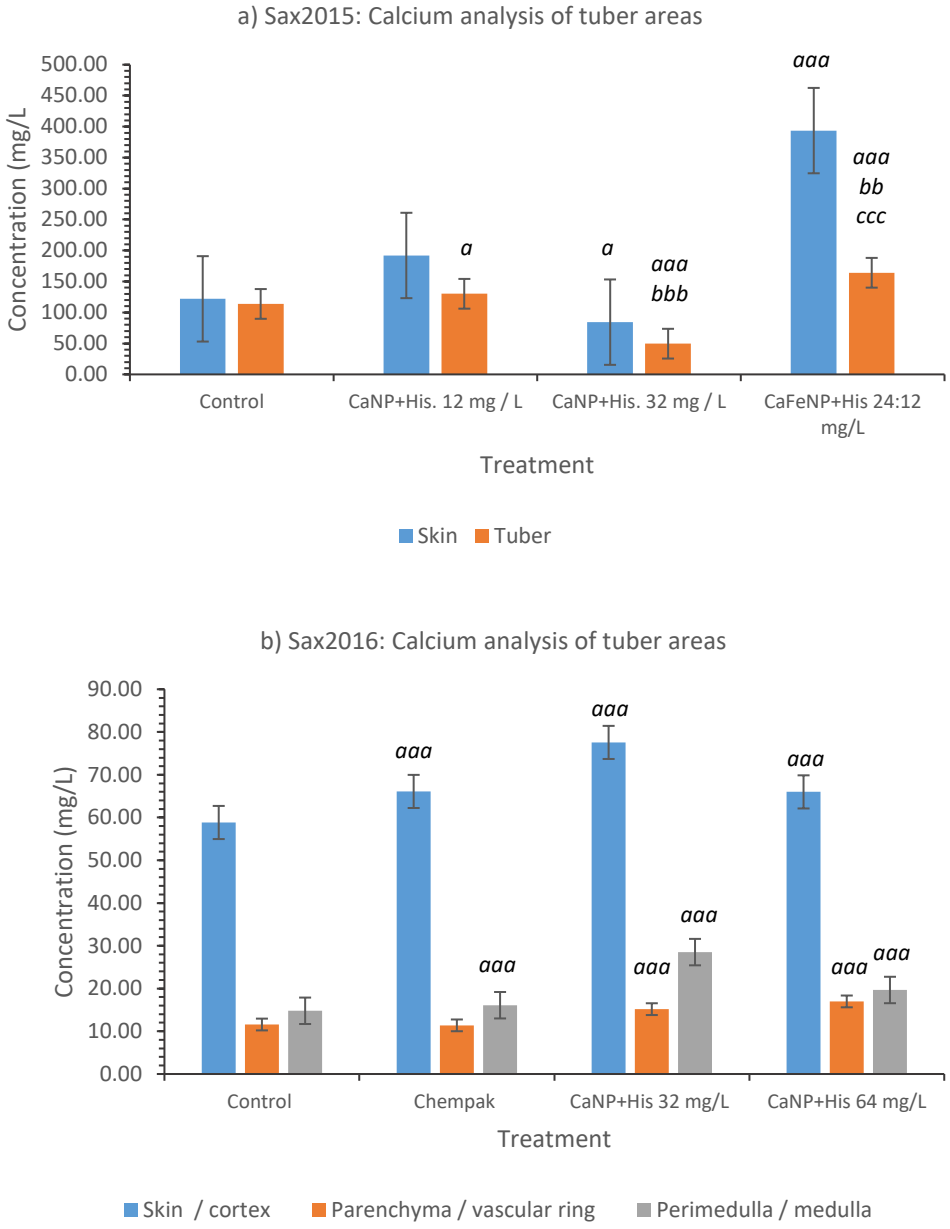

Figure 3.62 Ca content of areas of tuber. a) Sax2015 Sig. dif. indicated by the following: a = against control, b = against 12 mg / L, c = against 32 mg / L. b) Sax2016 Sig. dif. indicted by: a = against control. Sig. dif. obtained via ANOVA.

	Skin / cortex	Tuber	Parenchyma / vascular ring	Perimedulla / medulla
Control: Sax2016	69.05	30.95	13.59	17.36
Chempak: Sax2016	70.64	29.36	12.16	17.20
Control: Sax2015 (equiv. chempak2016	51.73	48.27		
CaNP+His. 12 mg / L: Sax2015	59.60	40.40		
CaNP+His 32 mg/L :Sax2016	63.97	36.03	12.51	23.52
CaNP+His. 32 mg / L: Sax2015	62.98	37.02		
CaFeNP+His. (24:12 mg / L): Sax2015	70.58	29.42		
CaNP+His 64 mg/L: Sax2016	64.30	35.70	16.55	19.15
His 32 mg/L:Sax2016	74.72	25.28	9.23	16.06
His 64 mg/L: Sax2016	59.34	40.66	21.27	19.38

Table 3.20 Calcium distribution (percentage) and comparison between trials Sax2015 and Sax2016.

Observing the percentage Ca distribution through the tuber, it becomes clear the application of CaNP+His. 32 mg / L, has the same distribution of Ca in consecutive years, therefore a consistent TF. It was also noted the His. 32 mg / L tubers had a higher Ca distribution in the skin than the CaNP counterparts. Amino acids increase the assimilation of minerals from the rhizosphere into the root / tuber, > 90 % are chloride, nitrates and other organic salts (Lisinska and Leszcaynski, 1989). From this data, it can be suggested that the calcium oxide nanoparticle offers a more bioavailable Ca as is it transported more freely through the tuber into the flesh, particularly into the perimedulla / medulla region, where it is then transported throughout the plant.

3.5.2 Fe fortification in potato tubers hydroponic and compost propagation; H2015, Sax2015, Sax2016, Field2015 and Field2016.

From the data obtained from hydroponic and compost propagation, a discrepancy of optimal concentration of FeNP application was observed, figure 3.28. Tubers propagated with FeNP+His. 12 mg / L under hydroponic conditions obtained an increase of 55.60 %, with a significant decrease of Fe when fed with FeNP+His. 16 mg / L, suggesting a detrimental effect to the plant as the growth rate is

decrease at this concentration. Sax2015 application of FeNP+His. 12 mg / L saw an insignificant increase of Fe content using ANOVA signal factor analysis nonetheless obtained a 26.71 % increase. A significant increase of Fe was found in the 16 mg / L, figure 3.28b, against all other applications including 12 mg / L ($p = 6.95 \times 10^{-6}$). This significant increase was repeated in the Sax2016 trial when compared against control plants and a 6.85 % increase against Chempak (comparable to 'control Sax2015'). Both trials using compost as the cultivation media (Sax2015 and Sax2016), there was a noted tolerance to the higher FeNP+His concentration. The composition of the compost media enables a retention of the Fe due to varying number of composites (i.e. sand, clay and organic matter) found in soil and compost. These constituents differ in negative charge, which attracts the positive charge of the Fe^{2+} and Fe^{3+}, thus enabling a buffering effect to the tuber and root system (Hinsinger, 1998). In a hydroponic environment, the reduced retention ability of the pebbles, exposes the tuber and root system to more readily to the nutrients, in theory enabling increased uptake.

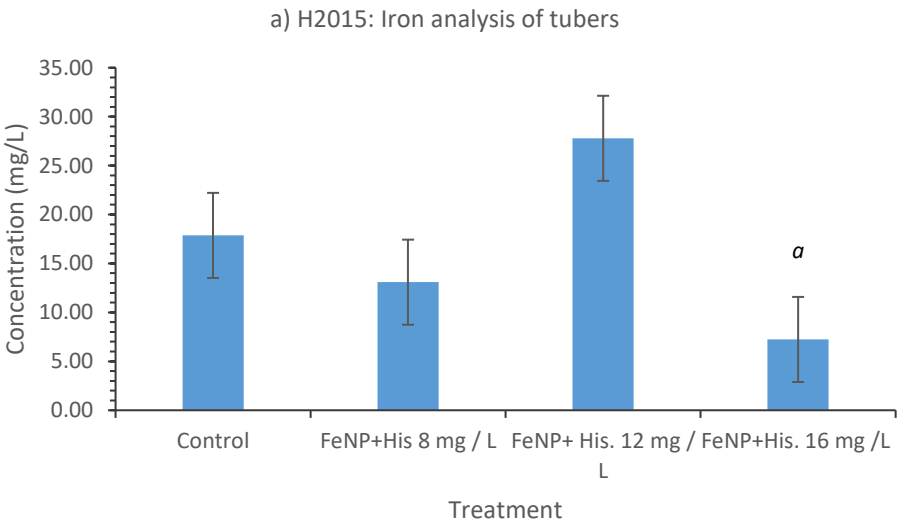

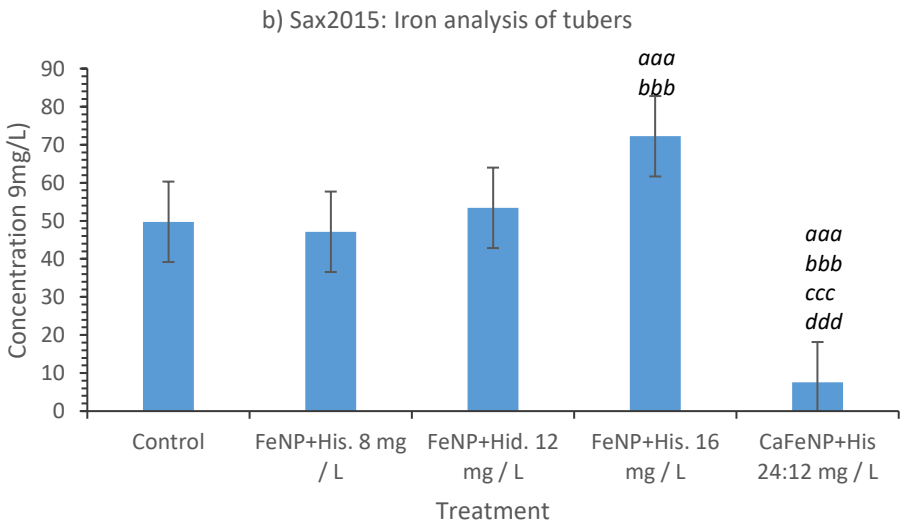

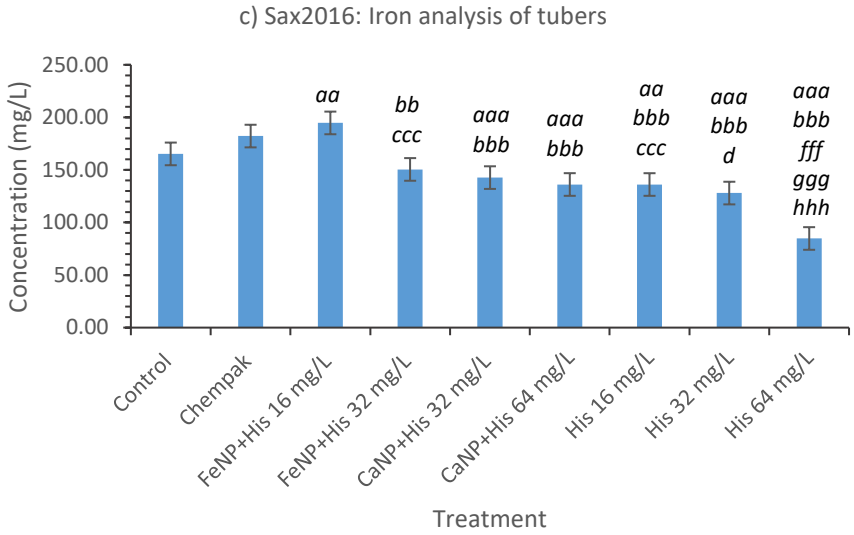

Figure 3.63 Fe content of whole tuber. a) H2015; influence of MONP in a hydroponic system on the mineral content of tubers. Sig. dif. between 'Control' and 'FeNP+His.16 mg / L' = a. b) Sax2015; Fe content of tubers propagated in greenhouse conditions in multipurpose compost. Sig. dif. indicted by: a = against control, b = against Chempak, c = FeNP+His. 16 mg / L, d = FeNP+His. 32 mg / L, e = CaNP+His. 32mg / L, f = CaNP+His. 64 mg / L, g = His. 16 mg / L, h = His. 32 mg / L. Sig. dif. obtained via ANOVA.

Using a H_o *"the application of FeNP did not affect the Fe content of the tubers",* the Fe content of tubers treated with FeNP+His and His equivalent concentration. From figure 3.28c, it is shown the FeNP have a significantly increased amount of Fe, (16 mg / L, $p = 6.81 \times 10^{-7}$ and 32 mg / L, $p = 0.0148$), concluding the FeNP has fortified the tuber and not the increased mineral assimilation amino acids can induce (Sánchez *et al*., 2005; Tegeder, 2012). With these results the H_o is rejected.

The tubers treated with calcium oxide nanoparticles where also analysed for their Fe content to compare / observe any suppression of Fe. From 3.28, the data shows a significant suppression of Fe when the CaFeNP+His was applied, although a significant increase in Ca content was obtained.

Data from segregated areas of the tuber displays the translocation and potential utilisation of Fe sources from the nanoparticle throughout the plant. Figure 3.29a, demonstrates the high proportion of Fe is retained in the skin (Lisinska and Leszcaynski, 1989). The application of 'FeNP+His. 16 mg / L' in both trials significantly increased the Fe concentration in skin and tuber over 'control' and 'Chempak' concluding the FeNP+His. is passing thought the pores in the cell wall, however, when the data is displayed in percentage distribution to observe TF. A decrease in the amount of Fe in the tuber areas differs between trials. This is possibly due to variation in climatic conditions or genetic variation (Lisinska and Leszcaynski, 1989) that are beyond the control of the trial conditions.

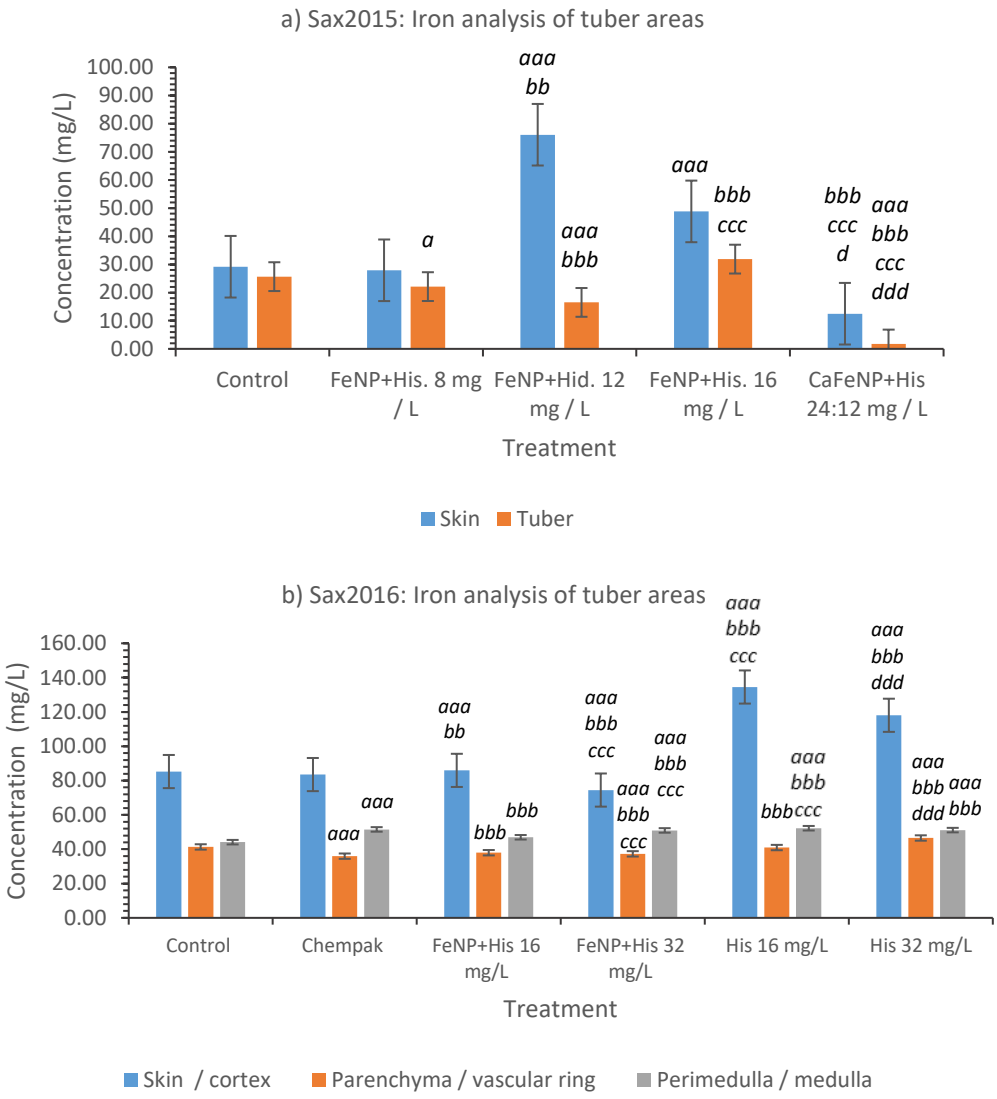

Figure 3.64 Fe concentration in areas of tubers. a) Sax2015; sig dif indicated by; a = control, b = FeNP+His. 8 mg / l, c = FeNP+His. 12 mg / L, d = FeNP+His. 16 mg / L. b) Sax2016; sif. dif indicated by; a = control, b = Chempak, c = FeNP+His. 16 mg / L, d = FeNP+ His. 32 mg / L. Sig. dif. obtained via ANOVA.

Iron concentration in the tubers treated with His. displayed a high concentration retention of Fe in the skin, 16 mg / L = 134.54 mg / L and 32 mg / L = 118.06 mg / L (figure 3.29b) with 59.07 to 54.73 %. Due to the nanoparticles ability to passively enter the skin via the pores in the cell wall (Navarro, *et al*., 2008), plus amino acids increase the assimilation of nitrogen and chelation of metal present in the rhizosphere, increases uptake of FeNP in the skin (Sánchez *et al*., 2005; Tegeder, 2012). Due to the high Fe^{+2} intake, it is possible that the excess Fe is retained as the protein ferritin to prevent cellular

oxidation damage until it is chelated and transported via protein transported to organelles that utilise the Fe^{2+} (Marschner, 2011; Zhang *et al*., 2014).

The distribution observed from 'FeNP+His. 32 mg / L' displays a phenomenon among the percentage distribution as the total tuber percentage, 54.24 % is higher than skin, concluding a high TF. This data also displays a high proportion of the Fe located in the centre of the tuber (perimedulla / medulla), 31.31 % when applied at 32 mg / L.

It is well documented that high content of Ca in calcareous soil limits the reduction of Fe^{3+} and uptake of Fe^{2+} coursing the deficiency chlorosis (White and Broadley, 2009; Marschner, 2011). The high pH of calcareous soils reduces the solubility of iron oxides by reducing H^+. Ca may be transferred by mass flow into the tuber / root system and accumulates in the rhizosphere, consequently calcium carbonate precipitation, with the formation of bicarbonate when increased CO_2 is produced by a developing root system (Hinsinger, 1998; White and Broadley, 2003; Pradsad and Djanaguiraman, 2017).

$CaCO_3 + CO_2 + H_2O \rightarrow Ca^{2+} + HCO_3^-$

Plants suffering from chlorosis display stunted growth, yellowing of the vein area of young leaves and a significant reduction in yield. No yellowing or discolouration of the leaves treated with CaNP or CaFeNP where observed. Average height increase was 9.95% above control, showing no detrimental effect to the plant when fed CaFeNP. There was a decrease in the average number of tubers per plant, however, the average tuber weight was significantly higher than control and as previously mentioned, tuber initiation was shortened, signified by the lack of < 30 mm when harvested. Therefore, with these number of contrasting results it is difficult to say without further investigation that the application of CaFeNP would course chlorosis or be an application to further improve the Ca fortification.

Fortification of tubers propagated in collaboration with Branston (Field2015 and Field2016) show an increase in Fe content, figures 3.30 and 3.31.

Statistical comparison to control (T1) in trial Field2015 showed no significant difference for data obtained from midway (12 weeks after planting) and harvested (21 weeks). When ICP data from midway T2 tubers (drench only application), the T2 tubers were found to contain highly significantly lower than T3 ($p = 7.88x10^{-6}$) and T4 ($p = 1.25x10^{-3}$). However, at the end of the trial, T2 tubers gained a highly significant increase in Fe content over T4 ($p = 6.16x10^{-3}$).

Highly significant Fe fortification where found in all treatments when comparing midway Fe content and harvested Fe content (figure 3.30). Generally, the foliar applications gained a reduced amount of Fe in tubers at the end of harvest (T3 = 67.58 mg / L and T4 = 55.57 mg / L) compared to drench only

applied FeNP+His, 50 mg / L, T2. The foliar applications appear to inhibit the Fe uptake from the soil source suggesting the Fe from the foliar application it utilised by the leaves in the process of chlorophyll production, reducing the requirement to take up Fe via the root system thus reducing the amount of Fe passing and stored within the tuber.

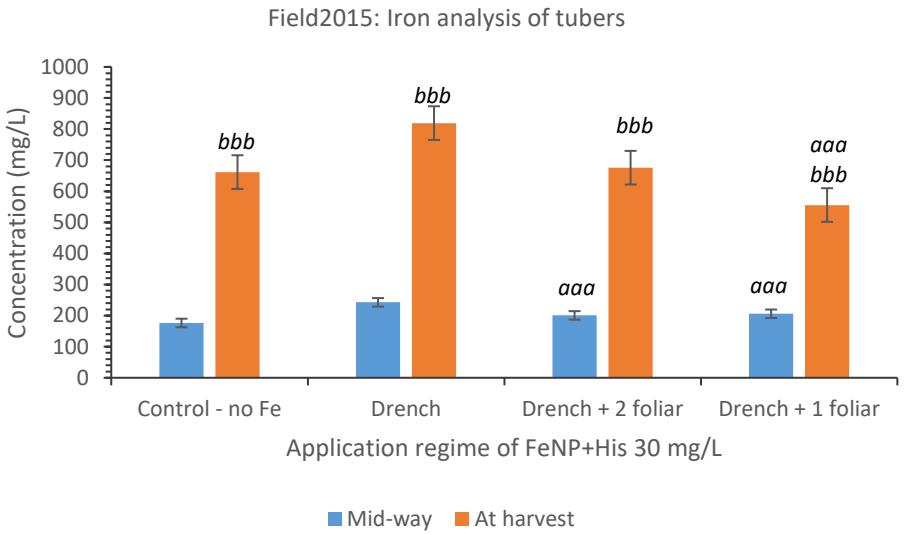

Figure 3.65 Fe content of tubers from trial Field2015, propagating the red variety Mozart. Significant difference against drench application = a, between midway and harvest Fe content = b.

As the drench only (T2) application of FeNP+His, Field2015 was deemed a successful fortification method, the trial was repeated in two separate sites (A and B) within 5-mile radius, but site A contained an increase in loam than B. Both sites were not labelled as Fe deficient as with the previous site used in trial Field2015.

Two different varieties of potato were cultivated in both sites to observe the difference in response to an increased Fe availability Lisinska and Leszcaynski, 1989. Figure 3.31a. Both varieties of tuber increase in Fe content when exposed to FeNP+His, 50 mg / L, at planting through a drench application with Maris piper gaining a significant increase ($p = 0.0108$, 36.95% increase) with Inca bella gaining 6.41 % increase in Fe content.

From figure 3.31b, the influence in soil composition had an effect on the Fe content of the tubers, although with the application of FeNP+His., similar concentrations of Fe were obtained in both varieties. The increased loam at site A, increased the Fe in the control tubers in the Inca bella tubers, (6.38 mg / L, 13.27 %), but decreased the Fe content when compared to the sandy soil site B Maris

pipers, (18.00 mg / L, 30.31 %) observing the preference of varieties to differing soil environments, table 3.15 Lisinska and Leszcaynski, 1989.

	Percentage increase in Fe content (%)	
	Site A	Site B
Inca bella	1.61	11.85
Maris piper	68.56	14.91

Table 3.21 Percentage increase in the content of Fe between control and FeNP+His. application from trial Field2016

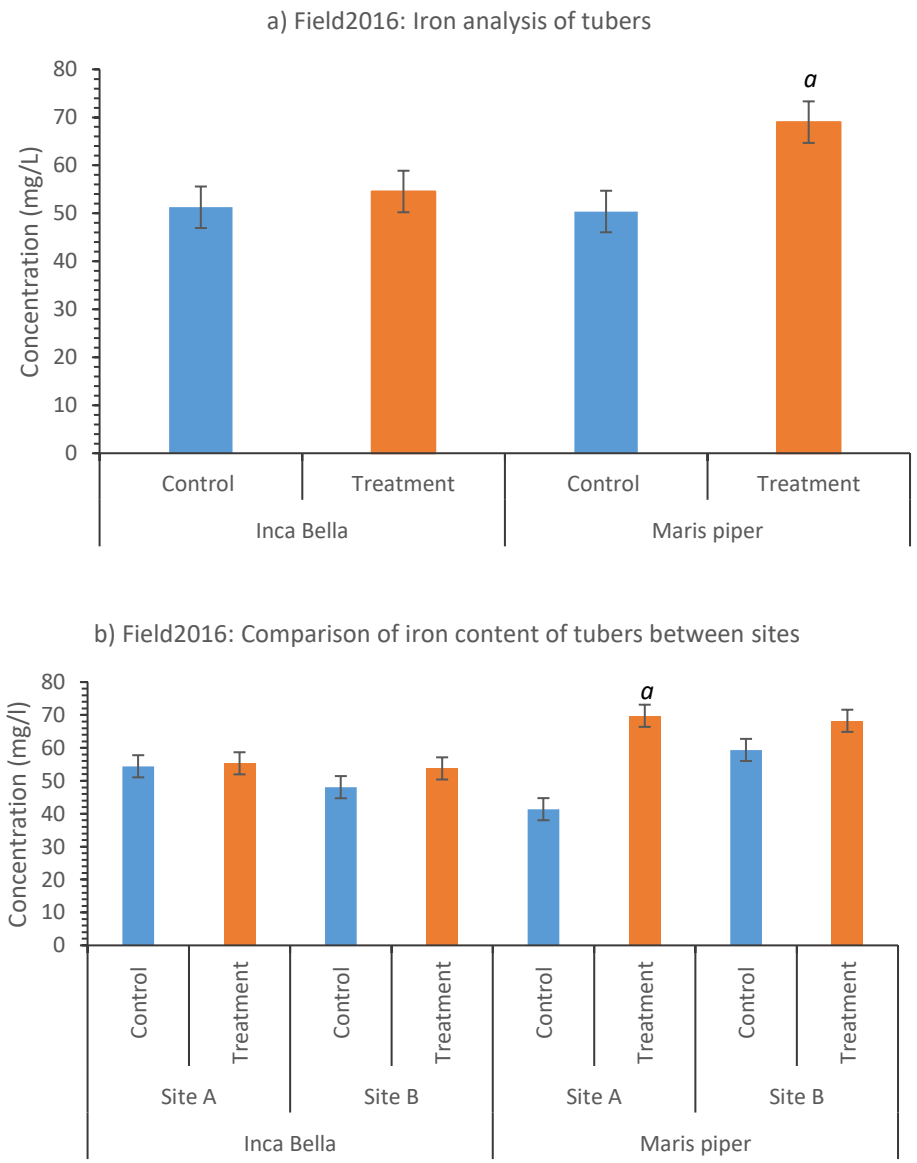

Figure 3.66 Field2016 ICP data showing the Fe content of tubers. a) Average Fe content collated from both sites comparing control and FeNP+His. treated. b) Comparison of tuber Fe content between sites, treatments and variety. Significant differences between control and treatment are indicated by a.

3.5.3 Zn fortification in potato tubers hydroponic and compost propagation: H2015, Sax2015, and Sax2016.

In both trials, H2015 and Sax2015 gained significant increases in Zn content. The 16 mg / L concentration produces a significant increase in Zn content in trial H2015 and a significant decrease was obtained in Sax2015.

The significant increase in Zn content in tubers increased with increasing ZnNP+His. application was noted in H2015 suggesting a successful fortification application however, the foliar growth was severely stunted then treated with ZnNP+His. leading to question the phytotoxic effect of ZnNP in a hydroponic system. In Sax2015 trial, figure 3.32a, contained greater amount of Zn compared to H2015 tubers with no detrimental effect to growth rate. This is due to the additional Zn present in the compost as the only source of Zn in the hydroponically propagated tubers was ZnNP+His. The decrease of Zn content at 16 mg / L in Sax2015 could be explained by published investigations into the uptake in ZnO nanoparticles presented the rapid aggregation of ZnO in an aqueous solution when in the nutrient solution is not continually agitated as in a hydroponic system (Lisinska and Leszcaynski, 1989). The increased size of aggregated ZnNP into the μm range, decreases the bioavailability as the particles are larger than cell wall pores (Sondi and Salopek-Sondi, 2004; Brayner at al., 2006; Navarro *et al*., 2008) Nano-scale pores 5 – 20 nm (Lin and Xing, 2007; Navarro *et al*., 2008)] located in the cell wall, allow the passive transportation of small molecules (< pore) while limiting the passage of larger modules (Lina and Xing, 2007). Zinc oxide nanoparticles also bind strongly with various organic ligands present in compost and soil, as Fe (Clemens, 2014), therefore, an increased concentration of ZnNP+His. along with the effects of nanoparticle aggregation, may have contributed towards the decrease in fortification of the tuber as observed in figure 3.32b.

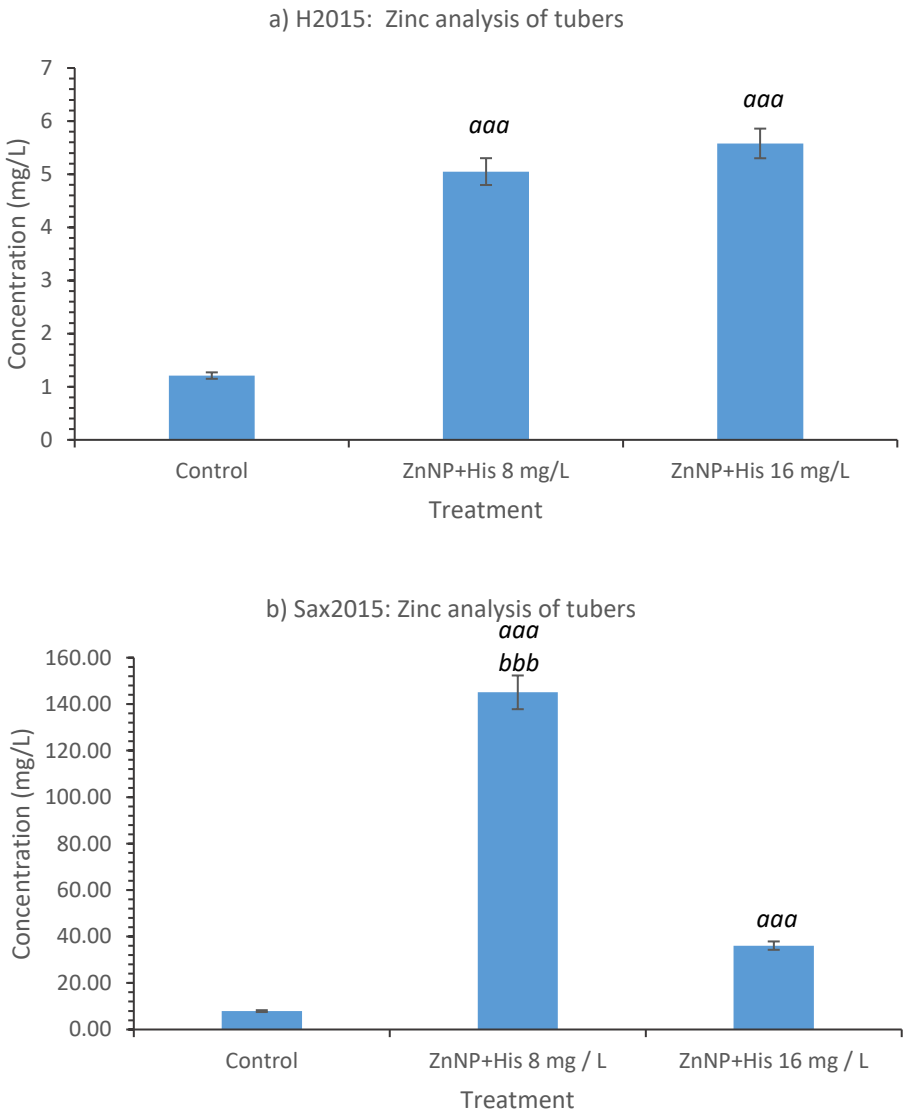

Figure 3.67 Average Zn concentration of tubers. A) H2015, hydroponic propagation; 'a' indicated the sig. dif. between control and ZnNP+His. applications. B) Sax2015, under greenhouse conditions with multi-purpose compost. Sif. dif. against control, a; between Zn applications, b. Statistical analysis via ANOVA single factor and ranked by p value as previously described.

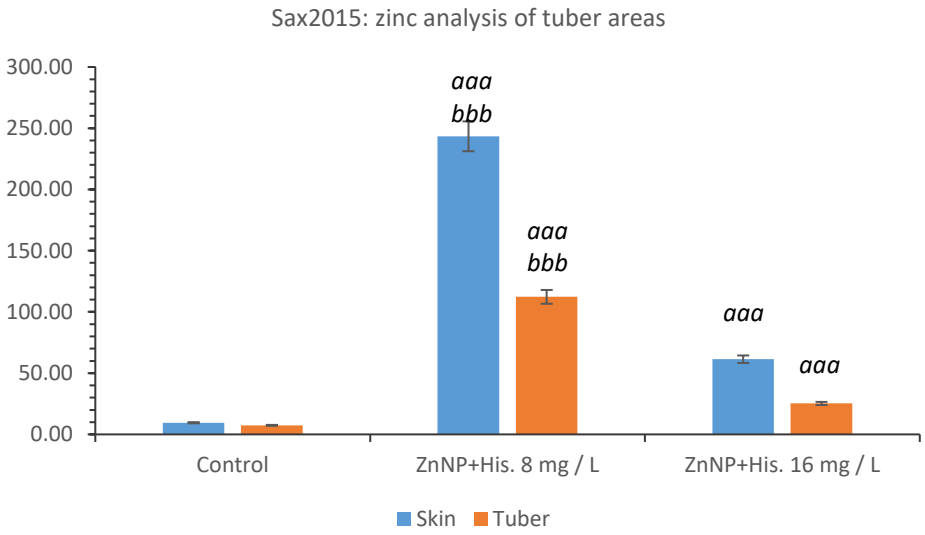

Figure 3.55 Zn content of areas of tuber from Sax2015. Sif. dif. against control, a, between Zn applications, b. Statistical analysis via ANOVA single factor and ranked by p value as previously described.

A significant increase in Zn concentration by means of ZnNP+His. application, by passive or active transportation, figure 3.33, with optimal fortification at 8 mg / L was found within the tubers Sax2015. Figure 3.33 shows a low TF as the tuber percentage is lower than the control 43.72 % by 14.57 – 12.14 %, therefore the TF is low possibly due to the tubers low tolerance to Zn.

The application of ZnO nanoparticles have a positive effect on the bofortification of tuber due to significant increase from application ZnNP+His. 8 mg / L in both hydroponic propagation and in a compost media. Investigation in to the retention and aggregation of Zn in a compost / soil media is required as the interaction between ZnO and organic ligands in order to develop Zn fortification with ZnO nanoparticles.

4 Tracing iron up take with ^{59}Fe: FeNP against Fe-EDTA

Due to the low mobility of Fe in soils due to the nature of Fe being readily oxidised to form salts and highly insoluble oxides and hydroxides as follows (Shenker and Chen, 2005):

$$Fe^{3+} + 3(OH)^{-} \leftrightharpoons Fe(OH)_{3\,(solid)}$$

Manly Fe applications use salts, such as $FeSO_4.7H_2O$ and Fe-chelates to increase soluble Fe and hence the availability to plants particularly in calcareous conditions. Salts are extremely soluble and easily leached through the soil (Shenker and Chen, 2005), therefore only used as a sort-term delivery. Chelates have been used since the early 1950's, as they have a high affinity constant to form a highly stable complex, delivering Fe at a reduced rate than $FeSO_4.7H_2O$ (Oviedo and Rodríguez, 2003; Shenker and Chen, 2005; Wagner and Baran, 2010; López-Rayo *et al*., 2015).

Ethylenediamineteraacetic acid (EDTA) is a potentially hexadentate chelating ligand (figure 4.1) with each N contains a free pair of electrons and the molecule possesses four acidic hydrogens (Schaider *et al*., 2006; Wagner and Baran, 2010). Other chelating agents include HEDTA, 2-hydroxyethylenediaminetriacetic acid; DTPA, diethylenetriaminepentacctic acid; EDDSA, ethylenediaminediscuccinic acid and IDSA, iminodisuccinic acid that are applied either as a foliar or root solution to increase Fe availability (Lucena, 2006). EDTA along with other chelates are used as a metal 'stripping agents', in the form of a treatment method to remove heavy metals from water courses due to its rapid strong chemical bond (Liu *et al*., 2016).

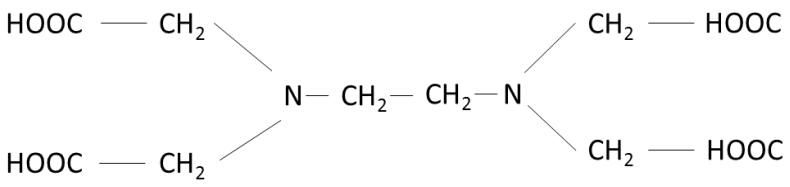

Figure 4.56 Schematic structure of ethylenediaminetetraacetic acid (H4EDTA).

Published data from Shenker and Chen (2005) observed Fe-EDTA had an increased stability constant (K_{app}) above other Fe-chelates, table 6.1, especially for Fe^{2+} is the most commonly used chelating agent. However, 81% of soil applied Fe-EDTA has been shown to leach and lost the surrounding environment, rendering the availability of Fe as poor (Boxma and De Groot, 1971).

Fe-Chelate	Log K_{app}	
	Fe^{2+}	Fe^{3+}
EDTA	22.3	11.4
HEDTA	20.3	9.5
EDDHA	24.9	5.3

Table 4.22 Adapted from Shenker and Chen, 2005; comparison of Fe-chelates and stability constant (Kapp).

Although the Fe uptake mechanism, strategy I, involves the chelation of Fe^{2+} to enable transportation thought the plant and to avoid cellular damage from oxygenation damage of Fe^{2+}, this as a remedial ligand that is not as tightly bound as EDTA, therefore can be precipitated at the target site (Trampczynska *et al*.,2006; Kim and Guerinot, 2007).

The FeNP is consist of Fe^{3+} and Fe^{2+} as a stoichiometric ratio of 2:1 (Fe^{3+}/Fe^{2+}) (Laurent *et al*., 2008) allowing a duel delivery of Fe that is phytoavailable immediately (Fe^{2+}) and a more stable Fe supply (Fe^{3+}) (White and Broadley, 2009). The amino acid coating prevents the formation of insoluble complexes with retention in the growth media to allow slow delivery of bioavailable iron.

Using the radioactive isotope ^{59}Fe, FeNP+His. and FeEDTa were synthesised and applied to the compost as a solution at a concentration of 12 mg / L. Using seral dilutions of the stock solution of the FeNP and FeEDTA, MBq was converted into mg / L.

4.1 Methods and materials

To directly compare the uptake of Fe from FeNP+His. and commonly used iron delivery method of Fe-EDTA, both iron compounds were synthesised using the radioisotope ^{59}Fe, 1 mCi, purchased from Perkin Emler. The isotope allows tracking of the iron through the plant as well as quantity of iron utilised through the plant. Thirdly, the retention of iron in the soil can be observed. Chemicals for Fe-EDTA synthesis were purchases from Sigma Aldrich and the precursor chemicals for the FeNP+His. synthesis was purchased as for pervious method.

The synthesis of this trial was adapted from Lauret *et al*. (2008) ^{59}Fe solution (10 mL) was added to a solution of iron (III) chloride (0.1 mol^{-1}, 30 mL) and iron (II) chloride (0.05 mol^{-1}, 30 mL), a 2:1 ration by

molarity. This mix was added by continuous drip via a pressure equalising funnel, into sodium hydroxide (3 mol^{-3}, 60 mL). The sodium hydroxide was heated to 60^{o}C with continuous stirring at 500 rpm in a 250 mL a round bottom flask for 1 hour. The black nanoparticles were filtered through a grade 2 glass sintered funnel via vacuum filtration and washed with deionised water (3 x 50 mL) then ethanol (20 mL) and left to dry over night before in fume hood being ground for further use. Equal weight of histidine monochloride to iron oxide nanoparticle was ground using a pestle and mortar. The ^{59}FeNP+His, (3.30 g) was suspended into distilled water (1000 mL) making a stock solution. The stock solution (66.6 mL) was diluted to into distilled water (433.4 mL) before application to the plants.

The synthesis of Fe-EDTA (Stiener and Van Winde, 1970) involved the preparation of two precursor solutions; Solution A: Disodium EDTA (1.9g) into a solution of sodium hydroxide (1 mol^{-1}, 5 mL); Solution B: Iron (III) chloride hexahydrate (1.25 g) into distilled water (2.5 mL). Solution A was added to solution B with continual stirring and heated to 60 ^{O}C until a yellow precipitate formed. The precipitated was obtained by filtration and washed with ice cold water (2 x 50 mL) and once with ethanol (20 mL). No coating method was required as Fe-EDTA is soluble. Fe-EDTA (4.64 g) into distilled water (1000 mL). The stock solution (66.6 mL) was diluted with distilled water (433.4 mL) before application to plants.

The treatment (500 mL) was added once a week to the potato plants around the base of the stem, watering with tap water every other day. Erin Multipurpose compost, purchased from LBS Horticulture, was used as the propagation media, to emulate previous trials. Three replicates of each application were cultivated. Samples of the compost, tuber and stem (lower, mid and upper) were taken and analysed for gamma radiation activity using a Hidex AMG Gamma Counter.

4.2 Results and discussion

Calibration graphs see app. 55, section 11.5

Using ANOVA single factor statistical analysis, with a p ranking as follows; < p = 0.05 *, < p = 0.01 ** and < p = 0.001 ***, all data collected from FeNP+His showed a '***' of significance over Fe-EDTA concluding that the nanoparticle retained in the compost at a highly increased amount than the Fe-EDTA., figure 4.2a Figure 4.2b, demonstrates a 578.4 fold increase in the amount of iron in the tubers propagated in the trial treated with FeNP+His application over Fe-EDTA. The amount of Fe distributed through the stem of the plant, figure 4.2c, was significantly higher for the application of Fe from the

nanoparticle over the chelate. The Fe-EDTA distribution shows a decline in Fe content progressing up the potato plant stem. The Fe content of the stems from application of FeNP+His display a high Fe content at the lower stem like the Fe-EDTA, however, the top of the stem contains 109.07 % (1.33 mg / L) more Fe than mid stem. Due to radioactive regulations limiting the contact with the radiation and plants, the growth rates were unable to be observed. The increased Fe concentration suggests the escalated production of chlorophyll, which Fe plays a key part, suggesting new leaf development.

Repetition of the experiment to include other Fe-chelates over a larger sample number would enable a comprehensive view of the increased uptake, utilisation and retention the iron oxide has above Fe-chelates and $FeSO_4$. It was noted that during the experiment that the foliage of all participating plants where suppressed or damaged due to the strength of the gamma and beta radiation produced from ^{59}Fe. The initial dosage of 1 mCi was deemed to be too strong even with the occurrence of two half-lives (28 days), due to laboratory and personnel availability, it is deemed that a stock sample from which the FeNP and Fe-chelated would be synthesised would be 500 µCi.

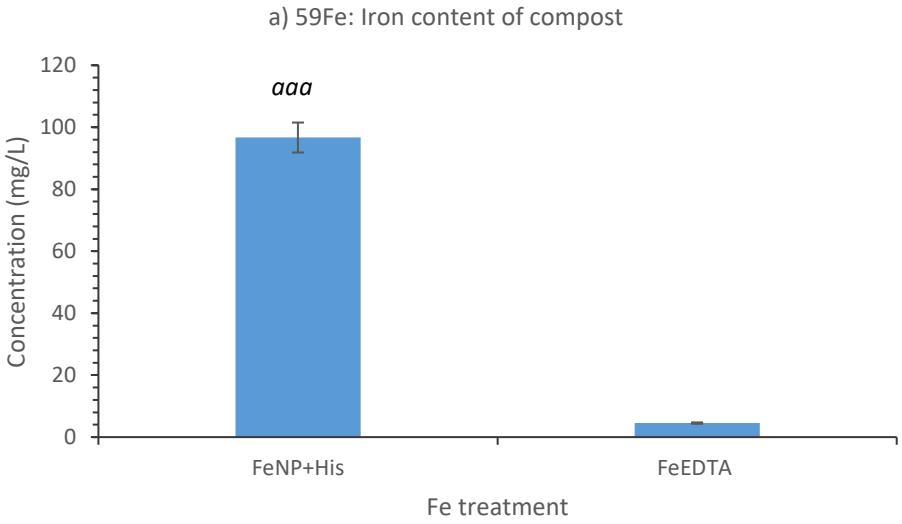

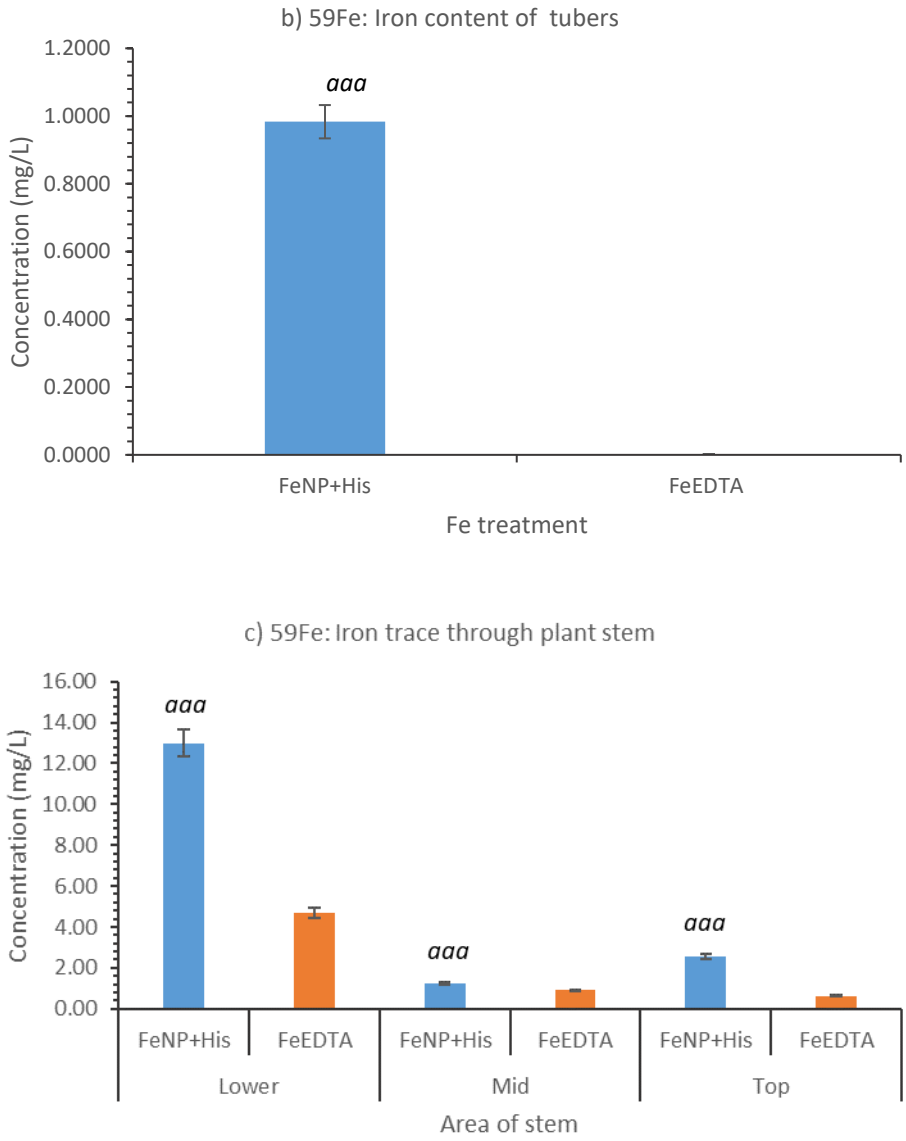

Figure 4. 57 Comparison of the Fe content recorded from the MBq reading produced from ^{59}Fe isotope and converted into mg / L per gram of sample. a) Fe content from the growth media, multi-purpose compost, after the trial was completed) Fe content from tubers propagated in trial and c) areas of stem sampled at the end of the trial. 'a' indicates the level of significant difference.

5 Tomato trials

Previous potato trials established a successful fortification of tubers using MONP. In ordered to understand that the fortification occurring in the potato trial was due to physiological processes and not passive transpiration in to the root system and tubers by diffusion.

The tomato (*Lycopersicon esculentum*) plant belongs to the deadly nightshade family *Solanum lysopersicum* of which other crop plants derive from such as the potato and chili. Tomato is popular worldwide fruit and the second most produced and consumed in the western countries (Willcox *et al.,* 2003 and Toor *et al*., 2006). The tomato fruit is a sink organ and provides an excellent source of many nutrients and antioxidants including vitamin C, lycopene and phenolic acids (Bressy *et al.,* 2013 and Chen *et al.,* 2013).

Fertilisers are used to improve the quality and quantity of the tomato crop. The three main nutrients in fertilisers are nitrogen, phosphorous and potassium (N, P and K). N promotes leaf growth, formation of proteins and chlorophyll. P promotes flower, fruit development and root growth. K is involved in the synthesis of proteins and contributes to health of the stem and root too (Corradini *et al*., 2010).

The surface of the tomato seeds, figure 5.1, provide an ideal surface for MONP coating, for a instantaneous supply of Fe at germination, or promoting germination as the nanoparticle enters the seed via diffusion.

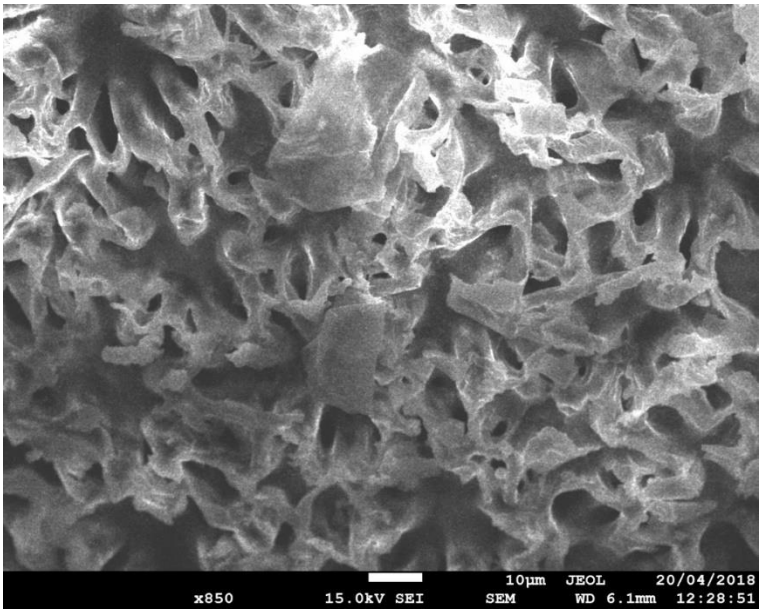

Figure 5.58: SEM of tomato seed used in trial. The irregular surface allows particle attachment and immediate contact with the FeNP the seed coating provides.

5.1 Materials and method

The following trials took place under glasshouse conditions, without additional heating and lighting. The variety Gardeners Delight was used throughout purchased from ++++ seeds, batch ****. During propagation, side shoots where not removed, as is common practice to encourage flowing, and supported by canes when necessary.

The synthesis and coating of the FeNP+His used in the following trials are synthesised as previously described.

To observe FeNP application effects the growth rate of the plants stems (Growth rates, yield and DM % recorded to observe the effect of the seed coating and FeNP application

5.1.1 Tomato 'Gardeners Delight'; FeNP application effects on plant growth rate and fruit production (T2014)

Seeds (*purchase from Simply Seeds, Nottingham*) sown on 17th February 2014, using rehydrated Jiffy peat pellets (Purchased from LBS Horticulture, UK) allocating one seed sown per pellet. Those seeds began treatment from sowing were planted in a pre-soaked pellet of the test solution (100 mL) as allocated in table 5.1. The seedlings germinated in individual non-heated propagators (purchased from B&Q). Once a week the seedlings were fed of the designated test solution (15 mL per pellet), increasing at week 4 (25 mL) and further increased (50 mL) due to demand by the plants, figure 5.2, at 8 w.a.p.

Treatment	When treatment began	Number of seeds sown	
Control (water only)	*Sowing*	*8*	
Commercial (MircleGro)	*From flowering**	*8*	
FeNP+His 6 mg / L	*Sowing*	*8*	*All treatments applied*
FeNP+His 12 mg / L	*Sowing*	*8*	*weekly with 500 ml of*
FeNP+His 24 mg / L	*Sowing*	*8*	*allocated feed.*
His 6 mg / L	*Sowing*	*8*	
His 12 mg / L	*Sowing*	*8*	
His 24 mg / L	*Sowing*	*8*	

*Table 5.23 Summery of trial conditions, T2014. *As recommended by manufacture.*

Figure 5.59 'Gardeners Delight' in trial T2014. Plants were randomly distributed thought the greenhouse bay to ensure all treatments were subjects to variants that maybe present, i.e. shading or draft.

After 6 weeks, the seedlings transferred into 30 cm diameter pots containing all-purpose compost. Feeding regime continued on a weekly basis with one litre of treatment per plant throughout the trial. Application of Miracle Gro All Purpose feed began when flowering commenced, as recommend by the company; feed rate was the same as the rest of the treatments. Previously these plants where treated as control plants, no additional fertiliser or feed applications Control plants continued the trial.

5.1.2 FeNP applied as a seed coating (TSC2014)

A solution of FeNP+His, 200 mg/L, 100 mL, was compared to a coating using the hydroponic nutrient solution (HNS) as described previously described, plus an equal combination of FeNP+His, 200 mg/L and nutrient solution FeNP+HNS 200 mg / L, 100 mL (1:1). A pump spray, allowing drying in-between each application, applied three applications of the solutions. Eight seeds were planted into separate Jiffy plug, cultivated in propagators as in previous trials and watered when required. No further application was given during propagation.

Application	Percentage emerged after 4 weeks (%)	Percentage survived to produce fruit (%)
Control	43.75	73.33
HNS	25	25.00
FeNP	37.5	66.67
FeNP+HNS	37.5	0.00
FeNP+His 6 mg / L	25	100.00
FeNP+His 12 mg / L	25	100.00
FeNP+His 24 mg / L	25	33.33
His 6 mg / L	25	66.67
His 12 mg / L	62.5	100.00
His 24 mg / L	87.5	100.00

Table 5.2: Emergence of seeds treated from sowing by solution application or coating.

5.2 Results and discussion

5.2.1 The effect of MONP on germination rate

The seeds coated with hydroponic fertiliser solution (coating: HNP), FeNP+His 200 mg/L (coating: FeNP+His) and a combination of hydroponic fertiliser solution and FeNP+His 200 mg/L (coating: FeNP+His+HNP). From table 5.2, the coating application have an inhibitory effect on emergency of sedlings as the emergence percentage is 18.75 % lower for coating HNS and 6.25 % for FeNP and FeNP+HNS when compared to control. Furthermore, the data from the percentage of plant that went on to produce fruit are less likely to with an application of HSN coating. During the cultivation of these plants, it was noted at six weeks in after sowing, the seedling was likely to bolt, causing stem weakness and ultimately death. This condition was observed in the application of FeNP+His. 24 mg/L where 33.33% of plants went onto produce fruit, as seen in table 5.2. Applications of FeNP+HIS and His. 6 and 12 mg / L increased the likelihood of the plant to achieve fruit production.

5.2.2 The effect of FeNP on the growth rate.

From figure 5.3a, the effect of the application of the commercial fertiliser, Miracle Gro, are observed after 8 weeks after sowing (w.a.s.) as the increase in N, increases the growth rate; however, this is not significant against control. Tomatoes treated with FeNP+His. 24 mg / L observed to have an increased growth rate over other applications, figure 5.3c. Those treated with His. 24 mg / L quickly preceded in an increased growth rate with a significant difference in height over control, weeks 4 to 13, Miracle Gro in 7, and 10 w.a.p. Other applications of His. 6 and 12 mg / L also increase growth rate over control and significantly over Miracle Gro treated plants. It was also observed those plants treated with His. gained taller plants as the concentration of His. increased.

Application of FeNP+His. 6 mg / L significantly gained taller plants when compared against other FeNP+His and His. 6 mg / L treated plants (figure 5.3a), suggesting the presence of FeNP promotes growth rate.

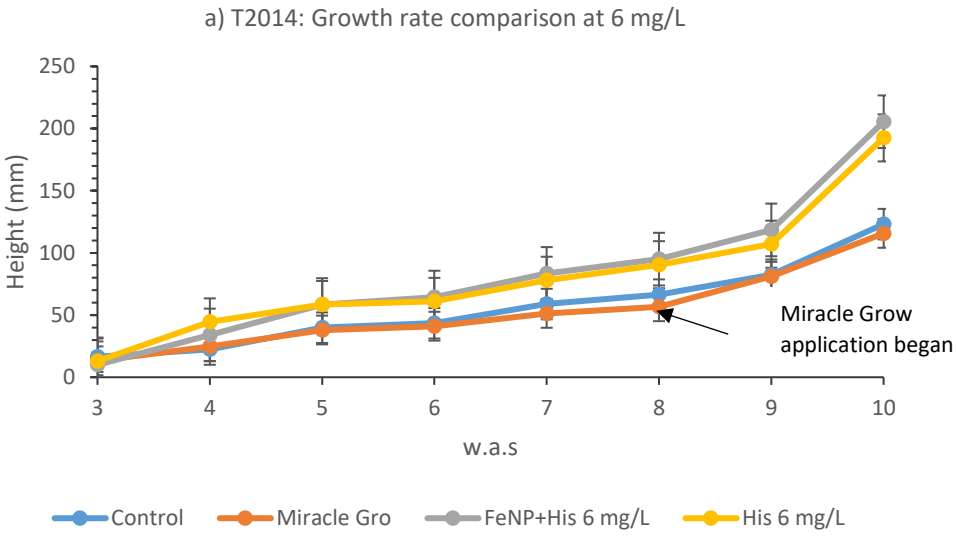

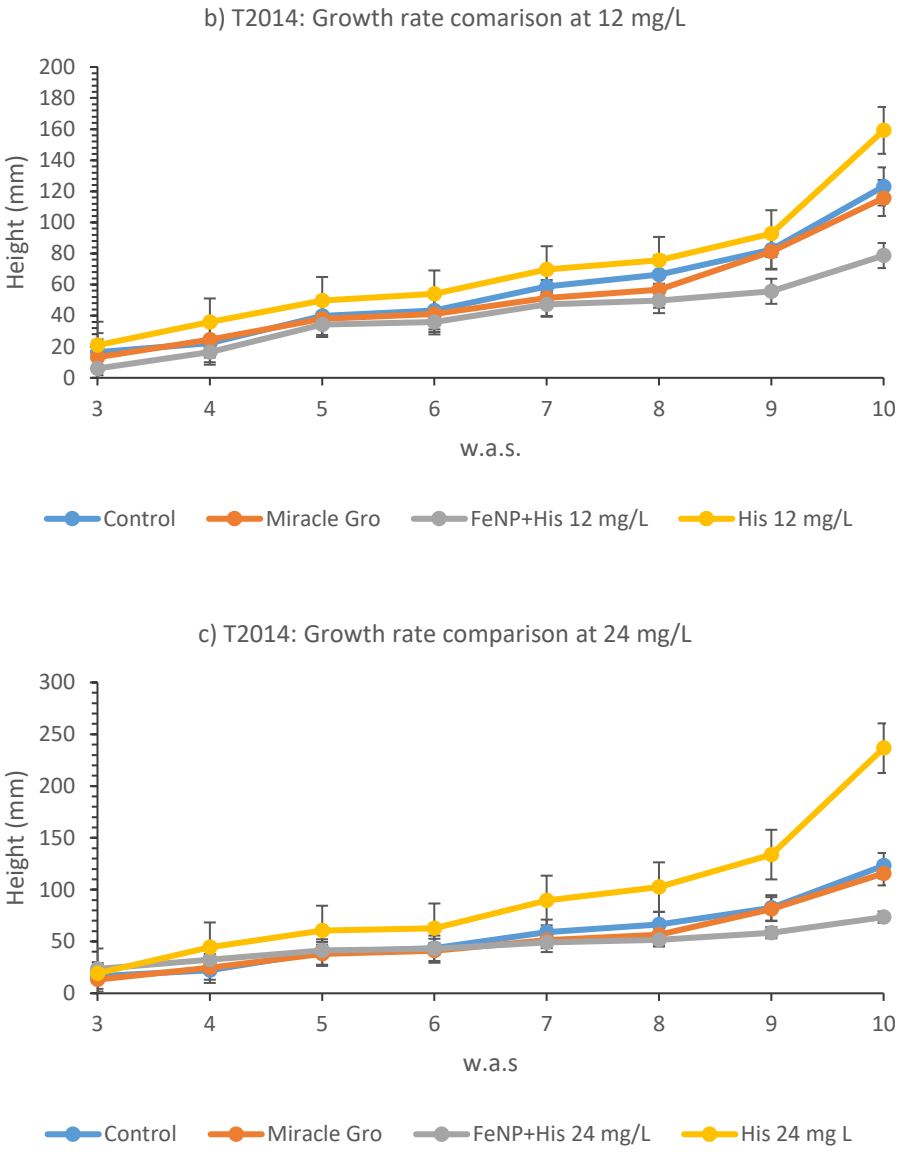

Figure 5.60 Average growth rate of tomato plants 'Gardeners Delight' cultivated in trial T2014. Each plant was cultivated from seed and treated from the onset. Application of Miracle Gro began at 8 w.a.p. as indicated in a).

In figure 5.3b, the treatment His 12 mg / L at week 7 has significantly increased in height than the FeNP counterpart, indicating the possibility of a threshold to the positive effect the FeNP has on foliar development at certain periods of the plants life cycle. This theory is supported by the reduced growth rate exhibited by FeNP+His. 24 mg / L, although the height gained by FeNP+His 24 mg / L at week 13 was significantly greater than plants treated with Miracle Gro (figure 5.4). The tomato plants fed with His, demonstrated similar or greater growth than control as observed in figures 5.3 a,b and c. Again suggesting the presence of FeNP 12 and 24 mg/L may supress foliar development as the His. equivalent promotes growth. Tomato plants treated with FeNP+His. display no phytotoxic effects of excess Fe as

shown in figure 5.5. Toxicity caused by excess Fe courses magnesium (Mg) deficiencies as well as free radical damage, (Chatterjee *et al*., 2006; Abadía *et al*., 2011). This is displayed by bronzing and stripping of the leaves at are similar to chlorosis under Fe deficiencies. Fe toxicity is suggested to stunt growth, which is suggested by figure 5.12. (Chatterjee *et al*., 2006; Abadía *et al*., 2011).

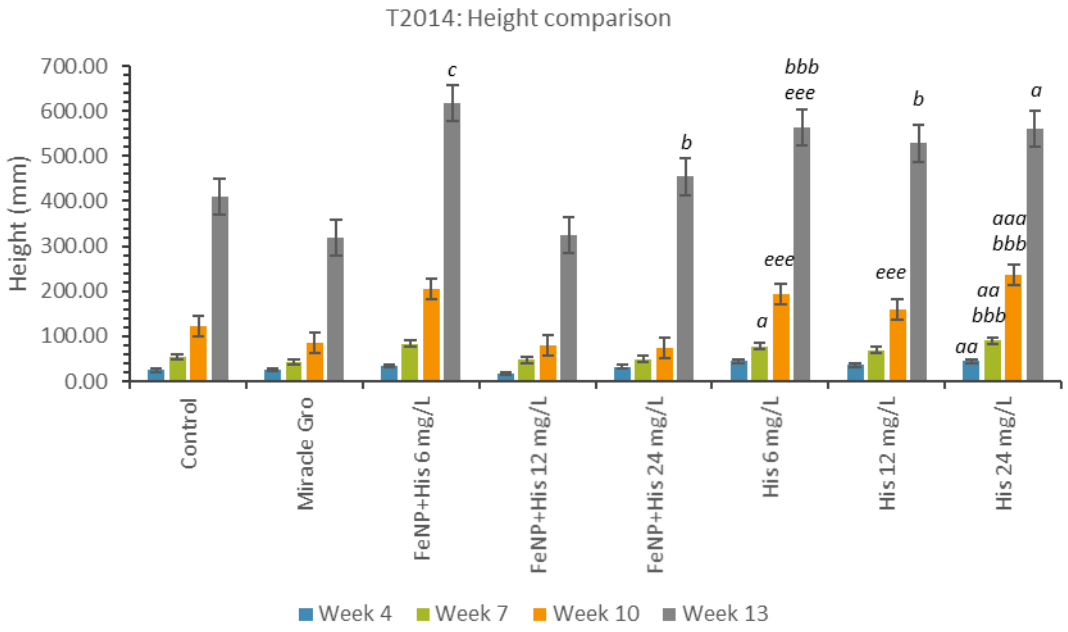

*Figure 5.61Average height of tomato plants after 13 weeks since sown. Using ANOVA single factor statistical analysis, p-values were ranked; * p=0.05>, ** p=0.01, *** p=0.005. Letters; 'a', against Control; 'b', against Miracle Gro; 'c' between the FeNP+His applications; 'd', between His treatments; 'e' FeNP+His against His equivalent.*

Application of FeNP as a seed coating, no significant difference found between the growth rate of control against HNS, FeNP and FeNP+HNS plants cultivated from coated seeds. From figure 5.7, the HNS plants had an increased height of 142.00 mm over control plants, 123.14 mm, and an increase of 15.31 % 10 weeks from being sown. HNS coated also gained a 22.81 % and 32.71 % increase in height over control at week 4 and 7.

Plants propagated from seeds coated with FeNP+HNS, did not survive past week 6 (figure 5.6) due to stem bolt leading to weakness and death. It is also observed that the presence of FeNP 200 mg/L had no beneficial effect at the time of germination.

Figure 5.75 T2014 Example of plants cultivated in T2014. Seven weeks since sown.

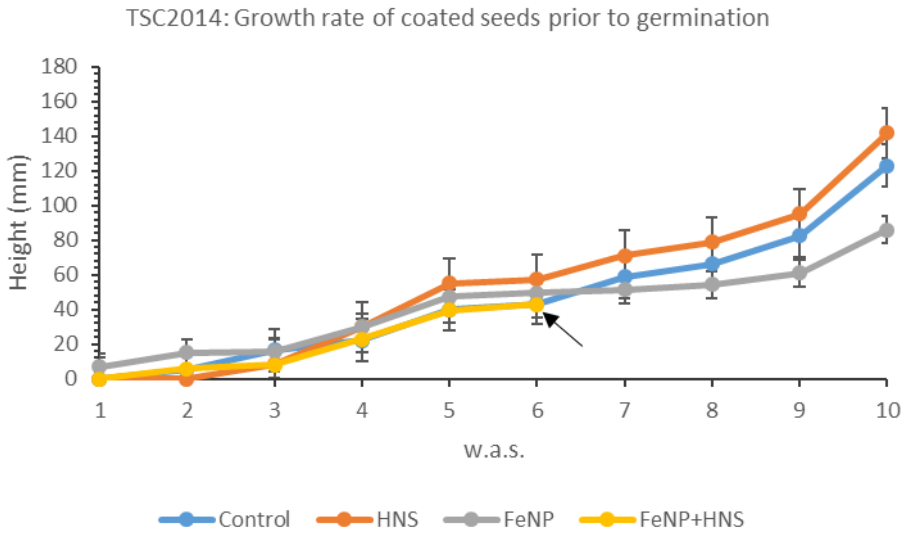

Figure 5.63 Average growth rate of tomato plants cultivated from coating seeds. The arrow indicates the demise of all seedling propagated from FeNP+HNS coated seeds

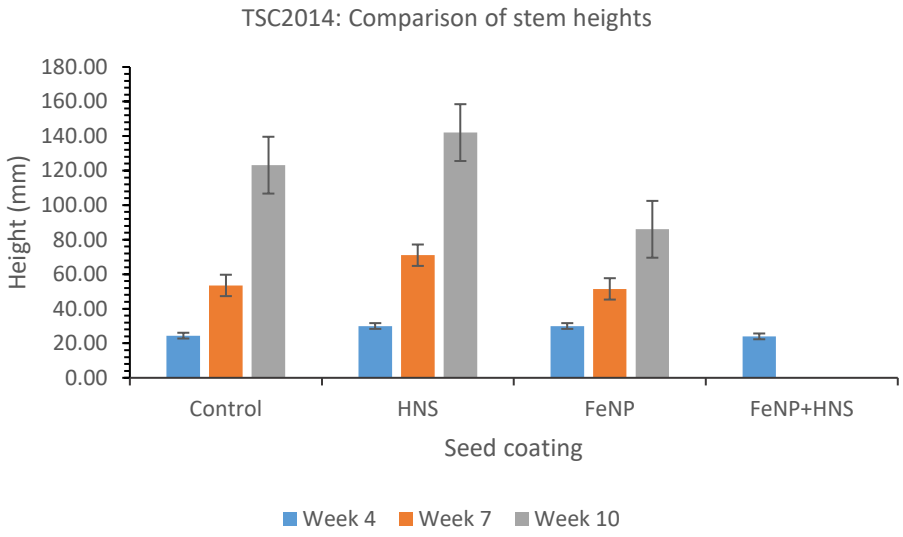

Figure 5.64 Height comparisons at allotted times for tomato plants cultivated from seed coatings in trial TSC2014.

5.2.3 Effect of MONP on yield

Ripening of tomatoes fluctuated greatly in a commercial greenhouse hydroponic environment (Adams) even with stringent control of N:P:K, EC levels and addition nutrients, it has been published that temperature is the main determinate in ripening (Verkerk, 1955; Hurd and Graves, 1985; Adams *et al*., 2001). Constancy of yield is required by the grower to supply the increasing demands of the market under current commercial pressure (Adams *et al*,. 2001; Smith 2013).

Data collected from T2014 and TSC2014 displayed the inconstant ripening of fruit, figure 5.9. It would be of commercial interest to provide a methodology to assist in the production of consistent rate of ripening of a good quality.

a) T2014: Control and Mircale Gro

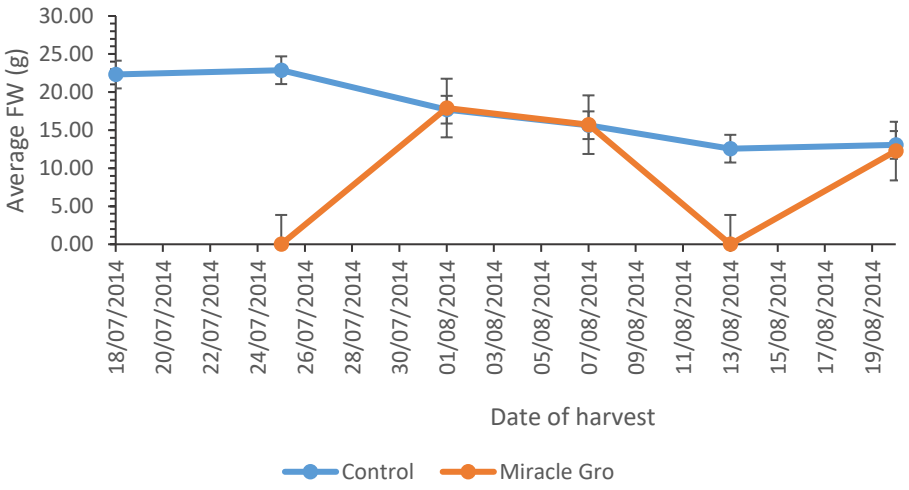

b) T2014: 6 mg/L

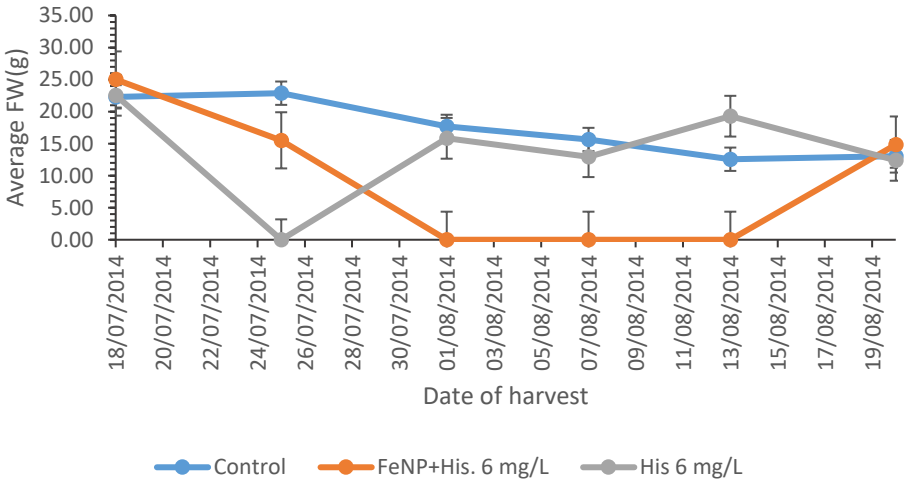

c) T2014: 12 mg/L

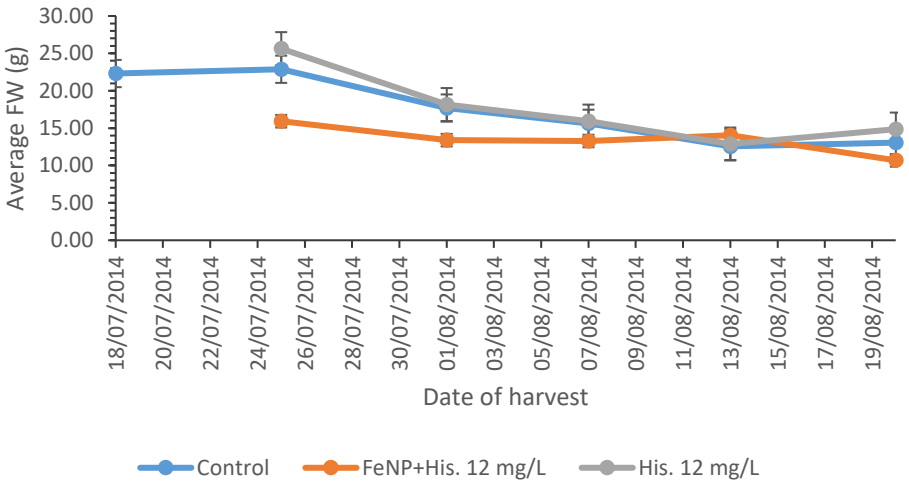

d) T2014: 24 mg/L

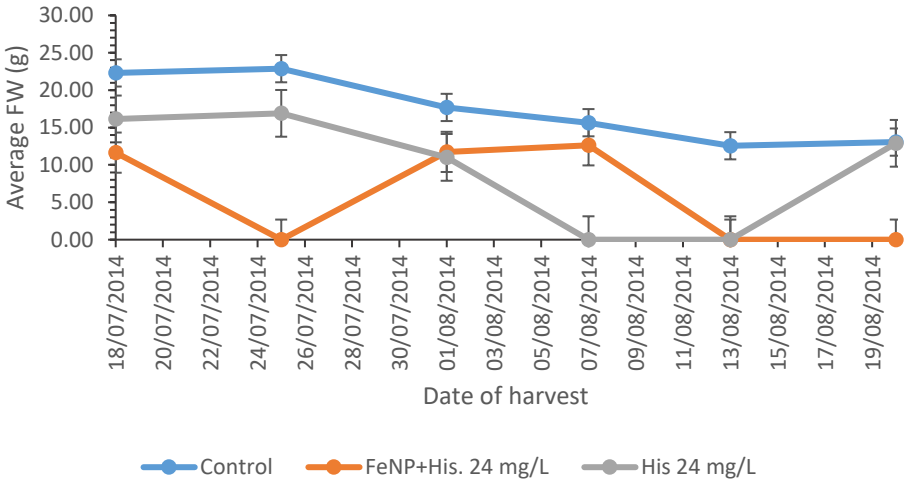

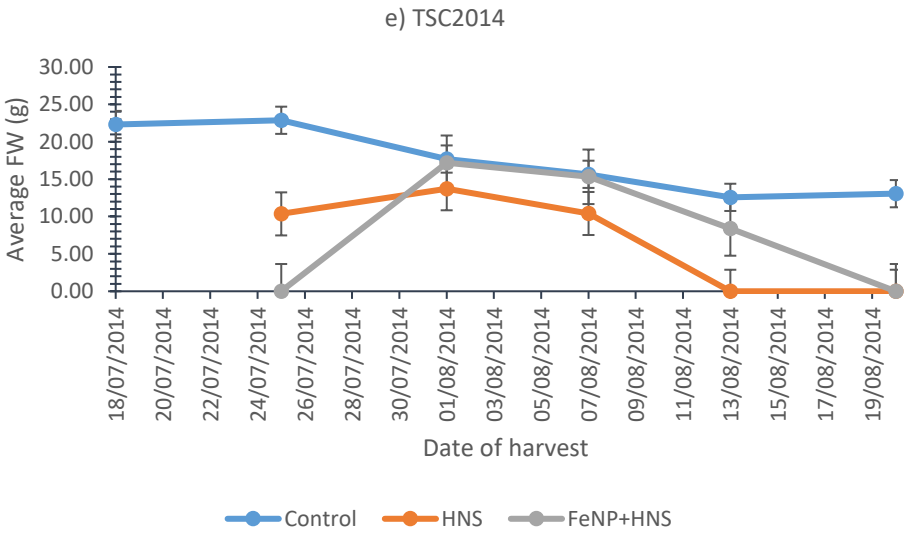

Figure 5.65 Average fresh weight (g) of tomatoes harvest during trials T2014 (a to d) and TSC2014 (e), harvested HP. T2014 graphs compare control FW with FeNP+His and His of comparative concentration.

Comparing average fresh weights obtained during the harvest period (HP), control plant gradually produced tomatoes decreasing in weight, figure 5.8a. A similar harvest pattern was observed in figure 5.8c, although this data displayed an anomaly of increased harvest weight, FeNP+His. 12 mg/L mid HP where as other treatments produced a decrease in fruit weight or no ripe fruit. This suggests the application of FeNP+His and His. at a concentration of 12 mg / L has enabled the plants to buffer against the environmental factor (i.e. decrease in temperature) (Verkerk, 1955; Hurd and Graves, 1985; Adams *et al*., 2001; Smith, 2013) that reduced the ripening rate in the other treated plants. The FeNP+His treatment was of particular interest as the ripened fruits increased in weight in this period and subsequently produced 146.38 % more tomatoes than control and 41.67% more than Miracle Gro. In comparison to His. 12 mg / L yield, it can be concluded that the concentration of 12 mg / L FeNP has a positive effect on the number of tomatoes produced and the ripening of the fruits.

Treatments of Miracle Gro, FeNP+His. 6 mg/ L and 24 mg / L, plus His. 24 mg / L and TSC2014 treatment (figure 5.8e) took a longer time for the fruit to ripen after the environmental stress occurred.

Comparing percentage difference of number of fruits harvested when compared against ‘Control’ and ‘Miracle Gro’ plants, was defined to be above or below 10%.

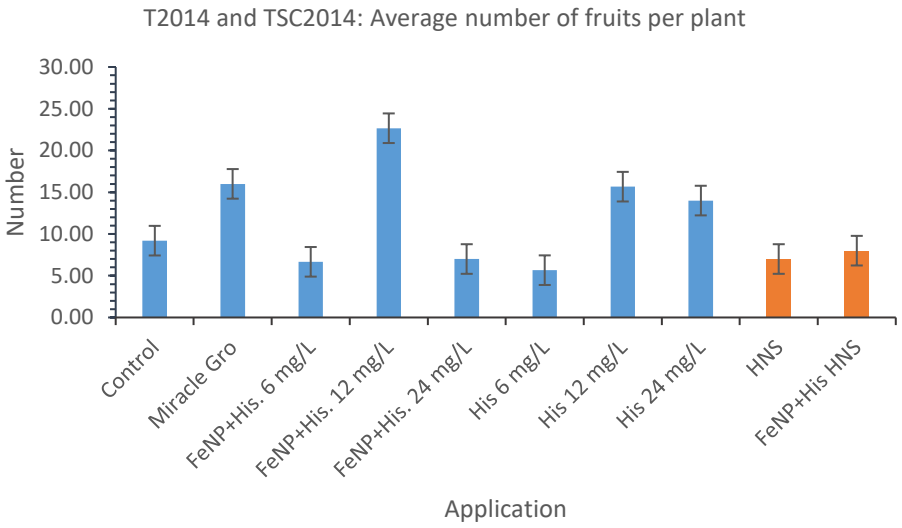

Figure 5.66 Average number of tomato fruits per plant from trials T2014 and TSC2014. Seed coatings (TSC2014) indicated in orange.

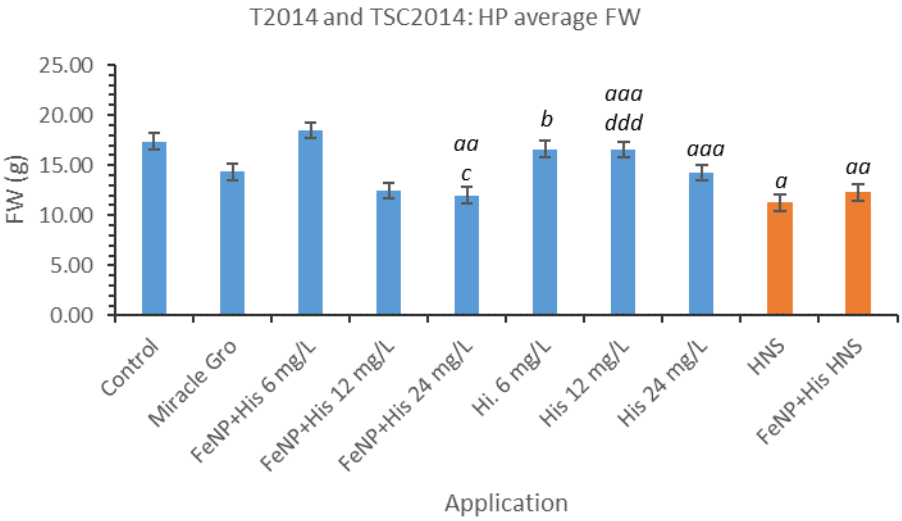

Figure 5.67 Average fresh weights (g) of tomatoes from trials T2014 and TSC2014. Significant differences were found using ANOVA single factor analysis and rank by p value as previously described. Analysis against Control,'a'; against Miracle Gro, 'b', against FeNP+ His. 6 mg / L 'c' and against FeNP+His. 12 mg / L 'd'.

Results of FW suggested that the lower concentration of FeNP+His 6 mg / L produced a significantly heavier crop, figure 5.9 and 5.10, which corresponds to publish data reported by Ejrari, (2013). The published results show an increase of Fe from 287.21 g per 'control' plant to 501.08 g when treated with a considerably low dose of 0.8 mg / L of chelated Fe (undisclosed chelating agent) using Hoglands solution under hydroponic conditions. The hydroponic conditions alone would increase yield (Sardare and Admane, 2013; Touliatos *et al*., 2016) and alter dynamics of the rhizosphere and the absorption of Fe. Navrot and Banin, (1975) observed the application of Fe from several sources ($FeCl_3$, $FeSO_4$, FeEDDHA and FeEDTA) in a hydroponic system and a Fe impregnated clay. None of the Fe applications were found to significantly increase FW, therefore the application of MONP influences FW than Fe counter parts (Navrot and Banin, 1975).

5.2.4 Effect of FeNP+His on DM %

As previously discussed in section 5.3.5 a number of factors course fluctuation in the quality of tomato crop (Adams *et al*., 2001). In contrast to potatoes, tomatoes consist of approximate 90 % water with 50 % of the remaining DM composed of carbohydrates (Ho *et al*., 1987; Adams *et al*., 2001). Using H_o^1; "a*pplication of FeNP+His has no effect on the DM% of tomatoes*", and H_o^2; *"application of His. has no effect on the DM% of tomatoes"*; it can be said that the H_o^1 is rejected as there is a significant decrease in DM% in fruit harvested from plants treated with FeNP+His. as the fruit contained a higher amount of water. This can be said for the application of His. (figure 5.11) therefore rejecting H_o^2.

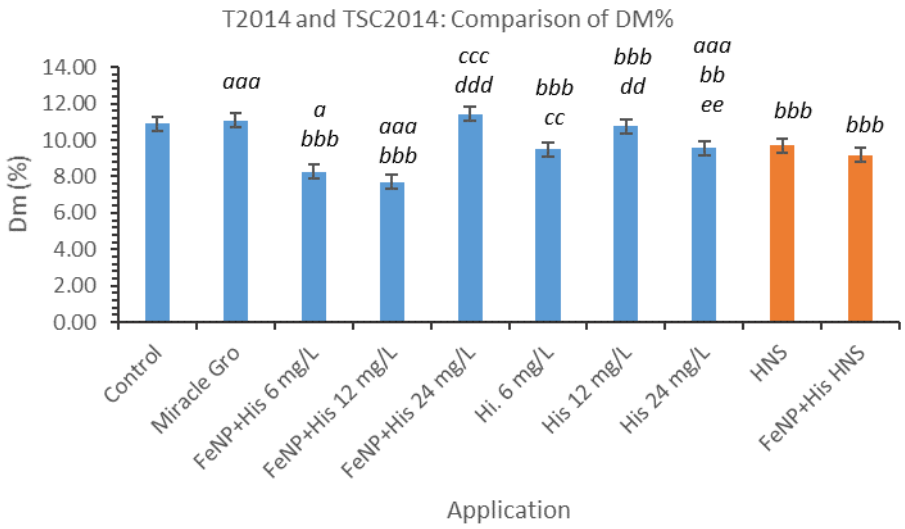

Figure 5.68 DM% of tomatoes harvested in trials T2014 and TSC2014 (orange). Significant differences were found using ANOVA single factor. 'a' indicates significant difference against control, 'b' against Miracle Gro, 'c' against FeNP+His. 6 mg / L, 'd' FeNP+His. 12 mg / L and 'e' FeNP+His. 24 mg / L.

The application of FeNP decreased the DM% of the fruit. In figure 5.11 it is observed the DM% obtained from His. 6 mg / L is significantly higher ($p=1.24 \times 10^{-3}$) than the FeNP counterpart. This is also reflected in the 12 and 24 mg / L applications, $p=7.80 \times 10^{-3}$ and $p=3.69 \times 10^{-3}$ respectively. This signifies the increase uptake of water by the plant possibly due to stress induced by the presence of the iron.

5.2.5 The effect of FeNP+His on mineral content of the crop

A significant increase in Fe was achieved by all three FeNP applications, with the greatest increase obtained by the concentration 6 mg / L, figure 5.12. It was noted the increasing amount of FeNP+His. saw a decrease in TF from roots to fruit, suggesting an optimal concentration for FeNP around 6 mg / L, as growth rate was significantly increased over control, Miracle Gro and other applications of FeNP (figure 5.12), suggesting the utilisation of FeNP through the plant including an increase in the average fresh weight of tomatoes harvested. Investigations into the amount of ferritin occurrence in areas of the plant i.e. Roots, leaves and fruit, would substantiate the possible Fe overload leading to phytotoxicty, the other FeNP+His present.

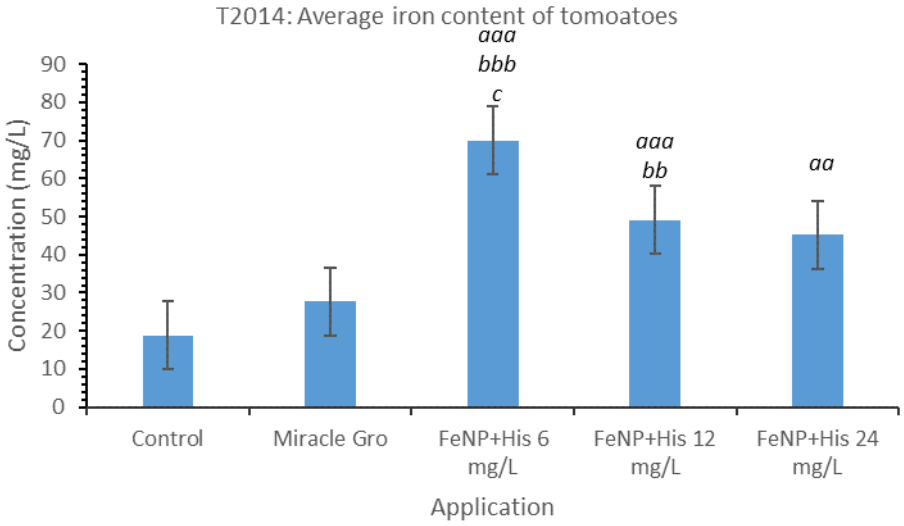

Figure 5.69 The average Fe content of tomatoes propagated in T2014. Level of significant difference determined by ANOVA single factor analysis, 'a' against control, 'b' against Miracle Gro, 'c' against FeNP+His 24 mg/L application.

Tomatoes fed with the application of FeN+His 6 mg / L, can be suggested as a method of increasing consumer Fe in diet. The FeNP+His 6 mg / L contained a higher content of water that (decrease in DM%), that would decrease the fruits value for processing. As UK produced tomatoes are mainly sold as fresh produce 85% (Caspell *et al*., 2006; FAO, 2014), a product such as the this, could be marketable. Investigations into FeNP tomato shelf life longevity, brix testing for sugar content and effect of FeNP on the vitamin concentration would be valuable in order to pursue marketability.

6 Chilli pepper trials

Chillies are the fruits of plants from the genus *Capsicum* and belong to the family *Solanaceae*. There are several domesticated species of chili peppers, among them *Capsicum annuum*, C. *frutescens* and *C. chinense*, which include many common varieties. These various peppers are widely used in many parts of the world and are particularly noted for their pungency, due to the unique presence of chemicals from the antioxidant capsaicinoid family of fatty acids (Arora *et al*., 2011; González-Zamora *et al*., 2013). There are five naturally occurring capsaicinoids: capsaicin, dihydrocapsaicin, nordihydrocapsaicin, homodihydrocapsaicin and homocapsacin (see figure 6.1) of which the two most prevalent in peppers are capsaicin (8-methyl-*N*-vanillyl-*trans*-6-nonenamide) and dihydrocapsaicin, together constituting about 90% of the capsaicinoids in chilli fruit, with capsaicin accounting for ~71% of the total capsaicinoid in most of the pungent varieties (Luo et a., 2011; Othman *et al*., 2011; González-Zamora *et al*., 2013) .

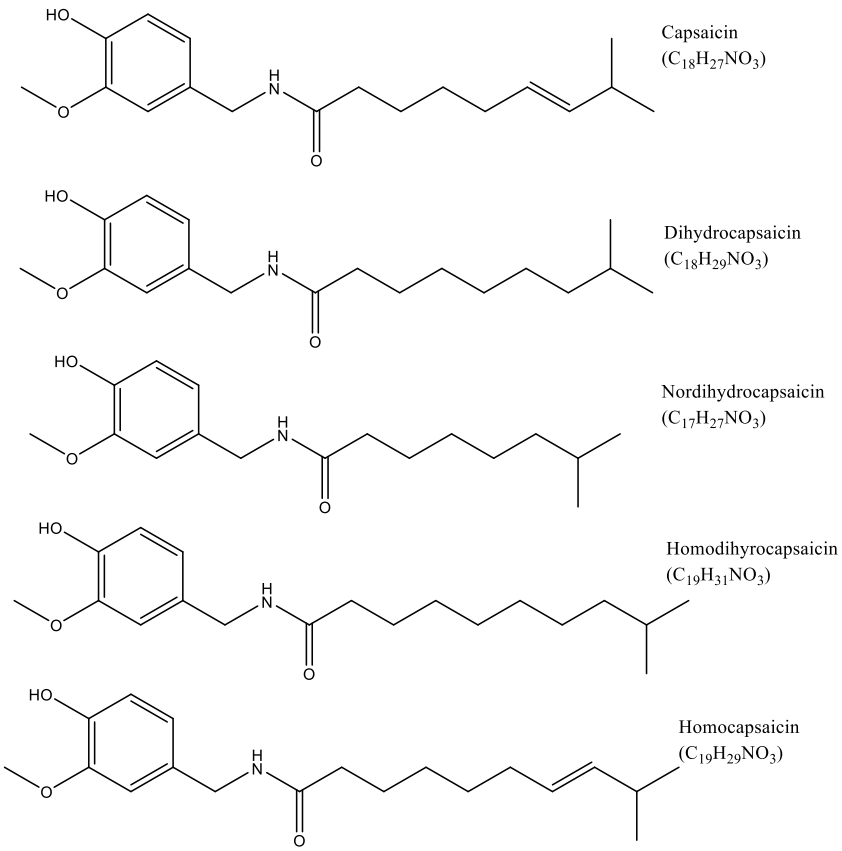

Figure 6.70 The chemical structure of the five main capsaicioids.

Isolated capsaicin is also reported to have anti-bacterial properties and medical applications in pain relief (Deal *et al*., 1999; Luo at al, 2011). Chillies may contain significant amounts of vitamins and antioxidants, including vitamins A, B6 and C and various carotenoids (Fray and Fray, 2012). The levels of these nutrients vary widely depending on the cultivar and growing conditions. Chillies contain the highest amounts of vitamin C of any plant, with levels as high as three times that of citrus fruit; as such, they can be an important dietary source of this vitamin (Cruz-Rus *et al*., 2012). In order to further improve growth and increase the nutritional value of the edible fruit, numerous studies have been undertaken to examine the nutritional uptake of chilli plants under diverse conditions (Rahman and Inden, 2012; Kenie at al., 2013) and with the addition of various organic or inorganic additives (Kasar at al., 2010) or in the presence of symbiotic microorganisms (Christinal and Tholkkappian, 2013). This study focuses on the effects of iron (Fe) fortification in order to improve yield and growth rate together with an increase in the capsaicin and iron content of the chilli peppers.

6.1 Materials and methods

The synthesis and coating of the FeNP+His used in the following trials are synthesised as previously described. The growth rates, yield and DM% was recorded as de. The peppers were analysed for Fe content via ICP -OES.

6.1.1 Chilli pepper trial with FeNP (C2014*)*

Seedlings of the cultivar 'Cayenne' (6 x *Capsicum annnum var. annuum*) were purchased (Hollybeck Nursey, Nottingham), at 4 weeks' post germination and used for the trial, C2014. The seedlings were transferred to 15 cm / 5 Ltr pots filled with Erin multipurpose compost (LBS Horticulture) and placed on a pot saucer to insure no contamination from other applications. All propagation took place under glass house conditions without additional lighting or heating. Control plants were watered with tap water with no feed. Experimental plants were treated with FeNP+His solution at concentrations of 6 and 12 mg/L. In contrast, a cohort of chilli plants was treated with histidine (His) solution at concentrations of 6 and 12 mg/L to observe the influence of Fe and His independently. A number of plants were allocated a commercial fertiliser, Chilli Focus by Growth Technology (NPK: 3:1:4.4). All

experimental plants were fed the allocated solutions once a week 250 mL per plant to replicate the suggested treatment regime of the commercial fertiliser Chilli Focus.

The growth rates, yield and DM% was recorded as previously described. The peppers were analysed for Fe content via ICP -OES.

6.1.2 Collaboration with Chilli Bobs Chilli Farm and Doff Garden Products (CB2015)

In collaboration with Chilli Bob's Chilli Farm, Fiskerton, Nottinghamshire, a commercial trial was sponsored by Doff Garden Products. Three cultivars of *Capsicum chinense* were used; Scotch bonnet, Red habanero and Jamaican; plus, a variety from the species *C. annuum var. glabriusculum*, Pequin. Quadruplets of each treated were obtained using control, Fe+HisNP 6 and 12 ppm for each variety in the trial. The plants where cultivated from cuttings taken from previous years' plants supplied by Chilli Bob (2014). The plantlets had an establish root system (6 weeks after cutting) before treatment of Fe+HisNP was applied. The plants were propagated in an Autopot system under greenhouse conditions at the chilli farm (figure 6.2) using Gold Label 60/40 (60% coir, 40% clay particulates).

Figure 6.71 Autopot system (Source www.autopot.co.uk).

The Autopot system uses a reservoir of feed solution that is supplied under the plant. Each reservoir tank (50 L) fed 40 plants. The wicking system, supported by a valve, allowing 20 mm of nutrient solution to be available in the feed tray on the underside of the plant at all times. The feed solution

was changed once a week using a commercial hydroponic feed by Canna (CannaAqua) with the addition of FeNP at the allocated concentrations throughout propagation. No additional lighting or heat was provided in the Kelda Greenhouse

6.1.3 Capsaicin analysis

Dried fruit, 1g was suspended in ethanol, 2.5 mL and heated to 80ºC for 2 hours. After cooling to room temperature, the sample was then centrifuged at 5000 rpm for 5 mins. The supernatant was replaced with ethanol, 2.5 mL and the procedure repeated to obtain an ethanolic extract (5 mL). HPLC analysis was used to measure the capsaicin and dihydrocapsaicin content of the solution by comparison with calibration curves.

The calibration curve was produced by accurately weighing 50.0 mg of a mixture of capsaicin/dihydrocapsaicin (4:1) and making up a 400/100 ppm solution using distilled water (100 mL). Parallel serial dilution was used to produce solutions at the following concentrations: 400, 320, 250, 200, 160, 125, 100, 80, 50, 40, 25, 20, 12.5, 10, 6.25 and 5 ppm of capsaicin, dihydrocapsaicin and nonhydrocapsaicin. HPLC analysis of these solutions was performed with an isocratic elutant of acetonitrile/water (1:1) and formic acid (0.1%), a 10 µL sample injection and UV detection wavelength of 222 nm. Capsaicin, dihydrocapsaicin and nondihydrincapsaicin were observed to elute at approximately 6 and 7.5 minutes respectively and calibration curves used to correlate the areas of the HPLC peaks with concentration, figure

6.2 Results and discussion

6.2.1 The effect of FeNP+His on growth

As shown in figure 6.3, the FeNP+His 6 mg / L treatment produced the tallest plants with an increase of 70 mm between week 1 to 5 since treatment began. Comparing the height obtained by FeNP+His 6 m g / L to the increase of control and ‘Chilli Focus’ fed plants, 56 and 60 mm respectively. Performing the statistical analysis Z-Test with a 95 % confidence, there was no significant difference found between control and FeNP+His 6 mg / L, as the CI value was greater than 1 (CI = 1.96). Figure 6.3 suggests the other weekly treatments have not attained an improved or diminished height compared to control to note. Table 6.1, depicts the percentage difference in heights from the first week after the initial application to the fifth week. The applications ‘Chilli Focus’, FeNP+His 6 mg / L and His 12 mg / L gained a greater percentage in height increase than the control.

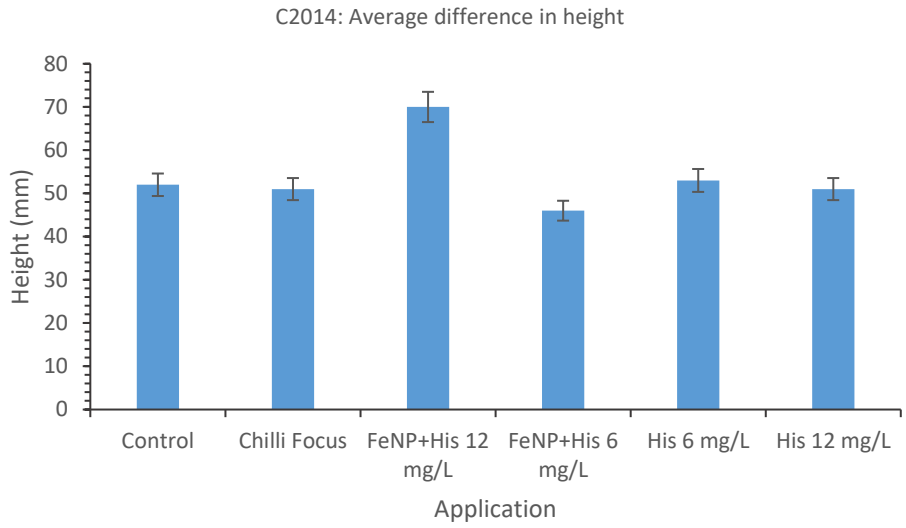

Figure 6.72 The average gain in stem height of chilli plants between the 1st and 5th week of treatment.

Treatment	*Percentage (%) increase between week 1 to 5, since the application of treatment*
Control	96.30
Chilli Focus	110.87
FeNP+His 6 mg / L	145.83
FeNP+His 12 mg / L	85.19
His 6 mg / L	88.33
His 12 mg / L	134.21

Table 6.24 Increase in height gained between first and fifth week of the allocated weekly treatment.

The growth rate of plants in trial C2014, had steady gain in heights comparable to control, figure 6.4a. Treatment FeNP+His 6 mg / L increased rate in growth from week 3. His 12 mg / L appear to increase growth rate between week 4 to 5, contrasting to the tapering rate noted in control and treatments of 'Chilli Focus', His 6 mg / L. The treatment of FeNP+His 12 mg / L fluctuates in growth rate with increases in weeks 1 to 2 and 4 to 5 (figure 6.4b).

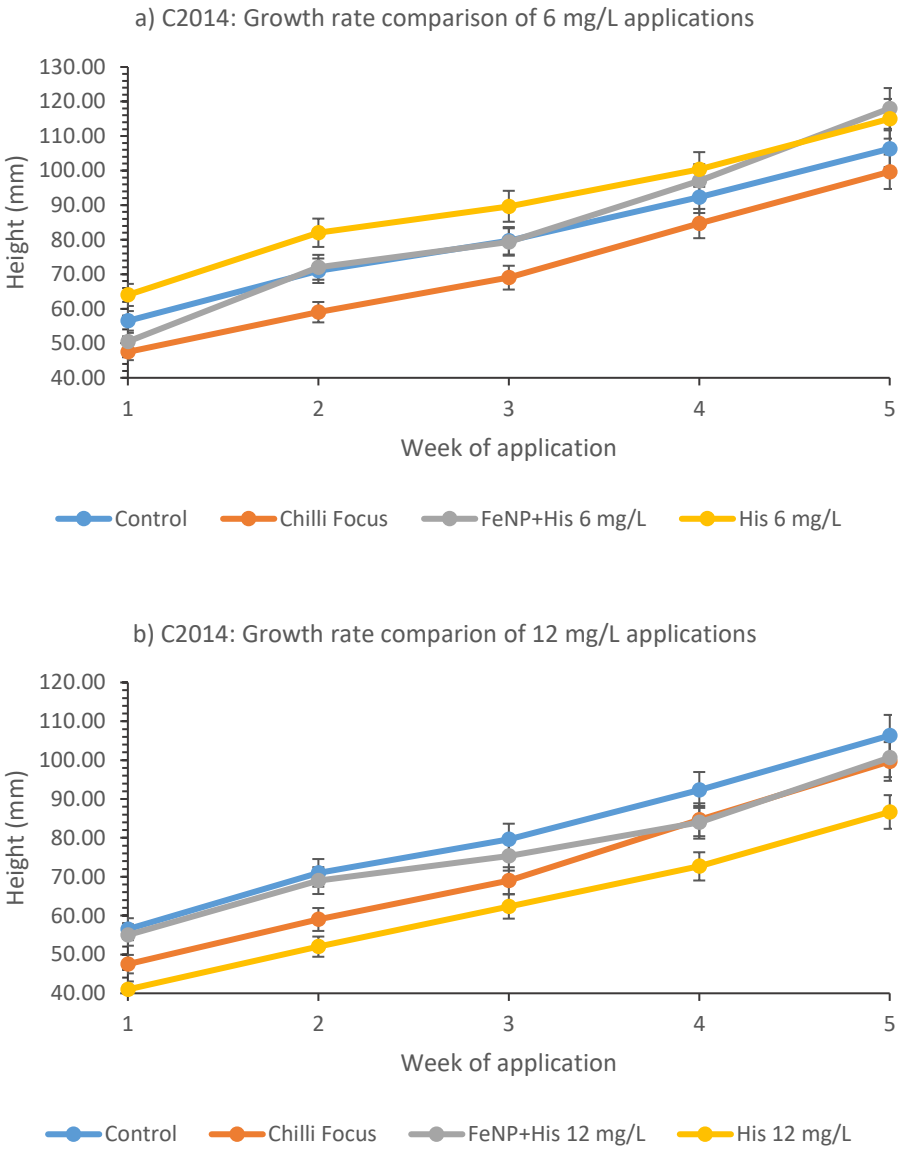

Figure 6.73 Rate of growth of 'cayenne' chilli pepper plants in trial C2014, comparing against control plants, Chilli Focus fed and; a) 6 mg/L FeNP+His and His; b) 12 mg/L FeNP+His and His.

Heights achieved by chilli pepper plants in trial CB2015, were observed to acquired taller plants when treated with of FeNP+His 12 mg / L compared to control; Habanero Red, 5.44 %; Jamaican, 9.28 %; Scotch Bonnet, 10.50 % and Pequin, 27.80 % (figure 6.5). Only Pequin chilli plants treated with FeNP+His 6 mg / L gained an increase in height (25.5 %) when compared to control. Despite the percentage increases, there was no significant difference found with ANOVA single factor. There were significant differences, $<p=0.05$, found between treatments with Pequin plants for both concentrations of FeNP+His using statistical a F-Test, plus a significant difference with t-Test assuming equal variances, one-tail (12 mg / L against control).

Jamaican chilli pepper plants, FeNP+His 12 mg /L, achieved a significant increase in height against control using f-Test analysis (p=0.0110), however a significant decrease in height was found when comparing Jamaican FeNP+His 6 mg / L against control (p=0.0401).

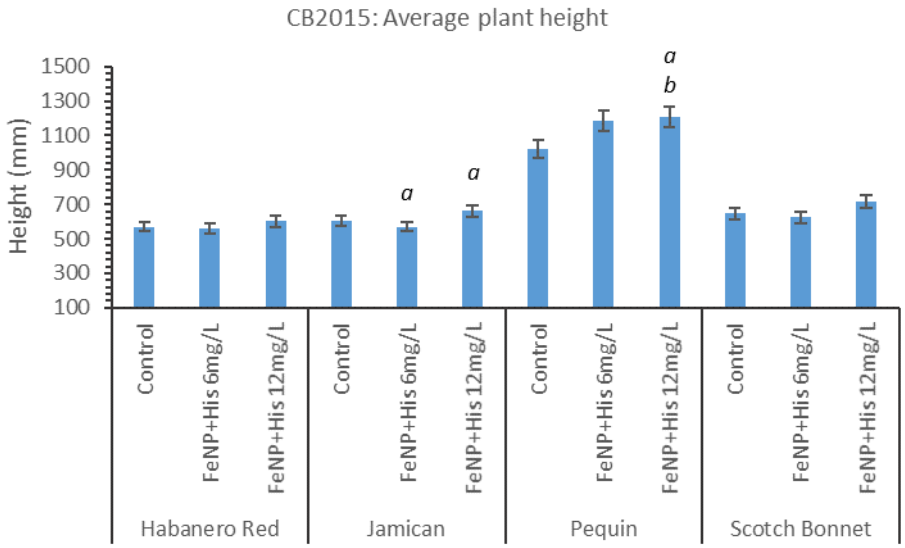

Figure 6.74 Average height gained by chilli pepper plants cultivated in CB2015 trial in a hydroponic Autopot propagation system. Significant difference, < p = 0.05 from F-Test, 'a' and t-Test: Two-Sample Assuming Equal Variances, one tail, 'b' are represented on the graph.

6.2.2 The effect of FeNP+His on yield

Comparing total FW (g) per plant and average FW (g) per chilli pepper, a pattern was observed indicating higher FW obtained per plant reduces FW per chilli. Treatments' Chilli Focus' and 'FeNP+His 6 mg / L' obtained FW per plant 100.89 and 109.14 g, average weight per chilli pepper, 'Chilli Focus' peppered average 0.64 g and 'FeNP+His 6 mg / L', 0.66 g. Concluding in an increase of 38.34 and 49.65 % per plant comparing against 'control' ('Chilli Focus' and 'FeNP+His 6 mg / L', respectively) with a decrease of -19.82 and -17.96 % when compared against control data. Contrasting data from treatment His 12 mg / L displayed an increase of 6.03 %, 77.33g total FW per plant and an average of 0.86 g per chilli, similar to that obtained by control (0.80 g).

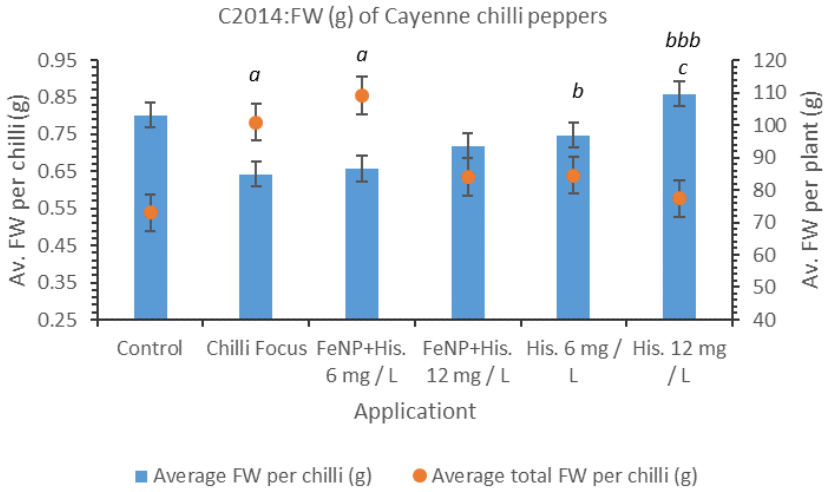

Figure 6.75 FW obtained from C2014 trial. ANOVA statistical analysis performed on average FW per chilli and ranked as with pervious data. Statistical difference against 'Control'= a, against' Chilli Focus' = b and FeNP+His 12 mg / L against His 12 m g / L = c.

The presence of FeNP+His appears to decrease FW per plant but increases FW per chilli pepper as observed in figure 6.6. The treatment 'His 12 mg / L' produced significantly heavier chillies that the FeNP. counterpart (p = 0.0263). These results indicate the FeNP induces a slight stress response (Rahman and Inden, 2012; Kehie *et al*., 2013) resulting in an increase in fruit production.

Variations of FW between cultivars and sub species of *C. annuum* in response to the presence of FeNP+His, are observe in figure 6.7. The three *C. chinense* varieties (Habanero Red, Jamaican and Scotch Bonnet) produced more FW (g) per plant at 12 mg / L than the control counterparts (figure 6.7).

Using a H_o: "*The application of FeNP+His 6 or 12 mg / L does not have an effect on the harvested FW",* was tested with ANOVA. At a concentration of 6 mg / L Habanero Red and Jamaican both produced significantly more FW (g) than control, (Habanero p = 5.13 X 10^{-3}, Scotch Bonnet p = 5.09 x 10^{-4}), thus rejecting H_o. From the statistical analysis, it was also noted that a large significant difference between applications of FeNP+His 6 and 12 mg /L were obtained for *C. chinense* varieties, disregarding Jamaican, as the FW for FeNP+His 6 mg / L were significantly lower than control.

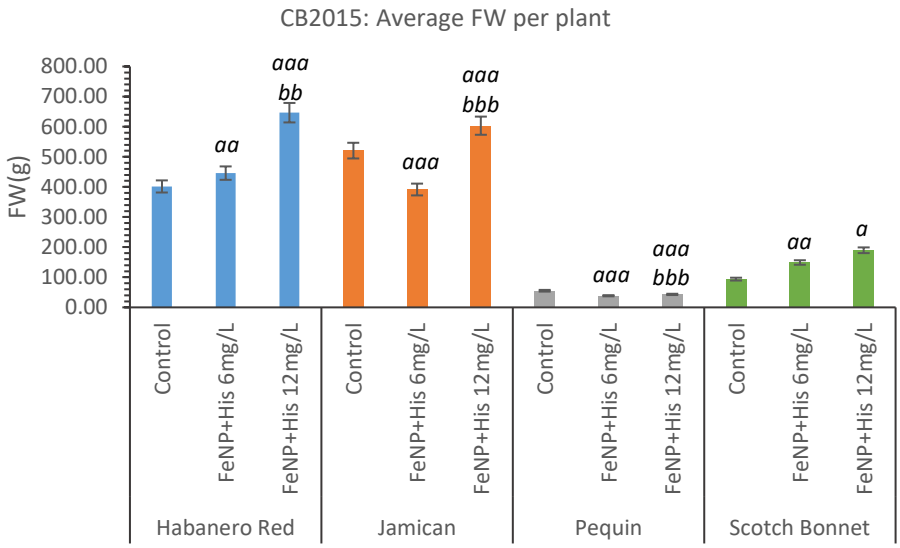

Figure 6.89 Average FW of chilli peppers harvested per plant from trial in collaboration with Chilli Bob's Chilli Farm, CB2015. a, indicates a sig.dif. against control plants;b, between FeNP+His applications, p-values ranked as previously described.

In contrast Jamaican chilli plants at 6 mg / L produced significantly lower FW than 'Control'. Comparing growth data, figure 6.5, a reduction in height obtained by Jamaican plants fed with FeNP+His 6 mg / L is observed leading to the conclusion that the application of 6 mg / L has a detrimental effect to the cultivation and production of fruit. Pequin cultivar also obtained significantly lower FW for both applications of FeNP+His leading to the suggestion that *C. annuum* sub species have a low tolerance to the presence of Fe. As only one cultivar of the *C. annuum* was propagated in this trial this is inconclusive.

Comparing average FW from trials C2014 and CB2015 (Habanero Red and Jamaican), figures 6.6 and 6.7, it is observed that a repetition of an increased FW obtained per plant coincides with increase amount of FeNP+His fed with no effect to vegetative growth.

6.2.3 The effect of FeNP+His on the DM%

Comparing average DW from C2014, obtained per plant (figure 6.4a) reflects the data collated for the FW (figure 6.6) with sig. dif. found between control and Chilli Focus ($p = 7.18 \times 10^{-3}$), control and FeNP+His 6 mg / L ($p = 0.0186$).

From figure 6.4b, 'Control' chillies produced the highest DM % with the applications of His producing significantly lower DM than 'Control', 'Chilli Focus' and applications of FeNP+His Using H_o "*Application of FeNP+His has no effect on the DM % of chilli peppers"*, the hypothesis can be accepted. DM % is

important to commercial production of chilli peppers in regard in economy of drying the fruit. In this instance the application of FeNP+His would not benefit commercial production economically nor would it be detrimental.

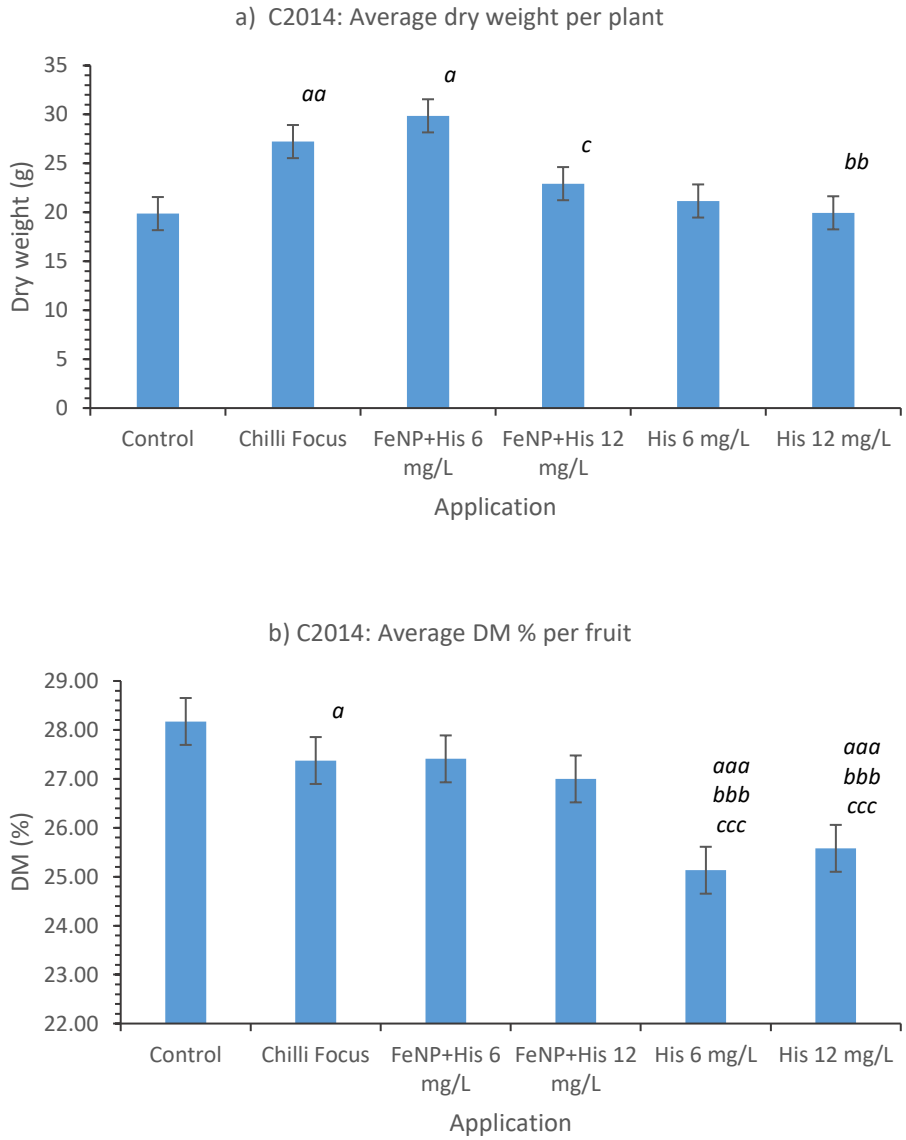

Figure 6.77 Cayenne chilli, C2014. Average DW obtained per plant (a) and DM % average per chilli (b). Significant differences indicated as follows; a, against control; b, Chilli Focus; c, FeNP+His compared against His counterpart. Differences were ranked as previously described.

The DM % obtained from Habanero red and Scotch bonnet chillies from trial CB2015, produced similar results to the C2014 trial with regards to the application of FeNP+His 6 mg / L obtaining no sif. dif. although C2014 FeNPHis 6 mg / L produced a 1.37 % increase, CB2015 Scotch bonnet 6 mg / /L = 5.33 % increase, figure 5.38. In contrast, CB2015 Habanero 6 mg / L produced a decreases of 4.99 %. Other application of FeNP+His 6 mg / L produced sig. dif. increase of DM % (Pequin $p = 4.90 \times 10^{-6}$), rejecting

H_o with a sig.dif. decrease of DM % (Jamaican p = 5.43 x 10^{-5}) therefore accepting H_o. All *C. chinense* varieties had significant decreases in DM % when treated with 12 mg / L, possibly causing a phytotoxic effect, however, without further investigation this cannot be conclusive. This detrimental effect was not observed in C2014, suggesting the compost substrate in which the cayenne peppers were cultivated, retained FeNP thus buffered the plant against overload of Fe.

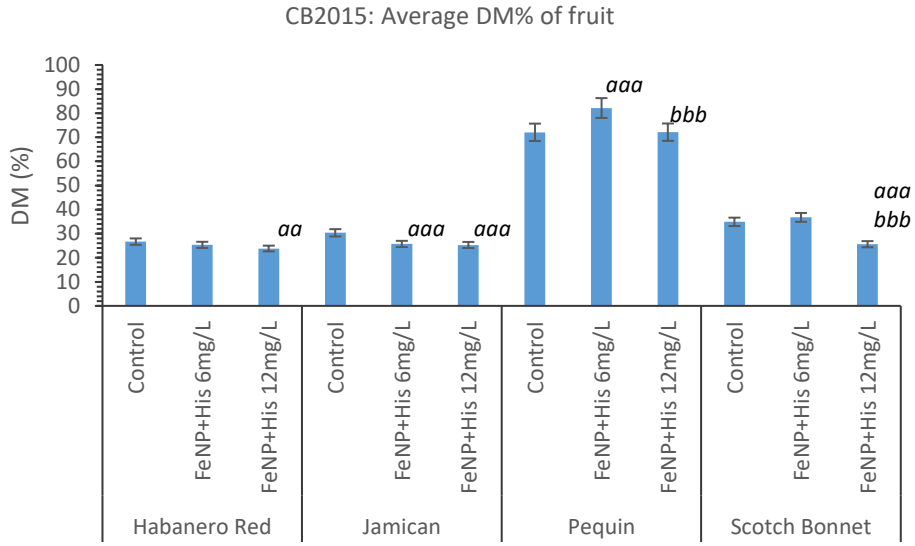

Figure 6.78 Average DM % of chilli pepper fruit from CB2015. significant differences found using ANOVA single factor analysis and ranked as before. Significant differences are indicated as follows; a, against control; b, between FeNP+His applications.

6.2.4 The effect of FeNP+His on the iron content of the crop

Data collected from the two chilli trials (C2014 and CB2015), conducted in consecutive years, demonstrates the variation in variety and sub species response to the presence of Fe.

From the hydroponic propagated varieties of *c. chinense*, figure 6.11, all three varieties gained a significant increase in Fe content when fed with FeNP+His 6 mg / L against control fruits Fe content. Jamaican and Scotch bonnet gained greater Fe fortification from FeNP+His 12 mg / L with significant increase over control fruits and FeNP+His 6 mg / L application. The variety pequin, *c. annuum var. capsicum*, appears to present sensitivity to Fe. Pequin plants gained significant increase in height over control, with increasing concentration of FeNP+His, figure 6.5. The detrimental effect of increasing Fe availability appears to be with yield and the TF of Fe to the fruit. Pequin peppers, unlike the *c. chinense*, are tall, small leaved bush plants. The iron seems to have been utilised for foliar growth.

The concentration of Fe determined from C2014 pepper is lower than that of the CB2015, figure 6.10 and 6.11. The C2014 cayenne peppers were cultivated in a compost media increasing the binding of the FeNP to organic ligand present. This has a positive effect as the retention of Fe enables supply of bioavailable Fe (Ebbs *et al*., 2016; Sawicka *et al*., 2016) but decreases the amount available to the plant due to Fe strong bond potential (Marschner, 2011). This can buffer the plant from hyper accumulation (Navarro *et al*., 2008), however when compared to hydroponically propagated chilli peppers, FeNP has a higher TF than in compost. Due to the small sample size in both trials this theory cannot be certain.

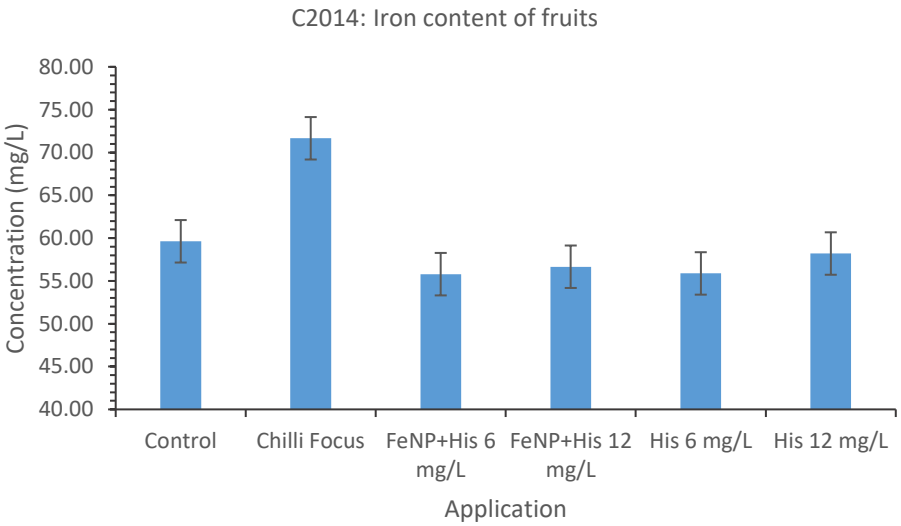

Figure 6.79 Fe content of Cayenne chilli pepper fruits after FeNP+His application during trial C2014.

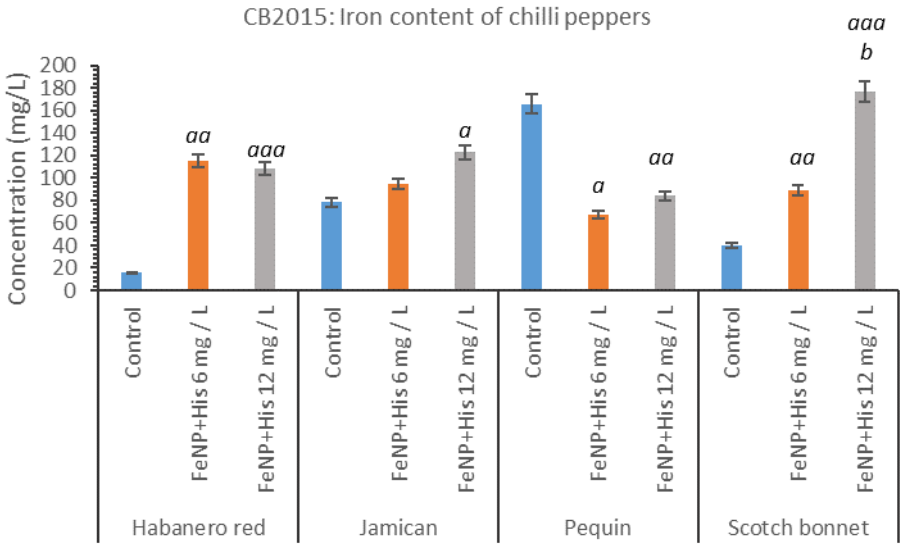

Figure 6.80 Iron content of chilli peppers from trial CB2015. Statistical analysis performed by ANOVA is illustrated by a, against control and b, between iron treatments.

6.2.5 FeNP fortification effects on the level of capsaicin, CB2015.

Using standards of capsaicin, dihydrocapsaicin and nordihydrocapsaicin from Sigma Aldrich to construct calibration graphs, (app.86) where by the concentrations of capsaicioids could be determined, mg / L per gram. Capsaicin data (mg / L) were finally converted into Scoville units (SHU) (table 6.2) to determine the 'heat' of the chilli peppers harvested by multiplying by 16 as 1 mg of capsaicin has a pungency of 16 million Scoville units (Islam *et al*., 2015).

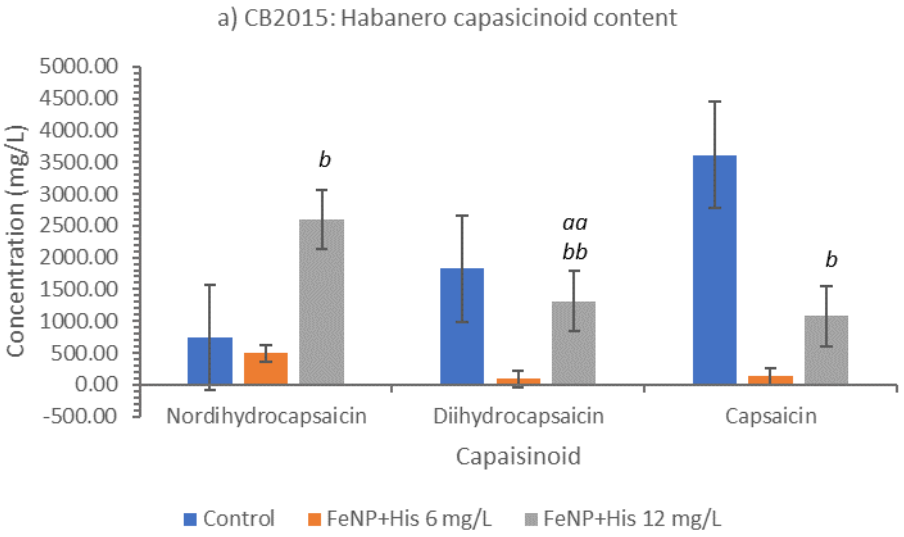
a) CB2015: Habanero capasicinoid content
Concentration (mg/L)
5000.00
4500.00
4000.00
3500.00
3000.00
2500.00
2000.00
1500.00
1000.00
500.00
0.00
-500.00
b
aa
bb
b
Nordihydrocapsaicin
Diihydrocapsaicin
Capsaicin
Capaisinoid
Control
FeNP+His 6 mg/L
FeNP+His 12 mg/L

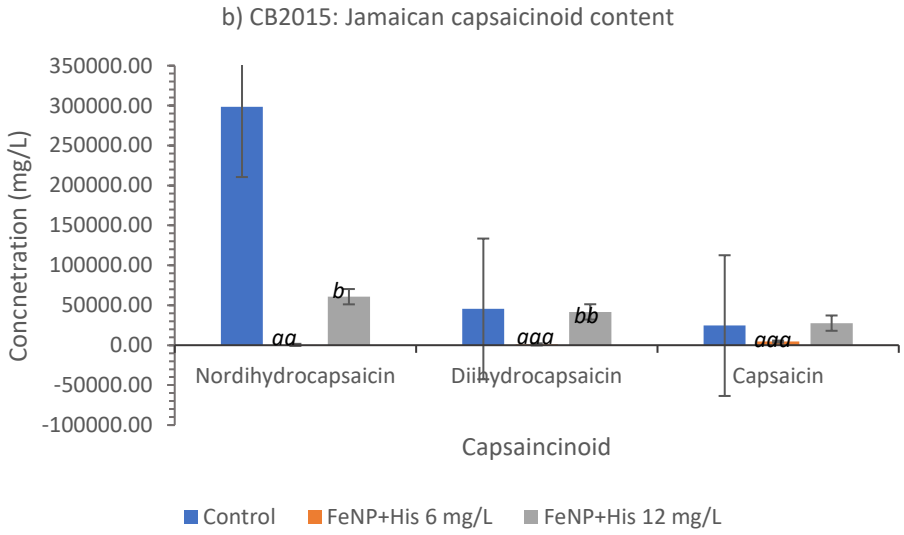
b) CB2015: Jamaican capsaicinoid content
Concnetration (mg/L)
350000.00
300000.00
250000.00
200000.00
150000.00
100000.00
50000.00
0.00
-50000.00
-100000.00
b
aa
aaa
bb
aaa
Nordihydrocapsaicin
Diihydrocapsaicin
Capsaicin
Capsaincinoid
Control
FeNP+His 6 mg/L
FeNP+His 12 mg/L

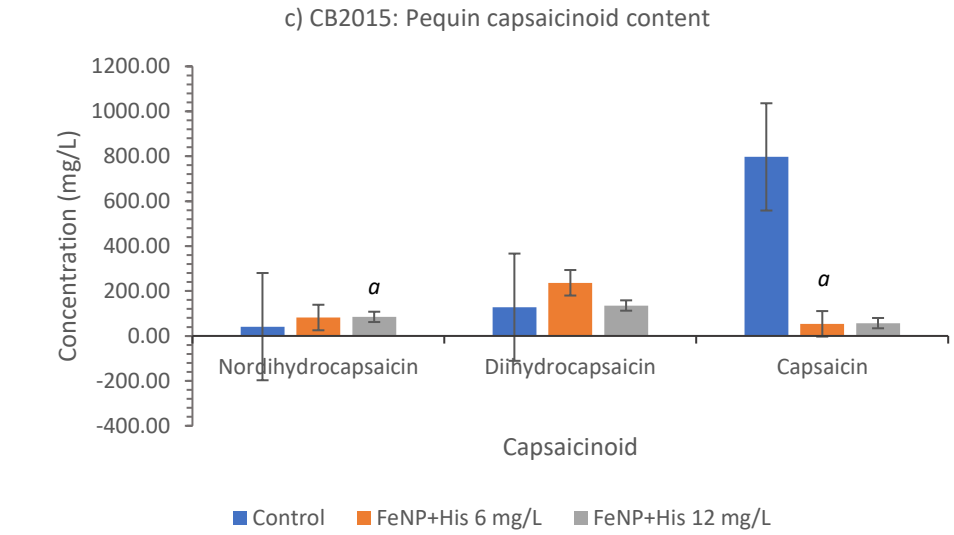

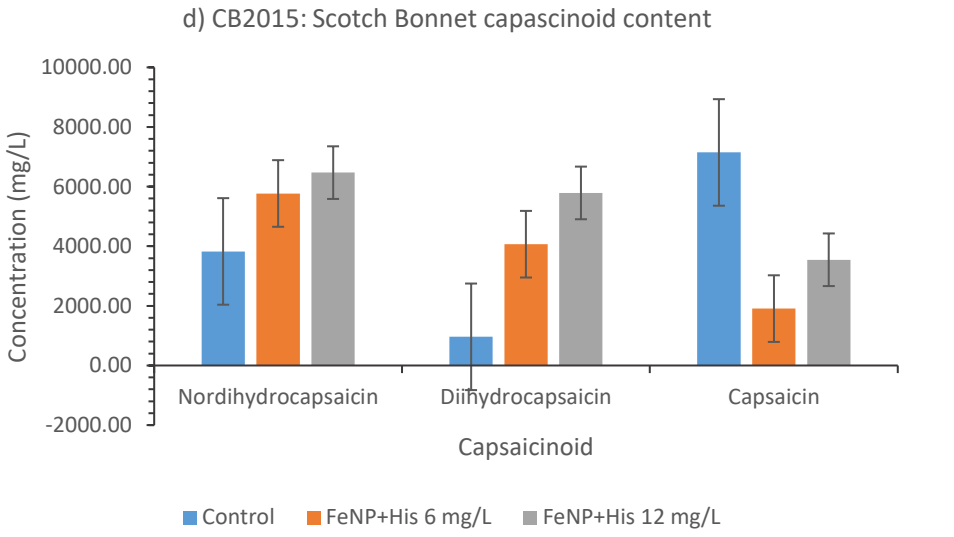

Figure 6.81 Capsaicinoid content of the four varieties of chilli pepper treated with FeNP+His during trial CB2015. Significant difference between control and FeNP+His application = a, between FeNP+His applications = b.

	Scoville unit (SHU)			
	Habanero red	*Jamaican*	*Scotch bonnet*	*Pequin*
Control	57750.2	423895.90	66772.65	663.41
FeNP+His 6 mg / L	2086.65	72576.29	92329.81 *	1312.08 **
FeNP+His 12 mg / L	17189.97	541025.82 *	103521.94 **	1357.87 **

*Table 6.25 Scoville units (SHU) of chilli peppers cultivated in CB2015. * = SHU increase above 25% over control, ** = SHU increase above 50 % over control.*

Using a null hypothesis; H_o, *"application of FeNP+His does not influence the capsaicioid content / SHU",* the following observations were made. From the Fe content of the chilli peppers collected via ICP, the nordihydrocapsiacin content of the chilli peppers increases with the FeNP+His application, as observed in figure 6.12a to d where the greatest concentration of nordihydrocapsaicin are obtained from those peppers treated with 12 mg / L. Scotch bonnet peppers increased in fortified Fe correlating with increase in the FeNP applied, figure 6.12; the correlation of fortification to capsaicioid content also followed this trend. No Signiant differences, using ANONA single factor analysis, was found therefore H_o was accepted but rejected when comparing the percentage increase of SHU over control, table 6.2 (sig. dif. >25%). The Pequin peppers obtained SHU increase over control content, even though the Fe content of the peppers was found to be significantly lower than control.

Jamaican peppers favoured 12 mg / L for increase in Fe fortification (figure 6.11) and the increase in nordihyrdocapsaicin and capsaicin content (mg / L), figure 6.12b, and increase in heat (SHU) table 6.2.

The application on FeNP+His 6 mg / L to Habanero red and Jamaican chillies, appears to have a detrimental impact on the capsaicinoid content of the peppers, figure 6.12a and 6.12b, with instances of significant decreases against control.

The application of FeNP+His 12 mg / L may induce stress to the plant that increases capsaicinoid content. An increase in capsaicinoid content has been proven to be a response in terms of water stress (Estrada *et al*., 1999; Ruiz-Lau *et al*., 2011) and saline conditions (Arrowsmith *et al*., 2012). To examine this response a more comprehensive trial with a larger number of plants, preferably taken form cuttings to reduce the genetic variation, with a much larger sample number and the inclusion of more varieties due to the range of response the data has shown. The use of hydroponic propagation would be advantageous as it reduced the great variation of mineral content provided from growth substrates of soil and compost.

7 Foliar transfer of FeNP+His

An alternative to current commercial applications of Fe, iron oxide nanoparticles have been used in variety of applications over a number of years due the in the ability to improve function, performance and increase cost-effectiveness in engineered materials. This novel application in agriculture observes the uptake of Fe_3O_4 when applied as a foliar application rather than to the soil. Currently foliar Fe application is problematic due to the mineral uptake mechanisms of the leaf and current commercial formulations. Treatments are limited when iron deficiency occurs, chlorosis, as it is deemed that plants will not take up or utilize Fe when they are not under stress.

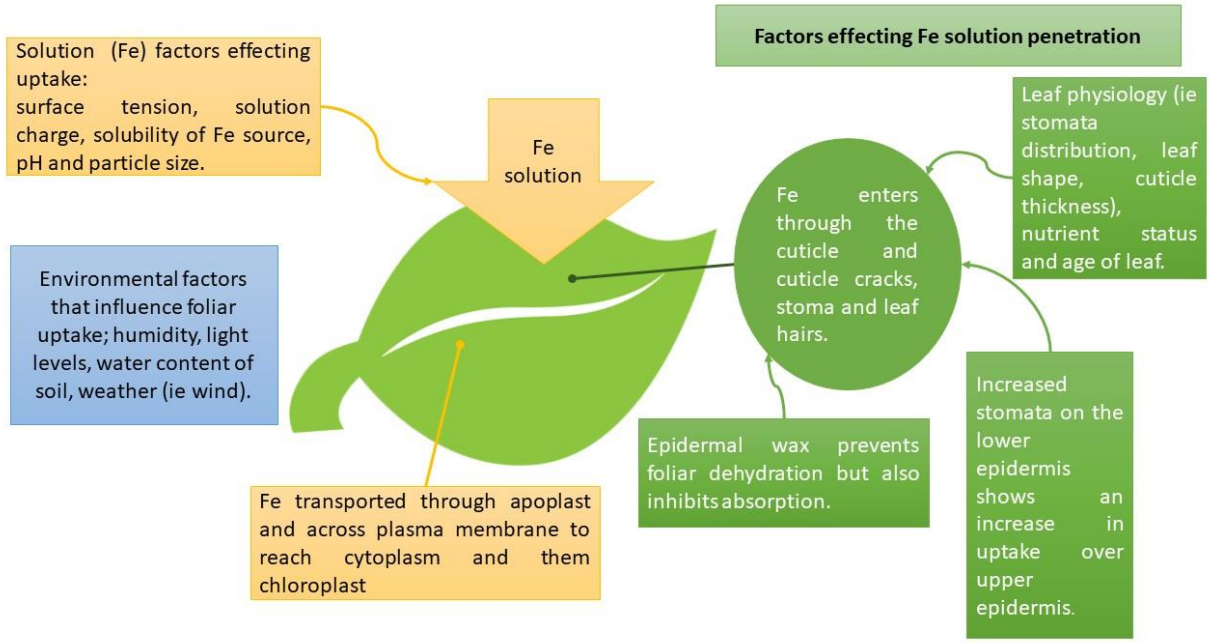

Figure 7.82 Summary of factors effecting the diffusion of Fe when applied as a foliar solution

Foliar application of Fe in the form of $FeSO_4$ or Fe-chelate for the rapid alleviation of, chlorosis, coursed by the calcareous soils and increased pH [9-11]. Using a foliar application eliminates the obstruction soil based fortification poses. Due to the cost implications, $FeSO_4$ is predominantly used for rapid application as it is a cheaper alternative than Fe-chelates and more soluble, resulting in more instantaneous 'greening' of the foliage (Fernández and Ebert, 2005). Due to the sulphates high solubility potential, foliar applications are regarded as an environmentally friendly approach to fortification as the contact with the soil is reduced (El-Jendoubi *et al.*, 2014) subsequently reducing

leaching of $FeSO_4$. Efficiency of a foliar application depends on many conditions; therefore, the uptake of Fe is complex, as illustrated in figure 7.1.

7.1 Materials and methods

The strawberry plants, variety Elsanta, were kindly supplied by S&A, Spalding, UK and cultivated in Erin multipurpose compost, individually planted in 1L pots purchased from LBS horticulture. The synthesis and coating of the FeNP+His used in the following trials are synthesised and coated as previously described. Statistical analysis was carried out using ANOVA single factor, Microsoft Excel and ranked in significance using the *p*-values obtained.

7.1.1. Foliar application of iron nanoparticles

This trial used one-year-old strawberry plants used to observe the translocation of Fe through the plant via foliar application of a water based FeNP+His, 60 mg / L. Each plant held a total of six tri-compound leaves with identical watering regimes with both cohorts had five replicated receiving no further fertiliser or feed during the trial period. The five plants only receiving water acted as controls. One tri-compound leaf was allocated for the application of FeNP+His per plant in the treated cohort. The solution (2 mL) to be applied on a weekly basis via a brush to ensure no cross contamination due to airborne particles.

7.1.2. Analysis of iron content and dry matter percentage

Foliage samples were washed in deionized water three times before being dried at room temperature for 30 min. Each sample's weight was recorded before drying in a vacuum oven at until the samples weight loss stabilized, obtaining DM %. A Milstone Ethos UP High Performance Microwave Digester was used to fully digest the foliage samples in a solution of nitric acid and hydrogen peroxide as suggested in the Milstone pre-set methodology 'Dried plant material'. The solution obtain was diluted to 20 % and converted to mg / L per gram sample using a Perkin Elma ICP-OES Optima 2100 DV.

7.2. Results and discussion

Leaves directly applied with FeNP+His, 60 mg / L, contained significantly higher amount of iron than control leaves and leaves untreated from the same plant (values) as observed in table 7.1. Interestingly, leaves from the treated plants that were not treated themselves, also contained significantly higher amounts of iron than control leading to the conclusion that the iron nanoparticle was successfully taken up and transported through the plant.

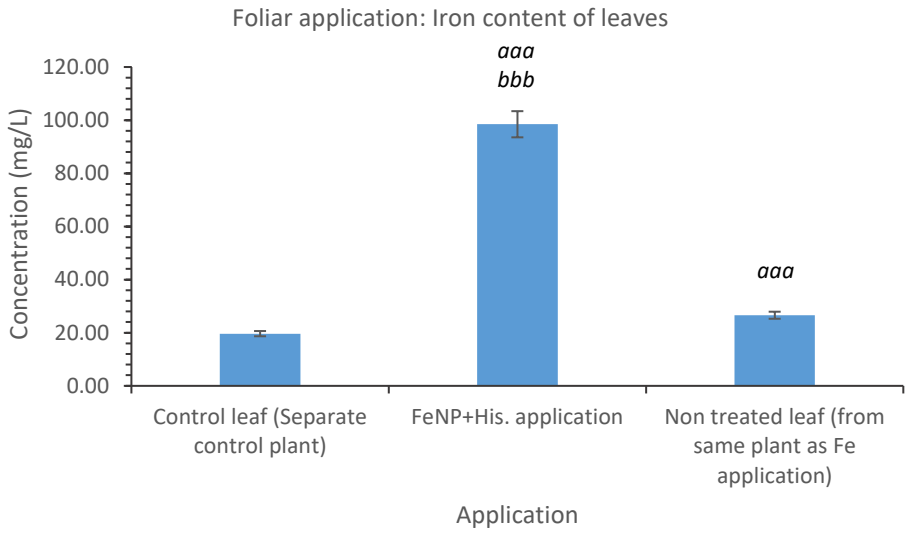

Figure 7.96 Iron content of leaves from control plant leaves and leaves from the FeNP+His foliar applied plants. Level of significant difference against control = a; between application leaf and non-application leaf = b.

From figure 7.2, the leaves that were directly applied with FeNP+His, 60 mg / L, contained significantly higher amount of iron than control leaves and leaves untreated from the same plant. Interestingly, leaves from the treated plants that were not treated themselves, also contained significantly higher amounts of iron than control leading to the conclusion that the iron nanoparticle was successfully taken up and transported through the plant.

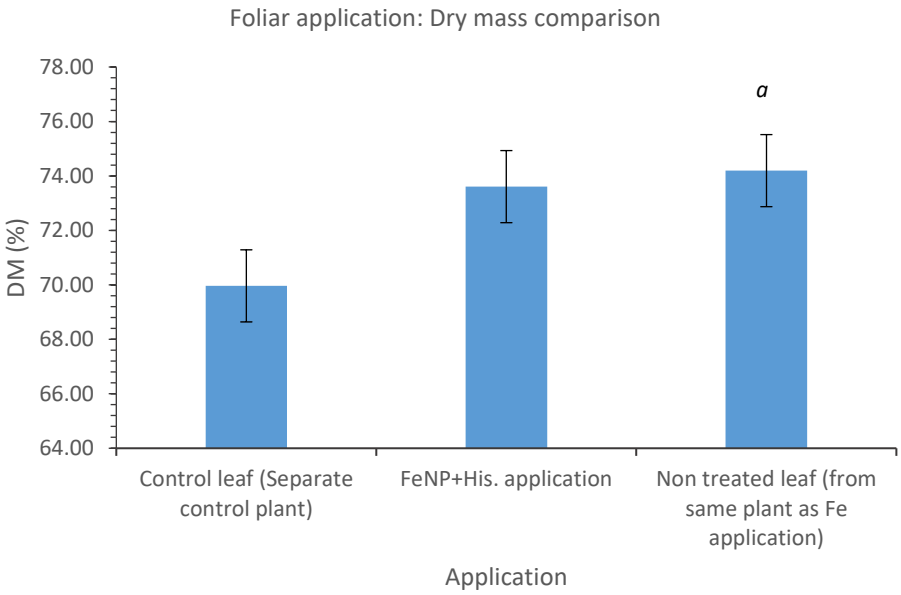

Figure 7.97 DM% of leaves in foliar application trial. Level of significance against control = a.

Figure 7.3 represents the dry mass percentage (DM%) of leaves sampled from control (no iron application), direct application leaves and leaves from treated plant that were untreated. The leaves that had the FeNP+His. directly applied increased in DM % by 3.65 %, however the non-treated leaves from the Fe fortified plant did increase significantly ($p = 0.0284$) in DM over control, leading to the conclusion the increased Fe content has had an impact on the physiology of the plant.

The FeNP+His, 60 mg / L solution was applied to upper and lower epidermis using a brush to ensure no cross contamination to surround leaves that would be tested for Fe transfer. Repetition of this trial would be recommended as the sample number ($n = 8$) was small. It would also be of interest to perform foliar application on leafy crops such as spinach or a variety of lettuce, where the positive influence the application of FeNP+His had had on the DM% would increase the crop value. Further to investigations, the concentration used in this trial, 60 mg / L was used to maximise uptake and to observe any detrimental effect a high FeNP would have on leaves applied with the solution. No leaf discolouration was observed, therefore it would be of interest to investigate the maximum and minimum FeNP concentration required to fortify leaves.

The dry mass percentage (DM %) of leaves sampled from control (no iron application), direct application leaves and leaves from treated plant that were untreated. The leaves that had the FeNP+His directly applied increased in DM % by 3.65 %, however the non-treated leaves from the Fe fortified plant did increase significantly ($p = 0.0284$) in DM% over control, leading to the conclusion the increased Fe content has had an impact on the physiology of the plant.

Caution into the use of a spray has been raised due concerns of nanomaterial increasing penetration and increased reactivity (through increased surface areas to volume ratio) (Nel *et al*., 2006) especially in contact with mucus membranes (lungs, nasal cavity) (The Royal Society, 2004). This is an ongoing investigation and discussion throughout nanomaterial research community. Regarding application of MONP as a spray, legislation in PPE (personal protective equipment) and guidelines for pesticide and fertiliser applications are already in place in the agricultural and horticultural industry that would safe guard users. Preliminary environmental assessments on the retention in the soil / compost and effects of MONP in an aquatic environment have been conducted in this project, however, in-depth studies across the metal oxide nanoparticle range at various concentrations is greatly required to give an indication into the behaviour of MONP in the environment.

8 Metal oxide nanoparticles in the environment.

The mineral content of soil is dependant of pH, organic matter and clay content, weather conditions and composition of parent material and exist as free ions or complexed with minerals or organic surfaces, soluble compounds or as precipitates (Evans, 1989; White, 2001; Kelling and Schilte, 2008; Schulte, 2008; Mousavi, 2011). Free metal ions that are released or added via fertiliser, the ions interact with the charged particulates that may form weak complexes through cation exchange or strong bond through ligand exchange. The associations these ions form largely depends on the nature of the ion and absorbing surface (Evans, 1989). Metal ions of calcium, iron and zinc (Ca^{2+}, Fe^{3+}, Fe^{2+}, Zn^{2+}) are unavailable as they form strong bonds with clay and organic matter in the form of oxides and hydroxides binding the metals into the soil / compost matrix (Marschner, 1993). Insoluble complexes are unable to move through the matrix to the root / tuber to compost interface where reduction in the pH enables chelation and uptake.

The histidine coating of the nanoparticles, increases mobility through the strata due to the ability to suspend the nanoparticle and move with water. This allows passive diffusion into the tuber/root membrane through a concentration gradient. The amino acid coating provides a barrier to limit the mineral to complexing with ligands in the compost that would otherwise decrease availability. However, increased mobility and reduced ability to complex may lead to leaching of the MONP to the lower level (30 cm) From section 5.5 it was observed there is fortification from the application of MONP. With this in mind, two null hypothesis formed:

H_o^1; the amount of mineral at the depth of 5 cm is less than at 30 cm due to leaching when MONP+His. applied.

H_o^2; there will be no significant change in the concentration of minerals when MONP+His applied when compared to control at depths of 5 and 30 cm due to increased assimilation of minerals from compost.

With increased mobility, it was question if excess nanoparticle will be leached through the strata with possible effects to the environment, in particular to watercourses, hence the requirement for the folloing observations of MONP+His retention in soil.

The high mobility of the FeNP due it the histidine coating, plus nano-size particles, allows the passive movement of Fe into the cell like Ca^{2+}. The coating provides a barrier to This feature has the potential to leach through the strata.

With the potential of MONP entering water systems through soil or foliar application, an aquatic ecotoxicology study was performed to observe potential effects. G Pulex used as a bioindicator species in freshwater systems for chemical stressors for a number of years (Chaumot *et al*., 2015). The shrimps inhabit the silt of water courses and feed from organic matter. If the MONP where to enter a water course or if organic matter treated with a foliar application of MONP where to come into contact with aquatic life, it is more likely the MONP will accumulate in the silt layer.

8.2 Methods and materials

Hydrochloric acid, 37 % and Nitric acid, 36 %, purchased from Fisher Scientific. Hydrogen peroxide 30% wt. in H_2O purchased from Sigma Aldrich UK. All chemicals used without further purification. Erin multipurpose compost was purchased from LBS Horticulture, UK and used as the propagation media in potato trials Sax2015 and Sax2016.

8.2.1 Determination of MONP retention in compost

Compost samples from the greenhouse trials where taken at depths of 5 and 30 cm to give an indication of transport of the MONP through the strata at the end of the propagation trial, Sax2015 and Sax2016 (figure 8.1).

Figure 8.85 Sampling of compost in trials Sax2015 and Sax2016.

Samples were dried at dried in dehydrator at 65°C for 20 hours, ground to a fine powder using a Tefal GT203840 Coffee Grinder. Digestion of compost and soil samples carried out using ETHOSUP High Performance Microwave Digester System using the pre-set methodology *'BSC 300 (soil)',* figure 8.2. All organic material was fully digested using nitric acid, 36 %, 10 mL apart from sand particulates. The fully digested material solution was diluted to 20% for ICP-OES analysis.

Sample weight and reagents

Sample weight	Up to 250 mg
Reagents	7 mL HNO3 3 mL HF

Microwave program

Step	Time	T1	Power
1	00:15:00	200C	1800 W*
2	00:15:00	200C	1800 W*

Figure 8.99 BSC 300 soil digestion program for ETHOS UP. www.milestonesrl.com.

8.2.2 Aquatic toxicology of MONP

Based upon paper published Vellinger *et al.* (2012), adult *G. pulex* (n = 8 per rep.) housed in opaque square containers (50 x 50 mm, 60 mm high, 200 mL capacity) with of test solution (100 mL) and 10 glass pebbles (thoroughly washed in distilled water) for the duration of the 96 hours. The *G.pulex* were not fed during the assessment, therefore the pebbles act as refuge to limit cannibalism. Each test solution will have three replicates and changed every 24 hours and kept at a constant temperature, 15°C (Vellinger *et al*., 2012). The MONP solutions were diluted with dechlorinated tap water as distilled water is low in oxygen and will affect the welfare of the shrimps. A control was tested against FeNP+His, 6, 12 and 24 mg / L; ZnNP+His 6 and 24 mg / L.

At the end of the trial the number of remaining alive *G. pulex* were recorded and washed with ultra-pure water, dabbed dry with filter paper and frozen. For mineral analysis, the shrimps were dried at 50 °C for 12 hours and the dry weight recorded before being fully digested in aqua regia, 5 mL (1:3 nitic acid 36% to hydrochloric acid 37%) for 12 hours and diluted to 10% by the addition of ultra-pure water. Mineral content was determined via ICP-OES and SEM-EDX.

8.3 Results and Discussion

8.3.1 MONP retention in growing media

$Ca^{2+}$is a large divalent cation in contrast to Fe and Zn ions (Hirschi, 2004) and moves in conjunction with water when free, however, this a rare occurrence as it forms a tight bond with particulates so much that Ca leaching through the soils strata does not normally occur (Kelling and Shcilte, 2008). Unlike other minerals such as Fe and Zn, Ca^{2+} passively diffuses into the root / tuber via a gradient caused by transpiration in the leaves (Hirschi, 2004; Kelling and Shcilte, 2008; Palta, 2010).

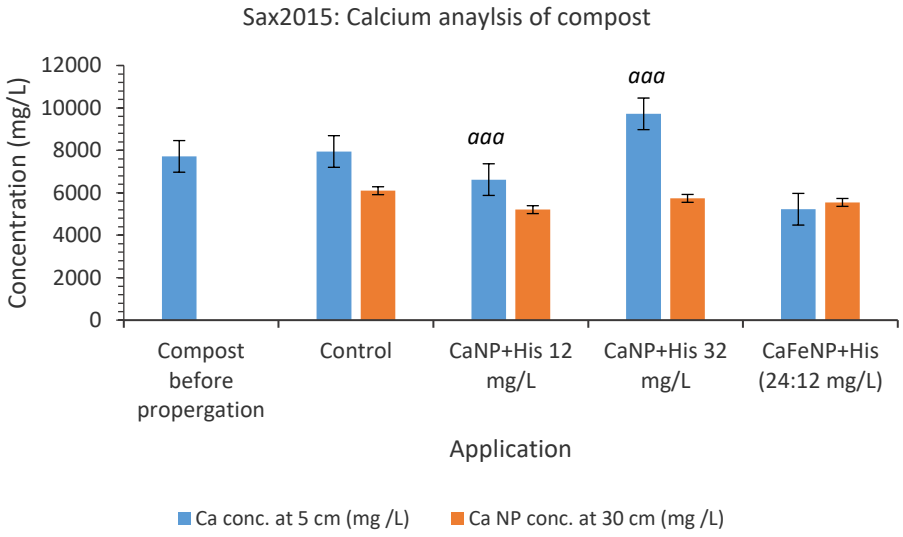

Figure 8.87 Ca content in compost after harvest Sax2015. Using 'a' to signify the sig.dif. between Ca concentrations at depths 5 and 30 cm with in the application using ANOVA single factor.

Data obtained for the growth media during the harvest of Sax2015 trial, the high organic matter composition of the multi-purpose compost naturally has a lower of pH of 5.5 than soils (e.g. from Branston field trial a pH of 6.5 was obtained). Due to an increase in organic acids from the increased organic material, minerals increase in phytoavailability via microbial decomposition (Schulte, 2008).

From figure 8.3, there was not a sig. dif. between Ca concentrations at 5 and 30 cm, with a decrease of 1895.9 mg / L, nor between the Ca concentration between control and compost before the trial commenced (accepting H_o^2). The nature of the compost with reduced pH and increase of organic acids that increase the uptake of calcium, as with other minerals, are responsible for the reduction at 30

cm. The control propagation fed with Chempak, as was the other Ca applications in Sax2015, thus increasing N and possible Ca phytoavailability.

There was no sig. dif. between control and Ca applications, however as figure 8.3 depicts, a sig dif. between 5 and 30 cm was found for applications CaNP+His 12 and 32 mg / L, therefore rejecting H_o^1. The application CaNP+His. 32 mg / L, increased Ca concentration at 5 cm by 25.60 % compared to 5 cm control. The application of calcium ferrite nanoparticles gained the highest concentration of Ca in the tubers harvested from Sax2015 than the application CaNP+His. 32 mg / L with a lower concentration of 12 mg /. There was a higher TF between in the skin of the tubers and compost which allows the conclusion that the reduced amount of Ca in the compost strata has increase the phytoavailability of Ca and thus taken up in the tuber.

The application of FeNP+His. allows the delivery of both Fe^{3+} and Fe^{2+} as a stoichiometric ratio of 2:1 (Fe^{3+}/Fe^{2+}) (Laurent *et al*., 2008), allowing a duel delivery of Fe that is phytoavailable immediately (Fe^{2+}) and a more stable Fe supply (Fe^{3+}), that will not be as readily complexed as Fe^{2+} but available to the plant when Fe^{3+} is reduced in the rhizosphere via a proton pump mechanism (Schulte, 2008; White and Broadley, 2009).

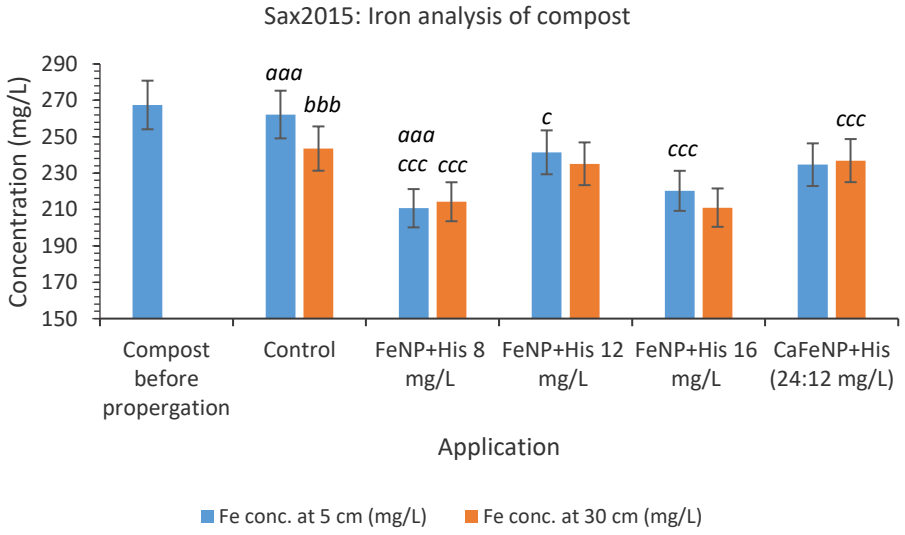

Figure 8.101 Fe content in compost after harvest Sax2015. Using ANOVA single factor significant differences where indicated; a = between depths 5 and 30 cm within application, b = against compost (control only tested), c = against control counterpart.

From data observing the whole tuber maximum uptake of Fe was with the application FeNP+His 16 mg / L with 12 mg / L producing the highest concentration in the skin giving an indication that FeNP+His successfully fortifies the tubers, whether from the nanoparticle supplied the Fe, and / or increased

assimilation with the presence of histidine. This notion was supported by the significant decreases found when comparing control concentrations at 5 and 30 cm with the FeNP+His counter parts concluding to reject H_o^2.

A significant higher concentration at a depth of 5 cm than 30 cm found with control with a significant decrease at 30 cm of the control against compost before application (figure 8.4). The decrease at 30 cm indicates the uptake of Fe around the tubers from the compost. Application of 8 mg / L produced an exception to the results obtained throughout this study, with a significant reduction of mineral content at 5cm.Due to significantly lower Fe concentration in the 5 cm when compared to control and compost before the trial, this suggests Fe released from complexes in the soil and subsequent leaching into the lower strata. The Fe content increases by 33.57 mg / L at 30 cm, accumulating around the areas of the tubers, concluding the acceptance of H_o^1. There was no notable increase in Fe concentration in the tuber. A possible explanation for the increased leaching of Fe could possibly due to a balance of the amino acid, histidine and the FeNP. Histidine could increase nitrogen assimilation and metabolism of the root and tuber, thus increasing mineral availability (Ghasemi *et al*., 2012; Tegeder, 2012). The concentration of iron released and Fe supplied by the FeNP is inadequate, or possible leached into lower strata (> 30 cm), to gain significant increase over control tubers. Another possible explanation could be due to the nature of the compost. Compost varies in composition and to overcome the differentials ten replicate were taken per sample. In hindsight, more replicates are required with increased samples taken in a border range of the strata.

Applications 12, 16 mg / L and CaFeNP+His. show Fe retention throughout the strata of the compost. From figure 5.42 B, the FeNP+His. application 16 mg / L tubers contained the most Fe (72.22 mg / L) with 12 mg / L application retained a significant amount in the skin. This was reflected in the compost Fe content as the applications of 12 and 16 mg/ L decreased in 30 cm compared to the 5 cm concentration, indicating retention of Fe at 5 cm and utilisation of minerals in the tuber region. These concentrations were lower than control counterparts, reaffirming uptake of Fe from the compost. Concentration results from CaFeNP+His compost, shows a decrease over control and compost before applications. A significant decrease in the amount of Fe in the tubers due to the presence of Ca as previously discuss.

Free Zn ions are bound in the soils matrix similarly to Fe (Marschner, 1993) and thus highly dependent in the pH of the growth media. Normality the Zn content of non-polluted soils is approximately $3 \times 10^{-8} – 5 \times 10^{-7}$ M (Barber, 1984) with 15 – 30 % as free ions. Zn acts similarly to Fe with release in the rhizosphere due to decrease of pH are a result of proton pump (White and Broadley, 2009). In figure

8.5, the pattern is repeated (with exception of FeNP+His. 8 mg / L) that has been found in applications of Ca and Fe, higher mineral contractions at 5 cm with a lower concentration obtained at 30 cm, the region of tuberisation and development.

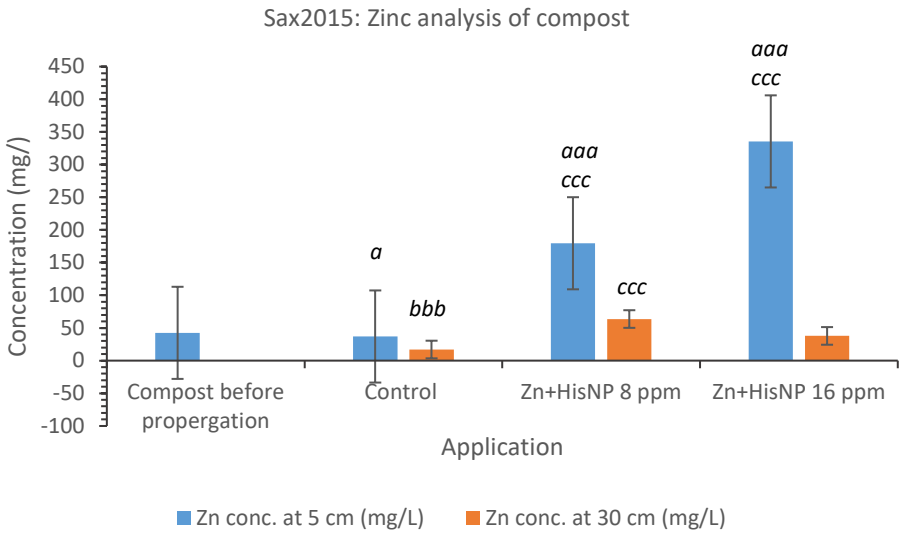

Figure 8.89 Zn content in compost after harvest Sax2015. Using ANOVA single factor significant differences where indicated; a = between depths 5 and 30 cm with in application, b = against compost (control only tested), c = against control counterpart.

Comparing the Zn content of tubers from figure 5.45 and compost Zn data, figure 8.5, the application of 8 and 16 mg / L produced significantly fortified tubers over control. The concentration of Zn through the application of zinc oxide nanoparticles resulted in a significant increase of Zn at the depths of 5 and 30 cm depth, therefore rejecting H_o^2. The data collected indicated highly significant decrease in the content of Zn at 5 than 30 cm following the pattern found for Ca and Fe concentration, withexception of FeNP+His. 8 mg / L thus rejecting H_o^1.

6.2 Aquatic toxicology using Common fresh water shrimps (Gammerus Pulrex)

From the below tables (8.1 and 8.2) it is concluded that the ZnNP have a higher mortality rate throughout the trial when compared to FeNP and control. Zinc oxide is harmful to aquatic life, classified according to Regulation (EC) no 1272/2008, acute aquatic toxicity (category 1), H400 and chronic aquatic toxicity (category 1), H410. The data collected in the trial observed toxic effect even at the low

concentration of 6 mg / L. It can also be concluded that increase concentration of FeNP+His trends with the increase in mortality (table 6.2 and 6.3). This can also be said for ZnNP, although the survival rate after 72 hours of treatment is higher in those treated with FeNP. Further observation conclude the MONP was readily taken up by the shrimps as figures 6.6 A and B show, which also correlated with mortality rate and increase in MONP concentration given.

	Start of test (number)	*Alive end of test (number)*	*Percentage mortality (%)*	*Percentage survival (%)*
Control (tap water)	25	24	4.00	96.00
FeNP+His. 6 mg / L	25	18	28.00	72.00
FeNP+His. 12 mg / L	26	5	80.77	19.23
FeNP+His. 24 mg / L	24	3	87.50	12.50
ZnNP+His. 6 mg / L	24	0	100.00	0.00
ZnNP+His. 24 mg / L	26	2	92.31	7.69

Table 8.26 Mortality of shrimps at end of trial.

	Mortality rate %		
	After 24 hours	*After 48 hours*	*After 72 hours*
Control (tap water)	4.17	0	0
FeNP+His. 6 mg / L	12	9.1	10
FeNP+His. 12 mg / L	19.23	47.62	57.55
FeNP+His. 24 mg / L	16.67	75	40
ZnNP+His. 6 mg / L	29.17	88.24	100
ZnNP+His. 24 mg / L	69.23	75	0

Table 8.27 Mortality rate of shrimps.

Using ANOVA single factor statistical test in Microsoft Excel, significant increases over Fe content of control shrimps where found in all Fe applications, figure 8.6a. Significant uptake of Fe was also observed over ascending concentrations for FeNP+His. applications. The Zn application of 24 mg / L was found to significantly increase the Zn content when compared to control shrimps.

The data collected in this trial correlated with those found using other indicator species such as muscles, *Mytulus galloprovincialis* (Taze *et al*., 2016), Zebrafish, *Danio rerio* (Xiong *et al*., 2011), plus

the bivalve *Dresissena polymorpha* and another shrimp *G. roeseli* (Garaud *et al*., 2015). Muscles where found to show toxicity stress at 10 and 50 mg / L of iron oxide nanoparticle (Taze *et al*., 2016), whereas zebrafish gained a 100 % mortality at 30 mg / L when subjected to zinc oxide nanoparticles at 30 mg / L (Xiong *et al*., 2011).

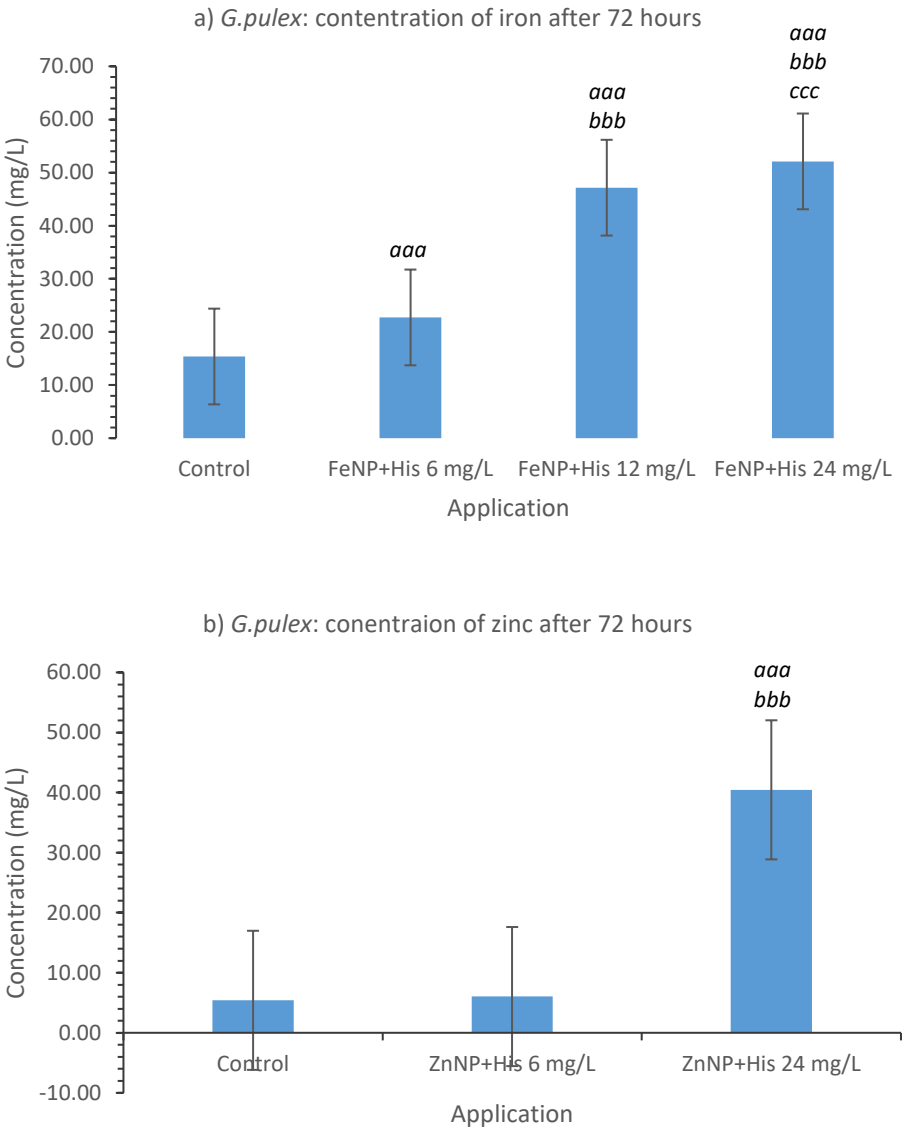

*Figure 8.103 Analysis of Fe (a) and Zn (b) content of G. pulrex to substantiate uptake of MONP. Using ANOVA single factor, significant differences were ranked; * = <0.05, ** = < 0.01 and *** = < 0.001, with a indicating sig.dif. against control, b = between 6 mg/L, c = against 12 mg/l.*

A reputation of this experiment based on Vellinger *et al.* (2012) would involve the inclusion of different biomarkers to provide an improved knowledge of the effect the presence of MONP would have upon an aquatic ecosystem (Garaud *et al*., 2015). The reactive oxygen species (ROS) of the

nanoparticle species disrupts anti-oxidant system and intercellular metabolic activities (Xiong *et al*., 2011) causing oxidative stress. Gammarid and zebrafish gills suffer oxidative stress whereas the digestive tract membranes of crustaceans are damaged (Xiong *et al*., 2011; Garaud *et al*., 2015; Taze *et al*., 2016). The concentrations at which the MONP is applied also requires review as Xiong *et al*. (2011) rationalised that a more realistic level of ZnO NP would be around 3.6 mg / L rather than the 30 mg / L tested, which in turn calls for a review of water courses content in minerals relating to possible application sites of MONP. Through the investigation of aquatic fatality of zinc oxide, it was found to have a significant effect on *Escherichia coil*, leading to an antibacterial effect (Xiong *et al*., 2011). Due to a number of unknowns and multiple chemical and environmental influences, a number of investigations are required into the durability and interactions of MONP in aquatic environment.

9 MONP effect upon bacterial

Understanding the effect that MONP potentially have on the in terrestrial and aquatic ecosystems extending to bacteria, particularly in the infection of *Pectobacterium carotovorum*, PCA in potato tubers when in storage. The soil dwelling bacterium PCA has a broad host worldwide and characteristically produce cell-wall-degrading enzymes, allowing infiltrations and macerations of plant tissue upon which they feed, known as soft rot when effecting potato tubers under storage (Barras *et al*., 1994). The term black leg refers to PCA infection in the potato stems, causing blackening during propagation (AHDB, 2013). During prolonged storage (>9 months), soft rot causes a large economic loss as the bacteria quickly spread between tubers when infected tubers go undetected.

Following data collected in previous trails (Sax2015 and Sax2016 in particular), the fortification of tubers and increased foliage growth thought the application of MONP, suggests a potential in suppressing PCA infection. The following work focuses on the anti-bacterial properties of MONP as a method of supressing soft rot in storage.

9.1 Methods

The following work was conducted at The AHDB Crop Storage Research Facility (CSRF), Sutton Bridge, Lincolnshire, UK.

Nutrient agar and broth was purchased from Fisher Scientific, UK and prepared as directed by the supplier. PCA inculcation used derived from AHDB with MONP synthesised as previously descried. Methodologies here in are developed by AHDB and used in quality control checks at CSRF.

Statistical analysis was conducted via Microsoft Excel, single factor ANOVA.

9.1.1 Antibacterial properties of CaNP+His solution (CaO and CaFe2O4)

Wash water (3 ltr) from potato washing was collected from Produce World, Sutton Bridge, and used as a general bacterial source. Buffered solutions of MONP+His (CaNP and CaFeNP) and His only solution (100 mg / L, 20 mL per rep) were inoculated with wash water (500 µL) and incubated for 2 hours at room temperature. The pH of the solutions was measured using a HI-98103 pH tester, to ensure the pH range ± 0.5. If pH was found to measure outside the range, the MONP was suspendered in pH7 buffer, purchased fromFisher Scientific, table 9.1.

The solutions where diluted x10^6 and spread onto nutrient agar plates with further incubation (24 hours at 17 ^oC). The colonies forming units (CFU) were then counted,

	Previous pH	*pH with buffer*
Control	pH 7	7.5
CaHisNP	pH 9	7.5
CaFeHisNP	pH 5	7
His	pH 4	7

Table 9.28 CFU and pH of solutions to observe the antibacterial effect of two forms of CaNP

9.1.2 Inoculation of potatoes (variety Maris piper) with pectobacteria pre-treated with MONP+His soak

Eight Maris piper potatoes where washed in a commercial washer (figure 9.1) and place in the wash water at ambient temperature for two hours to inoculate the potatoes with PCA. The potatoes where sampled by skin swabs and peel. A 25 mm^2 area of skin was swabbed in three areas and a peel sample was taken, figure 9.2. Peel samples were obtained with the use of a food grater, from the radius around the tuber (diameter of 10 mm) from apical to bud end until 2.5 g of skin was obtained. The peeling was homogenised with sterilised water (5 mL) and filtered gravitationally through a grade 1 filter paper.

Figure 9.91 Maris pipers washed in a commercial washer, Sutton Bridge Crop Storage Research Centre.

Figure 9.105 Skin swabbing process of tubers with the use of guide.

The skin swabs and peel samples were diluted (skin, 100 x and peelings 1000 x) through serial dilution and with sterilised distilled water. Samples were spread onto nutrient agar plate with two replicates of each sample. The plates were incubated at 17°C for 24 hrs. The pectobateria colonies leave wells in the agar which were counted to obtain a concentration figure of the bacteria and quoted as CFU in mL.

3.11.3 Inoculation of potatoes with pectobacteria (PCA).

Initial testing using variety Maris piper used three tubers per test. Two treatments were applied, calcium oxide (CaNP), 200 mg/ L and calcium ferrite (CaFeNP), Ca concentration of 200 mg / L both coated in amino acid histidine to aid dissolution in deionised water (2000 cm^3 di. Water per treatment).

- Test 1: No pre-treatment

Nine tubers were washed in a commercial washer until clean (c.a. 5 mins) then divided into the following treatments: Control (no treatment), CaNP+His and CaFeNP+His. These were left to soak at ambient temperature for 24 hours, figure 9.3. The tubers were removed from the solution then placed into PCA solution (10^6 concentration) for two hours at ambient temperature to induce inoculation via skin pores.

Figure 9.93 Tubers soaking in treatment solutions of MONP before inoculation of PCA.

- Test 2: Produce wash

Tubers (x 8) were washed in Produce Wash in a dilution of 1:200 as recommended by the manufacture. The tubers were divided into three per treatment and treated and inoculated as in test 1, see table 9.2.

The skin swabs and peel samples were diluted (skin, 100 x and peelings 1000 x) through serial dilution and with sterilised distilled water. Samples were spread onto nutrient agar plate with two replicates of each sample. The plates were incubated at 17°C for 24 hrs. The PCA colonies leave wells in the agar which were counted to obtain a concentration figure of the bacteria and quoted as CFU in mL.

	Conditions	*Washing*	*Treatment (24 hr soak) @ RT*		
1	Control	Water	Water		
2	Water/CaNP+His.	Water	CaNP+His		
3	Water/CaFeNP+His.	Water	CaFeNP+His	*PCA soak 2 hours @RT*	*Swab and peel samples taken onto LB plates (2 reps per sample)*
1a	PW/ no treatment	PW	Water		
2a	PW/CaNP+His.	PW	CaNP+His.		
3a	PW/CaFeNP+His.	PW	CaFeNP+His.		

Table 9.29 Washing applications and post-wash treatment with application of CaNP+His. and CaFeNP+His.

9.2 Results and discussions

Pectobacterium spp. (PCA) characteristically produce large quantities of pectolytic enzymes (Ngadze *et al.*, 2014) that are cell wall specific (Czajkowski *et al.*, 2011) which macerate plant tissue thus allowing infiltration and further tissue maceration (Barras *et al.*, 1994). PCA are one of a number of

bacteria that cause a storage disease known as soft rot. Contamination from PCA occurs from soil during propagation and at harvest (Barras *et al*., 1994; De Boer, 2002), plus pot-harvest handling, washing and packaging (Czajkowski *et al*., 2011) through damage or poor storage.

A number of publications have reported (Pérombelon and Kelman, 1980; McGuire and Kelman, 1984; Schöber and Vermeulen, 1999) on the increase in Ca content of tubers increasing the resistance to tissue maceration via bacterial pathogens. Calcium enhances the structural integrity of cellular walls and membranes (Pagel and Heitefuss, 1989; Ngadze *et al*., 2014), therefore increased strength through via Ca application through fertiliser or as a post-harvest treatment offers an alternative to current chemical applications that are under scrutiny (Pérombelon and Kelman, 1980).

9.2.1 Antibacterial properties of CaNP+His solution (CaO and CaFe2O4)

To establish the antibacterial effects of Ca upon a range of bacteria, a sample of wash water from a potato processor, Produce World, Sutton Bridge was used as the source. From figure 9.4, it can be observed that the His and CaFeNP+His gained significantly lass bacteria (CFU / mL) that control and CaNP+His. The treatment of CaNP had a very slight decrease in the nuber of CFU / mL observed, however, the addition of the Fe element may increase the antibacterial properties of calcium (McGuire and Kelman, 1984; Pagel and Heitefuss, 1989), thus requiring further investigation. The solutions where buffered prior to the waste wash water, therefore eliminating the acidic influence of the amino acid, histidine.

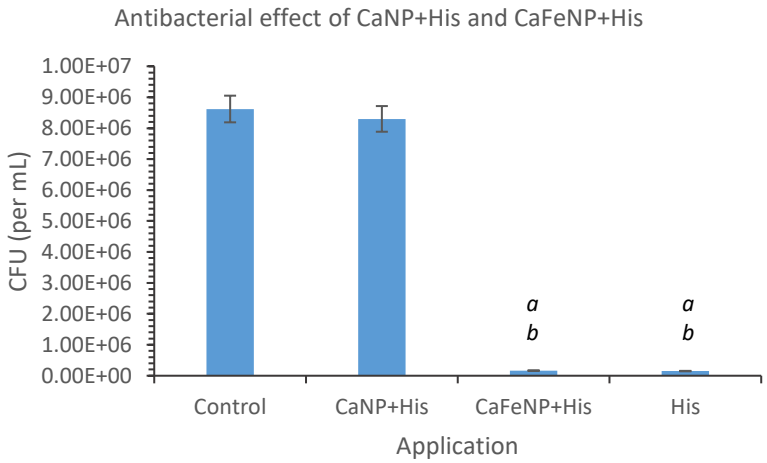

Figure 9.107 The antibacterial effect of two forms of Ca nanoparticle as an antibacterial against against soil bacteria. Sig. dif indicated between control = a, against CaNP+His = b.

9.2.2 Tuber inoculation using PCA soak to tubers pre-soaked with MONP.

A number of tubers from were collected from same storage conditions at CSRF, washed in water, dried then soaked in CaNP+His and CaFeNP+His. 100 mg / L, table 9.3, with 3 repetitions from each tuber. During periods of prolonged contact with moisture, the pores of the tuber open allowing the passage of PCA into the tuber. Utilising this period, a 'soak' method of fortification with the calcium oxide and calcium ferrite was utilised. The nano size of the particulates will increase the transfer into the tuber as they are sub size of the membrane pores (Livage *et al*., 1989). When membrane pores dilate in the soak, this will increase the uptake of nanoparticles but also increase the permeation of the bacteria into the cortex and parenchyma. Increased Ca concentration of the cells of the treated tuber will counteract any bacterial infection via the enhance structural integrity of cell walls and membrane (Candeia *et al*., 2004) preventing cellular damage from bacterial colonisation.

Soak treatment	*No. tubers per test*	*Length of soak period*	*PCA soak inoculation*	*Samples*
No soak *Dist H20* *CaNP+His.* *CaFeNP+His.* *FeNP+His* *His*	5	N/A Soak period of 24 hours	2 hours	Swab & peel 3 reps of each On LB plates (3 plate reps per sample)

Table 9.30 Conditions for the comparison of MONP against coating for antibacterial properties against PCA.

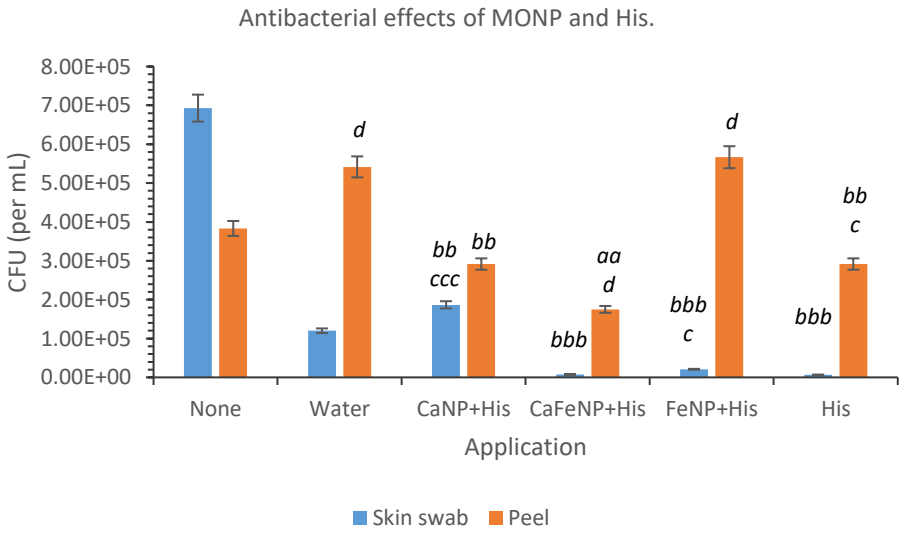

Figure 9.108 Antibacterial effects of MONP and histidine on PCA. Significant differences obtained from ANOVA single factor statistical test between non-soaked and other treatments are allocated= a, against water = b, against His. = c and swab against peel counterpart = d.

As on observed from figure 9.5, no significance was found between 'no soak' and other treatments even though the average PCA CFU / mL is considerably higher that other data collected. The action of the soak in itself will decrease the surface bacteria resulting in the reduction of CFU / mL from $6.90x10^5$ (none) to $1.20x10^5$ (water soaked). As expected the action of soaking the tuber enabled the bacteria to transport into cortex and parenchyma region of the tuber, as the peel data increase from $3.83x10^5$ CFU / mL (none) to $5.42x10^5$ (water soaked), figure 9.5.

CaNP+His. treated tubers gained a moderate significant increase in PCA in the skin swabs ($p = 4.98x10^{-3}$) against control, however, the peel PCA CFU / mL gained significantly less ($p = 2.58x10^{-2}$). The positive charge of the CaNP may 'attract' the bacteria to the skin surface and restrict bacterial progression into the cortex as a supplementary effect to the increased integrity of the cellular structures (Livage *et al*., 1989; Candeia *et al*., 2004; Zak *et al*., 2011).

Treatments CaFeNP+His, FeNP+His and His., all gained highly significant decreases in PCA concentration against water soak. Fe causes oxidative stress to the bacteria even if magnetite (Fe_3O_4) is fully oxidised to maghemite (γ-Fe_2O_3) (Wu *et al*., 2006; Wu and Wang, 2011; Khanna and Verma, 2013) resulting in the decrease of PCA on the surface of the skin. The absence of Ca in the FeNP+His. treatment saw an increase in the PCA CFU / mL on the peel sample from $1.75x10^5$ (CaNP+His.) to $5.67x10^5$ (FeNP+His). The application of His. observed a highly significant decrease in PCA on the skin surface suggesting the acidic nature of His. may be responsible for the CFU / mL decrease.

9.2.3 Comparison of the effect of MONP treatment on tubers; with and without PW. WH2O used as a bacterial source.

The potential anti-bacterial effect of MONP; CaNP+His. and CaFeNP+His. (200 mg/L) were compared against the commercial antibacterial application, Produce wash (PW), table 9.3. A second investigation observed the interaction of PCA with tuber treated with MONP when previously washed with PW, table 9.4.

For control tubers '1' and '1a', soaking in distilled water to be in conjunction with 'soak treatment' of CaNP and CaFeNP. During periods of prolonged contact with moisture, the pores of the tuber open allowing the passage of PCA into the tuber. Utilising this period, a 'soak' method of fortification with the calcium oxide and calcium ferrite was utilised. The nano size of the particulates will increase the

transfer into the tuber as they are sub size of the membrane pores (Srivastava *et al*., 2013). When membrane pores dilate, this could increase the uptake of nanoparticles. Treatment applied to 1 - 3 is a repetition of conditions with adjustments to the concentration (100 to 200 mg / L) and excluding FeNP+His. and His. as the commercial focus would preferably be on a Ca application.

	Conditions	*Washing*	*Treatment (24 hr soak) @ RT*		
1	Control	Water	Water	*PCA soak 2 hours @RT*	*Swab and peel samples taken onto LB plates (2 reps per sample)*
2	Water/CaNP+His.	Water	CaNP+His		
3	Water/CaFeNP+His.	Water	CaFeNP+His		
1a	PW/ no treatment	PW	Water		
2a	PW/CaNP+His.	PW	CaNP+His.		
3a	PW/CaFeNP+His.	PW	CaFeNP+His.		

Table 9.31 Washing applications and post-wash treatment with application of CaNP+His. and CaFeNP+His.

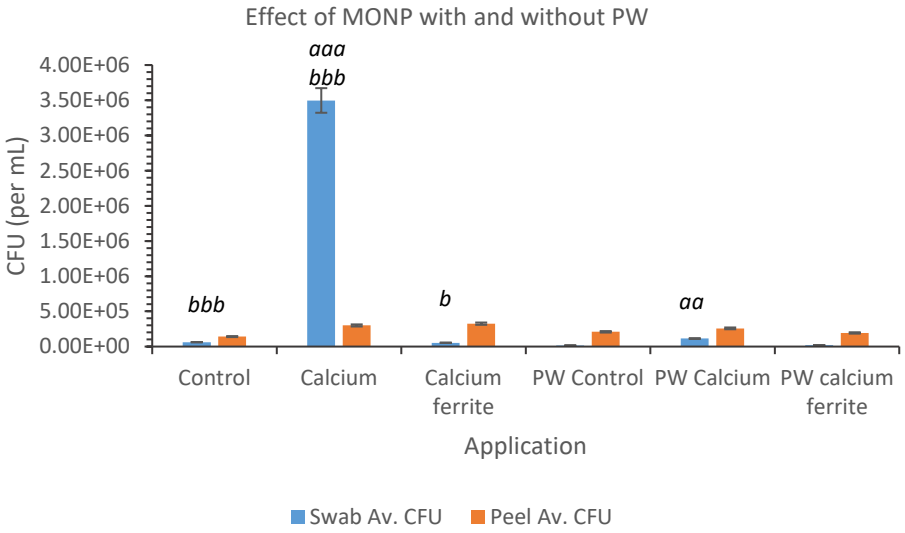

Figure 9.109 Comparison of PCA (CFU per mL) obtained from skin swab and peel to observe the action of CaNP and CaFeNP with the application of Produces wash before application. a = against 1,1a. b = against 'a' counterpart.

With a two null hypothesise; H_o^1= "*the use of Produce wash does not decrease the amount of PCA, CFU per mL*" H_o^2 = "*application of CaNP+His. or CaFeNP+His. does not decrease the amount of PCA, CFU per mL*". Using the statistical analysis test, ANOVA single factor and ranking the *p* value (< p = 0.05, *; < p = 0.01, **; < p = 0.001, ***) the data was analysed.

There was a significant increase in the concentration of PCA in swab samples taken from potatoes that were washed with water only (figure 9.6) indicating the use of PW reduces the presence of PCA on the potato skin surface, rejecting H_o^1. No significant difference was found in the peel data, concluding the

PW or nanoparticles have any reduction in the passage of PCA into the tuber, accepting both null hypothesise.

Application '2' obtained a significant increase in the amount of PCA on the skin swab but no difference was found between peel control, '1a' or '3a' suggesting the PCA does not transfer through the skin. H_o^1 is rejected for application '2' due the significant increase was obtained, and H_o^2 is accepted for application '2a' as there was not a significant difference obtained when compared to '1a'.

The application of CaFeNP+His., '3' and '3a' did not gain any significant difference when compared to controls, '1' and '1a', although a significant decrease ($p = 0.0248$) was found when PW was used.

10 Conclusion and further work

Increasing the production volume and reduced size range of MONP, was the criteria for the transferal of bench top MONP synthesis to the SDR. If successful, the applications of nanomaterial open a vast number of applications related to the understanding and manipulation of materials at the atomic, molecular, and macromolecular scale via the enhanced surface area per mass compared with larger-sized particles of the same chemistry (Oberdorster *et al*., 2005; Kalpana-Sastry *et al*., 2013). Applications of nanotechnology are conceded to provide solutions to some of the current challenges of food security concerns and can provide the needed tools to catalyse the entire agriculture and food value chain (Kalpana-Sastry *et al*., 2011). Formulating applications on a nanoscale can expected to revolutionize both agro-technology resulting in multiple benefits (Lane and Kalil, 2005).

10.1 MONP synthesis and scale up.

Successfully synthesis adaptation to the SDR were obtained of CaO, Fe_3O_4 and ZnO NP as the comparison with published data showed. Some further work is required for $CaFe_2O_4$ due to the combustible process involved. The SDR produced smaller nanoparticles when compared to published data as reviewed in section 2.3. Adaptation of ZnO NP synthesis to replace water with methanol and acetone, decreased the size range and sodium chloride content that become problematic in the first adaptation the ZnO NP synthesis to SDR.

Development of the SDR is required to incorporated a heated disc, or a disk that will retain the precursor mixing for a prolonged period of time. With the use of a 3D printer, Mackebot Replicator+, conditions of the disc are being investigated. Example of discs in development are shown in figure 10.1. Investigations into the depth, ridge frequency and disc diameter require further investigation into the effect these conditions have on the efficacy material synthesis and particle size. An introduction to a heated disc will enable more sol-gel based synthesis to be adapted to the SDR as these formulations require latent heating throughout synthesis.

Figure 10.01: changing the conditions of the disc to increase efficiency of the MONP synthesis.

Coating method of a 1:1 with a hydrolysed amino acid proved successful in the suspension of the nanomaterial with FTIR spectra confirming a chelation between the MONP and histidine allowing drying a resuspension of MONP+His particle. Results from the fortification trials would not have shown a significant increase in mineral content if the MONP was not transported in the soil / compost solution in order to reach the rhizosphere.

For MONP+His to increase in production 'bottlenecks' in the process must be resolved in order to increase production to commercial level. Through the synthesis methods herein the bottlenecks were identified as: 1) filtration and sufficient washing of the crude MONP slurry, 2) Drying, and 3) coating.

Filtration of FeNP is easier to overcome, due to the magnetic nature of the NP. A magnetised flatbed filtration system will retain the FeNP while surplus filtrate is disposed, figure 10.2. The collected FeNP can be washed in a similar way as the primary collection.

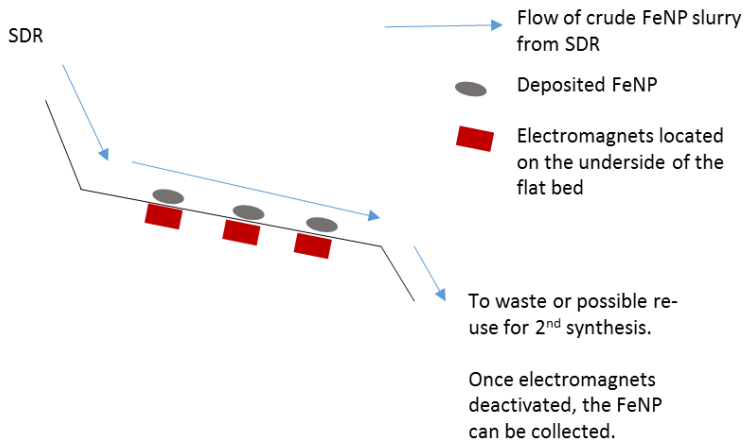

Figure 10.02: Electromagnetic flatbed design to aid the efficient collection and washing of FeNP.

The filtration of CaNP and ZnNP requires more knowledge in the available / possible commercial techniques that can be adapted especially when collecting nanomaterial.

A resolution to overnight drying of the uncoated NP is a spray dryer as used in the production of instant coffee or freeze drying as published by Abdelwahed *et al.* (2006).

The electrostatic coating currently using the coffee mill can be transfer to extruders, which are currently in the top-down production of nanomaterials for oral drug delivery systems (Baumgartner e*t al*., 2014).

Collaboration within the pharmaceuticals industry, particularly concerning spray drying, would be beneficial to the continuous flow process. An immediate drying after formation of the particles would provide a solution to ripening and interaction of excess precursor solutions after formation.

10.2 Effects of MONP on crop development.

The application of MONP+His had various effects in the growth rate in relation to MONP+His concentration and crop applied. FeNP+His. 16 mg / L optimised potato growth rate, whereas tomatoes favoured 6 mg / L. Growth rate response to the application of FeNP+His differed among chilli varieties. Increase in height was obtained with FeNP+His. 12 mg/ L, with little or lower growth rate (compared to control) with FeNP+His. 6 mg / L within the *C. chinense* varieties, whereas *C. annuum var. glabriusculum*, Pequin increased height with both 6 and 12 mg / L.

Interestingly the application of FeNP+His in the trial 'Field rep 2016', observed an increase in growth rate shortly after application, indicating an influence of the FeNP+His. Further investigation in the effect the FeNP+His or His has upon the growth rate and the timing of application (in the life cycle) is required in line with yield and DM%, speculating that increased energy going into vegetative production could hamper the tuber formation and loading.

The hydroponic application of ZnNP+His treated potatoes are significantly suppressed by the presence of ZnNP with increases of 13.73 mm and 13.18 mm, ZnNP+His 8 and 16 mg / L respectively. Ca+HisNP 12 mg / L did not grow as rapidly as expected with a height increase of 31.43 mm when compared to the increase of 216.63 mm obtained by Ca+HisNP 32 mg /L (figure 5.3 a). Compared to application to compost significant difference of stem height. Application of CaNP+His 32 and 64 mg / L has a significant increase in height over control, Chempak and the His. equivalent suggesting an influence in

the presence of CaNP. This is supported by an increase in growth rate in stems treated with CaNP+His 32 mg /L.

Yield analysis's using ANOVA single factor analysis, from trial Sax2015, a significant increase between control plants overall average weight (OAW) in grams, and treatments, CaNP+His 12 mg / L ($p = 0.01$), CaFeNP+His ($p = 1.43 \times 10^{-4}$), ZnNP+His 8 mg / L ($p = 3.21 \times 10^{-5}$) was found. Treatments CaFeNP+His and both ZnNP+His did not produce any sub 30 mm tubers where as FeNP+His did.

Treatments CaFeNP+His and both ZnNP+His did not produce any sub 30 mm tubers. Due to the harvest occurring at 14 weeks, approximately 20 days short of commercial harvest, the occurrence of <30 mm tubers would be expected as these tubers would go onto to produce 'salad' crop. The absence of these bud tubers (sub 30 mm) indicated the plant has halted tuber initiation early into the growth cycle. The presence of ZnNP or CaFeNP did not supress the vegetable development of the treated plants, nor did individual application of FeNP and CaNP supress development as previous discussed. This anomaly required further investigation in the form of repetition of the trial on a larger scale such as a field trial to observe an increase in environmental factors supress or increase this response. Investigation in to possible suppression of signalling pathways involved in tuber formation from the increased concentration of Zn, Ca or Fe in the rhizosphere, or the gene signalling involved in the uptake and transport in the plant, i.e. the expression of ZIP genes and ferritin (Guerinot, 2000; Tegegder, 2012).

The influence of FeNP+His upon the yield of larger tubers (<30 mm) was found to be significant in Sax2015, Sax2016, Feload2016 and an increase in the number of tubers harvested in Fieldrep2016. Field trials 2015 and 2016 did not observe any significant yield increases or decreases, but increase the DM %, which is of more economic importance to potato producers and production (Kolbe and Stephan-Beckmann, 1997; Pritchard and Scanlon, 1997). The application of CaNP+His at 12 and 32 mg / L, gained similar DM % as control, whereas the application of CaFeNP+His. (24:12 mg / L), ZnNP+His, 8 and 16 mg / L gained significantly less DM%. The application of ZnNP+His. 16 mg/ L did increase DM % over 8 mg / L; therefore, it would be of interest that investigations included increased concentrations of ZnNP+His to investigate increasing the DM% to improve the fusibility of a Zn fortified potato in the commercial environment.

10.3 MONP application as a fortification

The trials conducted here in found an increase in mineral content when applied to potato, tomato and chilli crops when treated with MONP+His. The optimal concentration of MONP+His differed between crops and with different trial environments. Fluctuations in uptake (i.e. preference in Ca concentration) are possibly due too climatic (extremes of heat, hydration) and genetic variation (Lisinska and Leszczynski, 1989; Tekalign and Hammes, 2005; Kelling and Schilte, 2008) that are beyond the remit of these trials. Increased collaborative work with commercial growers over a number of seasons would substantiate the influence of the environment (i.e. field trials) and delivery methods (hydroponic systems for tomato production, pellet or solution delivery in commercial potatoes cultivation).

More work is required in the uptake of other mineral influenced by the application of Fe, Ca and Zn, as previously documented that high content of Ca in calcareous soil limits the reduction of Fe^{3+} and uptake of Fe^{2+} coursing the deficiency chlorosis (Kelling and Schilte, 2008).

10.4 MONP in the environment.

Due the nanometre scale, particles properties have been investigated for centuries in the ability to improve function, performance and increase cost-effectiveness in engineered materials resulting in an extremely diverse research field. Many of the properties are dependent on the particle size therefore increased importance when synthesising nanoparticles especially when scaling up for commercial production (Lane and Kalil, 2005; Kalpan-Sastry *et al*., 2011). For these reasons, there is concern that nanomaterials will be unpredictable in the environment. Compost analysis and the use of ^{59}Fe observed the significant increase in the retention of MONP in the soil preventing leaching into the water system and increasing the mineral content of the substrate. Aquatic ecotoxicology test using *G. pulrex* did not highlight any increased hazards or increased accumulation that are not already documented already.

Increasing work with commercial sector has conclude to apply the MONP as a solution so to reduce airborne particulates that could potentially irritate and pass through mucus membranes, or as a pellet formation. Health and safety regulations that require applicants to wear PPE (personal protective equipment) can be utilised to NP.

It is accepted that a great deal of further work is required to understand the fate of NP through different soil strata, especially the micro fauna and flora. The aquatic ecotoxicology trial here in should be repeated with a large sample number with the inclusion of different biomarkers (Garud *et al*., 2015).

10.5 MONP application post-harvest

The application of CaNP is of great economic interest as a prevention of soft rot bacterial infection cause by pecobacteria. The application of CaNP and FeNP controlled / retained the PCA from entering the tuber, thus reducing infection rate and potentially reduce crop loss while in storage. An application at the washing stage at harvest could be incorporated in the current process as obverted at Produce World, Sutton Bridge. Further collaborative work would provide an opportunity to maximise application especially concerning refinement of TG2 activity analysis as observed in appendix 11.3, incorporating post-harvest application of CaNP or MONP that will supress TG2 and sprouting would be of economic interest with investigations into prolonging storage in the face of CIPC (isopropyl-N-(3-chlorophenyl) carbamate) restrictions.

11 Appendix

11.1 H2014 and H2015 statistical analysis

		Average height (mm) ± SD			
	Trial	Week 3	Week 4	Week 5	p -value against control (for corresponding year) week 5
Control 2014	H2014	524 ± 76.75	556.21 ± 92.95	578.08 ± 91.82	N/A
Control 2015	H2015	481 ± 152.14	613.79 ± 183.81	757.141 ± 91.82	N/A
CaNP+His 12 mg / L	H2015	35.57 ± 23.22	48.29 ± 22.26	66.00 ± 39.59	$3.29x10^{-7}$***
CaNP+His 32 mg / L	H2015	185.44 ± 117.08	284.44 ± 120.90	402.06 ± 119.63	$1.15x10^{-5}$***
FeNP+His 8 mg/L	H2015	477.2 ± 125.94	625.53 ± 96.33	791.40 ± 134.98	0.6308
FeNP+His 12 mg/L	H2015	444.64 ± 166.59	573.62 ± 159.06	736.69 ± 188.29	0.8058
FeNP+His 16 mg/L	H2015	390.35 ± 120.30	493.82 ± 108.83	654.41 ± 124.23	0.1783
Fe EDTA 8 mg/L	H2014	426.33 ± 133.54	441.06 ± 135.75	473.17 ± 150.57	0.0340*
ZnNP+His 8 mg / L	H2015	56.36 ± 41.40	60.91 ± 43.58	70.09 ± 41.69	$1.81x10^{-9}$***
ZnNP+His 16 mg / L	H2015	49.18 ± 28.03	51.73 ± 27.65	62.36 ± 36.93	$1.40x10^{-9}$***
His 8 mg/L	H2014	675.17 ± 977.77	728.75 ± 103.08	727.64 ± 129.68	$3.27x10^{-3}$**
His 20 mg/L	H2014	634.67 ± 149.31	677.33 ± 151.42	721.09 ± 161.12	0.0123*

App. 1 H2014 and H2015 growth data and statistical analysis

	Ca content (mg / L per gram of sample)	p-value against control	p-value against CaNP+His. 12 mg / L
Control 2015	346.86	N/A	N/A
CaNP+His 12 mg / L	480.04	0.0385	N/A
CaNP+His 32 mg / L	308.71	0.3621	$6.31x10^{-3}$**

App. 2 ICP analysis data of Ca content of tuber with statistical analysis

	Fe content (mg / L per gram of sample)	p-value against control	p-value against FeNP+His 8 mg / L	p-value against FeNP+His 12 mg / L
Control 2015	17.86	N/A	N/A	N/A
FeNP+His 8 mg/L	13.09	0.2781	N/A	N/A
FeNP+His 12 mg/L	27.79	0.5602	0.3868	N/A
FeNP+His 16 mg/L	7.24	0.0147*	0.0703	0.2295

App. 3 ICP analysis data of Fe content of tuber with statistical analysis

	Zn content (mg / L per gram of sample)	p-value against control	p-value against ZnNP+His. 8 mg / L
Control 2015	1.21	N/A	N/A
ZnNP+His 8 mg / L	5.05	$7.42x10^{-4}$***	N/A
ZnNP+His 16 mg / L	5.58	$2.19x10^{-7}$***	0.5816

App. 4 ICP analysis data of Zn content of tuber with statistical analysis

11.2 Sax2015 and Sax2016 statistical analysis

	Average height (mm) ± SD				
	Week since planting				
	2	3	4	5	6
Control	325.01 ± 30.24	665.63 ± 29.91	919.95 ± 52.32	1138.87 ± 41.17	1198.73 ± 15.07
CaNP+His 12 mg / L	357.60 ± 88.61	742.40 ± 94.71	1005.60 ± 108.04	1184.40 ± 28.76	1315.20 ± 45.54
CaNP+His 36 mg / L	321.27 ± 39.74	689.07 ± 63.26	964.13 ± 40.13	1145.00 ± 23.84	1164.70 ± 46.81
Ca.FeNP+His	355.80 ± 20.54	648.93 ± 48.72	902.60 ± 53.79	1147.73 ± 31.34	1318.00 ± 46.10
FeNP+His 8 mg / L	336.95 ± 62.19	671.51 ± 59.27	944.53 ± 71.06	1142.85 ± 97.18	1027.04 ± 64.50
FeNP+His 12 mg / L	337.14 ± 52.16	683.63 ± 76.54	960.77 ± 32.12	1152.66 ± 37.08	1234.40 ± 41.58
FeNP+His 16 mg / L	331.48 ± 57.20	672.24 ± 49.95	986.09 ± 14.12	1192.34 ± 42.39	1350.60 ± 51.73
ZnNP+His 8 mg / L	335.19 ± 99.22	675.79 ± 69.33	963.80 ± 56.76	1147.75 ± 28.41	1130.72 ± 37.05
ZnNP+His 16 mg / L	339.40 ± 52.00	697.87 ± 64.21	990.67 ± 9.98	1187.13 ± 57.07	1169.50 ± 137.04

App. 5 Sax2015 growth rate over a 5-week period

	Average height (mm) ± SD			
	Week since planting			
	3	4	5	6
Control (water only)	84.71 ± 66.85	442.89 ± 62.30	572.78 ± 32.26	637.83 ± 42.01
Chempak	207.75 ± 70.77	492.61 ± 101.48	622.61 ± 65.87	689.61 ± 56.76
CaNP+His 32 mg / L	116.06 ± 67.11	555.56 ± 76.58	700.39 ± 49.84	1175.22 ± 78.65
CaNP+His 64 mg / L	100.28 ± 62.62	550.78 ± 81.38	731.28 ± 40.55	806.06 ± 73.01
FeNP+His 16 mg / L	107.88 ± 69.85	496.94 ± 100.07	695.06 ± 38.64	736.17 ± 54.61
FeNP+His 32 mg / L	116.06 ± 54.54	510.44 ± 115.26	718.50 ± 85.48	819.33 ± 58.63
His 16 mg/L	104.73 ± 63.55	459.47 ± 106.76	676.88 ± 71.17	783.53 ± 60.05
His 32 mg/L	130.44 ± 48.11	499.67 ± 110.86	647.78 ± 95.42	776.56 ± 80.57
His 64 mg/l	127.56 ± 69.13	492.44 ± 101.49	636.33 ± 54.83	766.11 ± 41.50

App. 6 Sax2015 growth rate over a 5-week period

Sax2015	p-value against control	Sax2016	p-value against control	p-value against Chempak
CaNP+His 12 mg / L	0.2023	Chempak	$3.76x10^{-3}$**	N/A
CaNP+His 36 mg / L	0.2023	CaNP+His 32 mg / L	$6.27x10^{-7}$***	$2.00x10^{-3}$**
Ca.FeNP+His	0.9246	CaNP+His 64 mg / L	$6.77x10^{-10}$***	$6.17x10^{-6}$***
FeNP+His 8 mg / L	0.0501	FeNP+His 16 mg / L	$7.31x10^{-7}$***	0.0171*
FeNP+His 12 mg / L	0.2982	FeNP+His 32 mg / L	$2.13x10^{-12}$***	$9.46x10^{-8}$***
FeNP+His 16 mg / L	0.0210*	His 16 mg/L	$1.18x10^{-9}$***	$3.77x10^{-5}$***
ZnNP+His 8 mg / L	0.0201*	His 32 mg/L	$2.08x10^{-7}$***	$6.72x10^{-4}$***
ZnNP+His 16 mg / L	0.7160	His 64 mg/l	0.0219*	0.2764

App. 7 p-values of ANOVA single factor analysis of heights obtained at week 6 after planting.

		Percentage difference in height between week 3 and 6 (%)
Sax2015	Control	80.09
	CaNP+His 12 mg / L	77.16
	CaNP+His 36 mg / L	69.03
	Ca.FeNP+His	103.10
	FeNP+His 8 mg / L	52.95
	FeNP+His 12 mg / L	80.57
	FeN+His 16 mg / L	100.91
	ZnNP+His 8 mg / L	67.32
	ZnNP+His 16 mg / L	67.58
Sax2016	Control (water only)	653.00
	Chempak	231.94
	CaNP+His 32 mg / L	912.61
	CaNP+His 64 mg / L	703.82
	FeNP+His 16 mg / L	582.43
	FeNP+His 32 mg / L	605.96
	His 16 mg/L	648.12
	His 32 mg/L	495.35
	His 64 mg/l	500.58

App. 8 Percentage difference in height of stems between weeks 3 and 6 from trials Sax2015 and Sax2016, propagated in Erin multipurpose compost.

		Per plant	*Total number harvested*	*Number of >30mm*	*Number of <30 mm*	*% >30mm*	*% <30mm*
Sax2015	Control	7.86	165	115	50	69.70	30.30
	CaNP+His 12 mg / L	7	182	129	53	70.88	29.12
	CaNP+His 36 mg / L	9.89	157	109	48	69.43	30.57
	Ca.FeNP+His	5.56	138	95	43	68.84	31.16
	FeNP+His 8 mg / L	8.67	60	60	0	100.00	0.00
	FeNP+His 12 mg / L	7.48	61	61	0	100.00	0.00
	FeN+His 16 mg / L	6.57	63	47	16	74.60	25.40
	ZnNP+His 8 mg / L	6.57	89	60	29	67.42	32.58
	ZnNP+His 16 mg / L	6.67	50	48	2	96.00	4.00
Sax2016	Control	11.50	207	140	67	67.63	32.37
	Chempak	11.17	201	112	90	55.72	44.28
	FeNP+His 16 mg/L	11.56	208	133	75	63.94	36.06
	FeNP+His 32 mg/L	9.17	165	114	51	69.09	30.91
	CaNP+His 32 mg/L	9.72	175	128	47	73.14	26.86
	CaNP+His 64 mg/L	9.61	173	129	44	74.57	25.43
	His. 16 mg/L	9.67	174	130	44	74.71	25.29
	His 32 mg/L	10.78	194	133	61	68.56	31.44
	His. 64 mg/L	12.56	226	158	68	69.91	30.09

App. 9 Harvested number and segregation in to >30 mm and < 30 mm tubers

		Overall average weight (g)	*Average weight (g) > 30 mm*	*Average weight (g) < 30 mm*
Sax 2015	Control	39.81	55.01	4.83
	CaNP+His, 12 mg / L	49.09	63.82	5.82
	CaNP+His, 32 mg / L	35.52	50.36	4.81
	CaFeNP+His 24:12 mg / L	62.98	62.98	0.00
	FeNP+His 8 mg / L	41.71	55.87	7.23
	FeNP+His 12 mg / L	43.2	59.23	7.54
	FeNP+His 16 mg / L	40.46	55.37	6.73
	ZnNP+His 8 mg / L	49.67	49.67	0.00
	ZnNP+His 16 mg / L	55.43	55.43	0.00
Sax 2016	Control	29.81	41.51	5.36
	Chempak	29.79	48.21	6.55
	CaNP+His 32 mg/L	34.46	45.09	5.51
	CaNP+His 64 mg/L	33.89	43.93	4.45
	FeNP+His 16 mg/L	28.79	42.82	3.91
	FeNP+His 32 mg/L	31.45	43.34	4.88
	His. 16 mg/L	32.89	42.37	4.89
	His 32 mg/L	29.11	40.39	4.52
	His. 64 mg/L	29.03	39.04	5.77

App. 10 Harvested weights from trials Sax2015 and Sax2016, average tuber weight and average weight when segregated into >30mm and <30mm.

	Control	CaNP+His, 12 mg / L	CaNP+His, 32 mg / L	CaFeNP+His 24:12 mg / L	FeNP+His 8 mg / L	FeNP+His 12 mg / L	FeNP+His 16 mg / L	ZnNP+His 8 mg / L
CaNP+His 12 mg / L	0.0100	N/A	N/A	N/A	N/A	N/A	N/A	N/A
CaNP+His 32 mg / L	0.4479	0.1519	N/A	N/A	N/A	N/A	N/A	N/A
Ca.FeNP+His	$1.43x10^{-4}$	0.0330	$8.32X10^{-3}$	N/A	N/A	N/A	N/A	N/A
FeNP+His 8 mg / L	0.6359	0.1112	0.6910	$9.78x10^{-4}$	N/A	N/A	N/A	N/A
FeNP+His 12 mg / L	0.2816	0.0104	0.9567	$5.83x10^{-3}$	0.5363	N/A	N/A	N/A
FeN+His 16 mg / L	0.9573	0.0104	0.4601	$1.13X10^{-4}$	0.6838	0.3167	N/A	N/A
ZnNP+His 8 mg / L	$3.21x10^{-5}$	0.1240	$5.56X10^{-3}$	0.5860	$2.14x10^{-4}$	$1.59X10^{-3}$	$3.23X10^{-5}$	N/A
ZnNP+His 16 mg / L	0.8992	0.0162	0.3757	$6.69X10^{-5}$	0.8610	$1.59x10^{-3}$	0.6554	$1.71x10^{4}$

App. 11 Statistical analysis p-values comparing tuber weights from overall average harvested weight (g). Trial Sax2015

	CaNP+His, 12 mg / L	CaNP+His, 32 mg / L	CAFeNP+His 24:12 mg / L	FeNP+His 8 mg / L	FeNP+His 12 mg / L	FeNP+His 16 mg / L	ZnNP+His 8 mg / L	ZnNP+His 16 mg / L
Control >30 mm	0.1328	0.2953	0.1572	0.8495	0.3658	0.9568	0.2838	0.9756
Control <30 mm	0.1001	0.4134	N/A	0.0117	0.0032	0.0239	N/A	N/A

App. 12 Statistical analysis of tuber weight average when segregated into size. Trial Sax2015

	Control	Chempak	CaNP+His 32 mg/L	CaNP+His 64 mg/L	FeNP+His 16 mg/L	FeNP+His 32 mg/L	His. 16 mg/L	His 32 mg/L
Chempak	0.9576	N/A	N/A	N/A	N/A	N/A	N/A	N/A
CaNP+His 32 mg/L	0.1236	0.1635	N/A	N/A	N/A	N/A	N/A	N/A
CaNP+His 64 mg/L	0.1704	0.2147	0.8700	N/A	N/A	N/A	N/A	N/A
FeNP+His 16 mg/L	0.7131	0.7862	0.0781	0.1088	N/A	N/A	N/A	N/A
FeNP+His 32 mg/L	0.5597	0.5842	0.3668	0.4578	0.3820	N/A	N/A	N/A
His. 16 mg/L	0.2655	0.3155	0.6310	0.7565	0.1700	0.6366	N/A	N/A
His 32 mg/L	0.7947	0.8631	0.0875	0.1215	0.9098	0.4238	0.1825	N/A
His. 64 mg/L	0.7725	0.8403	0.0816	0.1147	0.9325	0.4124	0.1825	0.9763

App. 13 p-values comparing average tuber weight of all tuber harvested in trial Sax2016

	Chempak	FeNP+His 16 mg/L	FeNP+His 32 mg/L	CaNP+His 32 mg/L	CaNP+His 64 mg/L	His. 16 mg/L	His 32 mg/L	His. 64 mg/L
Control >30 mm	0.0784	0.6858	0.5626	0.3020	0.4724	0.7768	0.7123	0.415074
Chempak >30 mm	N/A	0.1969	0.2450	0.4791	0.3211	0.1451	0.0490	0.018389
Control <30 mm	0.0585	0.0020	0.4128	0.7983	0.1542	0.4361	0.114179	0.852794
Chempak <30 mm	N/A	3.38×10^{-6}	0.0150	0.1361	0.0051	0.0219	0.001276	0.689115

App. 14 Statistical analysis of tuber weight average when segregated into size. Trial Sax2015

Trial	Treatment	DM % ± SD
Sax2015	Control	36.67 ± 3.33
	CaNP+His 12 mg / L	35.24 ± 2.45
	CaNP+His 36 mg / L	36.29 ± 3.60
	Ca.FeNP+His	33.44 ± 2.14
	FeNP+His 8 mg / L	35.69 ± 3.50
	FeNP+His 12 mg / L	32.67 ± 4.24
	FeN+His 16 mg / L	35.03 ± 2.32
	ZnNP+His 8 mg / L	33.39 ± 2.85
	ZnNP+His 16 mg / L	34.17 ± 2.01
Sax2016	Control	39.59 ± 3.87
	Chempak	38.08 ± 3.19
	FeNP+His 16 mg/L	38.95 ± 2.53
	FeNP+His 32 mg/L	37.87 ± 2.79
	CaNP+His 32 mg/L	35.61 ± 3.08
	CaNP+His 64 mg/L	39.67 ± 2.64
	His 16 mg/L	36.69 ± 4.04
	His 32 mg/L	37.72 ± 2.71
	His 64 mg/L	49.92 ± 5.45

App. 15 Percentage of dry matter (DM%) Sax2015 and Sax2016

p-values DM% Sax2015	Control	CaNP+His, 12 mg / L	CaNP+His, 32 mg / L	FeNP+His 8 mg / L	FeNP+His 12 mg / L	ZnNP+His 8 mg / L
CaNP+His 12 mg / L	0.2595	N/A	N/A	N/A	N/A	N/A
CaNP+His 32 mg / L	0.7830	0.4823	N/A	N/A	N/A	N/A
Ca.FeNP+His	0.0126	0.1155	0.0582	N/A	0.6109	N/A
FeNP+His 8 mg / L	0.3607	N/A	N/A	N/A	N/A	N/A
FeNP+His 12 mg / L	1.54×10^{-3}	N/A	N/A	0.0159	N/A	N/A
FeN+His 16 mg / L	0.0725	N/A	N/A	0.4776	0.0308	N/A
ZnNP+His 8 mg / L	0.0467	N/A	N/A	N/A	N/A	N/A
ZnNP+His 16 mg / L	0.4776	N/A	N/A	N/A	N/A	0.4545

App. 16 p-value between DM % Sax2015

p-vlaues DM% Sax2016	Control	Chempak	CaNP+His 64 mg/L	FeNP+His 16 mg/L	FeNP+His 32 mg/L	His. 16 mg/L	His 32 mg/L
Chempak	0.1867	N/A	N/A	N/A	N/A	N/A	N/A
CaNP+His 32 mg/L	$9.24x10^{-4}$	0.0175	N/A	N/A	N/A	N/A	N/A
CaNP+His 64 mg/L	0.9355	0.0937	N/A	N/A	N/A	N/A	N/A
FeNP+His 16 mg/L	0.5427	0.3442	N/A	N/A	N/A	N/A	N/A
FeNP+His 32 mg/L	0.1150	0.8245	N/A	0.2055	0.0269	N/A	N/A
His. 16 mg/L	0.0264	0.2377	N/A	0.0411	N/A	N/A	N/A
His 32 mg/L	0.0857	0.7072	N/A	N/A	0.8705	0.3501	N/A
His. 64 mg/L	$1.85x10^{-8}$	$1.76x10^{-10}$	$2.06x10^{-9}$	N/A		$7.13x10^{-11}$	2.91x10-3

App. 17 p-value between DM % Sax2016

DM% comparison	p-value
FeNP+His. 16 mg / L	7.32E-06
CaNP+His. 32 mg / L	0.6085
Control with Chempak Sax2016	0.1737

App. 18 Comparison of DM % between same applications between trials Sax2015 and Sax2016

	Ca content (mg / L per gram)		
	Whole tuber	Skin	Tuber flesh
Control	115.82	121.95	113.77
CaNP+His. 12 mg / L	145.60	191.99	130.14
CaNP+His. 32 mg / L	49.58	84.39	49.58
CaFeNP+His. (24:12 mg / L)	221.45	393.58	164.08

App. 19 Concentration of Ca from tubers harvested from trial Sax2015, treated with MONP+His.

p-values Sax2015 Whole tuber	*CaNP+His. 12 mg / L*	*CaNP+His. 32 mg / L*	*CaFeNP+His. (24:12 mg / L)*
Control	0.0192	$2.62x10^{-16}$	$4.3x10^{-9}$
CaNP+His. 12 mg / L	*N/A*	$1.03x10^{-11}$	$2.97x10^{-4}$
CaNP+His. 32 mg / L	*N/A*	*N/A*	$2.47x10^{-9}$

App. 20 Figure 3.26: Statistical p-values for the comparison of whole tuber Ca content of Sax2015 tubers

p-values Sax2015 Skin	*CaNP+His. 12 mg / L*	*CaNP+His. 32 mg / L*	*CaFeNP+His. (24:12 mg / L)*
Control	0.4046	0.0461	$2.57x10^{-6}$
CaNP+His. 12 mg / L	*N/A*	0.0557 0.0278 *	$6.54x10^{-5}$
CaNP+His. 32 mg / L	*N/A*	*N/A*	$4.28x10^{-4}$
p-values Sax2015 Tubers	***CaNP+His. 12 mg / L***	***CaNP+His. 32 mg / L***	***CaFeNP+His. (24:12 mg / L)***
Control	0.0127	$1.95x10^{-19}$	$1.16x10^{-9}$
CaNP+His. 12 mg / L	*N/A*	$8.92x10^{-15}$	$1.48x10^{-3}$
CaNP+His. 32 mg / L	*N/A*	*N/A*	$5.24x10^{-17}$

*App. 21 Statistical p-values for the comparison of skin and tuber content of Ca from trial Sax2015. * p-value of one-way t-test.*

	Fe content (mg / L per gram)		
	Whole tuber	Skin	Tuber
Control	26.53	29.17	25.65
FeNP+His. 8 mg / L	23.56	27.91	22.11
FeNP+His. 12 mg / L	31.39	76.06	16.50
FeNP+His. 16 mg / L	36.11	48.82	31.87
CaFeNP+His. (24:12 mg / L)	15.72	12.48	1.71

App. 22 Concentration of Fe from tubers harvested from trial Sax2015, treated with MONP+His.

p-values Sax2015 Whole tuber	*FeNP+His. 8 mg / L*	*FeNP+His. 12 mg / L*	*FeNP+His. 16 mg / L*	*CaFeNP+His. (24:12 mg / L)*
Control	0.3686	0.5746	$5.60X10^{-3}$	$4.11x10^{-18}$
FeNP+His. 8 mg / L	*N/A*	0.320828	0.001641	$1.28x10^{-22}$
FeNP+His. 12 mg / L	*N/A*	*N/A*	0.0559 0.0280 *	$4.31x10^{-6}$
FeNP+His. 16 mg / L	*N/A*	*N/A*	*N/A*	$2.93x10^{-7}$

*App. 23 Statistical p-values for the comparison of whole tuber Fe content of Sax2015 tubers. * p-value of one-way t-test.*

p-values Sax2015 Skin	*FeNP+His. 8 mg / L*	*FeNP+His. 12 mg / L*	*FeNP+His. 16 mg / L*	*CaFeNP+His. (24:12 mg / L)*
Control	0.8716	0.0845	0.1471	0.1812
FeNP+His. 8 mg / L	*N/A*	0.0656 0.0328*	0.0648 0.0324*	$7.00x10^{-4}$
FeNP+His. 12 mg / L	*N/A*	*N/A*	0.3302	0.1171
FeNP+His. 16 mg / L	*N/A*	*N/A*	*N/A*	0.0430
p-values Sax2015 Tuber	FeNP+His. 8 mg / L	FeNP+His. 12 mg / L	FeNP+His. 16 mg / L	CaFeNP+His. (24:12 mg / L)
Control	0.0198	$7.88x10^{-7}$	0.0935	7.1710^{-24}
FeNP+His. 8 mg / L	*N/A*	$7.43x10^{-4}$	$7.96x10^{-3}$	$2.58x10^{-25}$
FeNP+His. 12 mg / L	*N/A*	*N/A*	$6.95x10^{-5}$	$1.72x10^{-11}$
FeNP+His. 16 mg / L	*N/A*	*N/A*	*N/A*	$1.09x10^{-7}$

*App. 24 Statistical p-values for the comparison of skin and tuber content of Fe from trial Sax2015. * p-value of one-way t-test.*

	Zn content (mg / L per gram)		
	Whole tuber	Skin	Tuber
Control	7.91	9.50	7.38
ZnNP+His. 8 mg / L	145.08	243.38	112.31
ZnNP+His. 16 mg / L	36.09	61.38	25.25

App. 25 Table 3.31: Concentration of Zn from tubers harvested from trial Sax2015, treated with MONP+His.

p-values Sax2015 Whole tuber	*ZnNP+His. 8 mg / L*	*ZnNP+His. 16 mg / L*
Control	8.65×10^{-8}	2.19×10^{-20}
ZnNP+His. 8 mg / L	*N/A*	9.30×10^{-3}

App. 26 Statistical p-values for the comparison of whole tuber Zn content of Sax2015 tubers.

p-values Sax2015 Skin	*ZnNP+His. 8 mg / L*	*ZnNP+His. 16 mg / L*
Control	2.84×10^{-5}	7.65×10^{-12}
ZnNP+His. 8 mg / L	*N/A*	0.0251
p-values Sax2015 Tuber	ZnNP+His. 8 mg / L	ZnNP+His. 16 mg / L
Control	1.98×10^{-4}	8.60×10^{-19}
ZnNP+His. 8 mg / L	*N/A*	0.0720 0.0232*

*App. 27 Statistical p-values for the comparison of skin and tuber content of Fe from trial Sax2015. * p-value of one-way t-test*

	Ca content (mg / L per gram)			
	Whole tuber	Skin / cortex	Parenchyma / vascular ring	Perimedulla / medulla
Control	242.41	58.84	11.58	14.79
Chempak	267.51	66.10	11.38	16.09
FeNP+His 16 mg/L	N/A	100.98	14.75	28.88
FeNP+His 32 mg/L	N/A	76.27	20.51	20.27
CaNP+His 32 mg/L	290.93	77.57	15.17	28.52
CaNP+His 64 mg/L	243.88	65.99	16.98	19.66
His 16 mg/L	N/A	73.35	14.46	22.21
His 32 mg/L	250.99	87.17	10.76	18.73
His 64 mg/L	140.77	45.91	16.46	15.00

App. 28 Concentration of Ca from tubers (and constituent parts) harvested from trial Sax2016, treated with MONP+His.

p-value of whole tuber	*Control*	*Chempak*	*CaNP+His 32 mg/L*	*CaNP+His 64 mg/L*	*His 32 mg/L*
Chempak	1.06×10^{-5}	N/A	N/A	N/A	N/A
CaNP+His 32 mg/L	0.0203	0.2572	N/A	N/A	N/A
CaNP+His 64 mg/L	0.9323	0.1820	0.0790 0.0395*	N/A	N/A
His 32 mg/L	0.6487	0.3874	0.1490	N/A	N/A
His 64 mg/L	4.19×10^{-24}	8.31×10^{-26}	N/A	3.74×10^{-7}	5.05×10^{-7}

*App. 29 p-value of Ca content of whole tuber analysis from Sax2016 trial. * p-value of one-way t-test*

p-values of Ca content Sax2016	*Skin / cortex*	*Parenchyma / vascular ring*	*Perimedulla / medulla*
Chempak	2.41×10^{-9}	0.0705	1.75×10^{-6}
CaNP+His 32 mg/L	1.12×10^{-13}	1.75×10^{-8}	1.62×10^{-13}
CaNP+His 64 mg/L	2.24×10^{-10}	8.48×10^{-10}	1.49×10^{-10}
His 32 mg/L	1.20×10^{-13}	4.77×10^{-4}	4.41×10^{-10}
His 64 mg/L	1.24×10^{-11}	2.84×10^{-9}	0.1253

App. 30 Statistical p-values for comparison of Ca content of tuber constituents from trial Sax2016.

Fe content (mg / L per gram)

	Whole tuber	Skin / cortex	Parenchyma / vascular ring	Perimedulla / medulla
Control	165.24	170.55	82.67	88.22
Chempak	182.21	167.03	71.93	103.11
CaNP+His 32 mg/L	142.69	224.84	89.99	102.78
CaNP+His 64 mg/L	136.13	156.36	96.38	100.90
FeNP+His 16 mg/L	194.70	171.92	75.94	93.93
FeNP+His 32 mg/L	150.48	148.96	74.62	101.91
His 16 mg/L	136.12	269.09	81.96	104.49
His 32 mg/L	127.99	236.12	93.10	102.29
His 64 mg/L	84.78	141.34	99.45	93.73

App. 31 Concentration of Fe from tubers (and constituent parts) harvested from trial Sax2016, treated with MONP+His.

	Control	*Chempak*	*FeNP+His 16 mg/L*	*FeNP+His 32 mg/L*	*CaNP+His 32 mg/L*	*CaNP+His 64 mg/L*	*His 16 mg/L*	*His 32 mg/L*
Chempak	0.01256	N/A	N/A	N/A	N/A	N/A	N/A	N/A
FeNP+His 16 mg/L	0.0011	0.1695	N/A	N/A	N/A	N/A	N/A	N/A
FeNP+His 32 mg/L	0.0886	1.70×10^{-3}	2.12×10^{-4}	N/A	N/A	N/A	N/A	N/A
CaNP+His 32 mg/L	1.62×10^{-5}	1.45×10^{-7}	N/A	0.3304	N/A	N/A	N/A	N/A
CaNP+His 64 mg/L	8.35×10^{-7}	6.85×10^{-11}	N/A	N/A	0.1886	N/A	N/A	N/A
His 16 mg/L	0.0041	2.40×10^{-5}	6.81×10^{-7}	N/A	N/A	N/A	N/A	N/A
His 32 mg/L	2.21×10^{-5}	2.57×10^{-8}	N/A	0.0148	0.0655	N/A	0.2766	x
His 64 mg/L	1.94×10^{-21}	1.65×10^{-23}	N/A	N/A	N/A	1.09×10^{-20}	9.36×10^{-12}	1.54×10^{-11}

App. 32 p-value of Ca content of whole tuber analysis from Sax2016 trial.

Skin / cortex	*Control*	*Chempak*	*FeNP+His 16 mg/L*	*FeNP+His 32 mg/L*
Chempak	0.0562	N/A	N/A	N/A
FeNP+His 16 mg/L	0.5612	0.0141	N/A	N/A
FeNP+His 32 mg/L	$7.49x10^{-9}$	$1.53x10^{-11}$	$4.90x10^{-9}$	N/A
His 16 mg/L	$1.20x10^{-15}$	$3.65x10^{-17}$	$0.77x10^{-15}$	N/A
His 32 mg/L	$1.49x10^{-14}$	$2.80x10^{-17}$	N/A	$2.80x10^{-18}$

App. 33 Statistical p-values for comparison of Fe content of tuber skin / cortex from trial Sax2016.

Parenchyma / vascular ring	*Control*	*Chempak*	*FeNP+His 16 mg/L*	*FeNP+His 32 mg/L*
Chempak	$4.09x\ 10^{-12}$	N/A	N/A	N/A
FeNP+His 16 mg/L	$8.58x10^{-7}$	$2.16x10^{-4}$	N/A	N/A
FeNP+His 32 mg/L	$2.22x10^{-9}$	$5.49x10^{-4}$	$1.02x10^{-6}$	N/A
His 16 mg/L	0.0690	$1.54x10^{-13}$	0.1542	N/A
His 32 mg/L	$3.20x10^{-14}$	$2.29x10^{-14}$	N/A	$6.57x10^{-13}$

App. 34 Statistical p-values for comparison of Fe content of tuber parenchyma / vascular ring from trial Sax2016.

Perimedulla / medulla	*Control*	*Chempak*	*FeNP+His 16 mg/L*	*FeNP+His 32 mg/L*
Chempak	$8.95x10^{-10}$	N/A	N/A	N/A
FeNP+His 16 mg/L	$1.43x10^{-7}$	$1.09x10^{-6}$	N/A	N/A
FeNP+His 32 mg/L	$3.93x10^{-9}$	0.4001	$7.10x10^{-6}$	N/A
His 16 mg/L	$9.49x10^{-5}$	0.2207	$1.97x10^{-10}$	N/A
His 32 mg/L	$2.33x10^{-13}$	0.4676	N/A	0.7412

App. 35 Statistical p-values for comparison of Fe content of tuber perimedulla / medulla from trial Sax2016.

11.3 FeLoad2016 statistical analysis

	Average height (mm) ± SD		
	Week 4	Week 5	Week 6
Control	379.44 ± 19.63	519.89 ± 41.57	584.11 ± 48.05
L1	438.22 ± 39.88	572.00 ± 25.31	640.67 ± 25.38
L2	386.33 ± 38.44	519.78 ± 27.25	597.00 ± 39.34
L3	361.44 ± 19.72	531.22 ± 31.65	607.33 ± 23.83

App. 36 Average growth rates ± SD from FeLoad2016.

	Control	L 1	L2	L3
Per plant	12.44	11.33	10.11	10.56
Total number of tubers >10 mm	112.00	102.00	91.00	95.00
Number of >30mm	69.00	77.00	65.00	63.00
Number of <30 mm	43.00	25.00	26.00	32.00
Percentage of >30mm	61.61	75.49	71.43	66.32
Number >30mm scab	12	4	6	1
Number >30mm virus	2	2	0	0
Soft rot	0	0	1	0
Total effected	14	6	6	1
Percentage virus or scab effected from > 30mm	49.11	69.61	64.84	65.26
Total harvested weight (g)	2820.44	3253.14	2995.44	3046.20
Total harvested weight >30mm (g)	2263.43	3120.93	2870.30	2882.93
Total harvested weight <30mm (g)	557.01	132.21	125.14	163.27
Percentage >30mm weight	80.25	95.94	95.82	94.64
Average harvested weight >30mm	32.80	41.09	44.16	45.76
Average harvested weight <30mm	12.95	5.29	4.81	5.10
Overall SD	39.24	26.82	27.49	29.52
SD >30mm	23.07	25.41	24.71	27.40
SD<30mm	54.40	2.54	2.84	2.85

App. 37 Harvest data from FeLoad2016 trial

p-values All tubers weights	L1	L2	L3
Control	0.1495	0.1135	0.1615
L1	na	0.7940	0.9659
L2	Na	na	0.9796
> 30 mm	L1	L2	L3
Control	0.057358	0.0068	0.0038
L1	na	0.3923	0.2443
L2	Na	na	0.7287
< 30 mm	L1	L2	L3
C	0.4852	0.4498	0.4182
L1	na	0.5321	0.7985
L2	na	na	0.7015

App. 38 p-values from comparison of harvest data from tubers harvested from trial FeLoad2016.

	Average DM % ± SD	ANOVA p-values			One way / Two-way t-test		
		Against control	Against L1	Against L2	Against control	Against L1	Against L2
Control	38.56 ± 3.22	N/A	N/A	N/A	N/A	N/A	N/A
L1	37.01 ± 3.95	0.3494	N/A	N/A	0.1747/ 0.3494	N/A	N/A
L2	37.93 ± 2.81	0.6476	0.5562	N/A	0.3238/ 0.6476	0.2781/ 0.5562	N/A
L3	39.44 ± 3.68	0.5745	0.1713	0.3154	0.2872/ 0.5745	0.0857/ 0.1713	0.1578/ 0.3154

App. 39 DM % and statistical analysis of tubers harvested from trial FeLoad2016

	Content of Fe (Mg/ L per gram)	p-value		
		Against control	Against L1	Against L2
Control	7.74 ± 0.8658	N/A	N/A	N/A
L1	6.06 ± 0.4533	0.005082	N/A	N/A
L2	5.60 ± 0.4860	0.001341	0.156358	N/A
L3	7.31 ± 0.7118	0.423434	0.010781	0.002162

App. 40 Fe content of whole tubers from FeLoad2016 with p-vaules.

11.4 Field2015 and Field2016 statistical analysis

Treatment	*Plot wt (kg)*	*Tuber numbers 10-20mm*	*Tuber wt (kg) 10-20mm*	*Tuber numbers 20-40mm*	*Tuber wt (kg) 20-40mm*	*Tuber numbers 40-65mm*	*Tuber wt (kg) 40-65 mm*	*Tuber numbers 65 +*	*Tuber wt (kg) 65 +*
1	2.78	0.00	0.00	24.25	0.97	17.50	1.75	0.00	0.00
2	3.14	0.00	0.00	24.00	0.94	21.00	2.12	0.00	0.00
3	2.99	0.00	0.00	24.25	0.99	19.00	1.87	0.00	0.00
4	3.08	0.00	0.00	24.00	0.94	20.50	2.00	0.00	0.00

App. 41 Harvest data collated by Branston Plc for Field2015

		Treatment 1 (control)	Treatment 2	Treatment 3	Treatment 4
DM% ± SD	Midway	39.94 ± 2.69	41.06 ± 3.52	38.82 ± 3.05	40.76 ± 3.45
	At harvest	34.36 ± 2.97	36.97 ± 3.41	37.48 ± 4.73	37.04 ± 3.99
Fe content (mg / L)	Midway	20.07	9.00	26.03	20.58
	At harvest	66.17	81.93	67.58	55.57

App. 42 Comparison of DM% and Fe content (mg / L per gram) midway (12th week after planting) and at harvest (21.5 weeks).

	p-values of DM% midway			p-value of DM% at harvest		
	Against control (T1)	Against T2	Against T3	Against control (T1)	Against T2	Against T3
T2	0.1578	N/A	N/A	$1.79x10^{-3}$	N/A	N/A
T3	0.1229	$8.37x10^{-3}$	N/A	0.0250	0.6276	N/A
T4	0.2940	0.7298	0.0200	$3.47x10^{-3}$	0.9458	0.6894

App. 43 Statistical comparison of DM% midway through trail and at harvest. Field2015.

	p-values between DM% midway and at harvest
T1	$6.41x10^{-11}$
T2	$1.38x10^{-5}$
T3	0.1814
T4	$1.73x10^{-4}$

App. 44 p-values of the comparison of DM% with in treatment midway and at harvest

	p-values of Fe content midway			p-value of Fe content at harvest		
	Against control (T1)	Against T2	Against T3	Against control (T1)	Against T2	Against T3
T2	0.0369	N/A	N/A	0.1787	N/A	N/A
T3	0.1263	$7.88x10^{-6}$	N/A	0.8872	0.1728	N/A
T4	0.8763	$1.25x10^{-3}$	0.0541	0.2300	$6.16x10^{-3}$	0.0952

App. 45 p-values of Fe content midway through trial (week 12) and at harvest (week 21).

	p-values between Fe content midway and at harvest
T1	$5.75x10^{-7}$
T2	$1.34x10^{-4}$
T3	$1.68x10^{-5}$
T4	$5.30x10^{-10}$

App. 46 p-values comparing the Fe content of tubers midway (week 12) and at harvest (week 21) with in treatments.

Against control (T1)	Number of tuber (p-value)	weight of tubers (p-vaules
T2	>0.25	>0.25
T3	>0.25	0.0005
T4	0.005	>0.25

App. 47 chi-squared analysis against Treatment 1 (control), 20-40 mm and 40-65 mm distribution in number and weight (kg).

Against control (T1)	Total no. of tubers	Total weight	No. of tubers 20- 40 mm	Wt. of tubers 20-40 mm	No. of tubers 40-65 mm	Wt. of tubers 40-65 mm
T2	0.8443	0.9363	1.0000	0.8575	0.8623	0.8133
T3	0.8362	0.5556	0.8356	0.7383	0.9442	0.8646
T4	0.7563	0.9344	0.2012	0.2899	0.4659	0.6169

App. 48 p-values from ANOVA one-way statistical analysis of tuber numbers and weights from Field2015.

	p-values of Fe content midway			p-value of Fe content at harvest		
	Against control (T1)	Against T2	Against T3	Against control (T1)	Against T2	Against T3
T2	0.7800	N/A	N/A	0.6942	N/A	N/A
T3	0.9281	0.6818	N/A	0.1480	0.2780	N/A
T4	0.2127	0.1071	0.2074	0.9780	0.6938	0.0808

App. 49 p-value of soil samples before and after trial, Field2015.

	p-values between Fe content midway and at harvest
T1	3.16×10^{-3}
T2	0.0410
T3	3.70×10^{-3}
T4	1.89×10^{-3}

App. 50 p-value from the comparison between Fe content of soil before and after trial, Field2015

Variety and treatment	Site 1	Site 2
Maris piper - Control	39.49 ± 3.62	36.86 ± 3.50
Maris piper - Treated	39.91 ± 3.31	38.87 ± 3.79
Inca bella - Control	38.38 ± 2.19	39.13 ± 1.94
Inca bella Treated	39.06 ± 2.01	39.71 ± 2.18

App. 51 DM % ± SD obtained from Field2016 trial comparing the effect of variety, treatment and location.

	Site 1	Site 2
Maris piper	0.5925	0.0157
Inca bella	0.1547	0.2095

App. 52 p-values of DM% of treatment against control.

		Fe content (mg / L per gram)	
		Control	Treatment
Inca Bella	Site A	54.45	55.32
	Site B	48.07	53.77
Maris piper	Site A	41.38	69.76
	Site B	59.38	68.24
Inca Bella	Overall av.	51.26	54.55
Maris piper	Overall av.	50.38	69.00

App. 53 Fe content of tubers segregated into different locations to compare uptake of Fe in different soils and varieties of potato.

.

		p-value
Inca Bella	Site A	0.8567
	Site B	0.1155
Maris piper	Site A	0.0167
	Site B	0.3002
Inca Bella	Overall av.	0.2766
Maris piper	Overall av.	0.0108

App. 54 Fe content of tubers across both locations.

11.5 59Fe statistical analysis

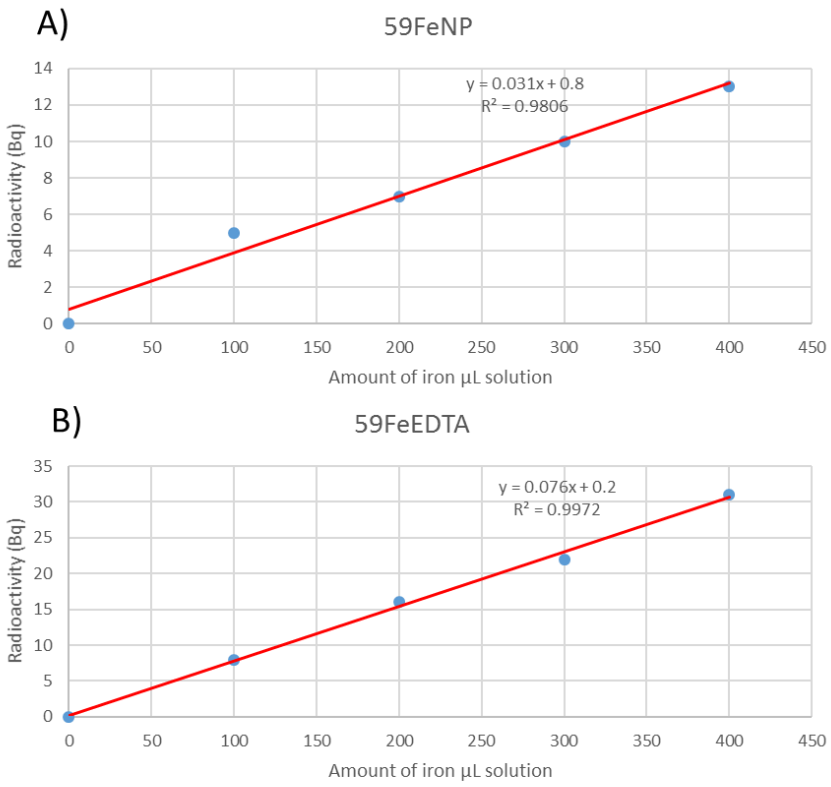

App. 55 Calibration of radioactive 59FeNP and 59Fe-EDTA to determine Fe content using Hidex AMG Gamma Counter measuring the gamma reading (MBq).

		Av. 59Fe (MBq)	Av .Fe conc (mg / L per gram)
FeNP+His	Soil	398.00	96.68
	Tuber	33.00	0.98
	Stem lower	13.00	12.99
	Stem mid	3.00	1.22
	Stem top	16.00	2.55
Fe-EDTA	Soil	24.29	4.52
	Tuber	0.22	0.00
	Stem lower	21.67	4.70
	Stem mid	10.67	0.92
	Stem top	5.83	0.62

App. 56 Data collected from trial 59Fe initially read in MBq then converted to Fe content via calibration graph.

	Fe-EDTA against ^{59}FeNP+His p-*value*
Soil	1.14×10^{-9}
Tuber	1.17×10^{-8}
Stem lower	1.61×10^{-8}
Stem mid	9.12×10^{-5}
Stem top	7.94×10^{-5}

App. 57 p-values of Fe content (mg / L) comparing 59Fe-EDTA to 59FeNP+His data.

11.6 T2014 statistical analysis

Application	*% emerged after 4 weeks*	*Percentage survived to produce fruit (%)*
Control	43.75	73.33
FeNP+His 6 mg / L	25	100.00
FeNP+His 12 mg / L	25	100.00
FeNP+His 24 mg / L	25	33.33
His 6 mg / L	25	66.67
His 12 mg / L	62.5	100.00
His 24 mg / L	87.5	100.00

App. 58 Effect of FeNP+His and His on the emergence and development of tomato seedlings and plants.

	Average height (mm) ± SD			
	Week 4	Week 7	Week 10	Week 13
Control	24.43 ± 11.23	53.50 ± 12.57	123.14 ± 51.20	410.71 ± 121.83
Miracle Gro	25.25 ± 9.81	42.00 ± 9.19	85.00 ± 12.73	319.00 ± 49.50
FeNP+His 6 mg / L	34.00 ± 5.66	83.50 ± 8.39	205.50 ± 17.68	617.50 ± 123.74
FeNP+His 12 mg / L	16.50 ± 4.95	47.33 ± 22.63	78.67 ± 7.23	323.33 ± 49.96
FeNP+His 24 mg / L	32.50 ± 21.95	49.00 ± 8.49	73.50 ± 2.12	454.00 ± N/A
His 6 mg / L	44.50 ± 2.12	78.00 ± 8.49	192.50 ± 2.12	563.50 ± 12.02
His 12 mg / L	36.00 ± 4.90	69.60 ± 2.88	159.20 ± 11.30	528.00 ± 12.71
His 24 mg / L	44.43 ± 11.22	89.57 ± 13.92	236.57 ± 32.08	561.29 ± 120.84

App. 59 Growth rate of tomatoes plants from trial T2014.

	p-value of heights against control.			
	Week 4	Week 7	Week 10	Week 13
Miracle Gro	0.9059	0.3100	0.3513	0.3504
FeNP+His 6 mg / L	0.2981	0.0725	0.0691	0.0726
FeNP+His 12 mg / L	0.3807	0.6149	0.1854	0.2765
FeNP+His 24 mg / L	0.4738	0.7806	0.2328	0.7509
His 6 mg / L	0.0475	0.1290	0.1108	0.1353
His 12 mg / L	0.0582	0.0958	0.1575	0.0605
His 24 mg / L	5.98×10^{-3}	1.27×10^{-3}	3.27×10^{-4}	0.0387

App. 60 p-values of growth rates when compared against control.

	p-values
	Week 13 against Miracle Gro
FeNP+His 6 mg / L	0.0210
FeNP+His 12 mg / L	1.68×10^{-4}
FeNP+His 24 mg / L	0.0323
His 6 mg / L	0.0210
His 12 mg / L	1.68×10^{-4}
His 24 mg / L	0.0323

App. 61 p-values at week 13 comparing average heights at week 13 to FeNP+His and His. applications.

	Fresh weight per plant (g)	Average number of fruits per plant	Average fresh weight per fruit
Control	172.85	9.20	18.79
Miracle Gro	214.06	16.00	13.81
FeNP+His. 6 mg / L	119.95	6.67	17.14
FeNP+His. 12 mg / L	254.65	22.67	12.96
FeNP+His. 24 mg / L	83.85	7.00	11.98
His. 6 mg / L	94.46	5.67	16.67
His. 12 mg / L	147.55	15.67	15.71
His. 24 mg / L	150.36	14.00	16.45

App. 62 Harvest data collated from T2014.

	Control	Miracle Gro	FeNP+His. 6 mg / L	FeNP+His. 12 mg / L	FeNP+His. 24 mg / L
Miracle Gro	6.24×10^{-5}	N/A	N/A	N/A	N/A
FeNP+His. 6 mg / L	0.2788	0.01590	N/A	N/A	N/A
FeNP+His. 12 mg / L	2.22×10^{-13}	3.10×10^{-3}	8.30×10^{-7}	N/A	N/A
FeNP+His. 24 mg / L	3.12×10^{-3}	0.2265	0.0302	0.6259	N/A
His. 6 mg / L	0.17753	0.0271	0.7904	N/A	N/A
His. 12 mg / L	3.63×10^{-3}	0.1651	N/A	5.47×10^{-6}	N/A
His. 24 mg / L	4.73×10^{-4}	0.2514	N/A	N/A	0.1376

App. 63 p-values obtained when comparing fresh weights from trial T2014.

	DM ± SD
Control	10.91 ± 0.52
Miracle Gro	11.06 ± 0.40
FeNP+His. 6 mg / L	8.27 ± 0.28
FeNP+His. 12 mg / L	7.71 ± 0.70
FeNP+His. 24 mg / L	11.43 ± 0.40
His. 6 mg / L	9.50 ± 0.92
His. 12 mg / L	10.77 ± 0.35
His. 24 mg / L	9.56 ± 0.55

App. 64 DM % with SD of tomato fruit from trial T2014

	Control	*Miracle Gro*	*FeNP+His. 6 mg / L*	*FeNP+His. 12 mg / L*	*FeNP+His. 24 mg / L*
Miracle Gro	$3.99x10^{-14}$	N/A	N/A	N/A	N/A
FeNP+His. 6 mg / L	0.0168	$2.71x10^{-13}$	N/A	N/A	N/A
FeNP+His. 12 mg / L	0.1953	$2.22x10^{-18}$	0.1741	N/A	N/A
FeNP+His. 24 mg / L	$3.24x10^{-5}$	0.2053	$3.79x10^{-8}$	$5.07x10^{-6}$	N/A
His. 6 mg / L	0.1879	$5.71x10^{-7}$	$1.24x10^{-3}$	N/A	N/A
His. 12 mg / L	0.2355	$8.89x10^{-17}$	N/A	$7.77x10^{-3}$	N/A
His. 24 mg / L	0.0340	$1.17x10^{-11}$	N/A	N/A	$3.37x10^{-3}$

App. 65 -value of DM % obtained from tomatoes propagated in trial T2014.

Fe content of tomatoes (mg / L per gram)

	Start (25/07/2014)	Mid (09/08/2014)	End (28/08/2014)	Harvest average of all fruit
Control	26.32	14.28	15.65	18.75
Commercial	16.93	26.83	39.56	27.78
Fe+His 6 ppm	52.84	67.48	89.43	69.92
Fe+His 12 ppm	46.14	49.97	51.22	49.11
Fe+His 24 ppm	26.42	55.98	53.09	45.16

App. 66 Fe content of tomato fruit. average over harvest and during harvest.

p-value against control Fe content

	Start (25/07/2014)	Mid (09/08/2014)	End (28/08/2014)	Harvest average of all fruit
Miracle Grow	0.1816	0.2783	0.1406	0.1711
Fe+His 6 ppm	0.2585	0.0111	4.53×10^{-3}	3.52×10^{-5}
Fe+His 12 ppm	0.0546	0.0430	0.0205	3.53×10^{-5}
Fe+His 24 ppm	0.9940	0.1085	0.1619	0.0248
	p-value against Miracle Grow Fe content			
	Start (25/07/2014)	Mid (09/08/2014)	End (28/08/2014)	Harvest average of all fruit
Fe+His 6 ppm	0.1575	0.0446	0.0176	8.06×10^{-4}
Fe+His 12 ppm	0.0284	0.1813	0.4625	9.19×10^{-3}
Fe+His 24 ppm	0.5280	0.2484	0.6081	0.1566

App. 67 p-values from the ICP data of Fe content of tomatoes through the harvest period and overall average content.

11.7 TSC2014 Data and statistical analysis

	Average height (mm) obtained after 'n' weeks after planting									
	1	2	3	4	5	6	7	8	9	10
Control	0.00	5.00	16.50	24.43	39.86	43.43	53.50	66.43	82.43	123.14
HNS	0.00	0.00	8.50	30.00	55.00	57.50	71.00	79.00	95.00	142.00
FeNP	7.00	15.00	16.00	30.00	47.30	49.70	51.50	54.50	61.00	86.00
FeNP+HNS	0.00	6.00	8.00	22.70	39.70	43.00				

App. 68 Growth rate of plants propagated from coated seeds.

	Week 4			*Week 7*		*Week 10*	
	HNS	FeNP	FeNP+HNS	HNS	FeNP	HNS	FeNP
Control	0.5256	0.5098	0.8050	0.4211	0.8980	0.7422	0.3854
HNS	N/A	1	0.1230	N/A	0.5332	N/A	0.4762
FeNP	N/A	N/A	0.4093	N/A	N/A	N/A	N/A

App. 69 p-values of growth rate of plants propagated form coated seeds. TSC2014

	Weight of harvest per plant (g)	*Average number of fruits per plant (n)*	*Average fresh weight per fruit (g)*	*p-value of fresh weight of tomatoes against control*
Control	172.85	9.20	18.79	N/A
HNS	127.01	7.00	14.11	0.0221
FeNP	111.39	8.00	13.92	2.47×10^{-3}

App. 70 Fresh harvest data collected from trial TSC2014 with p-vales against control comparing average fresh weights of tomato.

	DM % ± SD
Control	10.91 ± 0.52
HNS	9.71 ± 6.93
FeNP	9.17 ± 3.79

App. 71 Dry matter (%) of tomatoes from trial TSC2014.

	p-values		
	against control	against Miracle Gro	HNS against FeNP
HNS	0.0560	$3.79x10^{-3}$	0.1860
FeNP	0.6435	$4.24x10^{-8}$	

App. 72 p-values comparing DM% of tomatoes from trial TSC2014

11.8 C2014 data and statistical analysis

	Height (mm) after 'n' weeks into trial					*Height gained between weeks 1 to 5 (mm)*
	1	2	3	4	5	
Control	54	71	78	94	106	52
Chilli focus	46	59	69	87	97	51
FeNP+His. 6 mg / L	48	72	79	97	118	70
FeNP+His. 12 mg / L	54	69	75	84	100	46
His. 6 mg / L	60	82	88	102	113	53
His. 12 mg / L	38	52	63	72	89	51

App. 73 Growth rates of Cayenne plants in the first five weeks in the trial with weekly applications of the designated treatments.

	Total number of red chillies per plant	Average fresh weight (g) ± SD	Average % dry matter (DM %) ± SD
Control	91	0.8014 ± 0.58	28.17 ± 4.69
Chilli Focus	157	0.6426 ± 0.39	27.00 ± 2.67
FeNP+His. 6 mg / L	166	0.6575 ± 0.38	27.38 ± 3.67
FeNP+His. 12 mg / L	117	0.7185 ± 0.43	27.40 ± 3.82
His 6 mg / L	113	0.7478 ± 0.44	25.13 ± 3.66
His 12 mg / L	90	0.8592 ± 0.47	25.58 ± 2.35

App. 74 Harvest data and DM % of chilli peppers propagated in preliminary trial C2014

p-values of fresh weight (C2014)

	Control	FeNP+His. 6 mg / L	FeNP+His. 12 mg / L	His 6 mg / L	His 12 mg / L
Chilli Focus	0.0105	0.7287	0.1286	0.0392	1.35×10^{-4}
FeNP+His. 6 mg / L	0.0165	N/A	N/A	0.0672	N/A
FeNP+His. 12 mg / L	0.2354	0.2065	N/A	N/A	0.0263
His. 6 mg / L	0.4512	N/A	N/A	N/A	0.0839
His. 12 mg / L	0.4616	N/A	N/A	N/A	N/A

App. 75 p-values comparing fresh weights of chilli peppers harvested from trial C2014

p-values of DM % (C2014)

	Control	FeNP+His. 6 mg / L	FeNP+His. 12 mg / L	His 6 mg / L	His 12 mg / L
Chilli Focus	0.0125	0.2946	0.2962	$2.09x10^{-6}$	$3.77x10^{-5}$
FeNP+His. 6 mg / L	0.1325	N/A	N/A	$9.19x10^{-7}$	N/A
FeNP+His. 12 mg / L	0.1966	0.9398	N/A	N/A	$8.93x10^{-5}$
His. 6 mg / L	$4.78x10^{-7}$	N/A	N/A	N/A	0.3152
His. 12 mg / L	$5.29x10^{-6}$	N/A	N/A	N/A	N/A

App. 76 p-values comparing DM % of chilli peppers propagated C2014.

Fe content (mg / L) of cayenne peppers C2014 ± SD

Control	8.24 ± 7.27
Chilli focus	7.00 ± 3.24
FeNP+His 6 mg / L	4.58 ± 1.66
FeNP+His. 12 mg / L	5.23 ± 3.28
His. 6 mg / L	5.68 ± 3.36
His. 12 mg / L	5.11 ± 2.56

App. 77 Fe content of chilli peppers, Cayenne, from trial C2014

p-values of Fe content (C2014)

	Control	FeNP+His. 6 mg / L	FeNP+His. 12 mg / L	His 6 mg / L	His 12 mg / L
Chilli Focus	0.6236	0.5945	0.7212	0.3710	0.6422
FeNP+His. 6 mg / L	0.8455	N/A	N/A	0.4972	N/A
FeNP+His. 12 mg / L	0.8835	0.7084	N/A	N/A	0.9557
His. 6 mg / L	0.8216	N/A	N/A	N/A	0.7888
His. 12 mg / L	0.9081	N/A	N/A	N/A	N/A

App. 78 p-values of Fe content of cayenne peppers propagated in trial C2014.

11.9 CB2015 Data and statistical analysis

Average height (mm) gained by chilli plants ± SD

	Control	FeNP+His. 6 mg / L	FeNP+His. 12 mg / L
Habanero red	647.67 ± 46.05	624.33 ± 40.67	715.67 ± 184.33
Jamaican	569.67 ± 51.19	561.67 ± 41.02	600.67 ± 22.55
Scotch bonnet	606.25 ± 31.18	570.50 ± 102.78	662.50 ± 163.67
Pequin	1023.33 ± 145.66	1186.00 ± 416.01	1207.67 ± 15.04

App. 79 Average height (mm) gained by chilli peppers curing trial CB2015.

p-vales of heights against control CB2015

	FeNP+His. 6 mg / L	FeNP+His. 12 mg / L
Habanero red	0.8430	0.3915
Jamaican	0.5304	0.5245
Scotch bonnet	0.5466	0.5689
Pequin	0.5575	0.0947

App. 80 p-values of heights obtained from chilli peppers propagated in trial CB2015

		Average harvested weight per plant (g) ± SD	*Number of chillies total per plant (n)*
Habanero red	Control	401.63 ± 8.06	213
	FeNP+His. 6 mg / L	445.85 ± 11.13	205
	FeNP+His. 12 mg / L	646.58 ± 40.38	329
Jamaican	Control	520.60 ± 6.53	153
	FeNP+His. 6 mg / L	391.43 ± 15.93	143
	FeNP+His. 12 mg / L	603.41 ± 6.37	182
Scotch Bonnet	Control	93.89 ± 5.17	46
	FeNP+His. 6 mg / L	149.08 ± 7.55	62
	FeNP+His. 12 mg / L	189.73 ± 0.71	98
Pequin	Control	55.27 ± 3.21	343
	FeNP+His. 6 mg / L	38.60 ± 1.74	284
	FeNP+His. 12 mg / L	43.08 ± 5.68	295

App. 81 Harvest data from trial CB2015

p-vales of harvested weights per plant, against control CB2015

	FeNP+His. 6 mg / L	FeNP+His. 12 mg / L	Between FeNP+His treatments
Habanero red	5.14×10^{3}	5.01×10^{-4}	1.15×10^{-3}
Jamaican	2.37×10^{-4}	9.55×10^{-5}	3.11×10^{-5}
Scotch bonnet	5.09×10^{-3}	5.82×10^{-6}	0.5719
Pequin	1.28×10^{-3}	0.0311	0.2625

App. 82 p-values of harvested weights from trial CB2015

		Fe content (mg / L per gram) ± SD
Habanero red	Control	26.67 ± 5.25
	FeNP+His. 6 mg / L	25.34 ± 3.41
	FeNP+His. 12 mg / L	23.82 ± 4.04
Jamaican	Control	30.34 ± 4.55
	FeNP+His. 6 mg / L	25.71 ± 3.62
	FeNP+His. 12 mg / L	25.28 ± 5.74
Scotch Bonnet	Control	34.88 ± 6.04
	FeNP+His. 6 mg / L	36.74 ± 5.33
	FeNP+His. 12 mg / L	25.60 ± 5.32
Pequin	Control	72.05 ± 8.84
	FeNP+His. 6 mg / L	82.14 ± 6.48
	FeNP+His. 12 mg / L	72.12 ± 9.53

App. 83 Average DM % of chillies from trial CB2015.

p-vales of DM%, against control CB2015

	FeNP+His. 6 mg / L	FeNP+His. 12 mg / L	Between FeNP+His treatments
Habanero red	0.2482	0.0217	0.1209
Jamaican	5.43×10^{-5}	3.70×10^{-4}	0.7274
Scotch bonnet	0.2124	4.15×10^{-8}	4.26×10^{-11}
Pequin	4.90×10^{-6}	0.9795	1.31×10^{-5}

Table 3.98: p-values of DM% of chillies from CB2015

Fe content of chilli peppers (mg / L per gram)

Habanero red	Control	54.90 ± 9.55
	FeNP+His 6 mg / L	146.24 ± 65.83
	FeNP+His 12 mg / L	251.64 ± 129.42
Jamaican	Control	78.49 ± 23.83
	FeNP+His 6 mg / L	94.58 ± 31.12
	FeNP+His 12 mg / L	122.62 ± 35.79
Scotch bonnet	Control	40.21 ± 25.20
	FeNP+His 6 mg / L	88.93 ± 43.84
	FeNP+His 12 mg / L	176.93 ± 87.02
Pequin	Control	165.77 ± 84.79
	FeNP+His 6 mg / L	67.25 ± 58.77
	FeNP+His 12 mg / L	84.00 ± 29.94

App. 84 Fe content of chilli peppers from trial CB2015.

p-vales of Fe content, against control CB2015

	FeNP+His. 6 mg / L	FeNP+His. 12 mg / L	Between FeNP+His treatments
Habanero red	1.65×10^{-3}	7.51×10^{-4}	0.0592 0.0296*
Jamaican	0.2651	0.0116	0.1167
Scotch bonnet	0.0164	7.80×10^{-4}	0.0229
Pequin	0.0172	0.0222	0.0172

*App. 85 p-value of Fe content of chilli peppers CB2015. * t-test one-way p-value.*

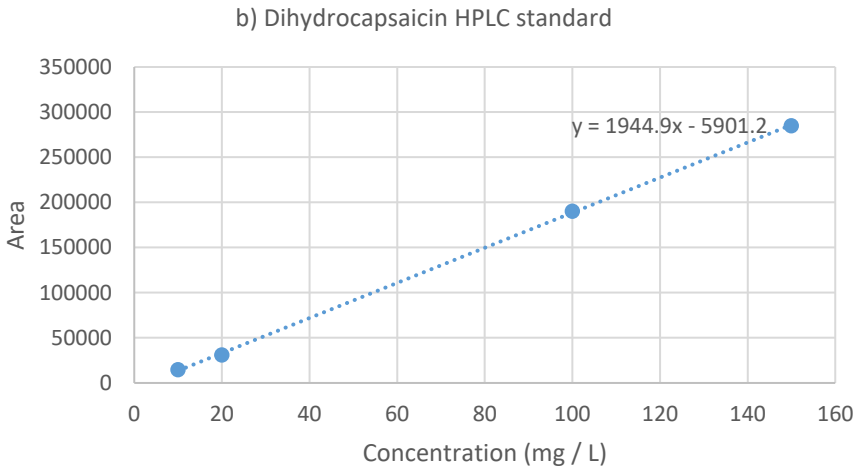

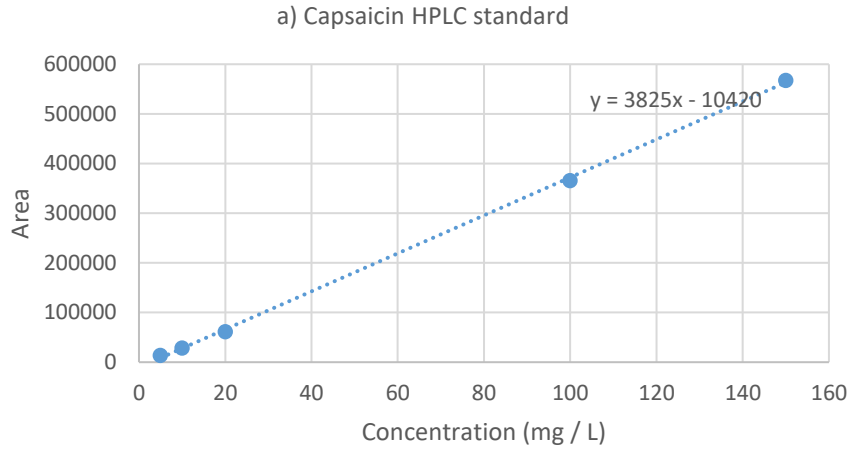

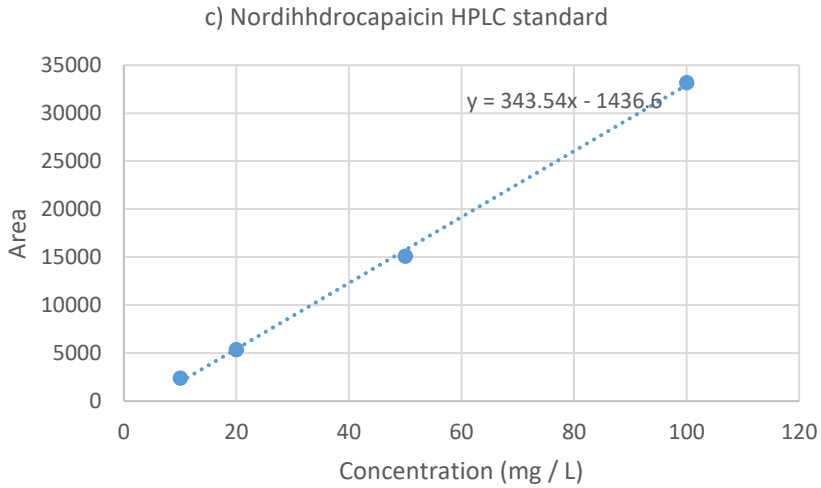

App. 86 Calibration of HPLC standards for the determination of capsaicinoids concentration, mg / L per gram of fruit.

		Capsaicinoid content (mg / L per gram)			Scoville unit (SHU)
		Nordihydrocapsaicin	Dihydrocapsaicin	Capsaicin	
Habanero red	Control	741.24	1823.32	3609.39	57750.20
	FeNP+His. 6 mg / L	493.03	91.71	130.42	2086.65
	FeNP+His. 12 mg / L	2596.67	1310.80	1074.38	17190.10
Jamaican	Control	37356.25	45442.71	26493.49	423896
	FeNP+His. 6 mg / L	414.90	818.12	4536.02	72576.30
	FeNP+His. 12 mg / L	60748.10	35737.00	33814.11	541026.00
Scotch Bonnet	Control	1799.67	961.97	4173.29	66772.60
	FeNP+His. 6 mg / L	1908.06	1036.19	5770.61	92329.80
	FeNP+His. 12 mg / L	3547.24	5788.38	6470.12	103522.00
Pequin	Control	24.51	137.15	41.46	663.41
	FeNP+His. 6 mg / L	53.87	236.63	82.00	1312.08
	FeNP+His. 12 mg / L	57.03	135.49	84.87	1357.87

App. 87 Capsaicinoid content and conversion to SHU (Collins et al., 1995)

		p-values of capsaicinoid		
	(*Against control)	Nordihydrocapsaicin	Dihydrocapsaicin	Capsaicin
Habanero red	*FeNP+His. 6 mg / L	0.5751	0.0159	0.1511
	*FeNP+His. 12 mg / L	0.0522	0.3617	0.1460
	Between FeNP+His. treatments	0.0413	2.15×10^{-5}	0.0310
Jamaican	*FeNP+His. 6 mg / L	1.34×10^{-3}	2.93×10^{-6}	2.92×10^{-4}
	*FeNP+His. 12 mg / L	0.3091	0.3643	0.6286
	Between FeNP+His. treatments	0.0177	1.09×10^{-3}	0.0947
Scotch Bonnet	*FeNP+His. 6 mg / L	0.8865	0.8186	0.1487
	*FeNP+His. 12 mg / L	0.4647	0.2002	0.6090
	Between FeNP+His. treatments	0.3268	0.0699	0.8195
Pequin	*FeNP+His. 6 mg / L	0.0801	0.4442	0.1870
	*FeNP+His. 12 mg / L	0.0374	0.9622	0.0259
	Between FeNP+His. treatments	0.8742	0.4074	0.9236

App. 88 Statistical analysis of capsaicinoid data from HPLC using ANOVA.

11.10 FoliarFe Data and statistical analysis

	Average Fe content (mg / L per gram) ± SD
Control leaf (Separate control plant)	19.65 ± 2.97
FeNP+His. applied leaf	98.45 ± 11.77
Non treated leaf (from same plant as Fe application)	26.58 ± 1.99

App. 89 Average Fe content obtained from leaves in trial FoliarFe

(against control)*	*p-value comparing average Fe content*
FeNP+His. applied leaf	2.50×10^{-3}
Non treated leaf (from same plant as Fe application)	4.96×10^{-7}
Treated against non-treated on same plant	8.86×10^{-7}

App. 90 p-values comparing Fe content in leaves from trial FoliarFe.

11.11 MONP in the environment data and statistical analysis

	Ca conc. at 5 cm (mg/L)	*Ca conc. at 30 cm (mg / L)*	*p-value between 5 and 30 cm*
Compost before application	7717.24		N/A
Control	7970.50	6074.60	0.0763
CaNP+His. 12 mg / L	7126.11	5213.85	$9.65x10^{-5}$
CaNP+His. 32 mg / L	9771.83	4781.88	$3.90x10^{-5}$
CaFeNP+His. (24:12) mg / L	7078.92	5638.41	0.0715
	Fe conc. at 5 cm (mg/L)	*Fe conc. at 30 cm (mg / L)*	p-value between 5 and 30 cm
Compost before application	267.45		N/A
Control	262.45	243.31	$4.41x10^{-3}$
FeNP+His. 8 mg / L	180.85	214.42	$5.51x10^{-4}$
FeNP+His. 12 mg / L	242.07	235.89	0.3996
FeNP+His. 16 mg / L	220.30	211.18	0.2347
CaFeNP+His. (24:12) mg / L	234.62	236.87	0.8629
	Zn conc. at 5 cm (mg/L)	*Zn conc. at 30 cm (mg / L)*	p-value between 5 and 30 cm
Compost before application	42.52		N/A
Control	37.01	17.54	0.0139
ZnNP+His. 8 mg / L	259.18	100.14	$3.88x10^{-8}$
ZnNP+is. 16 mg / L	321.34	36.45	$3.73x10^{-5}$

App. 91 ICP results from the retention of MONP from ICP of compost form trial Sax2015 with p-value comparing mineral concentrations between depth 5 and 30 cm.

CaNP	*5 cm*	*30 cm*
Compost before app.	0.8140	0.2252
CaNP+His. 12 mg / L	0.2126	0.2300
CaNP+His. 32 mg / L	0.0537	0.1035
CaFeNP+His. (24:12) mg / L	0.3583	0.5088

App. 92 p-value of CaNP retention in compost Sax2015 against control.

FeNP	5 cm	30 cm
FeNP+His. 8 mg / L	$1.86x10^{-6}$	$8.81x10^{-5}$
FeNP+His. 12 mg / L	0.0246	0.1159
FeNP+His. 16 mg / L	$2.64x10^{-4}$	$2.88x10^{-4}$
CaFeNP+His. (24:12) mg / L	0.0684	0.0630

App. 93 p-value of FeNP retention in compost Sax2015 against control.

ZnNP	5 cm	30 cm
Compost before app.	0.5963	$7.45x10^{-3}$
ZnNP+His. 8 mg / L	$1.92x10^{-9}$	$4.18x10^{-10}$
ZnNP+is. 16 mg / L	$3.52x10^{-5}$	0.0545

App. 94 p-value of ZnNP retention in compost Sax2015 against control.

	Start of test (number)	Alive end of test (number)	Percentage mortality (%)	Percentage survival (%)
Control (tap water)	25	24	4.00	96.00
FeNP+His. 6 mg / L	25	18	28.00	72.00
FeNP+His. 12 mg / L	26	5	80.77	19.23
FeNP+His. 24 mg / L	24	3	87.50	12.50
ZnNP+His. 6 mg / L	24	0	100.00	0.00
ZnNP+His. 24 mg / L	26	2	92.31	7.69

App. 95 Mortality of shrimps at end of trial

	Mortality rate %		
	After 24 hours	After 48 hours	After 72 hours
Control (tap water)	4.17	0	0
FeNP+His. 6 mg / L	12	9.1	10
FeNP+His. 12 mg / L	19.23	47.62	57.55
FeNP+His. 24 mg / L	16.67	75	40
ZnNP+His. 6 mg / L	29.17	88.24	100
ZnNP+His. 24 mg / L	69.23	75	0

App. 96 Mortality rate of shrimps

	MONP content ± SD	
	Fe (mg / L per gram)	Zn (mg / L per gram)
Control	15.38 ± 0.49	5.40 ± 0.80
FeNP+His. 6 mg / L	22.73 ± 0.06	N/A
FeNP+His. 12 mg / L	47.16 ± 0.22	N/A
FeNP+His. 24 mg / L	52.11 ± 0.05	N/A
ZnNP+His. 6 mg / L	N/A	6.03 ± 0.09
ZnNP+His. 24 mg / L	N/A	40.45 ± 0.72

App. 97 Fe and Zn content **of shrimps remaining after 72 hours.**

	p-values of Fe and Zn content in shrimps				
	FeNP+His. 6 mg / L	FeNP+His. 12 mg / L	FeNP+His. 24 mg / L	ZnNP+His. 6 mg / L	ZnNP+His. 24 mg / L
Control	1.36×10^{-5}	5.59×10^{-8}	2.19×10^{-9}	0.1691	8.81×10^{-10}
FeNP+His. 6 mg / L	N/A	5.44×10^{-9}	3.57×10^{-11}	N/A	N/A
FeNP+His. 12 mg / L	N/A	N/A	3.13×10^{-6}	N/A	N/A
ZnNP+His. 6 mg / L	N/A	N/A	N/A	N/A	9.40×10^{-11}

App. 98 p-values comparing Fe and Zn content of shrimps exposed to MONP's over 72 hours.

11.12 MONP as an antibacterial application for storage; date and statistical analysis

11.12.1 Antibacterial properties of CaNP+His solution (CaO and $CaFe_2O_4$)

	Previous pH	*pH with buffer*	*Average CFU / mL*
Control	pH 7	7.5	8.62E+06
CaHisNP	pH 9	7.5	8.30E+06
CaFeHisNP	pH 5	7	1.65E+05
His	pH 4	7	1.50E+05

App. 99 CFU and pH of solutions to observe the antibacterial effect of two forms of CaNP.

	Control	*CaHisNP*	*CaFeHisNP*
CaHisNP	0.8815	N/A	N/A
CaFeHisNP	0.0228	0.0276	N/A
His	0.0228	0.0276	0.8517

App. 100 p-values comparing CFU / mL using Ca nanoparticles as an antibacterial in waste wash water.

11.12.2 Inoculation of potatoes (variety Maris piper) with pectobacteria pre-treated with MONP+His soak

Soak	*Skin swab (CFU / mL)*	*Peel (CFU / mL)*
None	6.90E+05	3.83E+05
Water	1.20E+05	5.42E+05
CaNP+His	1.87E+05	2.92E+05
CaFeNP+His.	7.50E+03	1.75E+05
FeNP+His.	2.08E+04	5.67E+05
His	6.67E+03	2.92E+05

App. 101 CFU / mL obtained from MONP soak treated tubers to observe the antibacterial effect of the application.

	p-values of swab data			*p-values of peel data*		
	No soak	Water	His	No soak	Water	His
Water	0.4012	N/A	N/A	0.1169	N/A	N/A
CaNP+His	0.4568	$4.98x10^{-3}$	$5.30x10^{-7}$	0.1531	0.0258	*
CaFeNP+His.	0.3185	$8.78x10^{-7}$	0.8583	0.0139	$5.10x10^{-3}$	0.1793
FeNP+His.	0.3276	$3.79x10^{-6}$	0.0241	0.3549	0.9046	0.1852
His	0.3179	$1.29x10^{-6}$	N/A	0.2024	0.0352	N/A

*App. 102 p-values of swab and peel CFU / mL when MONP+His and His appled as a soak to tubers. * both sets of data contained the same sum and average rendering an ANOVA to be performed, using a T-test one tail p = 0.5, T-test two tail p = 1.*

11.12.3 Inoculation of potatoes with pectobacteria (PCA).

	Skin swab (CFU / mL)	*Peel (CFU / mL)*
1	6.17E+04	1.42E+05
2	3.50E+06	3.00E+05
3	5.40E+04	3.25E+05
1a	1.44E+04	2.09E+05
2a	1.14E+05	2.58E+05
3a	1.79E+04	1.93E+05

App. 103 CFU / mL obtained from MONP pretreated with PW (na) and not PW tubers to observe the antibacterial effect of the application.

	p-values of swab data				*p-values of peel data*			
	2	3	1a	2a	2	3	1a	2a
1	$6.87x10^{-4}$	0.4918	$1.72x10^{-5}$	N/A	0.1467	0.0801	0.2887	N/A
2	N/A	$6.88x10^{-4}$	N/A	N/A	N/A	0.8337	N/A	N/A
2a	$4.30x10^{-5}$	N/A	$1.81x10^{-3}$	N/A	0.6800	N/A	0.4039	N/A
3a	N/A	0.0248	0.5754	$2.33x10^{-3}$	N/A	0.2888	0.8677	0.5300

App. 104 p-values to compare the effect of MONP and PW

11.13 Tissue printing onto nitrocellulose Sample preparation

The following methods were refined from Cassab and Varner, (1989). A comparison of two transfer techniques of proteins onto nitrocellulose paper.

Method 1: Electrophoretic transfer

Method 2: Pressing transfer

A potato was cut in half vertically through the centre of an eye region. Slices 2 mm thick were then cut from the potato, and wedges were then cut from the slice, so that the eye region was in the centre of the wedge.

12 pieces of 3 mm filter paper, (40 x 35 mm) and two pieces of nitrocellulose paper (35 x 30 mm) in size were cut for each sample. All pieces were soaked in continuous transfer buffer (consisting of 0.19 M glycine, 20mM tris base, 0.1% SDS and 20% methanol). The electroblotter was moistened with continuous transfer buffer, and was loaded as shown in app. 105.

A glass rod was used to roll over the filter paper and the nitrocellulose once in position to ensure the exclusion of air bubbles.

Two samples were set up in the electroblotter which was run at 50mA (25mA per sample). One sample was removed after 1 hour and the second was allowed to run for 2 hours. After these time intervals, the pieces of nitrocellulose were removed to trays for further processing.

For the second method, twelve pieces of 3 mm filter paper, (40 x 35 mm) and two pieces of nitrocellulose paper (35 x 30 mm) in size were cut for each sample. All pieces were soaked in continuous transfer buffer as in method one.

Six pieces of the moistened filter paper were placed on a glass plate (see app. 106). A piece of nitrocellulose was placed on top, followed by the potato wedge. A second piece of nitrocellulose was placed on top of the potato sample, and a glass rod was rolled over the nitrocellulose to remove the air bubbles (app. 105).

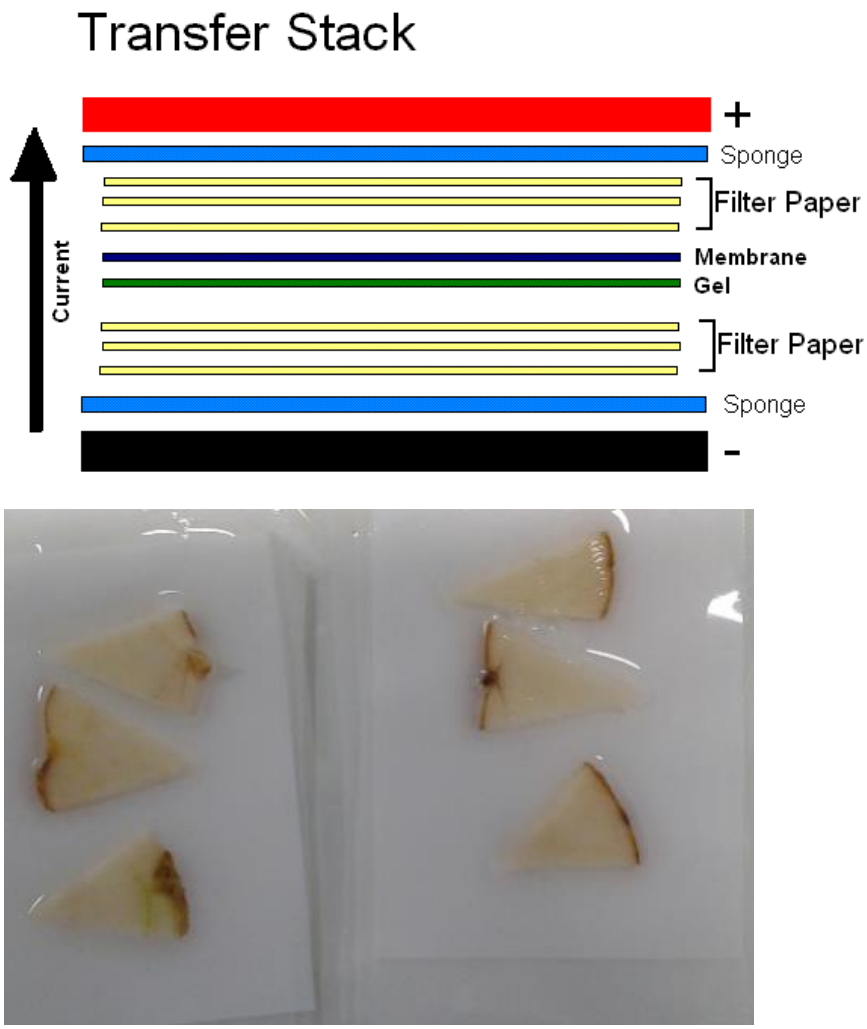

App. 105 Top; Set up of electroblotter for the transfer of proteins onto nitrocellulose paper. Bottomt; samples of potato prepared for transfer.

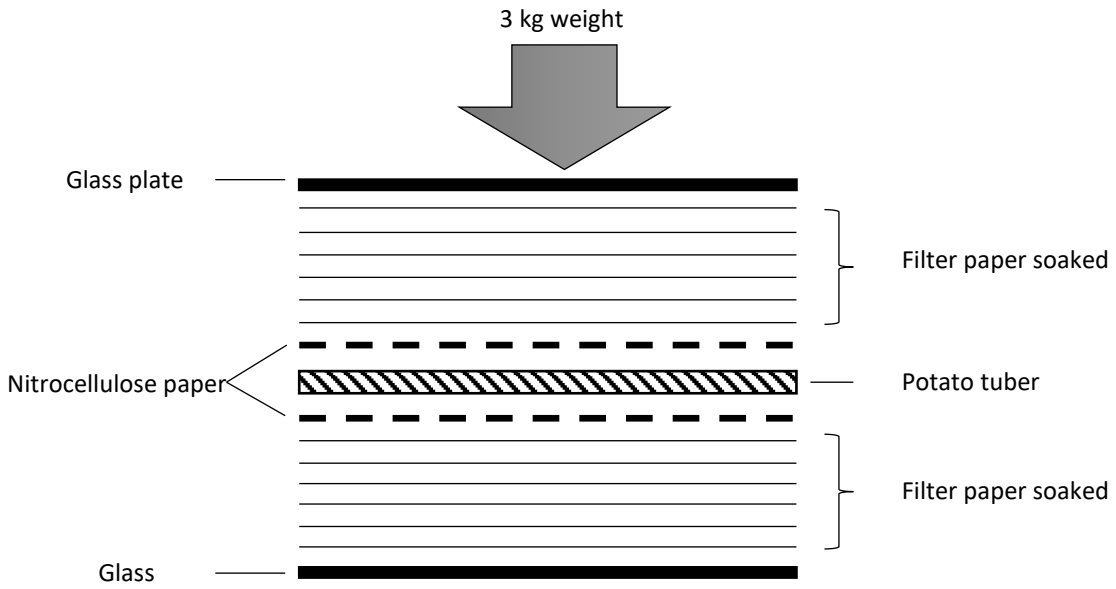

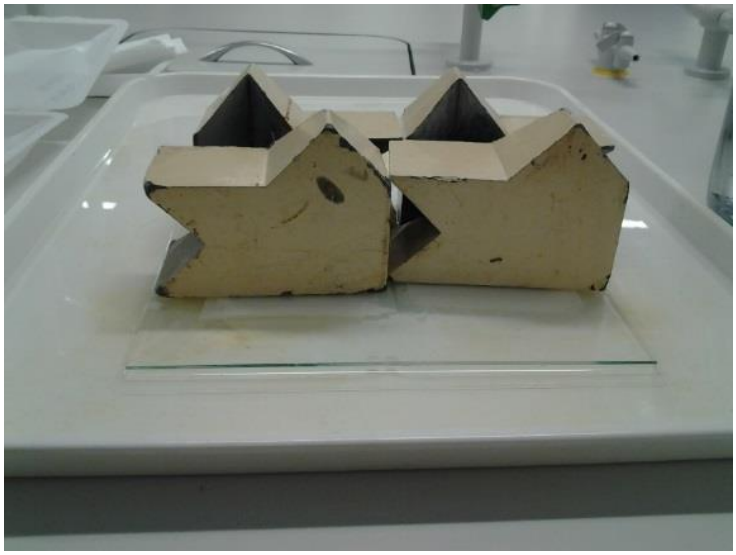

App. 106 Top; sematic of pressure transfer. Botom; in use in the lab

A further six pieces of moistened filter paper was placed on the top and a second glass plate was placed on top of this. A 3 Kg weight was then placed on the top of this, and left for 20 minutes. The procedure was repeated, leaving the weight in position for 1 hour. At the end of these time intervals the nitrocellulose was removed to trays for further processing.

The nitrocellulose from the blotting and from the pressing were all treated in the same manner.

Blocking solution of 5% (w/v), BSA in 150mM PBS (5 mL) was added to each piece of nitrocellulose. This was shaken at room temperature for 1 hour. After discarding the blocking solution, 5ml of a 1 in 10 dilution of primary monoclonal antibody was added, and was shaken at room temperature for 2

hours. The primary antibody used was ID10 which was raised against guinea pig liver transglutaminase and it was diluted in 5% (w/v) BSA in 150mM PBS. The nitrocellulose was then washed in blocking solution for 10 minutes, followed by 3 times for 10 minutes each in tris buffered saline (TBS). After washing, the secondary antibody was added. This was an anti-mouse antibody raised in sheep conjugated to horseradish peroxidase, and it was diluted 1 in 2000 in 5% (w/v) BSA in 150mM PBS before use. This was shaken at room temperature for 2 hours. The nitrocellulose was then washed 4 times for 10 minutes each in TBS, followed by once for 1 minute in distilled water. An addition of 5ml of substrate (3'3' diaminobenzidine (DAB)) was then added. This is specific for peroxidase and the development of a brown colouration denotes the presence of the enzyme. Colour development can take between 30 minutes and 2 hours. At the end of this time the nitrocellulose was washed thoroughly in distilled water. The experiment was repeated using the pressing technique only, the sample being pressed for 20 minutes. Three controls were also set up, these were: (a) No antibody control, (b) No primary antibody control (c) No secondary antibody control.

The experiment was further repeated incorporating an additional blocking step. This step was carried out after blocking with the 5% (w/v) BSA in 150mM PBS, the blocking solution consisting of a 1:1 mixture of 5%(v/v) foetal calf serum and 5% (v/v) sheep serum, and was carried out for 1 hour.

Modifications were also made in the use of the primary and secondary antibodies. In the first modification the nitrocellulose paper was shaken with the primary antibody overnight instead of for 2 hours. In the second modification, anti-mouse Ig G alkaline phosphatase conjugate raised in sheep was used instead of the horseradish peroxidase conjugate. The substrate mixture used for the detection of alkaline phosphatase consisted of 33µl of 50mg ml-1 5-bromo-4-chloro-3-indolyl phosphate(BCIP) and 44 µl of 75 mg ml -1 nitroblue tetrazolium (NBT) in 20 ml substrate buffer (0.75M Tris pH 8.5). Both the BCIP and NBT were dissolved in dimethylformamide (DMF). Colour development can again take between 30 minutes and 2 hours.

11.13.1 *Investigation into the distribution of TG2*

The results obtained from the adapted method from that published by Cassab and Vaner (1989), app.107, produced a visual indication to the TG2 content of sprouting and non-sprouting eyes in the tubers.

From app. 107, using no anti-body displayed a higher content of TG2

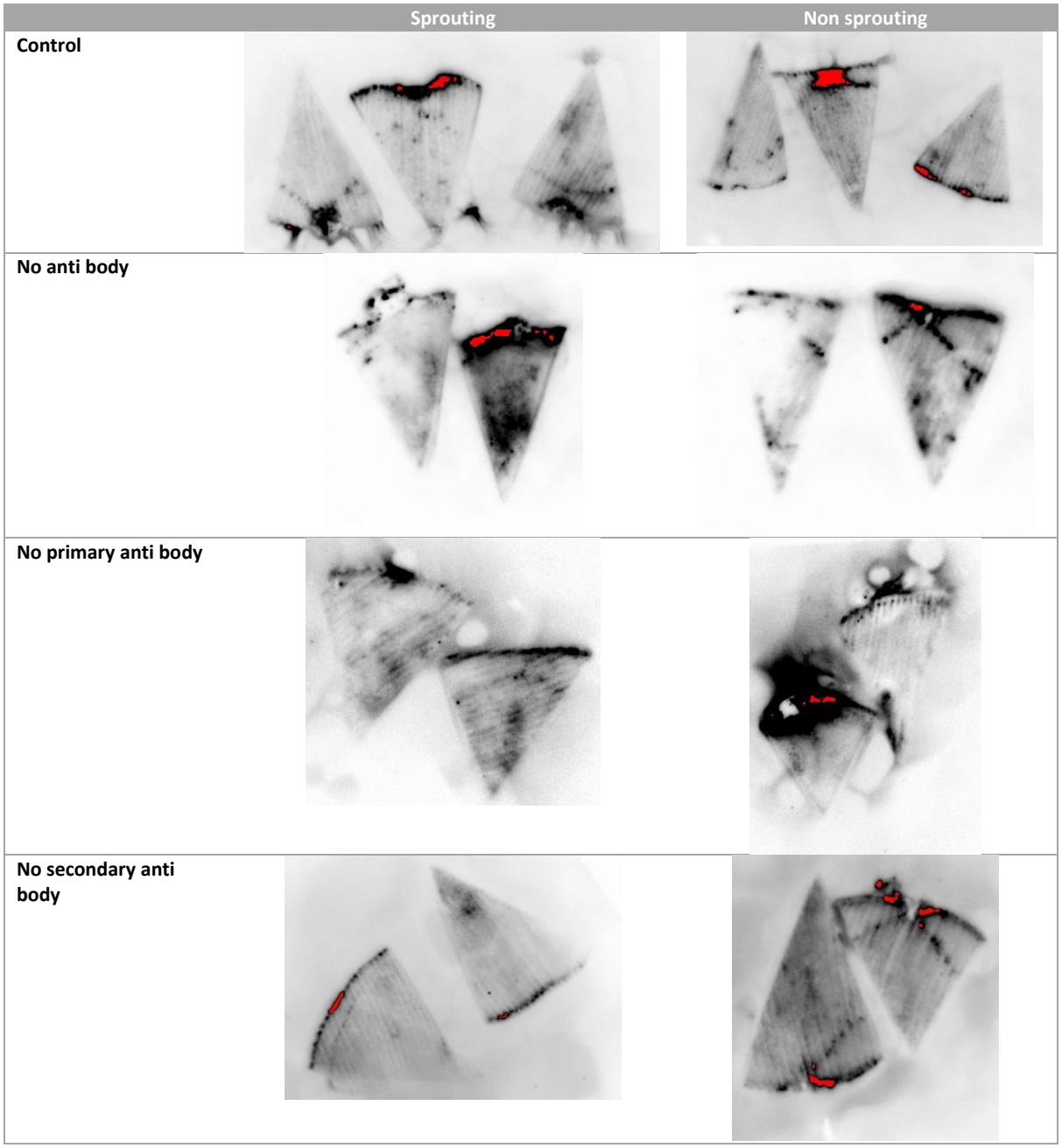

App. 107 Results from pressure transfer technique

Transglutaminases (TGases; EC 2.3.2.13) are a family of enzymes that catalyse the posttranslational modification of proteins by inserting an isopeptide bond within or between the polypep- tide chains (Chen and Mehta, 1999). When Ca^{2+} is ¯present an exchange of primary amine either a protein-bound lysine residue or other polyamine molecules, for ammonia at the g-carboxamide group of glutamine residues (Chen and Mehta, 1999, Pietsch et al., 2013).

Although there are a number of different transglutaminases, transglutaminase 2 (TG2), responsible for cell death and cell differentiation, matrix stabilization and an adhesion protein was investigated in the role of sprouting in potatoes (Griffin et al., 2002).
Higher the concentration of TG2 the darker the grey scale. Red areas indicate saturation. The control samples indicate clearly the areas of the sprout, periderm, cortex and vascular ring. More specific blocking is required to accurately detect TG2 activity.

Due to time, manpower and budget constraints, the investigation into the suppression of MONP fortified tubers effect on TG2 and sprouting was not carried out.

12 References

Abadía, J., Vázquez, S., Rellán-Álvarez, R., El-Jendoubi, H., Abadía, A., Álvarez-Fernández, A.,López-Millán.A.F., (2011) Towards a knowledge-based correction of iron chlorosis. *Plant Physiology and Biochemistry.* 49 (5), 471-482.

Abdelwahed, W., Degobert, G., Stainmesse, S. and Fessi, H., (2006) Freeze-drying of nanoparticles: Formulation, process and storage considerations. *Advanced Drug Delivery Reviews.* 58 (15), 1688-1713.

Adams, S.R., Cockshull, K.E., Cave, C.R.J., (2001) Effect of Temperature on the Growth and Development of Tomato Fruits. *Annals of Botany.* 88 (5), 869-877.

AHDB, 2013. Managing the Risk of Blackleg and Soft Rot. Stoneleigh Park, Kenilworth, CV8 TL, UK.

Akbar, A., and Anal, A.K., (2014) Zinc oxide nanoparticles loaded active packaging, a challenge study against Salmonella typhimurium and Staphylococcus aureus in ready-to-eat poultry meat. *Food Control.* 38, 88-95.

Akhter, P., Mohammad, D., Orfi, S. D., Ahmad, N., Rehman, K., (2005) Assessment of daily iron intake for the Pakistani population. *Journal of Nutritional and Food Science*. 35, 109–117.

Albornoz, C., Jacobo, S. E., (2006) *Preparation of a biocompatible magnetic film from an aqueous ferrofluid*. *Journal of Magnetism and Magnetic Materials.* 305, 12–15.

Alloway, B. J., Zhang, P., Mott, C., Smith, S. R., Chambers, B. J., Nicholson, F. A., Calton-Smith, C., Andrews A. J. (2000) The vulnerability of soils to pollution by heavy metals (Final Report for MAFF Project No. SP0127), London: MAFF.

Amin, M. T., Alazba, A. A., Manzoor, U., (2014) A Review of Removal of Pollutants from Water/Wastewater Using Different Types of Nanomaterials. *Advances in Materials Science and Engineering*. 825910, 1-24.

Aparicio-Caamaño, M., Carrillo-Morales, M., Olivares-Trejo, J.J., (2016) Iron Oxide Nanoparticle Improves the Antibacterial Activity of Erythromycin. *Journal of Bacterial Parasitology.* 7(2).

Arakha, M., Pal, S., Samantarri, D., Panigrahi, T.K., Mallick, B.C., Pramanik, K., Mallick, B., Jha, S., (2015) Antimicrobial activity of iron oxide nanoparticle upon modulation of nanoparticle-bacteria interface. *Scientific Reports.* 5, 14813.

Arora, R., Gill, N.S., Rana, A.C., (2011) An Overview about the Versatile Molecule Capsaicin. *International Journal of Pharmaceutical Sciences and Drug Research*. 3, 280-286.

Arora, R., Gill, N.S., Rana, A.C., 2011. An Overview about the Versatile Molecule Capsaicin. International. *Journal of Pharmaceutical Sciences and Drug Researc*h. 3, 280-286.

Arrowsmith, S., Egan, T.P., Meekins, J.F., Powers, D., Metcalfe, M., 2012. Effects of salt stress on capsaicin content, growth, and fluorescence in a Jalapeño cultivar of Capsicum annuum (*Solanaceae*) BioOne. 83 (1), 1-7.

Babu, K. S., Reddy, A. R., Sujatha, C., Reddy, K. V., Mallika, A. N., (2013) Synthesis and optical characterization of porous ZnO. *Journal of Advances Ceraminc,* 2 (3), 260-265.

Balarajan, Y., Ramakrishnan, U., Ozaltin, E., Shankar, A. H., Subramanian, S. V., (2011) Anaemia in low-income and middle-income countries. *Lancet*. 378, 2123–2135.

Balch, P. A., Balch, J. F., (2000) Prescription for Nutritional Healing. 3rd Edition. Avery, New York.

Barber, S.A., (1984) Soil nutrient bioavailability. A mechanistic approach. John Wiley and Sons, New York.

Barras, F., van Gijsegem, F., Chatterjee, A.K., (1994) Extracellular enzymes and pathogenesis of soft-rot Erwinia. *Annual Review of Phytopathology* 32, 201–34.

Bartz, J., (1999) Suppression of bacterial soft rot in potato tubers by application of kasugamycin. *American Journal of Potato Research*. 76, 127–36.

Basak, S., Chen, D.-. and Biswas, P., (2007) Electrospray of ionic precursor solutions to synthesize iron oxide nanoparticles: Modified scaling law. *Chemical Engineering Science.* 62 (4), 1263-1268.

Baumgartner, R., Eitzlmayr, A., Matsko, N., Tetyczka, C., Khinast, J. and Roblegg, E., (2014) Nano-extrusion: A promising tool for continuous manufacturing of solid nano-formulations. *International Journal of Pharmaceutics,* 477 (1), 1-11.

Bee, A., Massart, R., Neveu, S., (1995) Synthesis of very fine maghemite particles. *Journal of Magnetism and Magnetic Materials*.149 (1), 6-9.

Bouis, H.E., (2000) Enrichment of food staples through plant breeding: a new strategy for fighting micronutrient malnutrition. *Nutrition* 16, 701–4.

Bouis, H.E., (2003) Micronutrient fortification of plants through plant breeding: Can it improve nutrition in man at low cost? *Proceedings of the Nation Academy of Sciences: USA.* 62, 403–11.

Bouis, H.E., Hotz, C., McClafferty, B., Meenakshi, J.V., Pfeiffer, W.H., (2011) Biofortification: A new tool to reduce micronutrient malnutrition. *Food and Nutrition Bulletin.* 32, S31-S40.

Boxma, R., De Groot., A.J., (1971) Behaviour of iron and manganese chelates in calcareous soils and their effectiveness for plants. *Plant and Soil.* 34, 741-749.

Bradfield, S.J., Kumar, P., White, J.C., Ebbs, S.D., (2017) Zinc, copper, or cerium accumulation from metal oxide nanoparticles or ions in sweet potato: Yield effects and projected dietary intake from consumption. *Plant Physiology and Biochemistry.* 110, 128-137.

Brayner, R., Ferrari-lliou, R., Brivois, N., Djediat, S., Benedetti, M. F., Fie´vet, F., (2006) Toxicological Impact studies based on *Escherichia coli* bacteria in Ultrafine ZnO nanoparticles colloidal medium. *Nano Letters.* 6, 866–870.

Breitman, P. L., Fonseca, D., Cheung, A. M., Ward, W. E., (2003) Isoflavones with supplemental calcium provide greater protection against the loss of bonemass and strength after ovariectomy compared to isoflavones alone. *Bone.* 33(4), 597–605.

Bressy, F.C., Brito, G.B., Barbosa, I.S., Teixeira, L.S.G. and Korn, M.G.A., (2013) Determination of trace element concentrations in tomato samples at different stages of maturation by ICP OES and ICP-MS following microwave-assisted digestion. *Microchemical Journal,* 109 (0), 145-149.

Broadley, M.R., White, P.J., Hammond, J.P., Zelko, I., Lux, A., (2007). Zinc in plants. *New Phytologist.* 173 (6), 77-702.

Busse, J.S., Palta, J.P., (2006) Investigating the in vivo calcium transport path to developing tuber using ^{45}Ca: a new concept in potato tuber calcium nutrition. *Physiologia Plantarum.* 128, 313–323.

Camire, M.E., Kubow, S., Donnelly, D., (2009) Potatoes and Human Health. *Ritical Reviews in Food Science and Nutrition.* 49 (10), 823-840.

Candeia, R.A., Bernardi, M.I.B., Longo, E., Santos, I.M.G. and Souza, A.G., (2004) Synthesis and characterization of spinel pigment $CaFe_2O_4$ obtained by the polymeric precursor method. *Materials Letters.* 58 (5), 569-572.

Carmel, N., Tel-Or, E., Chen, Y. and Pick, U., (2014) Iron uptake mechanism in the chrysophyte microalga Dinobryon. *Journal of Plant Physiology.* 171 (12), 993-997.

Carvalho, M.D., Henriques, F., Ferreira, L.P., Godinho, M. and Cruz, M.M., (2013) Iron oxide nanoparticles: The Influence of synthesis method and size on composition and magnetic properties. *Journal of Solid State Chemistry.* 201, 144-152.

Carvalho, S.M.P., Vasconcelos, M.W., (2013) Producing more with less: strategies and novel technologies for plant-based food biofortification. *Food Research International.* 54, 961–971 10.1016/j.foodres.2012.12.021.

Caspell, N., Drakes, D., O'Neill,T., (2006) Pesticide residue minimization crop guide; tomatoes. *Food Standards Agency*. ADAS.

Cassab, G.I. and Varner, J.E., (1989) Tissue printing on nitrocellulose paper: a new method for immunolocalization of proteins, localization of enzyme activities and anatomical analysis, in Cytochemical and Immunological Approaches to Plant Cell Biology, (Vigil, E.L.and Hawes C (Edrs.), *Academic Press Ltd*., London, 147-152.

Chand V., Prasad S., (2013) ICP-OES assessment of heavy metal contamination in tropical marine sediments: A comparative study of two digestion techniques. *Microchemical Journal*. 111, 53-61.

Chatterjee, C., Gopal, R., Dube, B.K., (2006) Impact of iron stress on biomass, yield, metabolism and quality of potato (Solanum tuberosum L.). *Scientia Horticulturae,* 108 (1), 1-6.

Chatterjee, J., Haik, Y. and Chen, C., (2003) Size dependent magnetic properties of iron oxide nanoparticles. *Journal of Magnetism and Magnetic Materials.* 257 (1), 113-118.

Chen, J.S.K., and Mehta, K., (1999) Tissue transglutaminase: an enzyme with a split personality. *The International Journal of Biochemistry & Cell Biology,* 31 (8), 817-836.

Chin, A.B., Yaacob, I.I., (2007) Synthesis and characterization of magnetic iron oxide nanoparticles via w/o microemulsion and Massart's procedure. *Journal of materials processing technology* 191.1 (2007), 235-237.

Christinal, V., Tholkkappian, P., (2013) Interaction effects of AM fungi with Rhizobacteria and Phosphate solubilizing bacteria on the growth and nutrient uptake of chilli. *Journal of Applicable Chemistry*. 2, 33-41.

Chugh, V., and Dhaliwal, H.S., (2013) Chapter 9 - Biofortification of Staple Crops. *In:* G.S. Bhullar, and N.K. Bhullar, eds., *Agricultural Sustainability.* San Diego: *Academic Press.* 2013, 177-196.

CIP, (2017) Potato Facts and Figures [online]. CIP (International Potato Center). Available at: https://cipotato.org/potato2017].

Clemens, S., (2014) Zn and Fe biofortification: The right chemical environment for human bioavailability. *Plant Science.* 225 (0), 52-57.

Colangelo, E.P., Guerinot, M.L., (2006) Put the metal to the petal: metal uptake and transport throughout plants. *Current Opinion in Plant Biology*. 9, 322-330.

Cole, L., Kramer, P.R., (2016) Chapter 5.2 - Vitamins and Minerals. *In:* L. Cole, and P.R. Kramer, eds., *Human Physiology, Biochemistry and Basic Medicine.* Boston: Academic Press. 165-175.

Collins, M.D., Wasmund, L.M., Bosland, P.W., (1995). Improved method for quantifying capsaicinoids in Capsicum using high-performance liquid chromatography. *Hortscience.* 30 (1), 137-139.

Corradini, E., de Moura, M.R. and Mattoso, L.H.C., (2010) A preliminary study of the incorparation of NPK fertilizer into chitosan nanoparticles. *Express Polymer Letters.* 4 (8), 509-515.

Cruz-Rus, E., Amaya, I., Valpuesta, V., (2012). The challenge of increasing vitamin C content in plant foods. *Biotechnology Journal* 7, 1110-1121.

Czajkowski, R., Pérombelon, M.C. M., van Veen, J.A., van der Wolf, J.M., (2011) Control of blackleg and tuber soft rot of potato caused by *Pectobacterium* and *Dickeya* species: a review. *Plant Pathology.* 60, 999-1013.

D'Imperio, M., Renna, M., Cardinali, A., Buttaro, D., Serio, F., Santamaria, P., (2016) Calcium bofortification and bioaccessibility in soilless "baby leaf" vegetable production. *Food Chemistry.* 213, 149-156.

Darroudi, M., Bagherpour, M., Hosseini, H.A. and Ebrahimi, M., (2016) Biopolymer-assisted green synthesis and characterization of calcium hydroxide nanoparticles. *Ceramics International.* 42 (3), 3816-3819.

De Boer, S.H., (2002) Relative incidence of *Erwinia carotovora subsp*. atroseptica in stolon end and peridermal tissue of potato tubers in Canada. *Plant Disease.* 86, 960-964.

de Caprariis, B., Di Rita, M., Stoller, M., Verdone, N., Chianese, A., (2012) Reaction-precipitation by a spinning disc reactor: Influence of hydrodynamics on nanoparticles production. *Chemical Engineering Science.* 76 (0), 73-80.

Deal, C.L., Schnitzer, T.J, Lipstein, E., Seibold, J.R., Stevens, R.M., Levy, M.D., Albert, D., Renold, F., (1999) Treatment of arthritis with topical capsaicin: A double-blind trial. *Clinical Therapeutics*. 13, 383-395.

Deal, C.L., Schnitzer, T.J., Lipstein, E., Seibold, J.R., Stevens, R.W., Levy, M.D., Albert, D., Renold, F., (1999) Treatment of arthritis with topical capsaicin: A double-blind trial. *Clinical Therapeutics.* (13), 383-395.

DellaValle, D.M., Thavarajah, D., Thavarajah, P., Vandenberg, A., Glahn, R.P., (2013) Lentil (*Lens culinaris L*.) as a candidate crop for iron biofortification: Is there genetic potential for iron bioavailability? *Field Crops Research.* 144 (0), 119-125.

Ebbs, S.D., Bradfield, S., Kumar, P., Musante, C., White, J.C., Ma, X., (2016) Accumulation of zinc, copper, or cerium in carrot (*Daucus carota*) exposed to metal oxide nanoparticles and metal ions. *Environmental Science.Nano.* 3, 114–126.

Eide, D., Broderius, M., Fett, J., Guerinot, M. L., (1996) A novel iron-regulated metal transporter from plants identified by functional expression in yeast. *Proceedings of the National Academy of Sciences of the United States of America. 93*(11), 5624–5628.

Ejrari, A., (2013) Determination optimum concentration of iron in hydroponic medium of Tomato (*Lycopersicom esculentum*). *Journal of Novel Applied Sciences.* 2, 856-860.

El-Jendoubi, H., Vázquez, S., Calatayud, Á., Vavpetič, P., Vogel-Mikuš, K., Pelicon, P., Abadía, J., Abadía, A., Morales, F., (2014) The effects of foliar fertilization with iron sulfate in chlorotic leaves are limited to the treated area. A study with peach trees (*Prunus persica* L. Batsch) grown in the field and sugar beet (*Beta vulgaris* L.) grown in hydroponics. *Frontiers in Plant Science*. 5(2). doi:10.3389/fpls.2014.00002.

El-Jendoubi, H., Vázquez, S., Calatayud, Á., Vavpetič, P., Vogel-Mikuš, K., Pelicon, P., Abadía, J., Abadía, A., Morales, F., (2014) The effects of foliar fertilization with iron sulfate in chlorotic leaves are limited to the treated area. A study with peach trees (*Prunus persica* L. Batsch) grown in the field and sugar beet (*Beta vulgaris* L.) grown in hydroponics. *Frontiers in Plant Science*. 5 (2). doi:10.3389/fpls.2014.00002.

Estrada, A.B., Pomar, F., Díaz, J., Merino, F., Bernal, A., (1999) Pungency level in fruits of Padrón pepper with different water supply. *Scientia Horticultrae.* 81, 385–396.

Evans, L. J., (1989) Chemistry of metal retention by Soils. *Environmental Science & Technology.* 23 (9), 1046-1056. DOI: 10.1021/es00067a001

Fan, M.S., Zhao, F.J., Fairweather-Tait, S.J., Poulton, P.R., Dunham, S.J., McGrath, S.P., (2008) Evidence of decreasing mineral density in wheat grain over the last 160 years. *Journal of Trace Elements in Medicine and Biology*. 2 (2), 315-324.

FAO (Food and Agriculture Organization of the United Nations), (2016). *Statistics* [online]. Available at: http://www.fao.org/faostat/en/#data/QC2017].

FAO, (1996) Report of the World Food Summit. FAO, Rome.

FAO, (2014) FAOSTAT. Food and Agriculture Organization of the United Nations.

Fernández, V., Georg Ebert, G. (2005) Foliar Iron Fertilization: A Critical Review. *Journal of Plant Nutrition*, 28 (12) 2113-2124.

Fernández, V., Georg Ebert, G., (2005) Foliar Iron Fertilization: A Critical Review. *Journal of Plant Nutrition*. 28 (12), 2113-2124.

Fischer, W., André, B., Rentsch, D., Krolkiewicz, S., Tegeder, M., Breitkreuz, K., Frommer, W.B., (1998) Amino acid transport in plants. *Trends in Plant Science.* 3 (5), 188-195.

Fleischer, A., O'Neill, M.A., Ehwald, R., (1999) The pore size of nongraminaceous plant cell walls is rapidly decreased by borate ester cross-linking of the pectic polysaccharide rhamnogalacturonan II. *Plant Physiology.* 121, 829-838.

Frary, A., Frary, A., (2012) Physiology of Metabolites, In: Russo, V. (Ed.), Peppers: Botany, Production and Uses. *CABI*.176-188.

Frossard, E., Bucher, M., Miichler, F., Mozafar, A., Hurrell, R., (2000) Potential for increasing the content and bioavailability of Fe, Zn and Ca in plants for human nutrition. *Journal of the Science*. 861-879

Garaud, M., Trapp, J., Devin, S., Cossu-Leguille, C., Pain-Devin, S., Felten, V., Giamberini, L., (2015) Multibiomarker assessment of cerium dioxide nanoparticle ($nCeO_2$) sublethal effects on two freshwater invertebrates, *Dreissena polymorpha* and *Gammarus roeseli*. *Aquatic Toxicology.* 158 (0), 63-74.

Genet, R.A., (1992) Potatoes - the quest for processing quality. *Proceedings Agronomy Society of New Zealand.* 22.

Ghasemi, S., Khoshgoftarmanesh, A.H., Hadadzadeh, H., (2012) Synthesis of iron-amino acid chelates and evaluation of their efficacy as iron source and growth stimulator for tomato in nutrient solution culture. *Journal of Plant Growth Regulators.* 31 (4), 498-508.

Gnzález-Zamora, A., Sierra-Campos, E., Luna-Ortega, G., Pérez-Morales, R., Ortiz, J.C.R., García-Hernández, J.L., (2013) Characterization of Different Capsicum Varieties by Evaluation of Their Capsaicinoids Content by High Performance Liquid Chromatography, Determination of Pungency and Effect of High Temperature. *Molecules*. 18, 13471-13486.

González-Zamora, A., Sierra-Campos, E., Luna-Ortega, J.G., Pérez-Morales, R., Ortiz, J.C.R., García-Hernández, J.L., (2013) Characterization of Different Capsicum Varieties by Evaluation of Their Capsaicinoids Content by High Performance Liquid Chromatography, Determination of Pungency and Effect of High Temperature. *Molecules*. 18, 13471-13486.

Gray, D., Hughes, J.C., (1978) Tuber quality. In: The Potato Crop- the Scientific Basis for improvement, (ed. P.J. Harris). *Chapman and Hall, London*. 504-544.

Gregory, P.J., Ingram, J.S.I., Brklacich, M., (2005) Climate change and food security. *Philosophical Transactions of the Royal Society B: Biological Sciences.* 360, 2139-2148.

Griffin, M., Casadio, R., Bergaminil, C., (2002) Transglutaminases: Nature's biological glues. *Biochemical Journal.* 368 (2), 377-396

Grotz, N., Guerinot, M.L., (2006) Molecular aspects of Cu, Fe and Zn homeostasis in plants. *Biochimica et Biophysica Acta.* 1763, 595-608.

Grusak, M.A., Dellapenna, D., (1999) Improving the nutrient composition of plants to enhance human nutrition and health. *Annual Review of Plant Physiology and Plant Molecular Biology*. 50, 133-161.DOI: 10.1146/annurev.arplant.50.1.133

Grusak., M.A., Cakmak, I., (2005) Methods to improve the crop-delivery of minerals to humans and livestock. In: Broadly MR, White PJ, eds. Plant nutritional genomics. *Oxford, UK; Blackwell*. 265-286.

Guerinot, M.L., (2000) The ZIP family of metal transporters. *Biochimica Et Biophysica Acta (BBA) – Biomembrane.* 1465 (1), 190-198.

Gupta, U.C., Gupta, S.C., (2014) Sources and Deficiency Diseases of Mineral Nutrients in Human Health and Nutrition: A Review. *Pedosphere.* 24 (1), 13-38.

Hasany, S.F., Ahmed, I. and Rajan, J.A., (2012) Systematic Review of the Preparation Techniques of Iron Oxide Magnetic Nanoparticles. *Nanoscience and Nanotechnology.* 2 (6), 148-158.

Hinsinger, P., (1998) How Do Plant Roots Acquire Mineral Nutrients? Chemical Processes Involved in the Rhizosphere. *Advances in Agronomy.* 64, 225-265.

Hirschi, K.D., (2004) The Calcium conundrum. Both versatile nutrient and specific signal. *Plant Physiology*. 136(1), 2438-2442. doi:10.1104/pp.104.046490.

Hirschi, K.D., (2009) Nutrient biofortification of food crops. *Annual Review of Nutrition.* 29, 401–21.

Ho, L. C., Grange, R. I., Picken, A. J., (1987) An analysis of the accumulation of water and dry matter in tomato fruit. *Plant, Cell & Environment.* 10, 157–162. doi:10.1111/1365-3040.ep11602110

Hotz, C., Brown, K.H., (eds) (2004) Assessment of the Risk of Zinc Deficiency in Populations and Options for its Control. *Food and Nutrition Bulletin*. 25 (Supplement 2), S91-S204.

Hurd, R.G., Graves, C.J., (1985) Some effects of air and root temperatures on the yield and quality of glasshouse tomatoes. *Journal of Horticultural Science.* 60, 359-371.

Hwang, C., Wu, T., Wan, J., Tsai, J., (2004) Development of a novel combustion synthesis method for synthesizing of ceramic oxide powders. *Materials Science and Engineering: B.* 111 (1), 49-56.

Islam, M.A., Sharma, S.S., Sinha, P., Negi, M.S., Neog, B., Tripathi, S.B., (2015) Variability in capsaicinoid content in different landraces of Capsicum cultivated in north-eastern India. *Scientia Horticulturae.* 183, 66-71.

Jarrell, W. M., Beverly, R.B., (1981) The dilution effect in plant nutrition studies. *Advances in Agronomy.* 3 (4), 197-224.

Johnson, D. A., ed., (2008) Potato Health Management, 2nd ed., *American Phytopathological Society, St. Paul*, MN.

Kabata-Pendias, A., (2010) Trace elements in soils and plants. 4th ed. *Boca Raton, FL: CRC Press* (Taylor Francis Group).

Kalpana Sastry, R., Anshul, S., Rao, N.H., (2013) Nanotechnology in food processing sector-An assessment of emerging trends. *Journal of Food Science and Technology.* 50 (5), 831-84

Kalpana Sastry, R., Rashmi, H.B., Rao, N.H., (2011) Nanotechnology for enhancing food security in India. *Food Policy.* 36 (3), 391-400.

Karley, A.J., White, P.J., (2009) Moving cationic minerals to edible tissues: potassium, magnesium, calcium. *Current Opinion in Plant Biology.*12, 291–298.

Kasar, S,D., Jagtap, P.B., Kolape, S.S., Nimbalkar, C.A., Gaikwad, SP., (2010) Effect of application of humic acid and FYM on nutrient uptake, yield and quality of chilli. *Journal of Maharashtra Agricultural Universities*. 35, 187-194.

Kassaee, M. Z., Masrouri, H., Movahedi, F., (2011) Sulfamic acid-functionalized magnetic Fe_3O_4nanoparticles as an efficient and reusable catalyst for one-pot synthesis of α-amino nitriles in water. *Applied Catalysis A: General.* 395, 28-33.

Kaya, C., Higgs, D., (2002) Response of tomato (*Lycopersicon esculentum L.*) cultivars to foliar application of zinc when grown in sand culture at low zinc. *Scientia Horticulturae.* 93 (1), 53-64.

Kehie, M., Kumaria, S., Tandon, P., (2013) Manipulation of culture strategies to enhance capsaicin biosynthesis in suspension and immobilized cell cultures of Capsicum chinense Jacq. cv. Naga King Chili. *Bioprocess and Biosystems Engineering*. 37(6), 1055-63.

Kehie, M., Kumaria, S., Tandon, P., (2013) Manipulation of culture strategies to enhance capsaicin biosynthesis in suspension and immobilized cell cultures *of Capsicum chinense Jacq. cv.* Naga King Chili. *Bioprocess and Biosystems Engineering*. 37 (6), 1055-63.

Kelling, K.A., Schilte, E.E., (2008). A2523: Soil and applied calcium. *Understanding plant nutrients* (08). University of Wisconsin – Cooperative Extension.

Khalil, M.I., (2015) Co-precipitation in aqueous solution synthesis of magnetite nanoparticles using iron (III) salts as precursors. *Arabian Journal of Chemistry.* 8 (2), 279-284.

Khanna, L., Verma, N. K. (2013b). PEG/CaFe2O4 nanocomposite: Structural, morphological, magnetic and thermal analyses. *Physica B: Condensed Matter.* 427, 68–75.

Khanna, L., Verma, N.K., (2013) Size-dependent magnetic properties of calcium ferrite nanoparticles. *Journal of Magnetism and Magnetic Materials,* 336, 1-7.

Khot, L.R., Sankaran, S., Maja, J.M., Ehsani, R., Schuster, E.W., (2012) Applications of nanomaterials in agricultural production and crop protection: A review. *Crop Protection.* 35 (0), 64-70.

Kiekens L., (1995) Zinc in Heavy Metals. In B.J. Alloway (Ed.). Soils. London: Blackie Academic and Professional.

Kim, E.H., Lee, H.S., Kwak, B.K., Kim, B.K., (2005) Synthesis of ferrofluid with magnetic nanoparticles by sonochemical method for MRI contrast agent. *Journal of Magnetic Material.* 289, 328-330

Kim, S.A., Guerinot, M.L., (2007) Mining iron: Iron uptake and transport in plants. *FEBS Letters.* 581 (12), 2273-2280.

Kimata, M., Nakagawa, D., Hasegawa, M., (2003) Preparation of monodisperse magnetic particles by hydrolysis of iron alkoxide. *Powder Technology. 132*, *112–118*.

Kirby, E.A., Pilbeam, D.J., (1984) Calcium as a plant nutrient. *Plant Cell Environment.* 7, 397–405.

Kolbe, H., Stephan-Beckmann, S., (1997) Development, growth and chemical composition of the potato crop (*solanum tuberosum L.*). II. Tuber and whole plant. *Potato Research.* 40 (2), 135-153.

La Fontaine, S., Quinn J.M., Nakamoto S.S., Page M.D., Göhre V., Moseley J.L., (2002) Copper-dependent iron assimilation pathway in the model photosynthetic eukaryote *Chlamydomonas reinhardtii Eukaryot Cell.* 1. 736–757.

Lane, N., Kalil, T., (2005) The national nanotechnology initiative: present at the creation. *Issues Science Technology.* 21(4), 49–54.

Laurent, S., Forge, D., Port, M., Roch, A.C., Vander Elst, L., Muller, R., (2008) Magnetic Iron Oxide Nanoparticles: Synthesis, Stabilization, Vectorization, Physicochemical Characterizations, and Biological Applications. *Chemical Review.* 108 (6), 2064-2110.

Lemaga, B., Caesar, K., (1990) Relationships between numbers of main stems and yield components of potato (*Solanum tuberosum L*. cv. Erntestolz) as influenced by different daylengths. *Potato Research.* 33, 257. doi:10.1007/BF02358455

Lin, D., Xing, B., (2007) Phytotoxicity of nanoparticles: Inhibition of seed germination and root growth. *Environmental Pollution.* 150 (2), 243-250.

Lisinska, G., Leszczynski, W., (1989) Potato Science and Technology. London, New York: *Elsevier Applied Science Publishers Ltd*. 41-45.

Liu, T., Zhu, Y., Zhang, X., Zhang, T., Zhang, T., Li, X., (2010) Synthesis and characterization of calcium hydroxide nanoparticles by hydrogen plasma-metal reaction method. *Materials Letters.* 64 (23), 2575-2577.

Liu, Y., Fu, R., Sun, Y., Zhou, X., Baig, S.A., Xu, X., (2016) Multifunctional nanocomposites Fe_3O_4@SiO_2-EDTA for Pb(II) and Cu(II) removal from aqueous solutions. *Applied Surface Science.* 369, 267-276.

Livage, J., Sanchez, C., Henry, M., Doeuff, S., (1989) The chemistry of the sol-gel process. *Solid State Ionics.* 32–33, Part 2, 633-638.

Loladze, I., (2002) Rising atmospheric CO_2 and human nutrition: toward globally imbalanced plant stoichiometry. *Trends in Ecology and Evolution.* 17, 457-461.

Long T, Yin S, Takabatake K, Zhnag P, Sato T., (2009) Synthesis and Characterization of ZnO Nanorods and Nanodisks from Zinc Chloride Aqueous Solution. *Nanoscale Research Letters.* 4 (3), 247-253.

Lonnerdal, B., (2003) Genetically modified plants for improved trace element nutrition. *Journal of Nutrition.* 133, 1490S–1493S.

López-Rayo, S., Nadal, P., Lucena, J.J., (2015) Reactivity and effectiveness of traditional and novel ligands for multi-micronutrient fertilization in a calcareous soil. *Frontiers in Plant Science*. 6 (752). doi:10.3389/fpls.2015.00752.

Lucena, J.J., (2006) Synthetic Iron Chelates to Correct Iron Deficiency in Plants. Iron Nutrition in Plants and Rhizospheric Microorganism, editors Barton, L.L., Abadía, J. *New York, NY: Kluwer Academic Publishers.* 103–128.

Lulai, E.C., Orr, P.H., (1979) Influence of potato specific gravity on yield and oil content of chips. *American Potato Journal.* 56, 379-391.

Luo, S., Zheng, X., Xu, H., Mi, X., Zhang, L., Cheng, J.-P. (2007) Magnetic Nanoparticle-Supported Morita–Baylis–Hillman Catalysts. *Advanced Synthesis and Catalysis*. 349, 2431–2434. doi:10.1002/adsc.200700318.

Luo, X., Peng J., Li, Y., (2011) Recent advances in the study on capsaicinoids and capsacinoids. *European Journal of Pharmacology.* 650, 1-7 DOI:http://dx.doi.org/10.1016/j.ejphar.2010.09.074)

Luo, X., Peng, J., Li, Y., (2011) Recent advances in the study on capsaicinoids and capsinoids. *European Journal of Pharmacology.,* 650, 1-7. DOI:http://dx.doi.org/10.1016/j.ejphar.2010.09.074.

Mäder, P., Fliessbach, A,. Dubois, D., Gunst, L., Fried, P., Niggli, U., (2002) Soil fertility and biodiversity in organic farming. *Science.* 296, 1694-1697.

Mamalis, A.G., (2007) Recent advances in nanotechnology. *Journal of Materials Processing Technology.* 181 (1), 52-58.

Marschner, H., (1993) Zinc Uptake from soils. In: Robson, A.D., Ed., Zinc in Soils and Plants. *Kluwer Academic Publishers, Dordrecht*. 59-78.

Marschner, H., (1995) Mineral nutrition of higher plants. *London, UK: Academic Press.*

Masuda, H., Ishimaru, Y., Aung, M.S., Kobayashi, T., Kakei, Y., Takahashi, M., (2012) Iron biofortification in rice by the introduction of multiple genes involved in iron nutrition. *Scientific Repots*. 2, 543. doi: 10.1038/srep00543.

Mayer, J.E., Pfeiffer, W.H., Beyer, P., (2008) Biofortified crops to alleviate micronutrient malnutrition. *Current Opinion in Plant Biology.* 11 (2), 166-170.

McGuire, R.G., Kelman, A., (1984) Reduced severity of Erwinia soft rot in potato tubers with increased calcium content. *Phytopathology.* 74, 1250-1256.

Mengel, K., Kirkby, E.A., Kosegarten, H., Appel, T., (2001) Principles of plant nutrition. *Dordrecht: Kluwer Academic.*

Miller, A.J., Shen, Q., Xu, G., (2009) Freeways in the plant: transporters for N, P and S and their regulation. *Current Opinion in Plant Biology*. 12, 284–290.

Mirghiasi, Z., Bakhtiari, F., Darezereshki, E. and Esmaeilzadeh, E., (2014) Preparation and characterization of CaO nanoparticles from Ca(OH)2 by direct thermal decomposition method. *Journal of Industrial and Engineering Chemistry.* 20 (1), 113-117.

Miwa, K., Kamiya, T., Fujiwara, T., (2009) Homeostasis of the structurally important micronutrients, B and Si. *Current Opinion in Plant Biology.* 12, 307–311.

Morrison, S.A., Cahill, C.L., Carpemter, E.E., Calvin, S., Swaminathan, R., (2004) Magnetic and structural properties of nickel zinc ferrite nanoparticles synthesized at room temperature. *Journal of Applied Physics.* 95 (11), 6392-6395.

Mousavi, S.R., (2011) Zinc in crop production and interaction with phosphorus. *Australian Journal of Basic and Applied Sciences.* 5 (9), 1503-1509.

Nair, R., Varghese, S.H., Nair, B.G., Maekawa, T., Yoshida, Y., Kumar, D.S., (2010) Nanoparticulate material delivery to plants. *Plant Science.* 179 (3), 154-163. DOI:http://dx.doi.org/10.1016/j.plantsci.2010.04.012

Naqvi, S., Zhu, C., Farre, G., Ramessar, K., Bassie, L., Breitenbach, J., (2009) Transgenic multivitamin corn through biofortification of endosperm with three vitamins representing three distinct metabolic pathways. *Proceeding of the National Academy of Sciences*; *U.S.A*. 106, 7762–7767.

Navarro, E., Baun, A., Behra, R., Hartmann, N.B., Filser, J., Miao, A., Quigg, A., Santschi, P.H., Sigg, L., (2008) Environmental behaviour and ecotoxicity of engineered nanoparticles to algae, plants, and fungi. *Ecotoxicology.* 17 (5), 372-86.

Navrot, J., Banin, A., (1975) Tomato plant response to iron supply in various carrier forms. *Plant and Soil.* 42, 309-312.

Nel, A., Xia, T., Madler, L., Li, N., (2006) Toxic potential of materials at the nanolevel. *Science.* 311 (5761) 622-627.

Ngadze, E., Coutinho, T.A., Icishahayo, D., van der Waals, J.E., (2014) Effect of calcium soil amendments on phenolic compounds and soft rot resistance in potato tubers. *Crop Protection.* 62, 40-45.

Oberdorster, G., Oberdorster, E., Oberdorster, J., (2005) Nanotoxicology: an emerging discipline evolving from studies of ultrafine particles. *Environmental Health Prospectives.* 113, 823–1. 839

Obidiegwu, J.E., Bryan, G.J., Jones, H.G., Prasher, A., (2015) Coping with drought stress and adaptive responses in potato and perspectives for improvement. *Frontiers in Plant Science.* 6.

Ortiz-Lopez, A., Chang, H., Bush, D.R., (2000) Amino acid transporters in plants. *Biochimica Et Biophysica Acta (BBA) – Biomembranes.* 1465 (1–2), 275-280.

Othman, Z.A.A., Ahmed, Y.B.H., Habila, M.A., Ghafar, A., (2011) Determination of capsaicin and dihydrocapsaicin in Capsicum fruit samples using high performance liquid chromatography. *Molecules.* 16 (10), 8919-8929.

Othman, Z.A.A., Ahmed, Y.B.H., Habila, M.A., Ghafar, A.A., (2001) Determination of Capsaicin and Dihydrocapsaicin in Capsicum Fruit Samples using High Performance Liquid Chromatography *Molecules.* 16, 8919-8929.

Oviedo, C., Rodríguez, J. (2003) EDTA: The chelating agent under environmental scrutiny. *Química Nova*. 26 (6), 901-905. https://dx.doi.org/10.1590/S0100-40422003000600020

Paesano, R., Berlutti, F., Pietropaoli, M., Pantanella, F., Pacifici, E., Goolsbee W., Valenti, P., (2010) Lactoferrin efficacy versus ferrous sulfate in curing iron deficiency and iron deficiency anaemia in pregnant women. *Biometals*. 23, 411– 417.

Pagel, W., Heitefuss, R., (1989) Calcium content and cell wall polygalacturonans in potato tubers of cultivars with different susceptibilities to Erwinia *carotovora subsp*. atroseptica. *Physiological and Molecular Plant Pathology.* 32, 11-21.

Painem, J.A., Shipton, C.A., Chaggar, S., Howells, R,M., Kennedy, M.J., Vernon, G., (2005) Improving the nutritional value of Golden Rice through increased pro-vitamin A content. *Nature Biotechnology.* 23, 482–7.

Palta, J.P., (2010) Improving Potato Tuber Quality and Production by Targeted Calcium Nutrition: The Discovery of Tuber Roots Leading to a New Concept in Potato Nutrition. *Potato Research.* 53, 267-275.

Parak, W.J., Simmel, F.C., Holleitner, A.W., (2008) Top-down versus bottom-up. *In:* Schmid, G., Frug, G., Waser, R., Vogel, V., Fuchs, H., Grätzel, M., Kalyanasundaram, K., Chi, L., ed., Nanotechnology. Volume1: Principles and fundamentals. 1st ed. *Weinheim: Wiley-VCH*, 41-48.

Patel, G., Pal, U., Menon, S., (2009) Removal of Fluoride from Aqueous Solution by CaO Nanoparticles. *Separation Science and Technology.* 44 (12), 2806-2826.

Pérombelon, M.C.M., Kelman, A., (1980) Ecology of soft rot Erwinias. *Annu. Rev. Phytopathol*. 18, 361-367.

Pietsch, M., Wodtke, R., Pietzsch, J., Löser, R., (2013) Tissue transglutaminase: An emerging target for therapy and imaging. *Bioorganic & Medicinal Chemistry Letters.* 23 (24), 6528-6543.

Pilbeam, D. J., Marley, P. S., (2006) Calcium. In A. V. Barker & D. J. Pilbeam (Eds.), Handbook of plant nutrition. *USA: CRC Press.* 121–144.

Pirouz, M.J., Beyki, M.H., Shemirani, F., (2015) Anhydride functionalised calcium ferrite nanoparticles: A new selective magnetic material for enrichment of lead ions from water and food samples. *Food Chemistry.* 170 (0), 131-137.

Potato Council, (2015) Potato Council (AHDB Potatoes) Yearbook, 2015. *AHDB*.

Prasad, P.V.V., Djanaguiraman, M., (2017) Iron Chlorosis. In: B. Thomas, B.G. Murray and D.J. Murphy, eds., Encyclopedia of Applied Plant Sciences (Second Edition). *Oxford: Academic Press.* 2017, 246-255.

Pritchard, M.K., Scanlon, M.G., (1997) Mapping dry matter and sugars in potato tubers for prediction of whole tuber process quality. *Canadian Journal of Plant Science.* 77, 461-467.

Prucek, R., Tuček, J., Kilianová, M., Panáček, A., Kvítek, L., Filip, J., Kolář, M., Tománková, K., Zbořil, R., (2011) The targeted antibacterial and antifungal properties of magnetic nanocomposite of iron oxide and silver nanoparticles. *Biomaterials.* 32 (21), 4704-13.

Puig, S., Peñarrubia, L., (2009) Placing metal micronutrients in context: transport and distribution in plants. *Current Opinion in Plant Biology.* 12, 299–306.

Rahman, M. J., Inden, H., (2012) Effect of nutrient solution and temperature on capsaicin content and yield contributing characteristics in six sweet pepper (*Capsicum annuum L.*) cultivars. *Journal of Food, Agriculture & Environment.* 10, 524-529.

Rahman, M.J., Inden, H., (2012) Effect of nutrient solution and temperature on capsaicin content and yield contributing characteristics in six sweet pepper (Capsicum annuum L.) cultivars. *Journal of Food, Agriculture & Environment.* 10, 524-529.

Ramimoghadam, D., Bagheri, S., Hamid, S.B.A., (2014) Progress in electrochemical synthesis of magnetic iron oxide nanoparticles. *Journal of Magnetism and Magnetic Materials.* 368 (0), 207-229.

Ramos, J.P., Fernandes, C.M., Stora, T., Senos, A.M.R., (2015) Sintering kinetics of nanometric calcium oxide in vacuum atmosphere. *Ceramics International.* 41 (6), 8093-8099.

Rana, S., Philip, J., Raj, B., (2010) Micelle based synthesis of cobalt ferrite nanoparticles and its characterization using Fourier transform infrared transmission spectrometry and thermogravimetry. *Materials Chemistry and Physics.* 124, 264–269.

Rao, N.S., Rao, M.V.B., (2015) Structural and Optical Investigation of ZnO Nanopowders Synthesized from Zinc Chloride and Zinc Nitrate. *American Journal of Materials Science.* 5 (3), 66-68.

Raven, J.A., (2013) Iron acquisition in stramenopile algae. *Journal of Experimental Botany*. 64 (2013), 2119–2127.

Reddy, B.V.S., Ramesh, S., Longvah, T., (2005) Prospects of breeding for micronutrients and P3-carotene-dense sorghums. *International Sorghum and Millets Newsletter.* 46, 10-14.

Reilly, C.A., Crouch, D.J., Yost, G.S. and Fatah, A.A., (2001) Determination of capsaicin, dihydrocapsaicin, and nonivamide in self-defense weapons by liquid chromatography–mass spectrometry and liquid chromatography–tandem mass spectrometry. *Journal of Chromatography A.* 912 (2), 259-267.

Roth, H., Schwaminger, S.P., Schindler, M., Wagner, F.E., Berensmeier, S., (2015) Influencing factors in the CO-precipitation process of superparamagnetic iron oxide nano particles: A model based study. *Journal of Magnetism and Magnetic Materials.* 377 (0), 81-89.

Rude, R.K., Gruber, H.E., 2004. Magnesium deficiency and unexpected role as osteoporosis: animal and human observations*. Journal of Nutritional Biochemistry*. 15, 710-716.

Ruiz-Lau, N., Medina-Lara, F., Minero-García, Y., Zamudio-Moreno, E., Guzmán-Antonio, A., Echevarría-Machado, I., Martínez-Estévez. M., (2011) Water Deficit Affects the Accumulation of Capsaicinoids in Fruits of Capsicum chinense Jacq. *HortScience*. 3, *487-492*.

Safaei-Ghomi, J., Ghasemzadeh, M.A., Mehrabi, M., (2013) Calcium oxide nanoparticles catalyzed one-step multicomponent synthesis of highly substituted pyridines in aqueous ethanol media. *Scientia Iranica.* 20 (3), 549-554.

Saigusa, M., (2000) Broadcast application versus application of polyefin-coated fertilizer on green peppers grown on andisol. *Journal of Plant Nutrition.* 23, 1485-1492.

Salisbury, F.B., Ross, C.W., (1991) Plant physiology. 4th ed. *Wadsworth*.

Saltzman, A., Birol, E., Bouis, H.E., Boy, E., De Moura, F.F., Islam, Y., Pfeiffer, W.H., (2013) Biofortification: Progress toward a more nourishing future. *Global Food Security.* 2 (1), 9-17.

Sánchez, A.S., Juárez, M., Sánchez-Andreu, J., Jordá, J., Bermúdez, D., (2005) Use of humic substances and amino acids to enhance iron availability for tomato plants from applications of the chelate FeEDDHA. *Journal of Plant Nutrition.* 28, 1877–1886.

Sardare, M.D., Admane, S.V., (2013) A review on plant without soil - Hydroponics. *International Journal of Research in Engineering and Technology.* 2 (3), 299-304.

Sawicka, B., Noaema, A.H., Hameed, T.S., Skiba, D., 2016. Genotype and environmental variability of chemical elements in potato tubers. *Acta Scientiarum Polonorum,* 15 (3), 79-91.

Schaider, L.A., Parker, D.R., Sedlak, D.L., (2006) Uptake of EDTA-complexed Pb, Cd and Fe by solution and sand cultured *Brassica juncea*. *Plant and Soil.* (1-2), 377-391.

Schmid, G., (2010) Nanoparticles: From theory to application. 2nd ed. *Weinheim: Wiley-VCH*.

Schöber, B.M., Vermeulen, T., (1999) The role of calcium and nitrogen in susceptibility to witloof for soft rot coliforms. European Journal of Plant Patholgy. 105, 341 – 49.

Schulte, E.E., (2008.) A3554: Soil and applied iron. *Understanding plant nutrients*. University of Wisconsin – Cooperative Extension.

Shenker, M., Chen, Y., (2005) Increasing iron availability to crops: fertilizers, organo-fertilizers and biological approaches. *Soil Science and Plant Nutrition.* 51 (1), 1-17.

Shuman, L. M., (1998) Micronutrient fertilizers. *Journal of crop production.* 1, 165-195.

Smith, P., (2013) Delivering food security without increasing pressure on land. *Global Food Security.* 2 (1), 18-23.

Sondi, I., Salopek-Sondi, B., (2004) Silver nanoparticles as antimicrobial agent: a case study on *E. Coli* as a model for Gram-negative bacteria. *Journal of Colloid Interface Science.* 275, 177–182.

Soto, A.M., Morales, P., Haza, A. I., García, M. L., Selgas, M.D., (2014). Bioavailability of calcium from enriched meat products using CaCo-2 cells. *Food Research International.* 55, 263–270.

Srivastava, V., Gusain, D., Sharma, Y.C., (2013) Synthesis, characterization and application of zinc oxide nanoparticles (n-ZnO). *Ceramics International.* 39 (8), 9803-9808.

Stein, A.J., (2010) Global impacts of human malnutrition. *Plant Soil*. 335, 133–154

Stein, A.J., Meenakshi, J.V., Qaim, M., Nestel, P., Sachdev, H.P.S., Bhutta, Z.A., (2005). Technical monograph 4. Analysing the health benefits of biofortified staple crops by means of the disability-adjusted life years approach: A handbook focusing on iron, zinc and vitamin A. *Washington, WA, USA: HarvestPlus.*

Stein, A.J., Sachdev, H.P.S., Qaim, M., (2008) Genetic Engineering for the Poor: Golden Rice and Public Health in India. *World Development.* 36 (1), 144-158.

Stiener, A.A., Van Winden, H., (1970) Recipe for Ferric Salts of Ethylenediaminetetraacetic Acid. *Plant Physiology, Short communication.* 46, 862-863.

Struik, P.C., Geertsema, J., Custers, C.H.M.G., (1989) Effects of shoot, root and stolon temperature on the development of the potato (*Solanum tuberosum L.*) plant. III. Development of tubers. *Potato Research.* 151-158.

Sun, Y.K., Ma, M., Zhang, Y., Gu, N., (2004) Synthesis of nanometer-size maghemite particles from magnetite. *Colloids and Surfaces A: Physicochemical and Engineering Aspects. 245* (1), 15-19.

Suttle, J., (2008) Symposium Introduction: Enhancing the Nutritional Value of Potato Tubers. *American Journal of Potato Research.* 85, 266.

Tang, Z., Claveau, D., Corcuff, R., Belkacemi, K., Arul, J., (2008) Preparation of nano-CaO using thermal-decomposition method. *Materials Letters.* 62 (14), 2096-2098.

Taze, C., Panetas, I., Kalogiannis, S., Feidantsis, K., Gallios, G.P., Kastrinaki, G., Konstandopoulos, A.G., Václavíková, M., Ivanicova, L., Kaloyianni, M., (2016) Toxicity assessment and comparison between two types of iron oxide nanoparticles in *Mytilus galloprovincialis*. *Aquatic Toxicology.* 172, 9-20.

Tegeder, M., (2012) Transporters for amino acids in plant cells: some functions and many unknowns. *Current Opinion in Plant Biology.* 15 (3), 315-321.

Tekalign, T., Hammes, P.S., (2005) Growth and productivity of potato as influenced by cultivar and reproductive growth. *Scientia Horticulturae.* 105 (1), 29-44.

Thacher, T.D., Fischer, P.R., Strand, M.A., Pettifor, M., (2006) Nutritional food quality. Rickets around the world: causes and future directions. *Annals of Tropical Paediatrics.* 26, 1-16.

Thant, A.A., Srimala, S., Kaung, P., Itoh, M., Radzali, O,. Ahmad Fauzi, M.N., (2010) Low temperature synthesis of $MgFe_2O_4$ soft ferrite nanocrystallites. *Journal of the Australian Ceramic Society.* 46 (1) 11-14

The Royal Society, (2004) Nanoscience and Nanotechnologies: Opportunities and Uncertainties. Royal Society and Royal Academy of Engineering. Final report, UK, 2004. http://www.nanotec.org.uk/finalReport.htm.

Thomas, D., (2003) A study on the mineral depletion of the foods available to us as a nation over the period 1940–1991. *Nutritional Health.* 17, 85–115.

Touliatos, D., Dodd, I.C., McAinsh, M., (2016) Vertical farming increases lettuce yield per unit area compared to conventional horizontal hydroponics. *Food and Energy Security*. 5(3), 184-191. doi:10.1002/fes3.83.

Trampczynska, A., Böttcher, C., Clemens, S., (2006) The transition metal chelator nicotianamine is synthesized by filamentous fungi. *FEBS Letters,* 580 (13), 3173-3178.

Trenkel, M.E., (1997) Controlled-release and stailized fertilizers in agriculture. *International Fertilizer Industry Association, Paris.*

Ünal, B., Durmus, Z., Baykal, A., Sözeri, H., Toprak, M.S. and Alpsoy, L., (2010). l-Histidine coated iron oxide nanoparticles: Synthesis, structural and conductivity characterization. *Journal of Alloys and Compounds.* 505 (1), 172-178.

Vanaja, A., Ramaraju, G.V., Rao,K.S., (2016) Role of NaOH concentration on Structural, Morphological and Optical Properties of ZnO Nanopowders Synthesized by Solgel process. *International Journal of TechnoChem Research.* 2 (2), 110-120.

Vavrusova, M., and Skibsted, L.H., 2014. Calcium nutrition. Bioavailability and fortification. *LWT - Food Science and Technology,* 59 (2, Part 2), 1198-1204

Vazquez-Arenas, J., Sosa-Rodriguez, F., Lazaro, I. and Cruz, R., 2012. Thermodynamic and electrochemistry analysis of the zinc electrodeposition in NH4Cl–NH3 electrolytes on Ti, Glassy Carbon and 316L Stainless Steel. *Electrochimica Acta,* 79, 109-116.

Vellinger C, Felten V, Sornom P, Rousselle P, Beisel JN, et al. (2012) Behavioural and physiological responses of *Gammarus pulex* exposed to cadmium and arsenate at three temperatures: Individual and combined effects. PLOS ONE 7(6): e39153. https://doi.org/10.1371/journal.pone.0039153.

Verkerk K. (1955) Temperature, light and the tomato. *Mededelingen Landbouw Hogeschool, Wageningen* 55: 175-224.

Verma, S., Sharma, A., Kumar, R., Kaur, C., Arora, A., Shah, R. and Nain, L., (2015) Improvement of antioxidant and defence properties of Tomato (var. *Pusa Rohini*) by application of bioaugmented compost. *Saudi Journal of Biological Sciences.* 22 (3), 256-264.

Wagner, C.C., Baran, E.J., (2010) Vibrational spectra of two Fe(III)/EDTA complexes useful or iron supplementation. *Spectrochim Acta A: Molecular Biomolecular Spectroscopy* 75(2):807-10. doi: 10.1016/j.saa.2009.11.059.

Wan, J., Chen, X., Wang, Z., Yang, X., Qian, Y., (2005) A soft-template-assisted hydrothermal approach to single-crystal Fe_3O_4 nanorods. *Journal of Crystal Growth*. 276: 571–576. 10.1016/j.jcrysgro.2004.11.423

Welch, R. M., Graham, R.D., (2002) Food breeding crops for enhanced micronutrient content. *Plant and Soil*. 245, 205-214.

Welch, R.M., Graham, R.D., (2005) Agriculture: the real nexus for enhancing bioavailable micronutrients in food crops. *Journal of Trace Elements in Medicine and Biology.* 18 (4), 299-307.

Wheeler, R.M., (2006) Potato and human exploration of space: Some observations from NASA-sponsored controlled environment studies. *Potato Research.* 49 (1), 67-90.

White, P. J., Bradshaw, J. E., Finlay, M., Dale, B., Ramsay, G., Hammond, J. P., Broadley, M. R., (2009) Relationships Between Yield and Mineral Concentrations in Potato Tubers. *Horticultural Science.* 44 (1), 6-11.

White, P.J., (2001) The pathways of calcium movement to the xylem. *Journal of Experimental Botany*. 5 (2), 891-899.

White, P.J., (2005) Calcium. In: Broadley, M. R., White, P.J., eds. Plant nutritional genomics. *Oxford, UK: Blackwell.* 6 6-86.

White, P.J., (2017) Ion Transport. *In:* B. Thomas, B.G. Murray and D.J. Murphy, eds., Encyclopedia of Applied Plant Sciences (Second Edition). *Oxford: Academic Press*. 238-245.

White, P.J., and Broadley, M.R., (2005a) Biofortifying crops with essential mineral elements. *Trends in Plant Science.* 10 (12), 586-593.

White, P.J., and Broadley, M.R., (2009) Biofortification of crops with seven mineral elements often lacking in human diets – Iron, zinc, copper, calcium, magnesium, selenium and iodine. *New Phytologist.* 182 (1), 49-84.

White, P.J., Broadley, M.R,. (2005b) Historical variation in the mineral composition of edible horticultural products. *Journal of Horticultural Sciences Biotechnology.* 80, 660–7.

White, P.J., Broadley, M.R., (2003) Calcium in plants. *Annals of Botany.* 92, 487-511.

Willcox, J.K., Catignani, G.L., Lazarus, S., (2003) Tomatoes and cardiovascular health. *Critical Review in Food Science and Nutrition.* 43, 1–18.

Winkler, J.T., (2011) Biofortification: improving the nutritional quality of staple crops, in: C. Pasternak (Ed.), *Access Not Excess, Smith-Gordon, Cambs.* 100-112.

Wirth, J., Poletti, S., Aeschlimann, B., Yakandawala, N., Drosse, B., Osorio, S., (2009) Rice endosperm iron biofortification by targeted and synergistic action of nicotianamine synthase and ferritin. *Plant Biotechnology*. 7, 631–644.

World Health Organization (2002). World health report, 2002. Available at: <http://www.who.int/whr/2002/>.

Wu, K.H., Ting, T.H., Li, M.C., Ho, W.D., (2006) Sol–gel auto-combustion synthesis of SiO2-doped NiZn ferrite by using various fuels. *Journal of Magnetism and Magnetic Materials.* 298 (1), 25-32.

Wu, Y., Wang, X., (2011) Preparation and characterization of single-phase α-Fe2O3 nano-powders by Pechini sol–gel method. *Materials Letters.* 65 (13), 2062-2065.

Xiong, D., Fang, T., Yu, L., Sima, X., Zhu, W., (2011) Effects of nano-scale TiO_2, ZnO and their bulk counterparts on zebrafish: Acute toxicity, oxidative stress and oxidative damage. *Science of the Total Environment.* 409 (8), 1444-1452.

Ye, X., Al-Babili, S., Zhang, J., Lucca, P., Beyer, P., (2000) Engineering the provitamin A (β-carotene) biosynthetic pathway into (carotenoid-free) rice endosperm. *Science.* 287, 303-305

Zak, A.K., Razali, R., Majid, W.H.A., Darroudi, M., (2011) Synthesis and characterization of a narrow size distribution of zinc oxide nanoparticles. *International Journal of Nanomedicine.* 6, 1399-1403.

Zhang, T., Lv, C., Chen, L., Bai, G., Zhao, G., Xu, C., (2014) Encapsulation of anthocyanin molecules within a ferritin nanocage increases their stability and cell uptake efficiency. *Food Research International.* 62 (0), 183-192.

Zhao, F.J., McGrath, S.P., (2009) Biofortification and phytoremediation. *Current Opinion Plant Biology.* (12), 373-380.